Volatile in alkalinen Systemen – untersucht am Beispiel der Gardar Provinz, Südgrönland

Dissertation

zur Erlangung des Grades eines Doktors der Naturwissenschaften

der Fakultät für Geowissenschaften
der Eberhard-Karls-Universität Tübingen

vorgelegt von
JASMIN KÖHLER
aus Hechingen, Zollernalbkreis

2007

Tag der mündlichen Prüfung: 20. Dezember 2007

Dekan: Prof. Dr. Peter Grathwohl

1. Berichterstatter: Prof. Dr. Gregor Markl

2. Berichterstatter: Prof. Dr. Wolfgang Siebel

Inhaltsverzeichnis

Danksagung I

Zusammenfassung / Abstract II

Zielsetzung der Arbeit 1

Geologische Übersicht 3

Erweiterte Zusammenfassung der Publikationen 5

Literatur 20

Anhang

1	Magmatic halogen geochemistry in the Gardar Province, South Greenland: evidence for subduction-related mantle metasomatism.	24
2	Fluid geochemistry in the Ivigtut cryolite deposit, South Greenland.	53
3	REE-systematics of fluorides, calcite and siderite in peralkaline plutonic rocks from the Gardar Province, South Greenland.	91

Eidesstattliche Erklärung

Danksagung

An erster Stelle möchte ich mich herzlich bei Gregor Markl für die Betreuung dieser Arbeit bedanken. Darüber hinaus ermöglichte er mir Diskussionen mit Fachkollegen in Schottland und Dänemark und die Teilnahme an verschiedenen Tagungen. Wolfgang Siebel danke ich für die freundliche Übernahme des Koreferats.

Heiner Taubald danke ich für die Durchführung der RFA-Analysen, Helene Brätz für Spurenelement-Analysen mit LA ICP-MS, Bernd Steinhilber für Isotopenmessungen von Fluideinschlüssen und Joanne Potter für Gaschromatographie-Analysen an Fluideinschlüssen. Besonderer Dank gilt Gabi Stoschek für Sauerstoff-Isotopiemessungen an Quarz, aber vor allem für die tolle Teamarbeit und ihre unendliche Ruhe beim anspruchsvollen Aufbau der Ionenchromatographie. Thomas Wagner danke ich für seine Hilfe bei diversen thermodynamischen Modellierungen, Thomas Wenzel für das Korrekturlesen des RFA-Kapitels, Bernd Binder und Daniel Russ für ihre Unterstützung bei der Raman-Spektroskopie und Verena Krasz für ihre Hilfe bei Crush Leach Analysen. Mein herzlicher Dank geht außerdem an Frau Dimitrovice, Frau Gill-Kopp und an alle Kollegen der Arbeitsgruppe, insbesondere Gesa Graser und Michael Marks.

Bei Adrian Finch möchte ich mich herzlich für einen sehr fruchtbaren Aufenthalt in Schottland bedanken. Er verhalf mir durch anregende Diskussionen, mein Thema aus einem anderen Blickwinkel zu betrachten. Großer Dank geht auch an Brian Upton, der mir großzügigerweise Probenmaterial für RFA-Analysen zur Verfügung stellte und stets offen für Diskussionen war.

Jens Konnerup-Madsen danke ich für Einladung nach Kopenhagen und Ole V. Petersen für die zahlreichen Ivigtut-Proben aus dem Geologischen Museum in Kopenhagen. Ebenso möchte ich mich bei Ralf-Thomas Schmitt vom Naturkundemuseum Berlin für Bereitstellung von Ivigtut-Proben bedanken.

Es ist schwer in Worte zu fassen, wie dankbar ich meinem Freund Johannes Schönenberger bin. Sein stetes Motivieren, die Mitarbeit im Crush Leach Labor, seine unermüdliche Hilfe sowie unzählige Diskussionen trugen auch zum Erfolg dieser Arbeit bei.

Genauso sehr danke ich meinen Eltern und meiner Schwester für ihre grenzenlose Unterstützung und für ihr Aufbauen während mancher Durststrecken. Danke für Euer Vertrauen, und dass ich immer auf Euch zählen kann!

Der Graduiertenförderung des Landes Baden-Württemberg sowie Gregor Markl danke ich für die Finanzierung dieses Projekts.

Zusammenfassung

Die Gardar Provinz im Süden Grönlands ist ein *failed-rift* aus dem Mittleren Proterozoikum und gehört zu den weltweit großen Vorkommen alkaliner Gesteine. Erhöhte Gehalte an F im Mantel bzw. in den Schmelzen führten hier zur Bildung außergewöhnlicher Gesteine. Dazu gehören beispielsweise die HFSE- und SEE-reichen Agpaite der Ilímaussaq Intrusion oder die einzigartige Kryolithlagerstätte in Ivigtut. Ziel dieser Arbeit ist es, den Mantel unterhalb der Provinz zu charakterisieren sowie die Bildung und Entwicklung F-reicher Schmelzen und Fluide am Beispiel Ivigtuts nachzuvollziehen.

Ganggesteine in der Gardar Provinz repräsentieren die primitivsten Schmelzen und geben Auskunft über die Beschaffenheit der Mantelquelle. RFA Analysen von 114 fein- bis grobkörnigen Ganggesteinen weisen große Unterschiede hinsichtlich ihrer Chronologie, ihrer räumlichen Verbreitung und chemischen Zusammensetzung auf. So sind ältere Ganggesteine höher fraktioniert als jüngere und Ganggesteine aus unterschiedlichen Regionen haben einen stark variablen Chemismus. All diese Kriterien deuten daraufhin, dass die Schmelzen einem heterogenen Mantel entstammen, der im Zuge von Subduktionsprozessen metasomatisch verändert wurde. Dies zeigt sich vor allem in der Spurenelementverteilung der Ganggesteine, die stark jener von Shoshoniten ähnelt und sich durch eine Anreicherung an LILE, Sr und der leichten SEE, aber durch eine Verarmung an HFSE, Nb und Ti auszeichnet. Die Ganggesteine der Gardar Provinz weisen einen stets hohen Gehalt an F auf, der in der Region um Ivigtut sein Maximum (bis 1,2 Gew%) erreicht. Es wird vermutet, dass F dem lithosphärischen Mantel enstammt und im Zuge einer Teilaufschmelzung von F-reichem Apatit und F-Phlogopit freigesetzt wurde.

Eine Besonderheit innerhalb der Gardar Provinz ist die 1,27 Ga alte Ivigtut Intrusion mit der weltweit einzigen Lagerstätte von Kryolith [Na_3AlF_6]. Mit Hilfe einer detaillierten Untersuchung von Fluideinschlüssen wurde das Fluid näher charakterisiert, welches mit der Lagerstättenbildung in Zusammenhang steht. Mikrothermometrisch können drei Einschlusstypen unterschieden werden: (1) reines CO_2, (2) H_2O-CO_2 und (3) wässrig salinare Einschlüsse. Die finalen Schmelztemperaturen für Eis schwanken zwischen -23 und -15 °C für Typ (2) und von -15 bis -10 °C für Typ (3) Einschlüsse. Die meisten Fluideinschlüsse homogenisieren in die Flüssigkeit bei 110-150 °C. Die Isotopie des Einschluss-Wassers legt einen meteorischen Ursprung nahe (δD_{H2O} -19 bis -144 ‰ VSMOW und $\delta^{18}O_{H2O}$ -1 to -21.7 ‰ VSMOW). $\delta^{13}C$ von Einschluss-CO_2 beträgt ca. -5 ‰ PDB und entspricht typischen Mantelwerten. Die Unterschiede zwischen $\delta^{18}O_{CO2}$ (+21 to +42 ‰ VSMOW) und $\delta^{18}O_{H2O}$ ist

auf Isotopenaustausch bei geringen Temperaturen zurückzuführen. Mit Hilfe der Ionenchromatographie wurde der Reichtum an Na, Cl und F im Fluid nachgewiesen. Cl/Br Verhältnisse betragen 56-110 und lassen eine intensive Fluid-Gesteins-Wechselwirkung vermuten. Aus mikrothermometrischen Daten berrechnete Isochoren geben bei einem Druck von 1-1,5 kbar je nach Einschlusstyp Bildungstemperaturen von 100-400 °C an. Aufgrund thermodynamischer Modellierungen von Mineralparagenesen und des extrem hohen F-Gehalts wird angenommen, dass sich die Kryolith-Lagerstätte im Übergangsbereich von einer volatilreichen Schmelze zu einem Fluid bildete.

Um die Bildung und Entwicklung von F-reichen Schmelzen und Fluiden besser zu verstehen, wurden Fluoride, Calcit und Siderit in drei Gardar Intrusivkomplexen hinsichtlich ihres Seltenen Erd-Gehalts und Yttrium (SEE) untersucht. Die verschiedenen Fluorit-Generationen der agpaitischen Ilímaussaq, miaskitisch-agpaitischen Motzfeldt und granitischen Ivigtut Intrusionen weisen alle eine negative Eu-Anomalie auf, die auf Feldspat-Fraktionierung zurückzuführen ist. Die gleichen SEE-Muster primärer Fluorite von Ilímaussaq und Motzfeldt lassen ähnliche Magmenquellen und Bildungsbedingungen vermuten. SEE-Muster hydrothermaler Fluorite dieser beiden Intrusionen reflektieren verschiedene Mechanismen, die den Spurenelementeinbau steuern: Temperturabhängigkeit, Fluidmigration und –interaktion, Komplexierung und Fraktionierung. Die beobachtete SEE-Verteilung spiegelt den Einfluss eines F-CO_2-reichen Fluids wider, welches mit dem Nebengestein wechselwirkte. Hydrothermale Fluoride der Ivigtut Intrusion zeigen flache Muster, die teilweise auch an schweren SEE angereichert sind und einen prägnanten Tetrad-Effekt aufweisen. Dieser Effekt resultiert von intensiven Fluid-Gesteins-Wechselwirkungen und ist typisch für hoch fraktionierte, granitische Gesteine. Die großen Unterschiede in der Verteilung der SEE scheinen verschiedene Quellen zu reflektieren, denn während sich die benachbarten Intrusionen Ilímaussaq und Motzfeldt hinsichtlicher ihrer SEE-Verteilung stark ähneln, weisen die Fluoride Ivigtuts komplett andere Muster auf. Diese Unterschiede können auf die verschieden tektonische Lage und Heterogenitäten im Mantel zurückgeführt werden.

Abstract

The mid-Proterozoic Gardar failed-rift Province in South Greenland is world-famous for its alkaline rocks. Elevated contents of F in the mantle source and an F-enrichment in the parental melts have been suggested to account for the peculiarities of the Gardar rocks including the HFSE- and REE-enriched agpaites in the Ilímaussaq intrusion or the unique cryolite deposit at Ivigtut. The aim of this study was to characterise the mantle beneath the Province and to constrain the formation and chemical evolution of F-bearing melts and fluids with focus on the Ivigtut intrusion.

Dykes in the Gardar Province represent the most primitive melts and are thus suited to investigate the nature of the sub-Gardar mantle and the evolution of its partial melts. XRF analyses of 114 samples of fine- to coarse-grained dykes span the temporal, lateral and compositional range (basanites to trachytes) within the alkaline province. In terms of major and trace element geochemistry, older dykes are more highly fractionated than younger ones and dykes from different areas exhibit diverse geochemical characteristics suggesting a highly heterogeneous mantle. This mantle was intensively metasomatised during subduction processes as evidenced by the dykes' enrichment in LILE, LREE, Sr, their depletion in HFSE, Nb and Ti and their strong affinity with adakites and shoshonites. A typical feature of the magmatic Gardar rocks is their high content of fluorine which reaches up to 1.2 wt % in dykes around Ivigtut. Fluorine is interpreted to be derived from partial melting of F-apatite and F-phlogopite in the lithospheric mantle.

A peculiarity in the Gardar Province is the 1.27 Ga old Ivigtut intrusion. It hosts the world-wide unique cryolite [Na_3AlF_6] deposit situated within a metasomatised granite stock. A detailed fluid inclusion study helped to characterise the fluid present during the formation of the deposit. Microthermometry revealed three different types of inclusions: (1) pure CO_2, (2) aqueous carbonic and (3) saline aqueous inclusions. Final melting temperatures range between -23 to -15 °C for type 2 and from -15 to -10 °C for type 3 inclusions. Most inclusions homogenise between 110 and 150 °C into the liquid. Stable isotope compositions of CO_2 and H_2O were measured from crushed inclusions. $\delta^{13}C$ values are about -5 ‰ PDB and are typical of mantle-derived magmas. The differences between $\delta^{18}O_{CO2}$ (+21 to +42 ‰ VSMOW) and $\delta^{18}O_{H2O}$ (-1 to -21.7 ‰ VSMOW) suggest low-temperature isotope exchange. δD_{H2O} ranges from -19 to -144 ‰ VSMOW and the isotopic composition of inclusion water suggests a meteoric origin. Ion chromatography revealed the fluid's predominance in Na, Cl and F. Cl/Br ratios range between 56 and 110 and may imply intensive fluid-rock interaction with the host

granite. Isochores deduced from microthermometry suggest a formation temperature of 100 to 400 °C at a pressure of 1-1.5 kbar depending on inclusion type. Thermodynamic modelling of phase assemblages and the extraordinary high concentration in F (and Na) may indicate that the cryolite body formed during the continuous transition from a volatile-rich melt to a solute-rich fluid.

In order to constrain the formation and evolution of F-rich melts and fluids, fluorides, calcite and siderite from three intrusions in the Gardar Province were analysed for their trace element content focusing on the rare earth elements and yttrium (REE). The various generations of fluorites in the granitic Ivigtut, agpaitic Ilímaussaq and miaskitic to agpaitic Motzfeldt intrusions all share a negative Eu anomaly which is attributed to feldspar fractionation. The primary magmatic fluorites from Ilímaussaq and Motzfeldt display very similar REE patterns suggesting formation from related parental melts under similar conditions. Hydrothermal fluorites from these two intrusions reflect multiple effects responsible for the incorporation of trace elements into fluorides: temperature dependence, fluid migration/interaction and complexation resulting in REE fractionation. Generally, all REE patterns reflect the evolution and migration of a F-CO_2-rich fluid. This fluid partly inherited the REE patterns of altered host rocks. There is also evidence of an even younger fluid rich in REE which resulted in highly variable REE concentrations within one sample of hydrothermal fluorite. Fluorides from the granitic Ivigtut intrusion show flat to slightly heavy-REE-enriched patterns characterised by a strong tetrad effect. This effect resulted from extensive fluid-rock interaction in highly fractionated, Si-rich systems. In conclusion, the fluorides appear to record different REE source patterns, as the spatially close Motzfeldt and Ilímaussaq intrusions show strong similarities and contrast with the Ivigtut intrusion located 100 km NE. These variations may be attributed to differences in the tectonic position of the intrusions or mantle heterogeneities.

Zielsetzung der Arbeit

In magmatischen Systemen spielen volatile Elemente, insbesondere Fluor, eine wichtige Rolle, da sie zum einen die Schmelztemperatur von Gesteinen drastisch erniedrigen und zum anderen großen Einfluss auf die chemische Zusammensetzung einer sich bildenden Teilschmelze haben können. Fluor spielt dabei eine maßgebliche Rolle bei der Komplexbildung und dem Transport erzbildender Elemente, wie z.B. Li, Be, Sn oder den High Field Strength Elements (HFSE = u.a. Hf, Th, Zr, Ti), die dann meist in Form von Pegmatiten oder Greisen angereichert werden.

Die alkaline Gardar Provinz in Südgrönland eignet sich insbesondere für die Untersuchung von Fluor in magmatischen Systmen, da in dieser Region Fluor nicht nur in verschiedenster Form (z.B. in Kryolith [Na_3AlF_6], Villiaumit [NaF], Fluorit [CaF_2], Topas [$Al_2SiO_4F_2$]) auftritt, sondern sowohl in primitiven als auch in hochfraktionierten Gesteinen angereichert ist. Der Vergleich verschiedenster Gesteinstypen unterschiedlicher Fraktionierungsgrade lässt daher Aussagen über Quelle, Differentiations- und mögliche Anreicherungsprozesse für Fluor zu.

Im ersten Kapitel soll die Untersuchung der primitivsten Gesteine innerhalb der Gardar Provinz Auskunft über eine mögliche Magmenquelle bzw. den Mantel unter der Region geben. Hierzu eignen sich Ganggesteine, die die gesamte Gardar Provinz durchziehen, unterschiedlichen Generationen angehören und eine breite chemische Zusammensetzung aufweisen. Detaillierte RFA-Gesamtgesteinsanalysen sollen klären, ob die Ganggesteine aus einem primitiven oder aus einem bereits ab- bzw. angereicherten Mantel hervorgingen. Der Fluor-Gehalt dieser primitiven Gesteine lässt zudem Rückschlüsse zu auf eine mögliche Fluor-Quelle im Mantel oder auf eine Fluor-Anreicherung im Laufe von Subduktions- oder Fraktionierungsprozessen.

Im zweiten Kapitel werden die Entstehungsbedingungen der Ivigtut Intrusion untersucht, in der es aufgrund des außergewöhnlich hohen Fluor-Gehalts zur weltweit einzigen (abbauwürdigen) Anreicherung von Kryolith kam. Die detaillierte Untersuchung von Fluideinschlüssen hinsichtlich ihrer chemischen und isotopengeochemischen Zusammensetzung in verschiedenen Mineralen der Kryolith-Lagerstätte gibt Auskunft über den Ursprung und die Entwicklung des Fluids, welches mit der Lagerstättenbildung assoziiert ist. Die Kombination aus Fluideinschluss-Ergebnissen und thermodynamischen Modellierungen von typischen Phasenvergesellschaftungen in Ivigtut lässt eine genauere

Bestimmung der intensiven Parameter (T, p, a_{H2O}, a_{HF}, a_{SiO2}) zu, welche zur Entstehung der Kryolith-Lagerstätte führten.

Im letzten Teil wird mit LA ICP-MS Messungen die Verteilung der Seltenen Erden (SEE) in Fluorit, Kryolith, Kryolithionit, Siderit und Calcit untersucht. Hierzu wird eine Vergleichsstudie zwischen den drei Gardar Intrusionen Motzfeldt, Ilímaussaq und Ivigtut erstellt. Mit Hilfe der verschiedenen SEE-Verteilungsmuster sollen Fraktionierungsprozesse, unterschiedliche Komplexierungsphänomene, der Einfluss einer möglichen Fluidphase und die Abhängigkeit der SEE-Anreicherung vom geochemischen Milieu näher beleuchtet werden.

Geologische Übersicht

Die Gardar Provinz im Süden Grönlands erstreckt sich zwischen dem Archaischen Kraton im Norden und dem Ketilidischen Orogen im Süden. Die Provinz ist eine *failed-rift* Struktur aus dem mittleren Proterozoikum, die zwischen 1,35 und 1,14 Ga mehrmaligem, kontinentalem Rifting unterlag (Upton & Emeleus, 1987; Upton et al., 2003).

Das Grundgebirge der Gardar Provinz besteht im NW aus Archaischem Kraton, zum größten Teil jedoch aus dem 1,85-1,79 Ga alten, kalk-alkalischen Julianehåb-Batholith. Dieser ist 100-200 km breit, wird als magmatischer Bogen gedeutet und besteht überwiegend aus granodioritischen Gesteinen (Garde et al., 2002). Die Gesteine innerhalb der Gardar Provinz lassen sich in drei Einheiten untergliedern: a) eine Wechselfolge aus Sandsteinen und Basalten (Eriksfjord-Formation), b) weit verbreitete Ganggesteins-Schwärme sowie c) mehrere große und kleine Intrusivkomplexe (Escher & Watt, 1976).

Die basaltischen Laven der Eriksfjord-Formation wechsellagern mit fluviatil-lakustrinen Quarziten bzw. Arkosen und bilden insgesamt eine 3-4 km mächtige Einheit, welche heute zum größten Teil erodiert ist (Macdonald & Upton, 1993; Emeleus & Upton, 1976). Ganggesteine (*Dykes*) höchst unterschiedlicher Zusammensetzung durchziehen die gesamte Gardar Provinz, konzentrieren sich jedoch auf zwei Regionen um die Intrusivkomplexe Tugtutôq-Ilímaussaq bzw. Isortoq-Nunarssuit (Upton & Emeleus, 1987). Die Gänge können in drei verschiedene Gruppen eingeteilt werden. Die *Basischen Gänge* bestehen vorwiegend aus Doleriten und Gabbros, sind reich an Alkalien und werden aufgrund ihrer braunen Verwitterungsfarbe auch „Brown Dykes“ genannt (Upton et al., 2003; Emeleus & Upton, 1976). Nach Goodenough (1997) stammen die basischen Dykes aus dem lithosphärischen Mantel, welcher durch Subduktionsfluide an inkompatiblen Elementen angereichert wurde. Die WNW-ESE streichenden *Giant Dykes* sind 200-800 m breit und werden von (Syeno)Gabbros dominiert. Aufgrund ihrer Mächtigkeit besitzen sie aber oft einen mafischen Rand und ein SiO_2-reiches Zentrum und können als Binde- bzw. Übergangsglied zu den Intrusivkomplexen angesehen werden (Upton et al., 2003). Die dritte und kleinste Ganggesteinsgruppe umfasst ultramafische *Lamprophyre und Karbonatite*, die vor allem im Übergangsbereich zum Archaischen Kraton auftreten. Die Lamprophyre repräsentieren die primitivsten Gesteine innerhalb Gardars und entstammen einer OIB-ähnlichen Quelle (Goodenough, 1997). Die Karbonatite hingegen werden als Differentiationsprodukt eines CO_2-reichen, phonolithischen Magmas angesehen (Upton &

Emeleus, 1987) und gingen vermutlich aus einer Lamprophyr-Karbonatit-Schmelzentmischung hervor (Goodenough, 1997).

In der Gardar Provinz treten innerhalb des Julianehåb-Batholiths und vereinzelt im Archaischen Kraton 12 größere und mehrere kleine Intrusivkomplexe auf, deren Alter zwischen 1,35 und 1,14 Ga liegt (Upton et al., 2003). Trotz des lange andauernden Magmatismus in der Provinz zeichnen sich die Intrusionen durch große Homogenität hinsichtlich ihrer Petrologie und Geochemie aus (Upton & Emeleus, 1987; Marks et al., 2003; 2004). Allerdings lassen sich zwei Gruppen unterscheiden: die Intrusivkomplexe im Norden und Osten sind eher SiO_2-untersättigt, während jene im Süden und Westen meist SiO_2-übersättigt sind. Die Ausnahme bildet die Ilímaussaq Intrusion, in der sowohl SiO_2-untersättigte Sodalith-Foyaite als auch SiO_2-reiche Alkali-Granite auftreten. Ilímaussaq ist zudem die Typlokalität agpaitischer Gesteine. Dabei handelt es sich um peralkaline Nephelin-Syenite, die komplexe Ti-Zr-Silikate wie Eudialyt oder Rinkit führen (Emeleus & Upton, 1976; Upton & Emeleus, 1987; Sørensen, 1997; Markl et al., 2001; Sørensen et al., 2006). Im Gegensatz hierzu kristallisieren Miaskite normale Fe-Ti Oxide. Ein kleines Vorkommen agpaitischer Gesteine befindet sich zudem in der 1,27 Ga alten, überwiegend miaskitischen Motzfeldt Intrusion im NE der Gardar Provinz (Upton et al., 2003).

Eine Besonderheit unter den Gardar Intrusionen ist der 1,27 Ga (unveröffentlichte Daten, Upton) Ivigtut (auch *Ivittuut*) Komplex, der im NW der Provinz Archaikum intrudierte. Obwohl Ivigtut mit einem Durchmesser von 350 m die kleinste Intrusion der Region ist, wurde sie aufgrund ihrer weltweit einzigartigen Kryolith- [Na_3AlF_6] Lagerstätte berühmt. Die Intrusion umfasst den stockförmigen (A-Typ) Granitkörper, welcher von einer Intrusionsbrekzie umgeben ist. Ein zweites Brekzienvorkommen, die sog. „Bunkebrekzie“, ist in der Tiefe mit dem Granitstock verbunden. Der Granit selbst kann in einen oberen hypersolvus und einen unteren, metasomatisch stark veränderten subsolvus Bereich gegliedert werden, welche durch die 150 m mächtige Lagerstätte getrennt sind (Goodenough et al., 2000). Innerhalb der Lagerstätte ist Kryolith vorwiegend mit Siderit und Quarz (± Topas) vergesellschaftet, aber es treten auch Sulfide (z.B. Galenit, Sphalerit oder Cassiterit) und andere Fluoride wie z.B. Fluorit, Chiolith oder Kryolithionit auf. Nach Pauly & Bailey (1999) bildete sich die Lagerstätte, als F-reiche, postmagmatische Fluide aus dem tieferen Teil die zentralen und oberen Granitbereiche alterierten und metasomatisch überprägten/vergreisten. Dabei bildete sich eine Aluminofluorid-Schmelze, aus deren F-reicher Schmelzfraktion die Kryolith-Lagerstätte hervorging.

Kapitel 1 – Gardar-Ganggesteine

Bisher ist nur wenig über den Mantel unter der Gardar Provinz bekannt. Zahlreiche Studien gehen davon aus, dass der Großteil der Schmelzen einem metasomatisch veränderten, lithosphärischen Mantel entstammt, welcher nur geringer krustaler Kontamination unterlag (Goodenough, 1997; Goodenough et al., 2002; Upton et al., 2003; Halama et al., 2004). Dies belegen niedrige $^{86}Sr/^{87}Sr$ Verhältnisse von 0.703 and initiale ε_{Nd} Werte von +2 to +6 (Pearce & Leng, 1996; Andersen, 1997; Goodenough et al., 2002). Es wird angenommen, dass im Zuge von Subduktionsprozessen während der Ketilidischen Orogenese vor ca. 1,85 Ga der Mantel an Large Ion Lithophile Elements (LILE), Leichten Seltenen Erden (LSEE) und anderen inkompatiblen Elementen, insbesondere Fluor, angereichert wurde (Upton & Emeleus, 1987; Goodenough, 1997; Goodenough et al., 2002; Upton et al., 2003). In dieser Studie wurden über 110 Ganggesteine (*Dykes*) aus der ganzen Gardar Provinz hinsichtlich ihres Gesamtgesteinschemismus untersucht. Die Dykes repräsentieren die am wenigsten entwickelten Schmelzen der Region und lassen somit eine nähere Charakterisierung der Mantelquelle und Aussagen über die Herkunft/Entwicklung der Rift-bezogenen Schmelzen zu.

Die untersuchten Ganggesteine weisen eine breite Variation hinsichtlich ihrer Zusammensetzung auf. So sind sowohl primitive Basanite und Basalte als auch höher fraktionierte Phonolithe und Trachyte vertreten. Da der Na-Gehalt meist höher ist als der von K, können zahlreiche Ganggesteine als Mugearite, Benmoreite oder Hawaiite bezeichnet werden. Daneben weisen die Dykes Ähnlichkeiten mit K-reichen, kalk-alkalinen Gesteinen, insbesondere den Shoshoniten, auf. Nicht nur ihr durchschnittlicher Al_2O_3-Gehalt von 15 Gew%, sondern auch K_2O/Na_2O-Verhältnisse von 0,3-1,4 und ihr generell hoher Gehalt an Alkalien (K_2O > 2 Gew%; Na_2O+K_2O > 4 Gew%) sind typisch für Shoshonite (Le Maitre et al., 1989).

Innerhalb der Gardar Provinz treten verschiedene Dyke Generationen unterschiedlichen Fraktionierungsgrads auf. Als Maß für die Fraktionierung gilt hierbei die Mg-Zahl ([Mg# = 100*Mg/(Mg+Fe^{2+})). Dabei sind ältere Ganggesteine höher fraktioniert als jüngere, d.h. letztere haben einen geringeren Gehalt an inkompatiblen Elementen. Die Dykes lassen sich jedoch nicht nur chronologisch, sondern auch regional voneinander trennen. Dabei ähneln sich Ganggesteine in der Nähe folgender Intrusivkomplexe: 1) Tugtutôq-Isortoq-Nunarssuit-Narsarsuaq, 2) Ilímaussaq-Narsaq-Motzfeldt und 3) Ivigtut. Auf deren geochemische Charakteristika wird im Folgenden kurz eingegangen.

a) Hinweise auf Fraktionierungsprozesse

Die Korrelation verschiedener Elemente mit Mg# lässt Aussagen über mögliche Mineralfraktionierungen zu. So deutet die positive Korrelation zwischen TiO_2-Mg# und V-Mg# auf Fraktionierung von Fe-Ti Oxiden hin. Fraktionierung von Klinopyroxen ist wahrscheinlich, auch wenn die positive Korrelation zwischen CaO/Al_2O_3 und Mg# für einzelne Dyke-Regionen nur schwach ausgeprägt ist. Auch Ni, Fe und Cr korrelieren positiv mit Mg#, was Fraktionierung von Olivin und Orthopyroxen widerspiegelt. Allerdings beschreiben die Übergangsmetalle in der Region Ilímaussaq-Narsaq-Motzfeldt einen merkwürdigen Verlauf, denn ihr Gehalt steigt unterhalb einer Mg# von 30 wieder an. Diese Anreicherung bei Mg# < 30 ist am deutlichsten für Ni, Cr und Zn ausgebildet, aber auch für Fe_2O_{3total} und Co nachzuvollziehen. Derselbe Trend lässt sich auch in Abhängigkeit von MgO oder SiO_2 beobachten. Es ist rätselhaft, in welche Minerale diese Übergangsmetalle eingebaut wurden. Sulfide können ausgeschlossen werden, da die Elemente keine Korrelation mit S aufweisen. Auch die Fraktionierung von Mineralen der Spinell-Gruppe scheint keine Rolle gespielt zu haben, denn Elemente der verschiedenen Spinell-Endglieder (Ni, Cr, Al, Zn, Mn) korrelieren nicht miteinander. Nur Fe_2O_3 zeigt eine positive Korrelation mit TiO_2, was auf Fraktionierung von Ulvöspinell hindeuten könnte.

Im Vergleich zu den anderen Ganggesteinen sind die Dykes um Ilímaussaq-Narsaq-Motzfeldt bei gleichem Cr-Gehalt an Ni angereichert, was durch die Mischung einer *slab*-Schmelze mit Mantelperidotit erklärt werden könnte (Drummond et al., 1996; Tsuchiya et al., 2005). Nach Kelemen (1995) führt diese Interaktion zu einer Ni-Anreicherung in der Schmelze aufgrund der Bildung von Orthopyroxen auf Kosten des Olivins. Allerdings würde der Zerfall von Olivin nicht nur das Mg/Fe-Verhältnis, sondern auch den absoluten MgO-Gehalt in der Schmelze erhöhen, was in den untersuchten Ganggesteinen nicht der Fall ist. Eine Möglichkeit, den außergewöhnlichen Trend der Übergangsmetalle zu klären, wäre eine Änderung der Sauerstoff-Fugazität. Morse et al. (1991) fanden heraus, dass bei geringem f_{O2} etwa die Hälfte des Ni in der Schmelze als Ni^0 vorliegt und daher nicht in Olivin eingebaut wird. Kristallisationsbedingungen unter sehr geringen Sauerstoff-Fugazitäten bis zu FMQ -5 sind für die Younger Giant Dykes von Tugtutôq (Upton & Thomas, 1980) und aus dem frühen Stadium der Ilímaussaq Intrusion (Marks & Markl, 2001) bekannt. Es ist somit möglich, dass bereits frühere, primitive Schmelzen schon sehr reduziert waren. Ebenso wie Ni wäre auch Cr bei geringen Sauerstoff-Fugazitäten in der Schmelze verblieben und erst in späteren Kristallisaten angereichert worden.

b) Spurenelementverteilung während Subduktionsprozessen

Spurenelement-Gehalte, die auf den primitiven Mantel normiert wurden (McDonough & Sun, 1995), nehmen allgemein von primitiven zu höher fraktionierten Proben zu. Die primitivsten Ganggesteine aus der Region Tugtutôq-Isortoq-Nunarssuit-Narsarsuaq weisen eine deutlich positive Sr-Anomalie auf, die in entwickelteren Dykes kleiner wird. Im Gegensatz hierzu vergrößert sich die positive Ba-Anomlie im Laufe der Fraktionierung, und es bilden sich negative Ti- und positive Zr-Anomalien aus. In der Gegend von Ilímaussaq-Narsaq-Motzfeldt sind die primitiven Ganggesteine durch eine positive U- und negative Ba-, Nb- und Ti-Anomalien charakterisiert, die sich mit fortschreitendem Fraktionierungsgrad vergrößern.

Die generelle Anreicherung der Dykes an LILE, LSEE und Sr (> 400 ppm), die geringen Gehalte an High Field Strength Elements (HFSE) sowie deren charakteristische Spurenelementverteilung weisen typische Subduktionssignatur auf. Konvergente Plattenbewegungen sind auch aus Südgrönland bekannt, denn nach Chadwick & Garde (1996) entstand das Ketilidische Grundgebirge der Gardar Provinz tatsächlich im Zuge der Kollision zwischen dem Archaischen Kraton und einer nach Norden subduzierenden, ozeanischen Platte. Allgemein können bei Subduktionsprozessen zwei verschiedene Mechansimen zur Mantelmetasomatose, d.h. zur Anreicherung von LILE und LSEE, führen: a) Metasomatose durch freigesetzte *slab*-Fluide oder b) Metasomatose durch felsische, *slab*-Schmelzen (z.B. Arculus, 1994; Yogodzinski et al., 1994). Sehr wenig ist über die Subduktionsprozesse unter der Gardar Provinz bekannt. Es kann jedoch davon ausgegangen werden, dass der Mantel durch *slab*-Fluide metasomatisch verändert wurde, was fast konstante K/Rb-Verhältnisse zwischen 350 und 450 sowie geringe Verhältnisse von La/Nb (1-3) und Ba/Nb (ca. 39) in den Gardar-Ganggesteinen belegen (Rollinson & Tarney, 2005).

c) Herkunft und Entwicklung des Fluor(-Gehalts)

Die Gardar-Ganggesteine sind generell durch einen hohen Gehalt an F bis ca. 2500 ppm charakterisiert. Dabei sind die Dykes in der Gegend um Ivigtut mit bis zu 1,2 Gew.% am stärksten an F angereichert. Obwohl die Ganggesteine wenig P_2O_5 (meist < 2 Gew%) enthalten, kann aufgrund ihres Reichtums an Volatilen jedoch davon ausgegangen werden, dass Apatit-Sättigung im Laufe der Kristallisation erreicht wurde (Watson, 1980). Diese Vermutung wird durch die positive Korrelation von P_2O_5 mit F in Dykes der Tugtutôq-Isortoq-Nunarssuit-Narsasuaq Region bestätigt. Im Gegensatz hierzu beschreiben die Ganggesteine um Ivigtut eine andere Entwicklung: Bei einem fast gleichbleibend geringen Gehalt an P_2O_5 (< 0,5 Gew%) sind höher fraktionierte Dykes gegenüber primitiven stark an F

angereichert. Apatit-Sättigung wurde hier vermutlich nicht erreicht, so dass sich F progressiv anreichern könnte.

Um zu klären, wie es zu der generell hohen Anreicherung an F kam, müssen mögliche F-Quellen im Mantel in Betracht gezogen werden. Neueste Studien zeigen, dass F in nicht unbedeutenden Mengen in Olivin, Pyroxen oder Granat eingebaut werden kann (Bromiley & Kohn, 2007). Allerdings kann davon ausgegangen werden, dass im oberen Mantel der größte Teil von F vor allem in K-Richterit, F-Phologpit und F-Apatit eingebaut wird, da F in diesen Mineralen üblicherweise OH^- ersetzt (Smith et al., 1981; Edgar et al., 1996). Die untersuchten Gardar Dykes weisen allerdings nur eine schwach positive Korrelation zwischen K_2O und F auf. Würde alles F aus Glimmer kommen, müsste die Korrelation deutlicher ausgeprägt sein (Edgar et al., 1996). Auch wenn K-Richterit typischerweise im alkalinen, K-dominierten Milieu auftritt (Konzett et al., 1997) und sich vermutlich durch metasomatische Prozesse im oberen Mantel bildet (Erlank et al., 1987), so wird aus der Beziehung K-F deutlich, dass im Falle der untersuchten Ganggesteine F nicht aus Amphibol stammen kann. Typische K/F-Verhältnisse der primitivsten Gardar Dykes sind viel geringer als die von K-Richterit (Deer et al., 1997), liegen aber fast alle im Feld von Phlogopit (Fleet et al., 2003). Für jene Analysen, die außerhalb des typischen K/F-Bereiches für Phlogopit liegen, muss von einer anderen F-Quelle ausgegangen werden. Dabei könnte es sich um F-Apatit handeln, denn die P/F-Verhältnisse primitivster Ganggesteine überlappen mit repräsentativen Mantel-Apatiten (Hogarth, 1988; Boudreau et al., 1993; Campbell & Henderson, 1997; O'Reilly & Griffin, 2000; Bühn et al., 2001; Chakhmouradian et al., 2002) und liegen teilweise entlang der Linie für hypothetischen F-Apatit (P/F = 4,89; Smith et al., 1981; Sigvaldason & Óskarsson, 1986).

Zusammenfassend kann also davon ausgegangen werden, dass der Mantel unter der Gardar Provinz durch Subduktionsprozesse metasomatisch verändert wurde, und dass F im Mantel vor allem aus F-Phlogopit und F-Apatit stammt.

Kapitel 2 – Fluid-Geochemie in Ivigtut

Der Ivigtut Komplex im NW der Gardar Provinz intrudierte Archaischen Kraton und ist aufgrund seiner einzigartigen Kryolith- [Na_3AlF_6] Lagerstätte weltberühmt. Bisher haben sich jedoch nur wenige Arbeiten mit der Entstehung der Lagerstätte beschäftigt. Pauly & Bailey (1999) fassten petrographische und (isotopen)geochemische Ergebnisse der Gesteine innerhalb der Lagerstätte zusammen und diskutierten verschiedene Genesemodelle. Prokof'ev

et al. (1991) untersuchten erstmals Fluideinschlüsse in Kryolith und Siderit von Ivigtut, doch beschränkten sich die Analysen vor allem auf Mikrothermometrie. In der vorliegenden Arbeit wird erstmals das Fluid (isotopen)geochemisch charakterisiert, was Rückschlüsse auf dessen Ursprung, Entwicklung und seine Rolle bei der Lagerstättenbildung zulässt.

Fluideinschlüsse wurden in Kryolith, Fluorit, Siderit und Quarz (sowohl aus dem Granit als auch von der Lagerstätte selbst) untersucht. Dabei können drei Einschluss-Typen unterschieden werden, die meist sekundären Ursprungs sind: (1) reine CO_2, (2) wässrige-CO_2 und (3) wässrig-salinare Einschlüsse. Das eutektische Schmelzen von Eis liegt zwischen -50 und -30 °C, was die Dominanz von NaCl belegt (Shepherd et al., 1985). Allerdings deuten tiefere eutektische Temperaturen darauf hin, dass weitere Salze, wie z.B. $LiCl_2$, $CaCl_2$, $FeCl_2$, gelöst sind (Shepherd et al., 1985; Davis et al., 1989; Dubois et al., 1994; Borovikov, 2001). Die finalen Schmelztemperaturen für Eis liegen bei Typ (1) um -56,6 °C (Tripelpunkt von reinem CO_2), bei Typ (2) zwischen -23 und -15 °C und für Typ (3) bei -15 bis -10 °C. Die meisten Fluideinschlüsse homogenisieren im Bereich von 110-150 °C in die Flüssigkeit, während die Einschlüsse des Typ (2) oft vor kompletter Homogenisierung dekrepitieren. Einschlüsse des Typs (2) enthalten – je nach CO_2-Gehalt – CO_2-Klathrat [CO_2*5,7 H_2O], welches meist zwischen -9 und +4 °C schmilzt. Qualitative Raman-Spektroskopie zeigte vereinzelt Banden von CH_4 und C_3H_8 in Typ (2) und (3), doch konnten Kohlenwasserstoffe mikrothermometrisch nicht nachgewiesen werden. Tochterminerale treten selten auf: Wässrig-salinare Einschlüsse in Quarz vom Granit enthalten manchmal Halit. In Kryolith tritt in Fluideinschluss-Typen (2) und (3) stellenweise ein dunkler, stäbchenförmiger Tochterkristall auf, der zwischen 40 und 80 °C schmilzt und während des Kühlens rasch rekristallisiert. Raman-Spektroskopie gab kein Signal, so dass das Tochtermineral entweder Raman-inaktiv oder zu klein für die Analyse ist.

Fluidpetrographische Beziehungen und Mikrothermometrie belegen, dass die Einschlüsse aus einem unmischbaren Fluid hervorgegangen sind, was im Folgenden am Beispiel der Einschlüsse von Typ (2) erläutert wird. Die wässrigen-CO_2-Einschlüsse haben stark unterschiedlichen Füllgrad, der zwischen 0.65 und 0.95 schwankt. Daneben bestehen nicht alle Einschlüsse aus drei Phasen, d.h. sie beinhalten neben flüssigem H_2O und flüssigem CO_2 nur vereinzelt gasförmiges CO_2, was auf stark variable CO_2-Gehalte schließen lässt: So bildet sich bei höheren Gehalten CO_2-Klathrat, während in mikrothermometrisch „reinen“ H_2O-Einschlüssen geringste Mengen von CO_2 mit Hilfe der Raman-Spektroskopie nachweisbar sind. Aus diesen Beobachtungen wird deutlich, dass die Fluideinschlüsse die gesamte (NaCl-)H_2O-CO_2-Zusammensetzungsvariation repräsentieren. Prozesse wie

„leakage“ oder „necking down“ könnten vereinzelt unregelmäßige Fluideinschlüsse nach deren Bildung verändert haben. Die große Mehrheit jedoch hat gleichmäßige runde, rechteckige oder Negativkristall-Formen, so dass nachträgliche Umwandlungen ausgeschlossen werden können. Es kann daher angenommen werden, dass sich die Fluideinschlüsse aus einem unmischbaren Wasser-CO_2-Gemisch gebildet haben („heterogeneous trapping“). Diese Vermutung wird durch experimentelle Untersuchungen bestätigt. Im System NaCl-H_2O-CO_2 kommt es bei verschiedenen Druck- und Temperaturenbedingungen zu Fluidentmischung/-unmischbarkeit (z.B. Frantz et al., 1992; Sterner et al., 1984). Für Ivigtut werden Bildungsbedingungen von 400-450 °C und 1-1,5 kbar angenommen (Pauly & Bailey, 1999). Laut Duan et al. (1995) ist genau bei diesen Temperaturen das Unmischbarkeitsfeld minimal, was wiederum für die Entmischung des Ivigtut-Fluids spricht.

Aus mechanisch geöffneten Fluideinschlüssen wurde die Isotopensignatur von CO_2, H_2O und CH_4 bestimmt. Der $\delta^{13}C$-Wert von Einschluss-CO_2 liegt zwischen -4,1 und -9,3 ‰ PDB bei einem Mittelwert von ca. -5 ‰, was nach Taylor et al. (1967) typischen Mantelwerten entspricht. $\delta^{18}O_{CO2}$ schwankt zwischen 20,7 und 42,0 ‰ VSMOW und liegt weit außerhalb des für primäre Karbonatite typischen $\delta^{18}O$ (8-10 ‰ VSMOW; Taylor et al., 1967). Darüber hinaus weicht die Isotopie des Einschluss-CO_2 stark von jener von Calcit oder Lamprophyren aus der Gardar Provinz ab (Halama et al., 2005; Coulson et al., 2003), ist jedoch nahezu identisch mit der Isotopie von CO_2-Bläschen in MOR-Basalten (Pineau & Javoy, 1983).

Die isotopische Zusammensetzung des Einschluss-Wassers (δD -107 bis -45 ‰; $\delta^{18}O$ -21,7 bis -1,5 ‰ VSMOW) folgt dem Verlauf der heutigen meteorischen Wasserlinie und überlappt stark mit der Isotopie von Wasser aus Fluideinschlüssen in Mineralen der Motzfeldt Intrusion (Schönenberger & Markl, in Vorbereitung) und salinaren Lösungen vom Kanadischen Schild (Frape & Fritz, 1982; Frape et al., 1984; Bottomley et al., 1994). Somit kann angenommen werden, dass das Einschluss-Wasser meteorischen Ursprung hat. Der angereicherte $\delta^{18}O$-Wert von CO_2 (20-42 ‰ VSMOW) lässt sich durch Isotopenaustausch mit Sauerstoff von Einschluss-Wasser erklären. Die Fraktionierung für Sauerstoff zwischen H_2O und CO_2 bei Raumtemperatur beträgt laut Richet et al. (1977) 41-44 ‰, was genau dem Differenzbetrag von $\delta^{18}O_{CO2}$ und $\delta^{18}O_{H2O}$ dieser Studie entspricht. Von den geringen Mengen an Einschluss-Methan konnte lediglich die Isotopie des Kohlenstoffs ermittelt werden, dessen $\delta^{13}C$-Wert zwischen -40,8 und -28,0 ‰ PDB liegt. Nach Ohmoto & Goldhaber (1997) liegen die Gleichgewichtstemperaturen des gemessenen $\delta^{13}C_{CO2}$ und $\delta^{13}C_{CH4}$ ungefähr zwischen 175

und 320 °C. Das Auftreten geringer Mengen von Methan in Ivigtut kann auf Respeziation eines ursprünglichen CO_2-H_2O-Fluids zurückgeführt werden (Konnerup-Madsen et al., 1985). Ryabchikov & Kogarko (2006) zeigten, dass sich bei Sauerstoff-Fugazitäten um den QFM-Puffer in einem C-H-O Gasgemisch unterhalb 400 °C beträchtliche Mengen an Methan bilden können. Dieses Szenario wird daher auch für Ivigtut angenommen.

Mittels Ionenchromatographie (Crush Leach) wurde der genaue Fluidchemismus der Einschlüsse bestimmt. Aufgrund des hohen Gehalts an gelöster Ionen kann das Fluid als „Brine“ bezeichnet werden. Da sich Chlor und Brom (+ Iod) in Lösungen weitgehend konservativ verhalten, können diese als „Tracer“ für die Fluidherkunft verwendet werden (Bottomley et al., 1994; 2005). Das Cl/Br-Verhältnis liegt zwischen 53 und 110 mit einem Durchschnittswert von 84 und ist somit viel geringer als jenes von heutigem Meerwasser (288; Stober & Bucher, 1999; Millero, 2004). Nicht nur isotopengeochemisch, sondern auch mit Hilfe des Cl/Br-Verhältnisses lässt sich also ein mariner Ursprung des Einschluss-Wassers ausschließen. Allgemein scheinen die geringen Cl/Br-Werte typisch für Fluideinschlüsse in Gardar-Gesteinen zu sein: So beträgt das Verhältnis in Einschlüssen von Ilímaussaq 101-132 (Graser et al., in review) und in Fluideinschlüssen von Motzfeldt ca. 100 (Schönenberger & Markl, in Vorbereitung).

Die Crush Leach Analysen bestätigen mikrothermometrische Untersuchungen, dass in den Fluideinschlüssen Na^+ und Cl^- dominieren. Allerdings sind auch beträchtliche Mengen an K^+, Li^+ und F^- gelöst. Mit Hilfe der Li/Cl- und Li/Br-Verhältnisse lässt sich der Ursprung der Salinität näher beleuchten. Nach Bottomley et al. (1999) sind die beiden Verhältnisse stark von Mineral und Gesteinstyp abhängig, zeigen jedoch eine gute Korrelation, wenn Cl und Br marinen Ursprungs sind. Die Li/Cl- und Li/Br-Werte der analysierten Fluideinschlüsse weichen jedoch stark von den normalen marinen Verhältnissen ab. Auch das Fehlen mariner chemischer Sedimente in der Nähe um Ivigtut belegt die nicht-marine Herkunft der gelösten Stoffe. Analog zu Stober und Buchers (1999) Laugungsexperimenten an Schwarzwald-Gesteinen kann der Fluidchemismus in den Einschlüssen von Ivigtut auf intensive Wasser-Gesteins-Wechselwirkungen mit dem Ivigtut-Granit zurückgeführt werden, was auch die starke, metasomatische Alteration des Granits widerspiegelt. Der Na-Reichtum des Fluids scheint jedoch eine Folge der normalen Verteilung von Na und K während der Kristallisation zu sein. Orville (1963) diskutierte Fraktionierungsprozesse zwischen zwei Feldspäten und einer koexistierenden Fluidphase. Mit abnehmenden Temperaturen wird das Fluid stetig Na-reicher, während Feldspat bevorzugt K einbaut. Dies zeigt sich nicht nur in den spät-

magmatischen, Na-reichen Mineralparagenesen Ivigtuts, sondern auch in der Albitisierung des Ivigtut Granits selbst (Goodenough et al., 2000; Pauly & Bailey, 1999).

(Phasen)Petrographische Beziehungen des Ivigtut Granits (Goodenough et al., 2000) lassen auf einen Bildungsdruck von 1-1,5 kbar für die Lagerstätte, aber auch für die Fluideinschlüsse selbst schließen. Aus mikrothermometrischen Daten wurden nach Bakker (2003) Isochoren für primäre CO_2- und primäre CO_2-H_2O-Einschlüsse berechnet, die für einen Druck von 1-1,5 kbar je nach Einschlusstyp Entstehungstemperaturen zwischen 100 und 400 °C anzeigen.

Um die intensiven Parameter während der Kryolith-Lagerstättenbildung zu quantifizieren, wurden thermodynamische Modellierungen für die Stabilität möglicher Ivigtut-Paragenesen mit Hilfe der Programme TWQ (Berman et al., 1988) und Unitherm (Johnson et al., 1992) durchgeführt. Thermodynamische Daten für seltene Fluoride, wie z.B. Ralstonit [Al_2F_6*H_2O] oder Prosopit [$CaAl_2F_8$], wurden nach Van Hinsberg et al. (2005) und Mostafa et al. (1995) approximiert. Alle Mineralvergesellschaftungen sind für einen Druck von 1 kbar bei hohen Wasser- und Silika-Aktivitäten sowie Temperaturen von ≤ 450 °C stabil, was auch Fluideinschluss-Untersuchungen belegen. Diese Ergebnisse stimmen ebenso mit neuesten Phasenmodellierungen für F-reiche Systeme von Dolejš & Baker (2007 a,b) überein.

Die Entstehungstemperaturen der Lagerstätte von 400-450 °C legen einen spät-magmatisch – hydrothermalen Ursprung nahe. Allerdings kann aufgrund des extrem hohen F-Gehalts im Falle Ivigtuts nicht von klassisch hydrothermalen Bildungsbedingungen gesprochen werden. Denn gerade Alkali-reiche, silikatische Schmelzen mit einem hohen Gehalt an Volatilen (H, F, Cl oder B) können bis zu niedrigen Temperaturen bestehen und mit einem hydrothermalen Fluid über einen breiten p-T Bereich koexisiteren (Thomas et al., 2000; Veksler, 2004). Dolejš & Baker (2007 b) konnten experimentell nachweisen, dass in Anwesenheit von F die Granit-Kristallisation bei 1 kbar bis 540 °C gesenkt wird. Der hohe F-Gehalt führte vermutlich auch in Ivigtut dazu, dass die Schmelze immer noch um 450 °C existierte bzw. sich bei diesen Temperaturen vermutlich in ein überkritisches Fluid entwickelte.

Die vorliegenden Ergebnisse vervollständigen das Genesemodell von Pauly & Bailey (1999): F- und CO_2-reiche Fluide führten zur Auslaugung und Albitisierung des Ivigtut Granits. Gleichzeitig bildeten sie mit dem aus dem Zerfall von Feldspäten freigesetzten Na und Al eine Aluminofluorid-Schmelze, welche sich vermutlich zwischen 500-600 °C entmischte. Der massive Quarz-Körper im unteren Bereich der Lagerstätte bildete sich aus

dem silikatreichen Schmelzanteil. Die Kryolith-Lagerstätte selbst ging aus der F- und volatil-reichen Schmelzfraktion hervor und bildete sich in Anwesenheit eines unmischbaren (NaCl-) H_2O-CO_2-Fluids meteorischen bzw. magmatischen Ursprungs. Der graduelle Übergang von einer volatil-reichen Schmelzen zu einer Lösung fand dabei vermutlich zwischen 400 und 450°C statt.

Kapitel 3 – Seltene Erden in Gardar-Fluoriden

Der außerordentlich hohe F-Gehalt innerhalb der Gardar Provinz spiegelt sich im Vorkommen verschiedenster Fluoride wider: So treten beispielsweise primär magmatische Fluorite in der Motzfeldt Intrusion auf, während magmatischer Villiaumit in Ilímaussaq vertreten ist. In Ivigtut hingegen entstand die weltweit einzigartige Kryolith-Lagerstätte, in der auch zahlreiche seltene Fluoride, wie z.B. Kryolithionit [$Na_3Li_3Al_2F_{12}$], Ralstonit oder Prosopit, vorkommen. Um den Spurenelementeinbau in Minerale sowie die Entstehung und Entwicklung F-reicher Schmelzen und Fluide besser zu verstehen, wurden Spurenelemente – insbesondere die Seltenen Erd-Elemente und Yttrium (SEE) – in Fluoriden, Calcit und Siderit untersucht. Dabei wurden Minerale verschiedener Generationen aus den drei Intrusivkomplexen Motzfeldt, Ilímaussaq und Ivigtut analysiert, um Unterschiede bzw. einen möglichen systematischen SEE-Einbau herauszuarbeiten.

Die Geologie Ivigtuts wurde bereits ausführlich in der Geologischen Übersicht erläutert, so dass an dieser Stelle nur kurz auf Motzfeldt und Ilímaussaq eingegangen wird. Die Motzfeldt Intrusion kann nach Emeleus & Harry (1970) und Jones (1980, 1984) in sechs verschiedene Intrusivphasen (SM1-6) eingeteilt werden. Dabei treten in SM1 bis SM5 (per)alkaline, miaskitische Gesteine auf, während lediglich SM6 agpaitischer Zusammensetzung ist, was das Auftreten von Eudialyt belegt (Jones, 1980; 1984; Sørensen, 1997). In SM1 und SM6 tritt Fluorit als primär-magmatische Phase auf, wohingegen er in SM1, SM4 und SM5 spät- bis postmagmatische Adern bildet, die z.T. mit Calcit und Feldspat assoziiert sind. Die Ilímaussaq Intrusion ist die Typlokalität agpaitischer Gesteine und entstand im Zuge vier verschiedener Magmenschübe. Neben dem miaskitischen Augit-Syenit und Alkali-Granit machen die agpaitischen Nephelin-Syenite den Hauptteil der Intrusion aus. Diese bildeten Dach- (Naujaite) und Bodenkumulate (Kakortokite) sowie einen „Sandwich"-Horizont (Lujavrite; Sørensen et al., 2006). Villiaumit und Fluorit sind primär-magmatische

Phasen, während letzterer auch in Pegmatiten und als hydrothermales Alterationsprodukt auftritt.

Verschiedene Fluoride sowie Calcit wurden lichtmikroskopisch, mit Kathodolumineszenz (KL) und LA ICP-MS untersucht und sind zur besseren Übersicht in Tabelle 1 dargestellt:

Tab. 1: Übersicht über die analysierten Proben. LSEE, MSEE und HSEE beziehen sich auf die Anreicherung an leichten, mittleren bzw. schweren (heavy) Seltenen Erden (mit Y).

Intrusion	Einheit	Mineral	Charakteristika	Proben
Ilímaussaq	Naujait	Fluorit (primär)	LSEE angereichert	Ilm133, Ilm225, Ilm259, Ilm260
	Kakortokit	Fluorit	LSEE angereichert	XL30
	Naujait	Fluorit	geringe SEE Konzentration	Ilm77, Ilm99, Ilm325
	Naujait	Villiaumit	SEE unter Nachweisgrenze	
Motzfeldt	SM1	Fluorit (primär)	LSEE angereichert	JS193, JS195, JS197
	SM1	Fluorit	unterschiedlich LSEE angereichert	JS2, JS4, JS6, JS10, JS16
	SM1	Fluorit	geringe SEE Konzentration	JS9, JS10
	SM4	Fluorit	MSEE angereichert	JS34,JS 38, JS67, JS86, JS90, JS91, JS152, JS168, JS225, JS226
	SM4	Calcit	flach bis MSEE angereichert	JS67, JS152, JS226
	SM5	Fluorit	LSEE angereichert, Anomalien schwach ausgeprägt	JS109, JS110, JS175, JS183
	SM6	Fluorit (primär)	LSEE angereichert	JS88, JS122
Ivigtut		Siderit	HSEE angereichert	IV-CPH, IV1475, IV-Sid
		Kryolithionit	flaches SEE Muster, geringe Konzentration	IV30
		Kryolith	flaches SEE Muster, geringe Konzentration	IV20, IV30, IV33, IV35, IV-K1, IV-K4
		Fluorit	geringe SEE Konzentration	IV31-Fl, IV32-Fl
		Fluorit	leicht HSEE angereichert	IV80-Fl, IV79a-Fl, IV1479-Fl, IV33-Fl
		Fluorit	flaches SEE Muster	IV30-Fl, IV20-Fl

Im Gegensatz zu Motzfeldt und Ilímaussaq zeigen fast alle Fluorit-Proben aus Ivigtut deutliche Zonierungen (hell-dunkel) im KL-Bild, wobei die helleren Bereiche stets stärker an SEE angereichert sind als die dunklen. Dem über Chondrit normierten (McDonough & Sun, 1995) SEE-Muster wurde nach Bau & Dulski (1995) Yttrium zwischen Dy und Ho eingefügt, da es sich aufgrund seines dreiwertigen Oxidationzustands und nahezu identischen Radius den SEE sehr ähnlich verhält. Alle Proben sind durch eine deutlich negative Eu-Anomalie gekennzeichnet. Fluorite aus Motzfeldt und Ilímaussaq weisen stets eine positive Y-Anomalie auf, während die SEE Muster der Minerale aus Ivigtut durch eine negative Y-Anomalie charakterisiert sind. Negative Ce-Anomalien treten vereinzelt in Fluoriten von Motzfeldt und selten in jenen von Ilímaussaq auf. Die SEE Muster der Fluorite spiegeln meist den generellen

Trend der Gesamtgesteinsanalysen der jeweiligen Intrusionen wider und sind oft ähnlich stark an SEE angereichert (Jones, 1980; Jones & Larsen, 1985; Bradshaw, 1988; Goodenough et al., 2000; Bailey et al., 2001).

Die SEE-Muster der analysierten Fluoride variieren nicht nur zwischen den drei Intrusivkomplexen, sondern zeigen auch innerhalb einer Intrusion systematische Veränderungen. Generell weisen Fluoride aus denselben Einheiten bzw. aus den gleichen Entwicklungsstadien (d.h. primär, sekundär) ähnliche Charaktersitika auf und können zusammengefasst werden (Tab. 1). Zahlreiche unterschiedliche Prozesse und Mechanismen steuern dabei den systematischen Einbau der SEE bzw. deren Muster und werden im Folgenden näher erläutert.

a) Kristallographische Systematik

In Fluorit wird Ca durch die SEE ersetzt, wobei verschiedene Substitutionsmöglichkeiten denkbar sind: 1 SEE^{3+} + 1 Na^{+} ↔ 2 Ca^{2+} oder 3 Ca^{2+} ↔ 2 SEE^{3+} + □ (Leerstelle). In Kryolith [Na_3AlF_6] oder Kryolithionit [$Na_3Li_3Al_2F_{12}$] wird Na durch die SEE ersetzt, wobei die Ladungsdifferenz vermutlich mit Hilfe von Al ausgeglichen wird. Dies könnte auch erklären, warum Villiaumit [NaF] weniger SEE einbaut als Kryolith, da aufgrund seiner Zusammensetzung eine Ladungsbilanz schwerer zu erzielen ist (Na^{+} vs. Al^{3+}).

b) Einfluss der Quelle

Bereits Fleischer & Altschuler (1969) fanden heraus, dass nicht nur kristallographische Faktoren, sondern auch die „geologische Umgebung“, d.h. die Zusammensetzung der Gesteine/Quelle, die Verteilung der SEE beeinflusst. So sind in silika-reichen Magmatiten wie Graniten oder Pegmatiten HSEE angereichert, während silika-arme, alkaline bis mafische Gesteine eher LSEE-dominiert sind. Diese Systematik zeigt sich auch in den untersuchten Fluoriden: In den alkalinen Nephelin-Syeniten Motzfeldts und Ilímaussaqs sind die frühen Fluorite an LSEE angereichert, während die Fluoride in der pegmatitisch-granitischen Ivigtut Intrusion eher an HSEE angereichert sind. Darüberhinaus bestimmt die Menge an Spurenelementen in der Quelle deren Verfügbarkeit für den späteren Einbau in Minerale (z.B. Sallet et al., 2005). Sowohl die primär-magmatischen Fluorite, die Gesamtgesteinsdaten von Motzfeldt und Ilímaussaq als auch die SEE Muster der primitivsten Gardar-Ganggesteine zeigen alle eine Anreicherung an LSEE (Goodenough et al., 2002; Halama et al., 2007; Köhler et al., in Vorbereitung; s. Kapitel 1). Somit kann davon ausgegangen werden, dass bereits die Magmenquelle bzw. der Mantel unter Gardar reich an LSEE gewesen sein muss und diese metasomatische Anreicherung im Zuge von Subduktionsprozessen geschah (Goodenough et al., 2002; Upton & Emeleus, 1987).

c) Anomalien

Alle untersuchten Fluoride sind durch eine deutlich negative Eu-Anomalie charakterisiert, die auf frühe Plagioklas-Fraktionierung zurückgeführt werden kann. Dies wird durch das Auftreten großer Anorthosit-Körper unterhalb der Gardar Provinz (z.B. Halama et al., 2005), sowie durch die Feldspat-reichen Gesteine verschiedener Intrusionen gestützt.

Die negative Y-Anomlie in Ivigtut und die positive in Motzfeldt und Ilímaussaq könnte auf Unterschiede in der Quelle zurückzuführen sein. Dies belegen auch RFA-Gesamtgesteinsanalysen von Ganggesteinen in Gardar (Köhler et al., in Vorbereitung): Ganggesteine in der Gegend von Ilímaussaq und Motzfeldt haben bei gleichem Fraktionierungsgrad (Mg-Zahl) insgesamt höhere Y-Gehalte als jene in der Region um Ivigtut. Auf die Rolle des Y wird später noch näher eingegangen.

Die negative Ce-Anomalie in Fluoriten von Motzfeldt und Ilímaussaq könnte auf ein oxidierteres Bildungsmilieu oder einen sich ändernen pH-Wert (Bau & Möller, 1992; Hollings & Wyman, 2005) hindeuten. Oxidiertere Bedingungen während des späten Kristallisationsstadiums sind beispielsweise für Ilímaussaq sehr gut bekannt, wo Hämatit und Ägirin mit Fluorit koexistieren (Marks et al., 2003). Dieselben Beobachtungen treffen auch auf Motzfeldt zu, wo große Bereiche von SM1 stark alteriert sind und ebenfalls Hämatit mit sekundärem Fluorit auftritt.

d) Fraktionierung während der Kristallisation

Obwohl sich die SEE aufgrund ihres dreiwertigen Oxidationszustandes und ähnlichen Ionenradius nahezu gleich verhalten, fraktionieren sie im Laufe der Kristallisation. So erkannten Möller et al. (1976), dass LSEE bevorzugt in frühe Kristallisate eingebaut werden, während die MSEE eher im hydrothermalen Hauptstadium und die HSEE vorwiegend in späten Mineralpräzipitaten angereichert sind (Kempe et al., 1999; Wagner & Erzinger, 2001; Trinkler et al., 2005). Diese systematische Änderung des SEE-Einbaus kann deutlich in den Fluoriten von Motzfeldt und Ilímaussaq nachvollzogen werden: Primär-magmatische Fluorite zeigen eine starke Anreicherung an LSEE, wohingegen Fluorite aus Adern hydrothermaler Herkunft eher flachere Muster zeigen bzw. verstärkt MSEE einbauen. Sehr späte Fluorite, die beispielsweise nur eine dünne Kruste bilden oder Alterationsprodukte sind, weisen eine (leichte) Anreicherung an HSEE auf.

Eine weitere Möglichkeit, die Entstehungsbedingungen von Fluorit mit Hilfe der SEE abzuschätzen, bietet das Tb/Ca – Tb/La-Diagramm (Möller et al., 1976; Gagnon et al., 2003). Dabei repräsentiert das Tb/Ca-Verhältnis das chemische Milieu, während Tb/La den Grad der Fraktionierung darstellt. Die Grenzen der drei Entstehungsbereiche „pegmatitisch,

hydrothermal, sedimentär“ sind dabei als graduell anzusehen und dienen eher zur qualitativen/groben Abschätzung der Bildungstemperatur (Gagnon et al., 2003). Primäre Fluorite von Motzfeldt (SM1 und SM6) und Ilímaussaq fallen in das pegmatitische Feld, während die meisten sekundären Fluorite hydrothermaler Herkunft sind und nur krustige Fluorite aus z.T. stark alterierten Proben eine „sedimentäre“ Herkunft (d.h. niedrige Bildungstemperaturen) andeuten. Fluorit aus Ivigtut scheint überwiegend hydrothermal gebildet worden zu sein. Lediglich ein idiomorpher Fluorit, der laut Pauly & Bailey (1999) früh entstand, fällt in das pegmatitische Feld.

e) Entstehung von Zonierungen

Die alternierenden hell-dunkel Zonierungen im KL-Bild der Fluorite von Motzfeldt und Ivigtut entstanden vermutlich durch abrupte Änderungen der Fluidzusammensetzung. Beispielsweise zeigen Fluorite aus SM1 von Motzfeldt helle Bereiche im KL-Bild, die im Gegensatz zu den dunklen Stellen stark an SEE angereichert sind. Dabei können die Unterschiede im SEE-Gehalt innerhalb eines Korns mehr als zwei Größenordnungen betragen. Es wird angenommen, dass die komplexen Texturen und stark variablen SEE-Muster auf verschiedene Fluid-Generationen zurückzuführen sind und z.T. Fluid-Fluorit-Wechselwirkungn widerspiegeln.

f) Komplexierung und die Rolle von Y-Ho

Die Komplexierung der SEE mit F^-, CO_3^{2-}, Cl^- sowie anderer Liganden ist ein kritischer Prozess, der die Verteilung der SEE stark kontrolliert (Möller et al., 1976; Bau, 1991; Bau & Möller, 1992). Die Komplexbildung führt dazu, dass sich die SEE „non-CHARAC“ verhalten, d.h. weder gemäß ihrer Ladung (*CHA*rge) noch gemäß ihres *RA*dius, sondern dass sie zusätzlich durch ihre Elektronenkonfiguration beeinflusst werden (Bau, 1996; Irber, 1999). Im Allgemeinen nimmt die Komplexstabilität der SEE von La bis Lu (z.B. Möller et al., 1976; Ekambaran et al., 1986) und mit steigender Temperatur zu (z.B. Wood, 1990 a,b; Haas et al., 1995). Aus phasenpetrologischen Beziehungen und Untersuchungen von Fluideinschlüssen (Schönenberger & Markl, in Vorbereitung; Köhler et al., in press; Graser et al., in review; Pauly & Bailey, 1999) wird angenommen, dass in Motzfeldt und Ivigtut in der Fluidphase F^-, CO_3^{2-}, OH^--Komplexe den größten Einfluss auf die Verteilung der SEE ausübten. Dies gilt auch für Ilímaussaq, obwohl (Bi)Karbonatkomplexe wohl eher unbedeutend waren. Denn im Gegensatz zu Fluideinschlüssen aus Motzfeldt und Ivigtut treten in Ilímaussaq weder Calcit-Tochterminerale noch CO_2 auf (Köhler et al., in press; Schönenberger & Markl., in Vorbereitung; Graser et al., in review). Aufgrund des hohen F-Gehalts v.a. in Ivigtut scheint gerade die Komplexierung mit F^- ein wichtige Rolle gespielt zu haben, was anhand des Y/Ho-

Verhältnisses nachvollzogen werden kann. Y und Ho verhalten sich in magmatischen Prozessen kohärent und werden im Laufe der Kristallisation eigentlich nicht fraktioniert (Bau & Dulski, 1995). Während der Wechselwirkung mit einem F-reichen Fluid jedoch werden Y und Ho entkoppelt. Dabei sind Y-F Komplexe stabiler als jene mit Ho-F (Bau, 1996). Gleichzeitig steigt das Y/Ho-Verhältnis während der Infiltration F-reicher, hydrothermaler Fluide an (Bau & Dulski, 1995). Dies stimmt mit den hohen Y/Ho Verhältnissen bis 1375 in Fluoriten von Motzfeldt und Ilímaussaq überein. Die Fluoride Ivigtuts hingegen haben niedrigere Y/Ho-Verhältnisse, die mit einem Durchschnitt von 8-9 deutlich unter dem chondritischen Wert von 28 (McDonough & Sun, 1995; Irber, 1999) liegen. Die Experimente von Veksler et al. (2005) zeigten, dass der Verteilungskoeffizient zwischen einer Fluorid- oder Silikatschmelze und Kryolith für Ho doppelt so hoch ist wie der für Y. Dies kann die geringen Y/Ho-Verhältnisse in Kryolith erklären, jedoch nicht in Fluorit. Eine mögliche Erklärung wäre, dass die allgemein geringen Y/Ho-Verhältnisse in Fluoriden Ivigtuts bereits auf frühere Entkopplungsprozesse zurückzuführen sind. So wurde vermutlich im Zuge der Vergreisung des Granits und der eigentlichen Lagerstättenbildung Y im Granit zurückgehalten, während Ho mobilisiert und abgeführt wurde.

g) Tetrad Effekt

Gardar Gesamtgesteinsanalysen weisen keinen Tetrad-Effekt auf, so dass dieser vermutlich nicht auf Mineralfraktionierung zurückzuführen ist. Der Tetrad-Effekt ist vielmehr typisch für hoch fraktionierte, silikatische Magmen, die im Übergangsbereich Schmelze-Fluid entstanden bzw. starker Fluidwechselwirkung unterlagen (Bau, 1996). Er wird in Chondrit-normierten SEE-Mustern deutlich, die man nach Masuda et al. (1987) in vier Segmente, sog. Tetrade, unterteilen kann: T1 = La-Nd, T2 = (Pm)Sm-Gd, T3 = Gd-Ho und T4 = Er-Lu. Monecke et al. (2002) schlugen eine Methode zur Quantifizierung des Effekts vor. Während in den Fluoriten von Motzfeldt und Ilímaussaq der Tetrad-Effekt keine Rolle spielt, ist er in Fluorit und Kryolith von Ivigtut stark ausgeprägt. Dies impliziert, dass die Kryolith-Lagerstätte aus einer hochfraktionierten Schmelze hervorgegangen sein muss, die reich an F, CO_2, Li, B, Cl und H_2O war, starken Fluid-Gesteins-Wechselwirkungen unterlag und vermutlich graduell in ein überkritisches Fluid übergegangen ist (vgl. Pauly & Bailey, 1999; Köhler et al., in press).

Zusammenfassend kann gesagt werden, dass die unterschiedlichen SEE-Muster von Fluoriden aus drei verschiedenen Intrusionen unterschiedliche Entstehungsbedingungen reflektieren. Die Fluorite von Motzfeldt und Ilímaussaq scheinen aus derselben Quelle zu

stammen und unter ähnlichen Bedingungen gebildet worden zu sein. Primär-magmatische Fluorite weisen identische Charakteristika auf in Hinblick auf deren Y/Ho-Verhältnis, SEE-Gehalt und deren Anreicherung an LSEE. KL-Bilder und SEE-Verteilungsmuster der sekundären Fluorite spiegeln multiple Generationen innerhalb einer Einheit (SM1) wider. Sich verändernde, physiko-chemische Entstehungsbedingungen und ein oxidierteres Milieu zeichnen sich aufgrund der geringeren SEE-Gehalte bzw. durch die negative Ce-Anomalie ab. Die fast durchweg an HSEE angereicherten Muster der Fluoride aus Ivigtut unterscheiden sich stark von Motzfeldt und Ilímaussaq und reflektieren hydrothermale Bildungsbedingungen. Der Einbau der SEE scheint größtenteils von F-Komplexen gesteuert zu werden, und die starke Fluidwechselwirkung mit granitischem Nebengestein führte zur Ausbildung eines ausgeprägten Tetrad Effekts in den Fluoriden Ivigtuts. Diese Beobachtungen zeigen, dass die Verteilung der SEE einerseits stark von der Magmenquelle selbst, andererseits von Fraktionierungsprozessen im Zuge der Kristallisation sowie von der Zusammensetzung des Fluids bzw. dessen möglichen Komplexbildnern abhängt.

Literaturverzeichnis

ANDERSEN, T., 1997. Age and petrogenesis of the Qassiarsuk carbonatite-alkaline silicate volcanic complex in the Gardar rift, South Greenland. Mineralogical Magazine 61, 499-514.

ARCULUS, R.J., 1994. Aspects of magma genesis in arcs. Lithos 33, 189-208.

BAILEY, J.C., GWOZDZ, R., ROSE-HANSEN, J. & SØRENSEN, H., 2001: Geochemical overview of the Ilímaussaq alkaline complex, South Greenland. In: Sørensen, H. (Ed.), The Ilímaussaq complex, South Greenland: status of mineralogical research with new results. Geology of Greenland Survey Bulletin 190, 35-53.

BAKKER, R.J., 2003. Package FLUIDS 1. Computer programs for analysis of fluid inclusion data and for modelling bulk fluid properties. Chemical Geology 194, 3-23.

BAU, M., 1991. Rare earth element mobility during hydrothermal and metamorphic fluid-rock interaction and the significance of the oxidation state of europium. Chemical Geology 93, 219-230.

BAU, M., 1996. Controls on the fractionation of isovalent trace elements in magmatic and aqueous systems: evidence from Y/Ho, Zr/Hf, and the lanthanide tetrad effect. Contributions to Mineralogy and Petrology 123, 323-333.

BAU, M., DULSKI, P., 1995. Comparative study of yttrium and rare-earth element behaviours in fluorine-rich hydrothermal fluids. Contributions to Mineralogy and Petrology 119, 213-223.

BAU, M., MÖLLER, P., 1992. Rare Earth Element Fractionation in Metamorphogenic Hydrothermal Calcite, Magnesite and Siderite. Mineralogy and Petrology 45, 231-246.

BERMAN, R.G., BROWN, T.H., PERKINS, E.H., 1988. GEO-CALC update; software for calculation of pressure-temperature-XCO2 activity phase diagrams. In: Geological Association of Canada, Mineralogical Association of Canada, Canadian Society of Petroleum Geologists, 1988 joint annual meeting. Program with Abstracts – Geological Association of Canada; Mineralogical Association of Canada; Canadian Geophysical Union, Joint Annual Meeting. 13, p. A9.

BOROVIKOV, A.A., GUSHCHINA, L.N., BORISEKNO, A.S., 2001. Specific features of $FeCl_2$ and $FeCl_3$ solution behaviour at low temperatures (cryometry of fluid incluions). XVI ECROFI European Current Research On Fluid Incluions, Faculdade de Ciências do Porto, Departamento de Geologia, Memória 7, 61-63.

BRADSHAW, C., 1988. A Petrographic, Structural and Geochemical study of the Alkaline Igneous rocks of the Motzfeldt centre, South Greenland. PhD thesis, Univ. of Durham, UK.

BOTTOMLEY, D.J., GREGOIRE, D.C., RAVEN, K.G., 1994. Saline groundwaters and brines in the Canadian Shield: Geochemical and isotopic evidence for a residual evaporite brine component. Geochimica et Cosmochimica Acta 58, 1483-1498.

BOTTOMLEY, D.J., KATZ, A., CHAN, L.H., STARINSKY, A., DOUGLAS, M., CLARK, I.D., RAVEN, K.G., 1999. The origin and evolution of Canadian Shield brines: evaporation of freezing of seawater? New lithium isotope and geochemical evidence from the Slave craton. Chemical Geology 155, 295-320.

BOUDREAU, A.E., LOVE, C., HOATSON, D.M., 1993. Variation in the composition of apatite in the Munni Munni Complex and associated intrusions of the Wet Pilbara Block, Western Australia. Geochimica et Cosmochimica Acta 57, 4467-4477.

BROMILEY, D.V., KOHN, S.C., 2007. Comparisons between fluoride and hydroxide incorporation in nominally anhydrous and fluorine-free mantle minerals. Geochimica et Cosmochimica Acta 71, Goldschmidt Conference Abstracts, A124.

BÜHN, B., WALL, F., LE BAS M.J., 2001. Rare-earth element systematics of carbonatitic fluorapatites, and their significance for carbonatite magma evolution. Contributions to Mineralogy and Petrology 141, 572-591.

CAMPBELL, L.S., HENDERSON, P., 1997. Apatite paragenesis in the Bayan Obo REE-Nb-Fe ore deposit, Inner Mongolia, China. Lithos 42, 89-103.

CHAKHMOURADIAN, A.R., REGUIR, EKATARINA, MITCHELL, R.H., 2002. Strontium-apatite: new occurrences, and the extent of Sr-FOR-Ca Substitution in apatite-group minerals. The Canadian Mineralogist 40, 121-136.

CHADWICK, B., GARDE, A.A., 1996. Palaeoproterozoic oblique plate convergence in South Greenland: a re-appraisal of the Ketilidian orogen. From: Brewer, T.S., Atkin, B.P. (Eds.), Precambrian crustal evolution in the North Atlantic Region. Geological Society of London, Special Publication 112, 179-196.

COULSON, I.M., GOODENOUGH, K.M., PEARCE, N.J.G., LENG, M.J., 2003. Carbonatites and lamprophyres of the Gardar Province – a "window" to the sub-Gardar mantle? Mineralogical Maganzine 67, 855-872.

DAVIS, W.D., LOWENSTEIN, T.K., SPENCER, R.J., 1989. Melting behaviour of fluid inclusions in laboratory-grown halite crystals in the systems NaCl-H_2O, NaCl-KCl-H_2O, NaCl-$MgCl_2$-H_2O and NaCl-$CaCl_2$-H_2O. Geochimica et Cosmochimica Acta 54, 591-601.

DEER, W.A., HOWIE, R.A., ZUSSMAN, J., 1997. Rock-forming minerals. Volume 2B: Double-chain silicates. The Geological Society, London, 616-634.

DOLEJS, D., BAKER, R., 2007 a. Liquidus Equilibria in the System K_2O-Na_2O-Al_2O_3-SiO_2-F_2O_{-1}-H_2O to 100 Mpa: I. Silicate-Fluoride Liquid Immiscibility in Anhydrous Systems. Journal of Petrology 48, 785-806.

DOLEJS, D., BAKER, R., 2007 b. Liquidus Equilibria in the System K_2O-Na_2O-Al_2O_3-SiO_2-F_2O_{-1}-H_2O to 100 Mpa: II. Differentiation Paths of Fluorosilicic Magmas in Hydrous Systems. Journal of Petrology 48, 807-828.

DRUMMOND, M.S., DEFANT, M.J., KEPEZHINSKAS, P.K., 1996. Petrogenesis of slab-derived trondhjemite-tonalite-dacite/adakite magmas. Transactions of the Royal Society of Edinburgh: Earth Sciences 87, 205-215.

DUAN, Z., MØLLER, N., WEARE, J.H., 1995. Equation of state for the NaCl-H_2O-CO_2 system: Prediction of phase equilibria and volumetric properties. Geochimica et Cosmochimica Acta 59, 2869-2882.

DUBOIS, M., WEISBROD, A., SHTUKA, A., 1994. Experimental determination of the the two-phase (liquid and vapor) region in water-alkali chloride binary systems at 500 ° and 600 °C using synthetic fluid inclusions. Chemical Geology 115, 227-238.

EDGAR, A.D., PIZZOLATO, L.A., SHEEN, J., 1996. Fluorine in igneous rocks and minerals with emphasis on ultrapotassic mafic and ultramafic magmas and their mantle source regions. Mineralogical Magazine 60, 243-257.

EKAMBARAM, V., BROOKINS, D.G., ROSENBERG, P.E., EMANUEL, K.M., 1986. Rare-Earth Element Geochemistry of fluorite-carbonate deposits in western Montana, USA. Chemical Geology 54, 319-331.

EMELEUS, C.H., HARRY, W.T., 1970. The Igaliko nepheline syenite complex; general description. Meddelelser om Grønland, 186, 115.

EMELEUS, C.H., UPTON, B.G.J., 1976. The Gardar period in southern Greenland. In: Escher, A. & Watt, W.S. (Eds.), Geology of Greenland. Geological Survey of Greenland, Copenhagen, pp. 152-181.

ERLANK, A.J., WATERS, F.G., HAWKESWORTH, S.E., HAGGERTY, H.L., ALLSOPP, R.S., RICKARD, R.S., MENZIES, M., 1987. Evidence for mantle metasomatism in peridotite nodules from the Kimberley pipes, South Africa. In: Menzies, M.A., Hawkesworth, M.C. (Eds.), Mantle Metasomatism. London: Academic Press, 221-311.

ESCHER, A., WATT, W.S., 1976. Geology of Greenland. Geological Survey of Greenland, Copenhagen, 603 p.

FLEET, M.E., 2003. MICAS. In: Deer, W.A., Howie, R.A., Zussman, J. (Eds.), Rock-forming minerals, Volume 2B. The Geological Society, London, 354-369.

FLEISCHER, M., ALTSCHULER, Z.S., 1969. The relationship of the rare-earth composition of minerals to geological environment. Geochimica et Cosmochimia Acta 33, 725-732.

FRANTZ, J.D., POPP, R.K., HOERING, T.C., 1992. The compositional imits of fluid immiscibility in the system H_2O-NaCl-CO_2 as determined wit the use of synthetic fluid inclusions in conjuction with mass spectrometry. Chemical Geology 98, 237-255.

FRAPE, S.K., FRITZ, P., 1982. The chemistry and isotopic composition of saline groundwaters from the Sudbury Basin, Ontario. Canadian Journal of Earth Sciences 19, 645-661.

FRAPE, S.K., FRITZ, P., MCNUTT, R.H., 1984. Water-rock interaction and chemistry of groundwaters from the Canadian Shield. Geochimica et Cosmochimica Acta 48, 1617-1627.

GAGNON, J.E., SAMSON, I.M., FRYER, B.J., WILLIAMS-JONES, A.E., 2003. Compositional heterogeneity in fluorite and the genesis of fluorite deposits: insights from LA-ICP-MS analysis. Canadian Mineralogist 41, 365-382.

GARDE, A.A., HAMILTON, M.A., CHADWICK, B., GROCOTT, J., MCCAFFREY, K.J.W., 2002. The Ketilidian orogen of South Greenland: geochronology, tectonics, magmatism, and fore-arc accretion during Palaeoproterozoic oblique convergence. Canadian Journal of Earth Sciences 39, 765-793.

GOODENOUGH, K.M., 1997. Geochemistry of Gardar Intrusions in the Ivigtut area, South Greenland. PhD thesis, Edinburgh.

GOODENOUGH, K.M., UPTON, B.G.J., ELLAM, R.M., 2000. Geochemical evolution of the Ivigtut granite, South Greenland: a fluorine-rich "A-type" intrusion. Lithos 51, 205-221.

GOODENOUGH, K.M., UPTON, B.G.J., ELLAM, R.M., 2002. Long-term memory of subduction processes in the lithospheric mantle: evidence from the geochemistry of basic dykes in the Gardar Province of South Greenland. Journal of the Geological Society, London 159, 705-714.

GRASER, G., POTTER, J., KOEHLER, J., MARKL, G., in review. Isotopic, major, minor and trace element geochemistry of late-stage fluids in the peralkaline Ilímaussq intrusion, South Greenland.

HAAS J.R., SHOCK E.L., SASSANI D.C., 1995. Rare earth elements in hydrothermal systems: estimates of standard partial molal thermodynamic properties of aqueous complexes of the rare earth elements at high pressures and temperatures. Geochim. Cosmochim. Acta 59, 4329–4350.

HALAMA, R., MARKS, M., BRÜGMANN, G., SIEBEL, W., WENZEL, T., MARKL, G., 2004. Crustal contamination of mafic magmas; evidence from a petrological and Sr-Nd-Os-O isotopic study of the Proterozoic Isortoq dike swarm, South Greenland. Lithos 74, 3-4, 199-232.

HALAMA, R., VENNEMANN, T., SIEBEL, W., MARKL, G., 2005. The Grønnedal-Ika Carbonatite-Syenite Complex, South Greenland: Carbonatite Formation by Liquid Immiscibility. Journal of Petrology 46, 191-217.

HALAMA, R., JORON, J.L., VILLEMANT, B., MARKL, G., TREUIL, M., 2007. Trace element constraints on mantle sources druing mid-Proterozoic magmatism: evidence for a link between the Gardar (South Greenland) and Abitibi (Canadian Shield) mafic rocks. Canadian Journal of Earth Sciences 44, 1-20.

HOGARTH, D.D., 1988. Chemical composition of fluorapatite and associated minerals from skarn near Gatineau, Quebec. Mineralogical Magazine 52, 347-358.

HOLLINGS, P., WYMAN, D., 2005. The geochemistry of trace elements in igneous systems: principles and examples from basaltic systems. In: Linnen, R.L., Samson, I.M. (Eds.), Rare-Element Geochemistry and Mineral Deposits: Geological Association of Canada, GAC Short Course Notes 17, 1-16.

IRBER, W., 1999. The lanthanide tetrad effect and its correlation with K/Rb, Eu/Eu*, Sr/Eu, Y/Ho, and Zr/Hf of evolving peraluminous granite suites. Geochimica et Cosmochimica Acta 63, 489-508.

JOHNSON, J.W., OELKERS, E.H., HELGESON, H.C., 1992. SUPCRT92: A software package for calculating the standard molal thermodynamic properties of minerals, gases, aqueous species, and reactions from 1 to 5000 bars and 0 to 1000 °C. Computing Geosciences 18, 899-947.

JONES, A.P., 1980. Petrology and structure of the Motzfeldt centre, Igaliko complex, South Greenland. PhD thesis, Univ. of Durham, UK.

JONES, A.P., 1984. Mafic silicates from the nepheline syenites of the Motzfeldt centre, south Greenland. Mineralogical Magazine, 48, 1-12.

JONES, A.P., LARSEN, L.M., 1985. Geochemistry and REE minerals of nepheline-syenite from the Motzfeldt Centre, South Greenland. American Mineralogist 70, 1087-1100.

KEMPE, U., MONECKE, T., OBERTHÜR, T., KREMENETSKY, A.A., 1999. Trace elements in scheelite and quartz from the Muruntau/Myutenbai gold deposit, Uzbekistan: constraints on the nature of ore-forming fluids. In: Stanley, C.J., et al. (Eds.), Mineral Deposits: Processes to Processing. Balkema, Rotterdam, The Netherlands, 373-376.

KELEMEN, P.B., 1995. Genesis of high Mg# andesites and the continental crust. Contributions to Mineralogy and Petrolog 120, 1-19.

KÖHLER, J., KONNERUP-MADSEN, J., MARKL, G., in press. Fluid geochemistry in the Ivigtut cryolite deposit, South Greenland. Lithos: doi: 10.1016/j.lithos.2007.10.005.

KONNERUP-MADSEN, J., DUBESSY, J., ROSE-HANSEN, J., 1985. Combined Raman microprobe spectrometry and microthermometry of fluid inclusions in minerals from igneous rocks of the Gardar province (south Greenland). Lithos 18, 271-280.

KONZETT, J., SWEENEY, R.J., THOMPSON, A.B., ULMER, P., 1997. Potassium Amphibole Stability in the Upper Mantle: an Experimental Study in a Peralkaline KNCMASH System to 8.5 GPa. Journal of Petrology 38, 537-568.

LE MAITRE, R.W., BATEMAN, P., DUDEK, A., KELLER, J., LAMEYRE LE BAS, M.J., SABINE, P.A., SCHMID, R., SØRENSEN, H., STRECKEISEN, A., WOOLLEY, A.R., ZANETTIN, B., 1989. A classification of igneous rocks and glossary of terms. Blackwell, Oxford. 193 p.

MACDONALD, R., UPTON, B.G.J., 1993. The Proterozoic Gardar rift zone, South Greenland; comparisons with the East African Rift system. Journal of the Geological Society, London 76, 427-442.

MARKL, G., MARKS, M., SCHWINN, G., SOMMER, H., 2001. Phase Equilibrium Constraints on Intensive Crystallization Parameters of the Ilímaussaq Complex, South Greenland. Journal of Petrology 42, 2231-2258.

MARKS, M., MARKL, G., 2001. Fractionation and Assimilation Processes in the Alkaline Augite Syenite Unit of the Ilímaussaq Intrusion, South Greenland, as Deduced from Phase Equilibria. Journal of Petrology 42, 1947-1969.

MARKS, M., VENNEMANN, T., SIEBEL, W., MARKL, G., 2003. Quantification of Magmatic and Hydrothermal Processes in a Peralkaline Syenite-Alkali Granite Complex Based on Textures, Phase Equilibria, and Stable and Radiogenic Isotopes. Journal of Petrology 44, 1247-1280.

MARKS, M., VENNEMANN, T., SIEBEL, W., MARKL, G., 2004. Nd-, O-, and H-isotopic evidence for complex, closed-system fluid evolution of the peralkaline Ilímaussaq Intrusion, South Greenland. Geochimica Cosmochimica Acta 68, 3379-3395.

MASUDA, A., KAWAKAMI, O., DOHMOTO, Y., TAKENAKA, T., 1987. Lanthanide tetrad effect in nature: two mutually opposite types, W and M. Geochemical Journal 21, 119-124.

MCDONOUGH, W.F.M., SUN, S.S., 1995. The composition of the Earth. Chemical Geology 120, 223-253.

MILLERO, F.J., 2004. Physicochemical Controls on Seawater. In: Elderfield, H., Holland, H.D., Turekian, K.K. (Eds.), Treatise on Geochemistry, Volume 6, The Oceans and Marine Geochemistry. Elsevier Pergamon, Amsterdam.

MÖLLER, P., PAREKH, P., SCHNEIDER, H.-J., 1976. The application of Tb/Ca-Tb/La abundance ratios to problems of fluorspar genesis. Mineralium Deposita 11, 111-116.

MONECKE, T., KEMPE, U., MONECKE, J., SALA, M., WOLF, D., 2002. Tetrad effect in rare earth element distribution patterns: A method of quantification with application to rock an mineral samples from granite-related rare metal deposits. Geochimica et Cosmochimica Acta 66, 1185-1196.

MOSTAFA, A.T.M., EAKMAN, J.M., YARBRO, S.L., 1995. Prediction of Standard Heat and Gibbs Free Energies of Formation of Solid Inorganic Salts from Group Contributions. Industrial & Engineering Chemistry Research 34, 4577-4582.

OHMOTO, H., GOLDHABER, M.B., 1997. Sulfur and carbon isotopes. In: Barnes, H.L. (Ed.), Geochemistry of hydrothermal ore deposits. 3rd ed., Wiley, New York, 517-611.

O'REILLY, S.Y., GRIFFIN, W.L., 2000. Apatite in the mantle: implications for metasomatic processes and high heat production in Phanerozoic mantle, Lithos 53, 217-232.

ORVILLE, P.M., 1963. Alkali ion exchange between vapor and feldspar phases. American Journal of Science 261, 201-237.

PAULY, H., BAILEY, J.C., 1999. Genesis and evolution of the Ivigtut cryolite deposit, SW Greenland. Meddelelser om Grønland, Geoscience 37, 60 p.

PEARCE, N.J.G., LENG, M.J., 1996. The origin of carbonatites and related rocks from the Igaliko Dyke Swarm, Gardar Province, South Greenland: field, geochemical and C-O-Sr-Nd isotope evidence. Lithos 39, 21-40.

PINEAU, F., JAVOY, M., 1983. Carbon isotopes and concentrations in mid-oceanic ridge basalts. Earth and Planetary Science Letters 62, 239-257.

PROKOF'EV, V.B., NAUMOV, V.B., IVANOVA, G.F., SAVEL'EVA, N.I., 1991. Fluid inclusion studies in cryolite and siderite of the Ivigtut deposit (Greenland). Neues Jahrbuch für Mineralogie, Monatshefte 1, 32-38.

RICHET, P., BOTTINGA, Y., JAVOY, A., 1977. A review of hydrogen, carbon, nitrogen, oxygen, sulphur and chlorine stable isotope fractionation among gaseous molecules. Annual Reviews Earth Planetary Science 5, 65-110.

ROLLINSON, H.R., TARNEY, J., 2005. Adakites – the key to understanding LILE depletion in granulites. Lithos 79, 61-81.

RYABCHIKOV, I.D., KOGARKO, L.N., 2006. Magnetite compositions and oxygen fugacities of the Khibina magmatic system. Lithos 91, 35-45.

SALLET, R., MORITZ, R., FONTIGNIE, D., 2005. The use of vein fluorite as probe for paleofluid REE and Sr–Nd isotope geochemistry: The Santa Catarina Fluorite District, Southern Brazil. Chemical Geology 223, 227-248.

SHEPHERD, T.J., RANKIN, A.H., ALDERTON, D.H.M., 1985. A practical guide to fluid inclusion studies. Glasgow, Blackie, 239 p.

SMITH, J.V., DELANEY, J.S., HERVIG, R.L., DAWSON, J.B., 1981. Storage of F and Cl in the upper mantle; geochemical implications. Lithos 2, 133-147.

SIGVALDASON, G.E., ÓSKARSSON, N., 1986. Fluorine in basalts from Iceland. Contributions to Mineralogy and Petrology 94, 263-271.

SØRENSEN, H., 1997. The agpaitic rocks – a review. Mineralogical Magazine 61, 485-498.

SØRENSEN, H., BOHSE, H., BAILEY, J.C., 2006. The origin and mode of emplacement of lujavrites in the Ilimaussaq alkaline complex, South Greenland. Lithos 91, 286-300.

STERNER, S.M., KERRICK, D.M., BODNAR, R.J., 1984. Experimental determination of unmixing in CO_2-H_2O-NaCl fluids at 500 °C and 1 kbar using synthetic fluid inclusions: Metamorphic implications. Geological Society of America, Abstract with Programs 16, 668.

STOBER, I., BUCHER, K., 1999. Origin of salinity of deep groundwater in crystalline rocks. Terra Nova 11, 181-185.

TAYLOR, H.P.JR., FRECHEN, J., DEGENS, E.T., 1967. Oxygen and carbon isotope studies of carbonatites from the Laacher See District, West Germany and the Alno District, Sweden. Geochimica et Cosmochimia Acta 31, 407-430.

THOMAS, R., WEBSTER, J.D., HEINRICH, W., 2000. Melt inclusions in pegmatite quartz: complete miscibility between silicate melts and hydrous fluids at low pressure. Contributions to Mineralogy and Petrology 139, 394-401.

TRINKLER, M., MONECKE, T., THOMAS, R., 2005. Constraints on the genesis of yellow fluorite in hydrothermal barite-fluorite veins of the Erzgebirge, Eastern Germany: Evidence from optical absorption spectroscopy, rare-earth-element data and fluid-inclusion investigations. The Canadian Mineralogist 43, 883-898.

TSUCHIYA, N., SUZUKI, S., KIMURA, J.-I., KAGAMI, H., 2005. Evidence for slab melt/mantle reaction: petrogenesis of Early Cretaceous and Eocene high-Mg andesites from the Kitakami Mountains, Japan. Lithos 79, 179-206.

UPTON, B.G.J., THOMAS, J.E., 1980. The Tugtutôq Younger Giant Dyke Complex, South Greenland; fractional crystallization of transitional olivine basalt magma. Journal of Petrology 21, 167-198.

UPTON, B.G.J., EMELEUS, C.H., 1987. Mid-Proterozoic alkaline magmatism in southern Greenland: the Gardar province. From: Fitton, J.G. & Upton, B.G.J. (Eds.), Alkaline Igneous Rocks. Geological Society Special Publication No. 30, 449-471.

UPTON, B.G.J., EMELEUS, C.H., HEAMAN, L.M., GOODENOUGH, K.M, FINCH, A.A., 2003. Magmatism of the mid-Proterozoic Gardar Province, South Greenland: chronology, petrogenesis and geological setting. Lithos 68, 43-65.

VAN HINSBERG, V.J., VRIEND, S.P., SCHUMACHER, J.C., 2005. A new method to calculate end-member thermodynamic properties of minerals from their constituent polyhedra; II, Heat capacity, compressibility and thermal expansion. Journal of Metamorphic Geology 23, 681-693.

VEKSLER, I., 2004. Liquid immiscibility and its role at the magmatic-hydrothermal transition: a summary of experimental studies. Chemical Geology 210, 7-31.

VEKLSER, I.V., DORFMAN, A.M., KAMENETSKY, M., DULSKI, P., DINGWELL, D., 2005. Partitioning of lanthanides and Y between immischible silicate and fluoride melts, fluorite and cryolite and the origin of the lanthanide tetrad effect in igneous systems. Geochimica et Cosmochimica Acta 69, 2847-2860.

WAGNER, T., ERZINGER, J., 2001. REE geochemistry of fluid-rock interaction processes related to Alpine-type fissure vein mineralisation, Rheinisches Schiefergebirge, Germany. In: Piestrzynski, A. et al. (Eds.), Mineral deposits at the beginning of the 21st century. Proc. joint 6th biennial SGA-SEG meeting, Krakow, 929-932. Society for Geology Applied to Mineral Deposits (SGA).

WATSON, E.B., 1980. Apatite and phosphorus in mantle source regions: an experimental study of apatite/melt equilibria at pressures to 25 kbar. Earth and Planetary Science Letters 51, 322-335.

WOOD, S.A., 1990a. The aqueous geochemistry of the rare-earth elements and yttrium. 1. Review of available low-temperature data for inorganic complexes and the inorganic REE speciation of natural waters. Chemical Geology 88, 159-186.

WOOD, S.A., 1990b. The aqueous geochemistry of the rare-earth elements and yttrium. 2. Theoretical predictions of speciation in hydrothermal solutions to 350 °C at saturation water vapor pressure. Chemical Geology 88, 99-125.

YOGODZINSKI, G.M., VOLYNETS, O.N., KOLOSKOV, A.V., SELIVERSTOV, N.I., MATVENKOV, V.V., 1994. Magnesian andesites and the subduction component in a strong calc-alkaline series at Piip volcano, Far Western Aleutians. Journal of Petrology 35, 163-204.

Magmatic halogen geochemistry in the Gardar Province, South Greenland: evidence for subduction-related mantle metasomatism

Jasmin Köhler[1], Johannes Schönenberger[1], Brian Upton[2] and Gregor Markl[1]*

[1]Eberhard-Karls Universität Tübingen
Institut für Geowissenschaften
Wilhelmstraße 56
D-72074 Tübingen
Germany

[2]University of Edinburgh
School of Geosciences
Grant Institute
The King's Buildings
West Mains Road
Edinburgh, EH9 3JW
Schotland, UK

*Corresponding author

Telephone: +49 7071 2972930
Fax: +49 7071 293060
e-mail: markl@uni-tuebingen.de

Abstract

XRF analyses of 114 samples of dykes span the temporal (1280 to 1163 Ma), lateral (150 by 60 km) and compositional range (from basanites to trachytes with an alkalinity index of 0.3 to 1.5) of the mid-Proterozoic alkaline Gardar Province in Southern Greenland. These dykes are regarded to represent all possible mantle melts and their fractionation products which gave rise to gabbroic to syenitic complexes including the Ivigtut cryolite deposit or the agpaitic Ilímaussaq intrusion. Regarding geochemical signatures, dykes from different areas exhibit diverse characteristics suggesting a heterogeneous mantle which appears to have been intensively metasomatised during pre-Gardar subduction processes. This is evidenced by the dykes' enrichment in LILE, LREE and Sr and depletion in HFSE, Nb and Ti. All dykes are characterised by a high content of fluorine with up to 1.2 wt % in the dykes around Ivigtut. Fluorine is interpreted to be derived from the partial melting of lithospheric mantle regions enriched in F-apatite and F-phlogopite. Some dykes describe an unusual trend where compatible elements like Ni or Cr increase with decreasing Mg#. This behaviour probably documents the reduced nature of the primitive magma in which Ni is partly present as Ni^0 and thus retained in the melt instead of being incorporated into fractionating minerals.

Keywords: Gardar, dyke, halogen, fluorine, subduction, mantle metasomatism

1. Introduction

Halogens (F, Cl, Br) are useful geochemical tools as they behave differently in magmatic systems and provide constraints on the genesis of plutonic and volcanic rocks and the fluid evolution (Sigvaldason & Óskarsson, 1986; Kullerud, 1996; Markl & Schumacher, 1996; Bureau et al., 2000).

Chlorine can be highly concentrated either in melts or fluids (e.g. Carmichael et al., 1974; Metrich & Rutherford, 1992; Lowenstern, 1994; Bailey et al., 2001). Cl solubilities in aluminosilicate melts vary between few thousand ppm and up to more than 2 wt% in peralkaline systems (Metrich & Rutherford, 1992; Bailey et al., 2001). Generally, Cl is either lost during degassing or partitions into aqueous fluids (Nijland et al., 1993; Carroll &

Webster, 1994). During later magmatic stages, a Cl-rich aqueous phase (Carmichael et al., 1974) or a salt melt (Lowenstern, 1994) may even separate.

The combination of Cl with Br helps to constrain different reservoirs as the two elements behave as conservative tracers in geochemical processes (Bottomley et al., 2005). Therefore, it may be possible to reveal unmixing processes or fluid interaction by comparing Cl/Br ratios of rocks from different sources. Additionally, Br itself may be used to constrain processes like crystallisation and/or degassing and its high potential solubility in silicate melts makes it a sensitive tracer to the interaction of a magma with seawater or other Br-rich material (Bureau & Métrich, 2003).

Among the halogens, F is best soluble (> 10 wt%) in (alumino)silicate melts (Webster, 1990; Carroll & Webster, 1994). F generally remains in the residual magma where it enters hydroxyl-bearing minerals which are thus stabilised to higher temperatures (Candela, 1986; Edgar et al., 1996). In addition, F may play a crucial role in complexation processes in fluids and in the transport of ore-forming elements such as Li, Be, Sn and HFSE (Pan and Fleet, 1996; Salvi et al., 2000; Williams-Jones et al., 2000; Tagirov et al., 2002; Wood, 2003). Of all rock typies, alkaline rocks have the highest F content which increases with increasing peralkalinity index [molar (Na+K)/Al] (Bailey, 1977). In alkaline magmas, F rather forms bonds with alkali elements than with Si or Al (Kogarko, 1974; Kogarko & Ryabchikov, 1978) and may even generate fluoridic alkaline melts which show immiscibility with a silicate melt (Bailey, 1977; Veksler, 2004; Dolejš & Baker, 2007 a,b).

In order to study the behaviour of halogens in magmatic rocks, we investigated the halogen content in dykes from the alkaline Gardar Province in South Greenland. The magmatic rocks are characterised by very high F contents of different evolutionary stages and by the occurrence of various F-bearing minerals (like fluorite, villiaumite [NaF], cryolite [Na_3AlF_6]). The present study focuses on whole-rock geochemistry on 114 Gardar dykes from all over the province. The results help to understand the timing, distribution, source and significance of halogen enrichment and distribution in the Gardar rocks and their sources, particularly the sub-continental mantle.

2. Geology

The Gardar Province in South Greenland is situated between the Archaean craton in the north and the Ketilidian mobile belt in the south (Fig. 1). The Gardar Province represents a failed

rift structure where magmatic activity lasted from 1350 to 1160 Ma (Blaxland et al., 1978). The country rocks mainly consist of the calc-alkaline, 1855-1795 Ma old Julianehåb batholith (Garde et al., 2002) which was intruded by 12 major alkaline igenous complexes and numerous dyke swarms of different ages and highly variable chemical composition

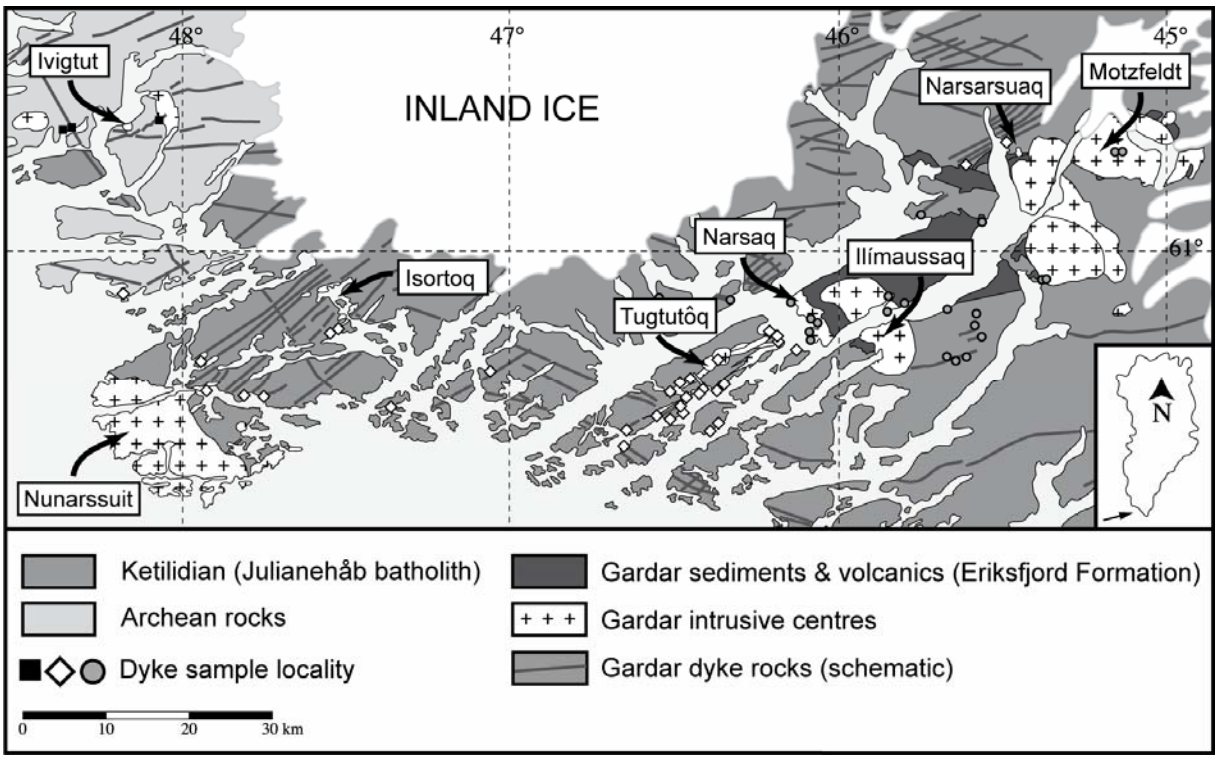

Fig. 1: Overview of the Gardar Province and the localities of the analysed dykes (except for Ivigtut) with respect to the different intrusive complexes. Map modified after Escher & Watt (1976).

The oldest, WNW-ESE trending dykes are called “Brown Dykes” (BD 0) due to their brown alteration colour. Their composition ranges from lamprophyric to (trachy)doleritic and gabbroic (Upton & Emeleus, 1987; Goodenough, 1997). The BD 0 have an average U-Pb age of 1280 Ma and are succeeded by the “Giant Dykes” (GD) which are younger than 1200 Ma (Upton et al., 2003). The GD follow an ENE-WSW trend, have a width of 200-800 m and are mainly concentrated in the area around Nunarssuit-Isortoq and on Tugtutôq. The latter comprises the Older and Younger Giant Dyke Complexes (OGDC and YGDC, respectively; Upton, 1962; Upton & Thomas, 1980; Martin, 1985). The OGDC has an age of 1184 ± 5 Ma and acted as a precursor to the larger, 1163-1166 Ma old YGDC (Upton et al., 2003). Generally, the GD are composed of augite syenite, quartz syenite and alkali granite. Where they are composite, the dykes have a mafic (gabbroic) margin and a salic centre (Upton & Emeleus, 1987; Halama et al., 2004). Due to their broadness, the GD can be regarded as the

transitional link between the dykes and the igneous complexes (Upton & Emeleus, 1987). These 12 alkaline Gardar intrusions exhibit a wide compositional range comprising silica-over- to silica-undersaturated rocks. The famous Ilímaussaq intrusion is the type locality of agpaitic rocks (Sørensen et al., 2006) and hosts one of the most Cl-rich magmatic rocks on Earth, with the sodalite cumulates ("naujaite") containing up to 2.3 wt.% of Cl in the whole rock (Bailey et al., 2001). Another specialty is the small Ivigtut complex (1270 Ma; Upton, unpublished data) in the NW of the Gardar Province which shows the highest enrichment in fluorine and became world-famous for its unique cryolite deposit (Pauly & Bailey, 1999, Köhler et al., in press). It only measures about 350 m across and consists of an A-type granite stock which intruded Archaean gneisses (Goodenough et al., 2002).

3. Analytical methods

Whole rock X-ray fluorescence analyses (XRF) were carried out on a Bruker S4 Pioneer machine at the Institut für Geowissenschaften, Universtität Tübingen and on a Philips PW-1450 XRF at the School of Geosciences, University of Edinburgh, respectively. USGS, CRPG and international rock standards were used for calibration. Detection limits vary between 1 to 10 ppm depending on (trace) element and instrument.

For major elements, the powdered sample was molten to glass discs whereas pressed powder pellets were used for trace element analyses. Loss on ignition (LOI) was usually positive with the majority varying between 0 and +1.5 %. Only two samples had a negative LOI (-0.77 and -0.18 %, respectively) indicating a mass increase upon oxidation from FeO to Fe_2O_3. XRF data from dykes of the Ivigtut area are from the archive of the Geological Survey of Denmark/Greenland (GEUS). The Ivigtut dyke samples are from drill cores and were analysed by the Outokumpu OY Exploration & Mining Services/Finland during 1985-1987. The XRF whole rock analyses were carried out at the the company's Geoanalytical Laborary on a Philips PW-1400 using the correction program "Leco". Carbon and sulphur were analysed by a Leco analyser and fluorine by a fusion procedure and selective ion electrode.
The analysis of the halogens in all samples except for those from the Ivigtut area was carried out at the Institut für Geowissenschaften, Universität Tübingen. For the quantification of the halogens (i.e. F, Cl and Br), a pyrohydrolysis extraction line in combination with ion chromatography was used.

The pyrohydrolysis extraction line was set up according to the method outlined by Dreibus et al. (1979). 10 to 120 mg sample powder washed with triple deionized water was thoroughly mixed with at least twice the amount of V_2O_5. Subsequently, the mixture was filled into small quartz-glass vessels and heated to 1100 °C in the extraction line. The released halogens were dissolved in a 0.02 mol NaOH solution. A second halogen trap was installed after the main trap in order to avoid any loss of halogens. The total time of the experiment was 20 min with 10 to 15 ml of solution being collected. Subsequently, this solution was analysed with a Dionex ICS-1000 ion chromatograph using an IonPac AS9-HC 2-mm anion column. Blank runs were performed after every sample in order to check for possible contamination. The blanks yielded values for F^- and Cl^- of below 30 ppb and Br^- below detection limit. The reproducibility of the measurements was regularly checked with reference materials (Govindaraju, 1994; Michel et al., 2003) and is above 90 %, even though triple deionised water is used instead of a NaOH halogen trap. A total error of 20 % (relative) can be assumed for the extraction/measurement process. For rock samples, detection limits are about 10 ppm for F and Cl and <1 ppm for Br.

4. Results

4.1 Petrography

Giant Dykes occur on the island of Tugtutôq and around Isortoq. They are generally composite and show signs of rhythmic layering and/or feldspar lamination (Upton, 1962). Their chilled gabbroic margin is mainly composed of olivine and primary zoned plagioclase, alkali feldspar and anhedral olivine with interstitial clinopyroxene, titanomagnetite, ilmenite and abundant apatite (Halama et al., 2004). Towards the syenitic centre, amphibole becomes abundant whereas plagioclase and olivine disappear. The syenitic centre itself consists of greyish-white, antiperthitic alkali feldspar, greenish-grey, euhedral pyroxene, sector-zoned epidote, titanite and biotite (Upton, 1962; Halama et al., 2004). The OGDC from Tugtutôq is made up of augite-syenite which grades into peralkaline nepheline-syenites (foyaites; Upton & Emeleus, 1987). The YGDC mainly consists of plagioclase-olivine rocks that comprise calcic pyroxene, ilmenite, titanomagnetite, apatite and biotite as a minor component. Quartz occurs interstitially in the syenitic parts with primary calcite (Upton & Thomas, 1980).

The dykes from the Ilímaussaq-Narsaq-Motzfeldt area are very fine-grained, holocrystalline and occasionally exhibit a porphyritic texture. Alkali feldspar forms up to 1 cm big phenocrysts in a matrix of feldspar laths, aggregates of green pyroxene, altered biotite

and opaque oxides. Interstitial quartz, fluorite and apatite occasionally occur while hypidiomorphic calcite is scarce.

In the Ivigtut region, olivine dolerite dykes (i.e. Brown Dykes) consist of augite, early olivine and plagioclase in an ophitic texture. Subordinate minerals are oxides and apatite. Younger, basaltic dykes around Ivigtut comprise plagioclase phenocrysts in a fine, olivine-free matrix of augite and andesine (Goodenough et al., 2002).

4.2 Whole-rock geochemistry

XRF whole-rock data are summarised in Table 1. In the TAS-diagram (Fig. 2; Le Maitre et al., 1989), the Gardar dykes span a wide compositional range from ultrabasic basanites to phonolites/trachytes. The dykes around Tugtutôq-Isortoq-Nunarssuit-Narsarsuaq are confined to (ultra)basic composition whereas most other dykes are more highly fractionated. Due to the rather strong predominance of Na over K, some dykes can be referred to as hawaiites, mugearites and benmoreites, respectively (Fig. 3).

The Gardar dykes exhibit similarities with high-K calc-alkaline rocks and particularly with shoshonites. Not only the dykes' average Al_2O_3 content of 15 wt% is very typical of shoshonites, but also their K_2O/Na_2O ratio (0.3-1.4) and the overall high alkali content ($Na_2O+K_2O > 4$ wt%; Le Maitre et al., 1989). Regarding the K_2O content itself, it generally exceeds 2 wt% in the Gardar dykes (Fig. 4). Their Na_2O content of 3 to 8 wt% (mean at 4.4 wt%) and the high Sr contents of > 400 ppm (Fig. 6 h) are similar to adakites (Defant & Drummond, 1990; Martin et al., 2005) although the dykes' La/Yb (<< 21) and Sr/Y ratios (mean at 23) are lower than that of adakites (50-72 and 21-39, respectively; Defant & Drummond, 1990).

Trace elements were normalised to primitive mantle (McDonough & Sun, 1995; Fig. 5). Due to the lack of data for the dykes in the Ivigtut area, only the differing patterns of the other dykes are compared. Generally, the trace element content increases from primitive to more fractionated dykes. The most primitive dykes in the Tugtutôq-Isortoq-Nunarssuit-Narsarsuaq area exhibit a pronounced positive Sr anomaly which diminishes in more evolved dykes. On the other hand, the positive Ba anomaly increases in more fractionated dykes combined with the appearance of negative Ti and positive Zr anomalies. In the Ilímaussaq-Narsaq-Motzfeldt region, the primitive dykes are characterised by a positive U anomaly and negative Ba, Nb and Ti anomalies. In more evolved dykes, these anomalies become more pronounced and strikingly, the positive K and Sr anomlies turn into negative ones.

Tab. 1: Representative XRF whole rock data from dykes in the Gardar Province.

Locality	Tugtutôq	Tugtutôq	Tugtutôq	Tugtutôq	Tugtutôq	Tugtutôq	Tugtutôq	Isortoq	Isortoq	Isortoq	Nunarssuit	Nunarssuit
Sample	40452	40455	86101	40583	40488	85997	86041	101337	101363	101438	101338B	101390
Dyke type	YGDC	YGDC	OGDC	YGDC	YGDC	OGDC	OGDC					
Rock type	tephrite/ basanite	basalt	trachy-basalt	basalt	trachy-basalt	tephrite/ basanite	basaltic trachy-andesite	basalt	phono-tephrite	basalt	basalt	hawaiite
Fe_2O_3/FeO	0.25	0.20	0.30	0.20	0.30	0.25	0.35	0.20	0.35	0.20	0.20	0.30
Major elements (wt.%)												
SiO_2	44.92	45.5	45.17	46.43	45.04	44.37	50.63	49.34	49.38	48.67	46.41	49.67
TiO_2	2.31	2.77	3.88	2.41	3.44	4.59	2.66	1.87	2.98	3.15	1.73	1.41
Al_2O_3	16.38	16.28	14.75	17.98	15.56	14.01	15.09	16.36	14.38	13.58	17.48	18.32
$Fe_2O_{3\ total}$	16.47	15.67	16.29	14.4	16.65	16.28	13.25	13.47	13.65	15.44	14.14	10.71
FeO_{total}												
MnO	0.19	0.19	0.23	0.17	0.23	0.2	0.19	0.18	0.19	0.21	0.19	0.16
MgO	8.48	6.4	4.15	5.77	5.1	4.51	2.37	5.43	3.05	4.2	7.53	5.14
CaO	7.57	8.01	7.84	7.93	7.76	7.14	6.42	7.89	6.76	7.41	9.1	7.72
Na_2O	2.91	3.28	4.03	3.62	3.6	3.62	4.65	3.85	4.54	3.18	3.01	3.79
K_2O	0.89	1.60	2.27	1.19	1.73	2.16	3.14	0.85	2.89	1.80	0.39	1.35
P_2O_5	0.6	0.97	2.66	0.56	1.21	2.26	1.1	0.41	1.51	0.75	0.23	0.24
LOI (%)	-	-	-	-	-	-	-	-	-	-	-	-
Mg# **	56	49	40	49	44	41	32	49	37	39	56	55
Alkalinity Index	0.4	0.4	0.6	0.4	0.5	0.6	0.7	0.4	0.7	0.5	0.3	0.4
Trace elements (ppm)												
Sc	15	18	19	14	22	18	30	20	18	28	21	22
V	164	134	110	191	165	166	35	270	66	214	158	175
Cr	24	22	7	43	18	6	6	65	3	60	41	170
Co	-	-	-	-	-	-	-	-	-	-	-	-
Ni	79	55	6	45	34	14	4	66	5	39	82	49
Cu	38	70	89	58	87	51	60	87	54	70	72	91
Zn	83	93	96	86	90	94	99	112	88	139	87	114
Ga	17	21	19	20	21	17	22	19	22	23	19	21
Rb	13	23	37	17	24	38	58	19	38	72	6	46
Sr	933	859	876	1002	769	818	753	798	379	424	429	506
Y	20	32	40	20	38	38	43	26	52	46	25	23
Zr	107	171	221	122	202	208	291	105	253	323	112	94
Nb	15	25	37	17	30	39	47	6	16	15	7	6
Ba	837	1166	1898	914	1357	2220	2554	1264	1440	783	245	539
Pb	4	4	8	5	6	8	10	3	9	7	3	3
La	38	50	53	36	51	60	65	17	42	34	6	14
Ce	39	67	129	48	86	123	129	36	101	77	18	23
Pr	0	0	13	0	0	12	13	0	13	0	0	0
Nd	19	36	68	24	46	66	59	23	59	40	12	15
Sm												
Eu	-	-	-	-	-	-	-	-	-	-	-	-
Gd	0	0	0	0	0	0	8	0	9	0	0	0
Dy	10	18	28	8	34	18	9	16	16	31	16	14
Yb	-	-	-	-	-	-	-	-	-	-	-	-
Lu	0.3	0.5	0.7	0.4	0.6	0.9	0.9	0.7	0.9	0.8	0.4	0.5
As	0	0	0	0	0	0	0	0	0	0	0	0
Hf	0	0	2.7	0	1.7	2.7	5.1	0	8.8	9.8	3.7	1.2
Ta	0	0	0	0	0	0	0	0	0	0	0	0
Th	0	0	0	0	0	0	0	0	0	0	0	0
U	0	2.8	1.1	0	5.3	0.0	5.6	5.6	9.3	8.1	2	6.9
Sn	1.4	2.7	3.9	1.6	2.5	3.0	4.8	2.9	3.1	3.3	1.6	2.7
Cs	0	0	0	0	0	0	4	4	0	0	0	3
S	557	855	149	710	1261	310	756	712	1825	711	690	334
Cl	245	110*	195	76*	224	341	280	148*	352	83*	198	459
F	473	1181*	2506	734*	974	2206	1380	692*	3025	1037*	302	529
La_{cn}/Lu_{cn}	13.1	10.4	7.9	9.3	8.8	6.9	7.5	2.5	4.8	4.4	1.6	2.9
Eu/Eu*	-	-	-	-	-	-	-	-	-	-	-	-

* Cl and F contents analysed with pyohydrolysis / IC

** Mg# = 100[Mg/(Mg+Fe^{2+})] - = not detected

*** Eu/Eu* with Eu* = $(Sm*Gd)^{0.5}$

Tab. 1 continued

Locality	Nunarssuit	Narsarsuaq	Narsarsuaq	Narsarsuaq	Ilímaussaq	Ilímaussaq	Ilímaussaq	Ilímaussaq	Ilímaussaq	Narsaq
Sample	101374	101249	101250	101469	GD22	GD23b	GD26	GD27	GD31a	GD5
Rock type	trachy-basalt	trachy-basalt	hawaiite	trachy-basalt	trachy-andesite	tephri-phonolite	hawaiite	trachy-andesite	phonolite	tephrite/ basanite
Fe_2O_3/FeO	0.30	0.30	0.30	0.30	0.40	0.40	0.30	0.40	0.50	0.25
Major elements (wt.%)										
SiO_2	45.43	45.62	48.04	44.5	55.49	54.94	47.10	56.74	53.30	43.64
TiO_2	2.04	2.99	3.21	3.52	1.53	1.23	2.80	1.02	0.56	3.48
Al_2O_3	16.08	15.21	13.94	16.27	17.37	17.08	15.05	17.95	19.32	15.07
$Fe_2O_{3\ total}$	14.18	15.64	13.54	15.1	8.28	7.29	14.36	7.35	7.13	15.70
FeO_{total}										
MnO	0.18	0.19	0.21	0.18	0.17	0.20	0.18	0.18	0.27	0.19
MgO	6.73	5.28	3.64	5.07	1.39	0.94	4.47	0.86	0.54	4.68
CaO	8.98	7.74	7.37	7.61	3.40	3.08	7.16	2.28	1.80	6.72
Na_2O	1.94	3.13	4.82	3.39	5.08	4.96	4.50	5.43	8.16	2.92
K_2O	3.32	2.15	1.79	2.25	5.22	5.84	0.91	5.10	6.23	3.92
P_2O_5	0.37	1.06	1.7	1.47	0.56	0.42	0.54	0.33	0.17	1.14
LOI (%)	-	-	-	-	0.47	2.93	1.69	1.19	1.46	1.44
Mg# **	55	47	41	46	32	26	45	25	18	42
Alkalinity Index	0.4	0.5	0.7	0.5	0.8	0.8	0.6	0.8	1.0	0.6
Trace elements (ppm)										
Sc	26	25	20	17	13	22	22	14	3	24
V	226	235	139	150	25	12	236	12	6	215
Cr	77	41	4	27	0	3	73	0	8	42
Co	-	-	-	-	7	0	39	4	3	42
Ni	91	37	4	41	42	47	92	48	126	91
Cu	108	88	59	75	73	66	87	77	91	97
Zn	103	109	156	81	95	129	139	105	168	146
Ga	21	20	23	19	24	27	26	27	41	25
Rb	66	137	38	43	92	121	27	86	186	154
Sr	299	865	608	1066	648	333	520	331	42	644
Y	29	31	43	32	42	40	46	40	91	40
Zr	117	139	218	189	312	343	249	334	984	201
Nb	7	23	32	33	76	78	20	84	261	34
Ba	975	1189	1378	1584	2812	1830	715	2043	54	1128
Pb	2	3	9	4	22	7	6	28	41	7
La	11	32	62	49	31	36	24	47	138	0
Ce	20	65	139	89	121	122	77	134	289	56
Pr	0	0	16	0	14	17	0	17	30	0
Nd	15	37	74	48	58	67	51	59	112	50
Sm					8	10	8	9	20	8
Eu	-	-	-	-	2	2	2	2	2	2
Gd	0	0	11	0	11	12	0	13	21	0
Dy	47	27	9	32	145	8	34	239	329	36
Yb	-	-	-	-	3.2	3.0	3.6	3.1	6.7	3.1
Lu	0.8	0.9	0.9	0.6	0.7	0.7	0.8	0.6	1.3	0.8
As	0	0	0	0	0	0	0	0	13.6	0
Hf	5.0	0.0	4.4	0.0	6.6	12.8	4.4	11.5	36.0	2.5
Ta	0	0	0	0	8.0	0	0	8.3	24.3	0
Th	0	0	0	0	0.0	0	0	0.0	21.1	0
U	8.0	6.1	9.3	3.5	188.0	13.6	12.6	232.2	267.6	9.7
Sn	2.3	4.7	5.3	2.4	4.0	5.6	4.8	5.3	8.5	5.1
Cs	3	8	2	0	3	12	6	11	19	8
S	18	1371	39	993	56	0	435	0	103	538
Cl	184	262	241*	249	291	281	300	297	1058*	359
F	570	1260	1983*	1238	543	520	520	466	2819*	1728
La_{cn}/Lu_{cn}	1.4	3.7	7.2	8.5	4.5	5.4	3.1	8.2	11.0	0.0
Eu/Eu*	-	-	-	-	0.7	0.4	-	0.4	0.3	0.0

Tab. 1 continued

Locality	Narsaq	Narsaq	Narsaq	Motzfeldt	Motzfeldt	Ivigtut	Ivigtut	Ivigtut	Ivigtut	Ivigtut	Ivigtut	Ivigtut
Sample	GD7	GD9	GD13	JS147	JS89	BB 7	BB 8	BB 11	BB 15	BB 16	BB 18	BB 23
Rock type	ben-moreite	trachyte	tephri-phonolite	phonolite	phonolite	trachy-andesite	phono-tephrite	ben-moreite	trachyte	trachy-andesite	tephri-phonolite	basalt
Fe_2O_3/FeO	0.40	0.50	0.40	0.50	0.50	0.40	0.35	0.40	0.50	0.40	0.40	0.20
Major elements (wt.%)												
SiO_2	57.48	59.85	53.91	58.69	55.42	59.6	48.2	59.5	62.1	57.5	54.2	50.2
TiO_2	0.77	0.90	0.85	0.72	0.54	0.62	1.94	0.67	0.542	0.619	0.44	1.08
Al_2O_3	15.08	14.36	18.12	12.25	16.57	18.7	15.6	16.4	14.8	14.5	17.9	12
$Fe_2O_{3\ total}$	10.11	8.43	8.44	9.97	8.91							
FeO_{total}						4.17	11.6	5.28	6.7	6.07	6.37	12.2
MnO	0.25	0.21	0.35	0.58	0.24	0.066	0.181	0.091	0.157	0.111	0.208	0.19
MgO	0.44	0.50	0.46	0.26	0.34	1.13	2.09	2.46	0	0.33	0	4.14
CaO	2.66	2.03	2.56	1.39	2.06	5.09	5.68	5.06	2.17	3.08	3.03	8.84
Na_2O	6.76	6.07	3.80	7.58	7.25	4.31	4.01	4.75	4.85	4.4	3.25	3.21
K_2O	3.51	4.81	7.62	5.28	5.36	3.23	3.21	2.18	5.14	4.81	7.26	1.02
P_2O_5	0.16	0.18	0.13	0.19	0.11	0.362	1.26	0.239	0.093	0.113	0.234	0.15
LOI (%)	1.40	1.43	1.88	0.58	1.66	-	-	-	-	-	-	
Mg# **	11	15	13	7	9	40	30	54	0	12	0	52
Alkalinity Index	1.0	1.1	0.8	1.5	1.1	0.6	0.6	0.6	0.9	0.9	0.7	0.5
Trace elements (ppm)												
Sc	8	13	0	0	8	-	-	-	-	-	-	-
V	9	6	4	3	5	-	-	-	-	-	-	-
Cr	11	14	0	0	15	5	9	70	9	9	0	21
Co	6	4	1	3	3	-	-	-	-	-	-	-
Ni	174	60	0	133	103	-	-	-	-	-	-	-
Cu	96	58	82	160	91	22	59	18	68	< 5	130	62
Zn	238	169	252	365	199	66	880	87	188	< 5	728	158
Ga	46	32	25	51	40	-	-	-	-	-	-	-
Rb	86	106	99	185	180	244	170	126	180	188	368	52
Sr	158	32	2913	1471	3	1006	905	423	863	364	127	668
Y	184	76	72	166	101	25	18	26	50	< 10	44	26
Zr	1532	527	871	1760	857	207	318	370	518	5256	1288	104
Nb	246	94	403	303	194	69	91	96	233	182	606	32
Ba	207	131	3339	160	9	743	1908	770	439	690	493	242
Pb	59	26	43	83	54	39	60	67	100	< 5	148	94
La	223	101	300	480	141	-	-	-	-	-	-	-
Ce	446	212	474	778	289	31	58	69	191	166	165	24
Pr	45	27	31	76	37	-	-	-	-	-	-	-
Nd	184	97	153	276	116	-	-	-	-	-	-	-
Sm	30	16	27	48	19	-	-	-	-	-	-	-
Eu	3	2	8	7	2	-	-	-	-	-	-	-
Gd	27	15	16	49	26	-	-	-	-	-	-	-
Dy	53	21	11	171	483	-	-	-	-	-	-	-
Yb	14.2	6.2	4.6	11.8	8.0	-	-	-	-	-	-	-
Lu	2.0	1.0	1.0	2.1	1.6	-	-	-	-	-	-	-
As	26.7	0	0	0	0	-	-	-	-	-	-	-
Hf	51.1	20.8	10.0	71.8	38.0	-	-	-	-	-	-	-
Ta	24.4	6.5	40.4	90.6	16.8	-	-	-	-	-	-	-
Th	36.1	14.0	0.0	129.4	20.5	-	-	-	-	-	-	-
U	36.5	15.7	20.9	73.3	290	-	-	-	-	-	-	-
Sn	14.1	7.8	9.6	22.1	10.4	< 10	< 10	< 10	< 10	< 10	17	< 10
Cs	21	10	3	30	21	-	-	-	-	-	-	-
S	39	148	160	0	429	100	1100	100	400	1700	200	300
Cl	159*	300	143*	57	1279*	-	-	-	-	-	-	-
F	3928*	1258	3536*	410	2468*	5100	6600	3400	5400	12000	8800	3700
La_{cn}/Lu_{cn}	11.6	10.5	31.1	23.7	9.1	-	-	-	-	-	-	-
Eu/Eu*	0.3	0.3	1.1	0.4	0.2	-	-	-	-	-	-	-

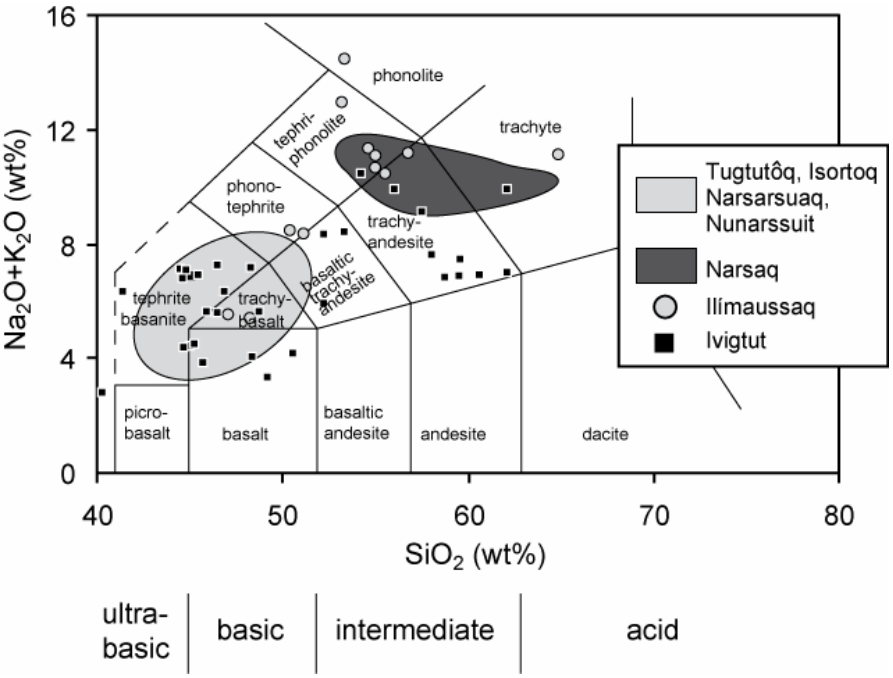

Fig. 2: TAS Diagram after Le Maitre et al. (1989). The Gardar dykes cover a wide compositional range with the majority of dykes being restricted to (ultra)basic rocks.

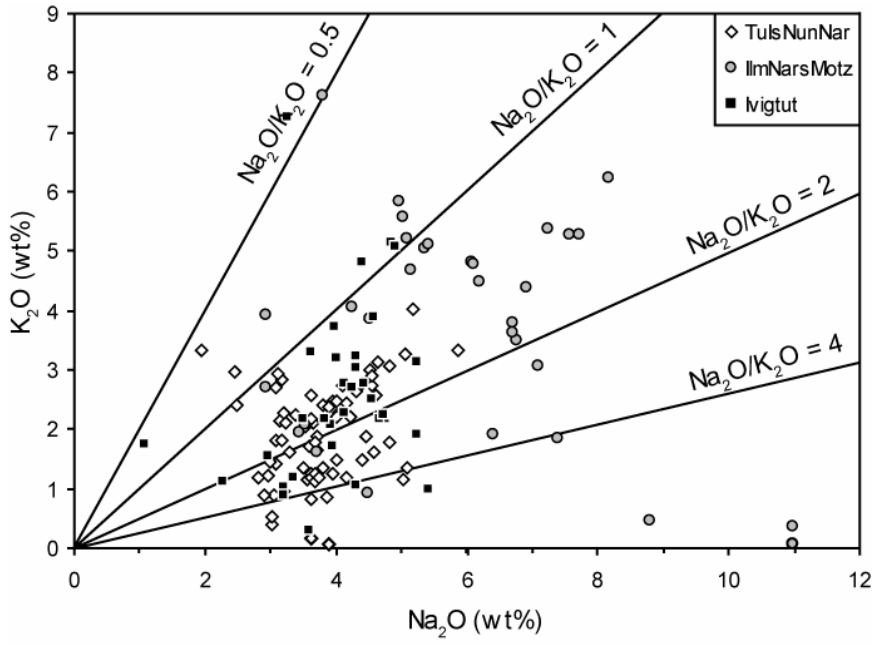

Fig. 3: Na_2O (wt%) vs. K_2O (wt%). Due to the predominance of Na_2O over K_2O, some dykes can be referred to as hawaiites, mugearites or benmoreites, respectively. [TuIsNunNar = Tugtutôq-Isortoq-Nunarssuit-Narsarsuaq; IlmNarsMotz = Ilímaussaq-Narsaq-Motzfeldt]

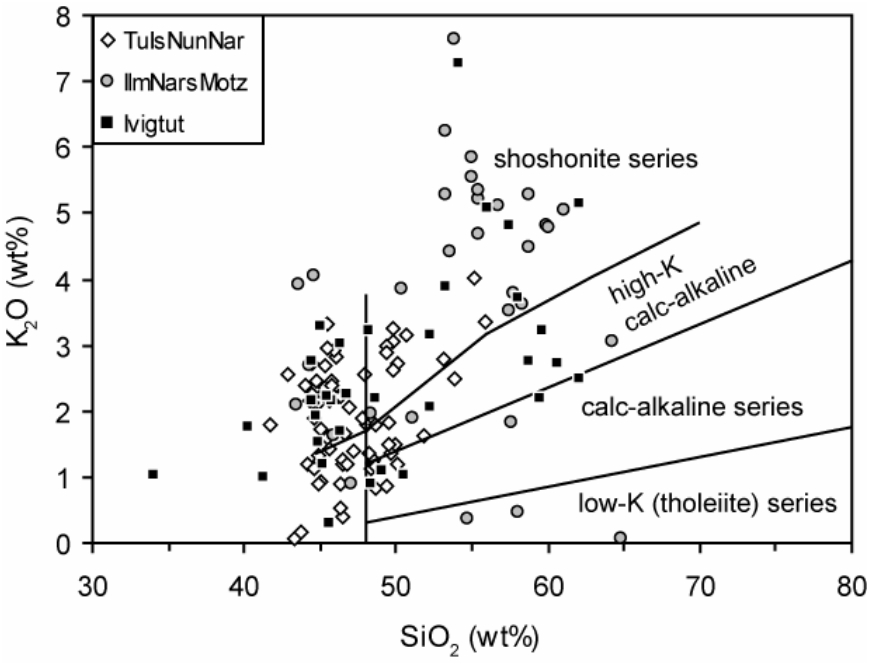

Fig. 4: SiO_2-K_2O discrimination diagram for K-rich magmas after Le Maitre et al. (1989). Most dykes with SiO_2 > 48 % can be referred to as shoshonites suggesting their derivation from a subduction-related, metasomatised mantle [TuIsNunNar = Tugtutôq-Isortoq-Nunarssuit-Narsarsuaq; IlmNarsMotz = Ilímaussaq-Narsaq-Motzfeldt].

Compositional variation and possible fractionation trends are shown with respect to the Mg-number (Fig. 6). Mg-numbers [Mg# = 100*Mg/(Mg+Fe^{2+}) atomic] were calculated using different Fe_2O_3/FeO ratios from 0.15 to 0.5 for the various rock types according to Middlemost (1989). Generally, the Gardar dykes are moderately to highly evolved and seem to be derived from fractionated melts. This is indicated by their low Cr and Ni content (mostly < 100 ppm) and the enrichment of incompatible elements like Zr (100 to > 1000 ppm; Fig. 6 d, e, f) and La (10-300 ppm). Incompatible elements are especially concentrated in the dykes around Motzfeldt, Ilímaussaq and Narsaq. The dykes' F content does not exceed a value of 2000 ppm except for the dykes in the Ivigtut area (Fig. 6 g). There, fluorine correlates negatively with Mg# and reaches an F content of up to 12 000 ppm in the most highly fractionated samples. Two trends can be observed in Fig. 6 g: the first one is rather steep and comprises F-rich dykes from the Ivigtut area while the other Gardar dykes describe a much flatter trend with maximum F contents of about 4000 ppm. Both trends can be also recognised in Andean (e.g. Morgan et al., 1998; Halter et al., 2004), but not in Aleutian rocks (Coats, 1953; Coats et al., 1959; Drewes et al., 1961; Nye & Turner, 1990).

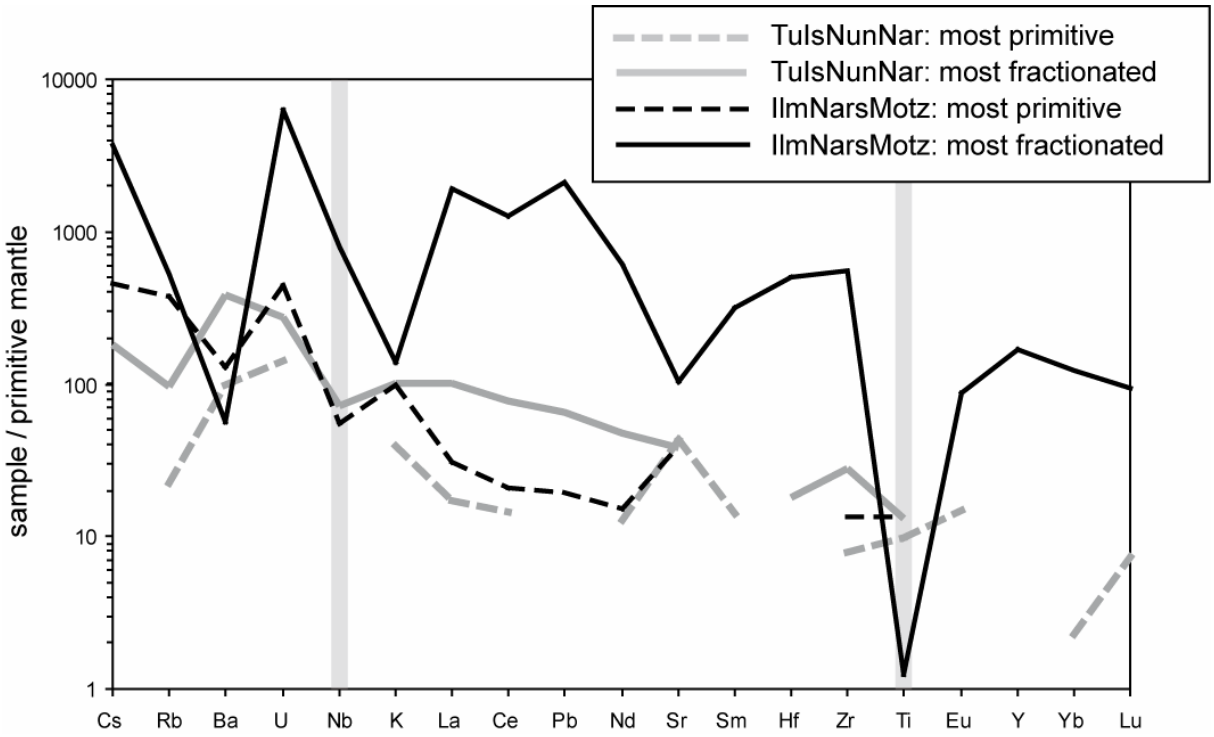

Fig. 5: Primitive mantle-normalised (McDonough & Sun, 1995) trace element diagram for Gardar dykes. The ranges are given for the most primitive and most highly fractionated rocks, respectively [TuIsNunNar = Tugtutôq-Isortoq-Nunarssuit-Narsarsuaq; IlmNarsMotz = Ilímaussaq-Narsaq-Motzfeldt; Ivigtut no data].

The dykes in the Gardar Province do not only vary regionally, but also differ regarding their temporal appearance/age. The Brown Dykes (BD 0) and the Older Giant Dyke Complex (OGDC) display large similarities in terms of their evolved composition. In contrast, the Younger Giant Dykes (YGDC) are more primitive which is evidenced by their higher Mg# and higher contents of compatible elements (Cr, Ni; Fig. 7 a) Incompatible elements like Rb, Ba, Zr, F and the alkalis describe negative correlations with Mg# and are more abundant in the OGDC (Fig. 7 b, c). The fact that older dykes are more highly fractionated than the younger ones is in accordance with results by Upton et al. (1985). Upton & Thomas (1980) found that the F content in the chilled margin of the OGDC is higher than in the YGDC. This agrees with results from this study: whole rock analyses of OGDC mostly have a F content > 2000 ppm whereas F in the YGDC commonly does not exceed 950 ppm (Fig. 7 d).

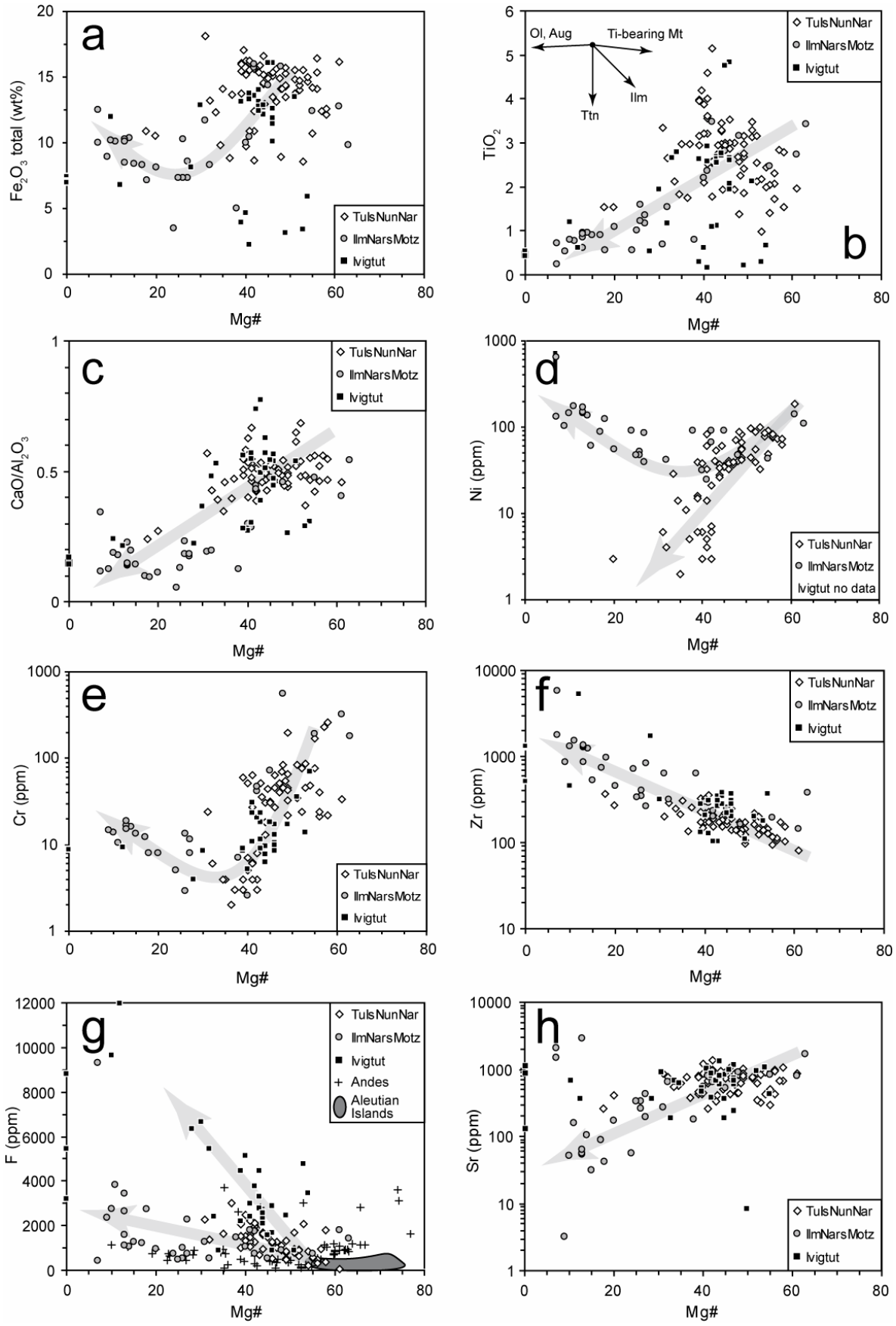

Fig. 6: Whole rock variation diagrams for Gardar dykes with Mg# = Mg/(Mg+Fe^{2+}) as fractionation index. b) Arrows indicate qualitative mineral fractionation. g) Comparative data for Andean rocks from Morgan et al. (1989) and Halter et al. (2004) and for Aleutian Islands from Coats (1953), Coats et al. (1959), Drewes et al. (1961) and Nye & Turner (1990). See text for further discussion.

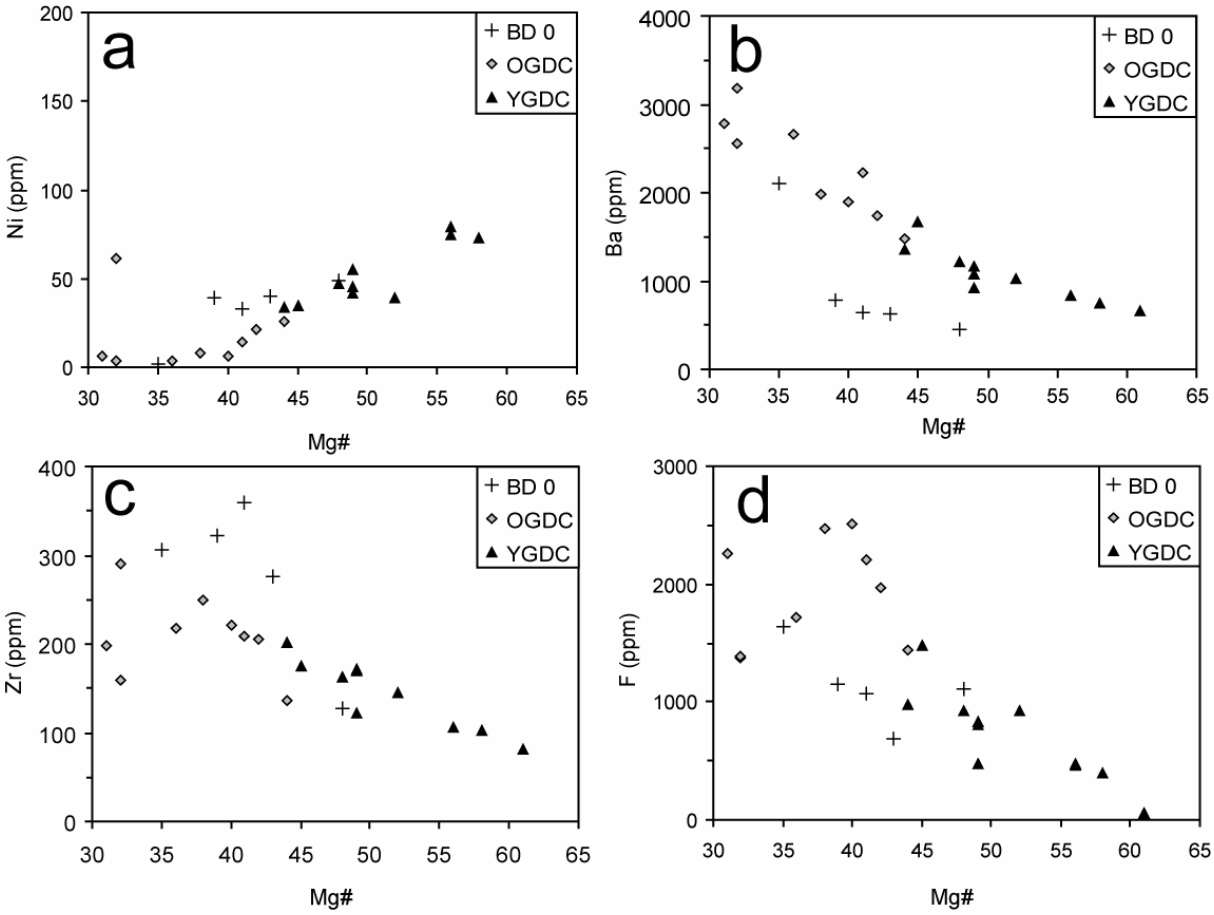

Fig. 7: Chronological differences for Gardar dykes with Mg# = Mg/(Mg+Fe^{2+}) as fractionation index [BD 0 = Brown Dykes, 1.28 Ga; OGDC = Older Giant Dyke Complex, 1.18 Ga; YGDC = Younger Giant Dyke Complex, 1.16 Ga; Upton et al., 2003].

5. Discussion

5.1 Melt or cumulate?

The question arises whether the studied samples represent true melts or are affected by cumulate effects. The dykes are commonly very fine-grained and do not show any signs of typical cumulate textures. Plagioclase laths are uniformly distributed and not aligned within the mafic matrix. There are no euhedral cumulus grains as the great majority of minerals are subhedral to xenomorphic. Porphyritic textures are rare and neither interstitial melt fractions nor melt inclusions are present. Geochemical characteristics also argue against any cumulate effects: The dykes' MgO content is much lower (0.3-10 wt%, mean at 3.7 wt%) than that of typical mafic cumulates (13-20 wt%; Bağci et al., 2005). The same applies to the CaO content (1-12 wt% in this study vs. 7-18 wt% in cumulates; Bağci et al., 2005). Generally, the dykes exhibit a continuous fractionation trend if major or trace elements are plotted against SiO_2 or

Mg#. There are no kinks in the Harker diagrams except for the transition metals in dykes from the Ilímaussaq-Narsaq-Motzfeldt region. However, this peculiar feature will be scrutinised in more detail below. Anomalies in the trace element patterns may be interpreted to result from cumulate processes. However, positive Sr and Eu anomalies typically observed in cumulates due to plagioclase accumulation (Schmidberger et al., 2007) are neither present in trace nor in rare earth element patterns of the studied dykes (Fig. 5). Therefore it can be assumed that most studied samples do represent true melts and no cumulates.

5.2 Evidence for mineral fractionation

Generally, all Gardar dykes describe clear fractionation trends, i.e. incompatible trace elements correlate negatively with Mg# whereas compatible elements commonly decrease with decreasing Mg#.

The positive correlation between Fe_2O_3-Mg#, TiO_2-Mg# (Fig. 6 a, b) and V-Mg# (not shown as no data for Ivigtut are available) indicates fractionation of Fe-Ti-oxides. CaO/Al_2O_3 decreases with decreasing Mg# which suggests fractionation of clinopyroxene (Fig. 6 c). However, this trend is not clearly defined within one single dyke region, but is evident for all Gardar dykes. The same holds true for the Sc-Mg# diagram (not shown). Mattsson & Oskarsson (2005) proposed Sc/Y against Mg# as another test for clinopyroxene fractionation, because Sc is compatible, but Y incompatible in augite. For the Gardar dykes (Ivigtut no data), Sc/Y correlates positively with Mg# which further suggests a certain amount of clinopyroxene fractionation.

Fractionation of olivine and orthopyroxene is highly likely for Gardar dykes, because Ni correlates positively with Mg# (Ivigtut no data available, Fig. 6 d). A similar trend can be followed for Cr, Fe, Co and Zn vs. Mg# (Fig. 6 a, e). However, the dykes in the vicinity of Ilímaussaq-Narsaq-Motzfeldt describe a different development for those elements which will be scrutinised in more detail below.

The Gardar dykes generally have a low P_2O_5 content which commonly does not exceed 2 wt%. However, due to their high abundance of volatiles (esp. F), apatite saturation may have actually been attained (Watson, 1980). This is evidenced by the perfect correlation of F with P_2O_5 for the dykes in the Tugtutôq-Isortoq-Nunarssuit-Narsasuaq region (Fig. 9 b) which describes a normal fractionation trend. In contrast, more evolved dykes in the Ivigtut area are up to three times more F-enriched at the same P_2O_5 content than primitive ones. Therefore, the extraordinarily high F content in the Ivigtut area may not be explained by

apatite fractionation. Possibly, apatite saturation was not achieved in these dykes (Watson, 1980) and therefore, fluorine became progressively enriched in more fractionated dykes.
The negative Eu-anomaly in chondrite-normalised (McDonough & Sun, 1995) REE patterns (Tab. 1) can be attributed to early-magmatic plagioclase fractionation as evidenced by the large occurrence of anorthosites underlying the Gardar Province (Schönenberger & Markl, in press; Halama et al., 2002).

5.3 Late-stage enrichment of Ni, Cr, Fe, Zn, Co

The transition metals Ni, Cr, Fe, Zn and Co are positively correlated with Mg# for most Gardar dykes implying normal fractionation trends. However, the dykes in the region Narsaq-Ilímaussaq-Motzfeldt describe a concave trend with a minimum at a Mg# of about 30 (Fig. 6 a, d, e). This trend is most obvious for Ni, Cr and Zn and appears to be independent of the Mg#, because the same trends can be seen if plotted against MgO or SiO_2.

No mineral phase was observed which could have accounted for the enrichment of these transition metals. It is doubtful that the metals were incorporated into sulphides, because they only show a weak (if any) correlation with sulphur. Spinels also appear to have played a minor role, because there are no strong correlations among the elements of the different (Fe-Al-Zn-Mn-)spinel group members. Only total Fe_2O_3 displays a positive trend with TiO_2 for all Gardar dykes suggesting that ulvöspinel may have fractionated.

Cr/Ni is positively correlated with Mg# even though the dykes in the Ilímaussaq-Narsaq-Motzfeldt area are restricted to lower Cr/Ni ratios and lower Mg# (Fig. 8 a). The overall positive correlation indicates that the Cr/Ni ratio is dependent on fractionation processes (Martin et al., 2005). In Fig. 8 b, the Gardar dykes fall near, but largely plot above a mixing line between a slab melt and a mantle peridotite (Drummond et al., 1996; Tsuchiya et al., 2005). A simple mixing process would result in a Ni decrease in the modified mantle (Tsuchiya et al., 2005), i.e. the dykes should lie below the mixing line. The higher Ni contents relative to Cr could result from interaction of a slab-derived adaktic melt with mantle peridotite. According to Kelemen (1995), this interaction would cause an increase in the melt's Ni content due to the dissolution of olivine and the formation of orthopyroxene (which incorporates less Ni relative to olivine). However, dissolution of olivine would not only increase the Mg/Fe ratio, but also the absolute MgO concentration both of which is not observed for the dykes in the Ilímaussaq-Narsaq-Motzfeldt area. Hence, the interaction of an

adakitic melt with the overlying mantle wedge cannot fully explain the high Ni contents at low Mg#.

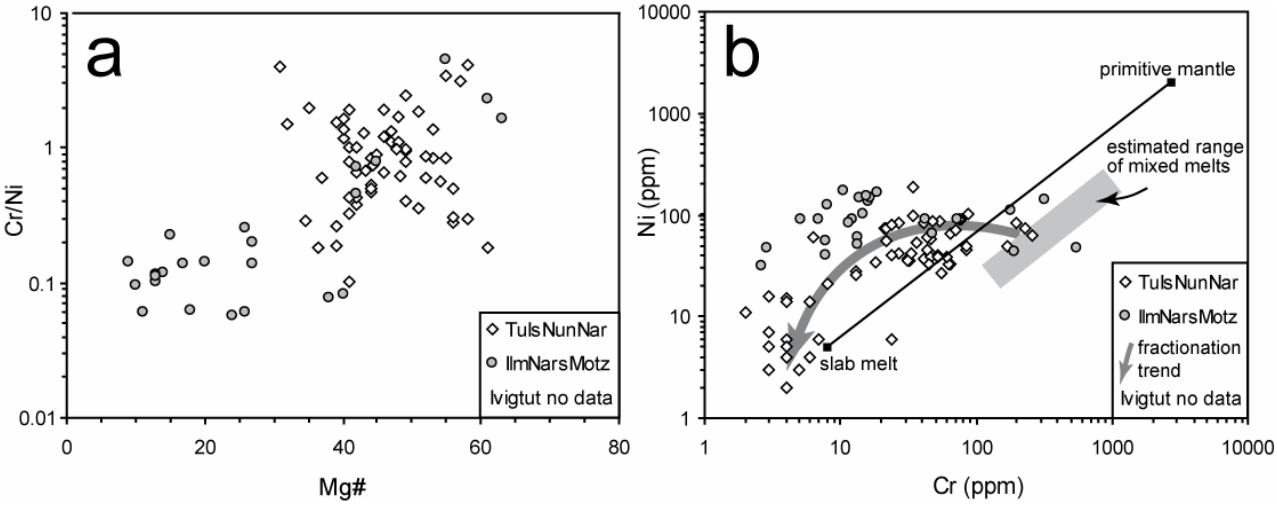

Fig. 8: Peculiar trends for transition metals in the Ilímaussaq-Narsaq-Motzfeldt area. a) The dykes in this region are restricted to lower Cr/Ni ratios and Mg# compared to the rest. According to Martin et al. (2005), the overall positive correlation can be attributed to fractionation processes. b) Most dykes lie above the potential mixing line of the primitive mantle with a slab melt.

The extraordinary trend of the transition metals may be attributed to changes in oxygen fugacity. Morse et al. (1991) showed that the fractionation of Ni in olivine depends on the oxygen fugacity. At low oxygen fugacities near the wüstite-magnetite buffer, about half of the total Ni content in the magma may be present as Ni^0. This part would be retained in the melt and not incorporated into olivine, but later fractionating minerals. Accordingly, Cr was most likely not incorporated into liquidus phases at such low oxygen fugacities and high temperatures (Shearer & Papike, 2005). Marks & Markl (2001) constrained very reduced formation conditions (FMQ -4) for an augite syenite in the 1.16 Ga old (Krumrei et al., 2006) Ilímaussaq intrusion. The dykes from the Ilímaussaq area investigated by us are cut by the intrusive Ilimaussaq complex implying an earlier age. It may therefore be likely that the dyke magma which preceded the Ilímaussaq one was also rather reduced. This in accordance with results from Upton & Thomas (1980) who derived reducing conditions (FMQ down to -5) for the crystallising YGDC magma on Tugtutôq.

5.4 Crustal contamination

The lack of a positive Pb-anomaly in primitive mantle-normalised trace element patterns (Fig. 5) may suggest no or an insignificant upper crustal contamination and indicates negligible late-stage alteration (Le Roex et al., 2001). Assimilation of lower crustal rocks also seems to be insignificant for most of the Gardar dykes, because there is no obvious positive correlation between Zr – Zr/Nb, K/Nb – Zr/Nb or K/Nb – SiO_2 (not shown). Zr/Nb ratios for the majority of dykes vary from 2 to 7. However, the dykes in the region of Isortoq and Nunarssuit (± Tugtutôq) seem to be partly contaminated by lower crustal rocks, because their Zr/Nb ratio ranges from 10 to 29 consistent with Zr/Nb ratios of the continental crust (Taylor & McLennan, 1985). This is also in accordance with results from Halama et al. (2004) who showed that the Isortoq dykes assimilated up to 10 % lower crustal Archaean gneisses. Thus, crustal contamination cannot be entirely ruled out as was also shown by Taylor & Upton (1993). The Pb isotopes they analysed in the Gardar complexes Kûngnât and Tugtutôq showed that the more evolved rocks have lower μ_1 resulting from increasing crustal control in the course of fractional crystallisation (Taylor & Upton, 1993).

6. Constraints on mantle source

Numerous studies dealt with the potential magma source of the Gardar melts. There is general consensus that the majority of melts was derived from a metasomatised, lithospheric mantle and that the melts were only little affected by crustal contamination (Goodenough, 1997; Goodenough et al., 2002; Upton et al., 2003; Halama et al., 2004). This is evidenced by low $^{86}Sr/^{87}Sr$ ratios of 0.703 and initial ε_{Nd} values of +2 to +6 (Pearce & Leng, 1996; Andersen, 1997; Goodenough et al., 2002). However, temporal differences, i.e. differences in the course of the Gardar cycles, can be seen.

The predominating Gardar basalts show trace element patterns different from OIB and preclude an asthenospheric derivation (this study; Upton & Emeleus, 1987). They rather formed by partial melting of sub-continental mantle lithosphere which had been metasomatised by subduction-related fluids rich in LILE and incompatible elements like K, Ba, P and LREE (Upton & Emeleus, 1987; Upton et al., 2003; Goodenough,1997).

Upton (1991) analysed mantle xenoliths from Igdlutalik which are situated within the Tugtutôq-Ilímaussaq-Nunataq lamprophyre suite. The phlogopite-bearing xenoliths comprise can be referred to as garnet-peridotites which may represent the lithospheric mantle at a depth

of more than 60 km. Analysed basaltic dykes have rather low Ce/Yb ratios (mean: 14) and are generally enriched in LREE. According to Mattsson & Oskarsson, 2005, these characteristics could result from small degrees of melting in a garnet-bearing mantle source as garnet retains HREE (McInnes & Cameron, 1994; Martin, 1999). However, the HREE in dykes of this study are still 20 to 100 times enriched relative to chondrite which renders the importance of residual garnet unlikely. It can be rather assumed that the enrichment of LREE over HREE in fact reflects the mantle source which was metasomatised by subduction processes (e.g. Upton & Emeleus, 1987; see below). This is not only evidenced by the LREE enrichment in the dykes, but also in the Gardar intrusions and in the Ketilidian basement itself, i.e. the Julianehåb batholith (Garde et al., 2002).

7. Potential source of F

Smith et al. (1981) and Edgar et al. (1996) considered the various source minerals in the upper mantle that could possibly store volatiles, in particular F and Cl, in their crystal structure. They ruled out dry silicates like olivine, garnet or pyroxene and considered hydrated minerals like amphibole, phlogopite or apatite in which F substitutes for OH^-. However, recent experiments have shown that even nominally F-free minerals like olivine can incorporate remarkable amounts of F up to 0.45 wt% (Bromiley & Kohn, 2007).

7.1 Phlogopite

According to Smith et al. (1981), phlogopite occurs in all rock types of the upper mantle and is the main carrier of H_2O and alkalis. Kushiro et al. (1967) pointed out that F-phlogopite is more stable at higher temperatures than OH-phlogopite. Edgar & Arima (1985) concluded from experiments that F is rather partitioned into phlogopite than apatite making phlogopite a more likely source of F in the mantle. They further showed that the F-content in phlogopite is independent of pressure, but increases with decreasing temperature.

The analysed Gardar dykes only show a weak positive correlation between K_2O and F (Fig. 9 a). If the dykes were derived as partial melts from a phlogopite-bearing mantle source and if all F was stored in mica, the correlation should be more pronounced (Edgar et al., 1996).

7.2 Amphibole

In the mantle, the typical amphibole is K-richterite (ideally $K[NaCa]Mg_5Si_8O_{22}[OH,F]_2$) in which K substitutes for Na at high pressures (Harlow & Davies, 2004). However, the occurrence of K-richterite is mainly restricted to alkaline, K-dominated environments which are not only poor in Al, but can also be Si-undersaturated (Konzett et al., 1997). K-amphiboles may be an important source for alkalis, water and/or trace elements in the mantle (Konzett et al., 1997). Harlow & Davies (2004) found a positive correlation between K and p which in agreement with Konzett et al. (1997) who observed an increase in K/(K+Na) with increasing pressure. In contrast, F is negatively correlated with p, but positively with T. From the K-F relationship of the studied samples (Fig. 9 c), it is evident that not only primitive dykes with a lower K- and F-content, but also more evolved ones lie outside the richterite field (Deer et al., 1997 and references therein). Thus it can be assumed that K-richterite was an insignificant source of F in the mantle.

7.3 Apatite

Smith et al. (1981) pointed out that Cl-bearing, F-rich apatite may be present in the source region of carbonatites derived from the upper mantle. It may thus play an important role in the Gardar Province since there are carbonatitic dykes/complexes (Upton et al., 2003).

According to experiments by Watson (1980), the occurrence of residual apatite in magma source regions is generally precluded since as much as 3-4 wt% P_2O_5 (at 50 wt% SiO_2) are soluble in basic magmas. Therefore, even at low degrees of partial melting, apatite would not be a residual phase. According to that and taking into account the (relatively) high content of phosphorus in most primitive dykes, it can be assumed that apatite has been in the mantle source. This apatite was most likely removed from the mantle source region.

Brenan (1993) experimentally investigated the composition of apatite at high p and T (10-20 kbar, ~ 1000 °C). He found out that only low concentrations of F and Cl in an acidic (H_2O-HCl or CO_2-H_2O) fluid are required to achieve a high X_{FClAp}/X_{OHAp} in apatite. This ratio also rises with aqueous NaCl in direct proportion of F-concentration. Fluid inclusion studies in various Gardar intrusions have shown that the fluid is generally NaCl-dominated and that CO_2 can be a major component, too (Köhler et al., in press; Graser et al., in review; Schönenberger & Markl, in prep.; Konnerup-Madsen et al., 1985; Konnerup-Madsen, 1984). Taken these considerations into account, we suggest that apatite must have been rather enriched in F.

This may have been apatite, because some of those primitive dykes which fall off the phlogopite field do in fact lie within the apatite one (Hogarth, 1988; Boudreau et al., 1993; Campbell & Henderson, 1997; O'Reilly & Griffin, 2000; Bühn et al., 2001; Chakhmouradian et al., 2002; Fig. 9 d). Some primitive dykes from Tugtutôq-Isortoq-Nunarssuit-Narsarsuaq actually coincide with the line defined by a hypothetical fluorapatite with a P/F ratio of 4.89 (Smith et al., 1981; Sigvaldason & Óskarsson, 1986).

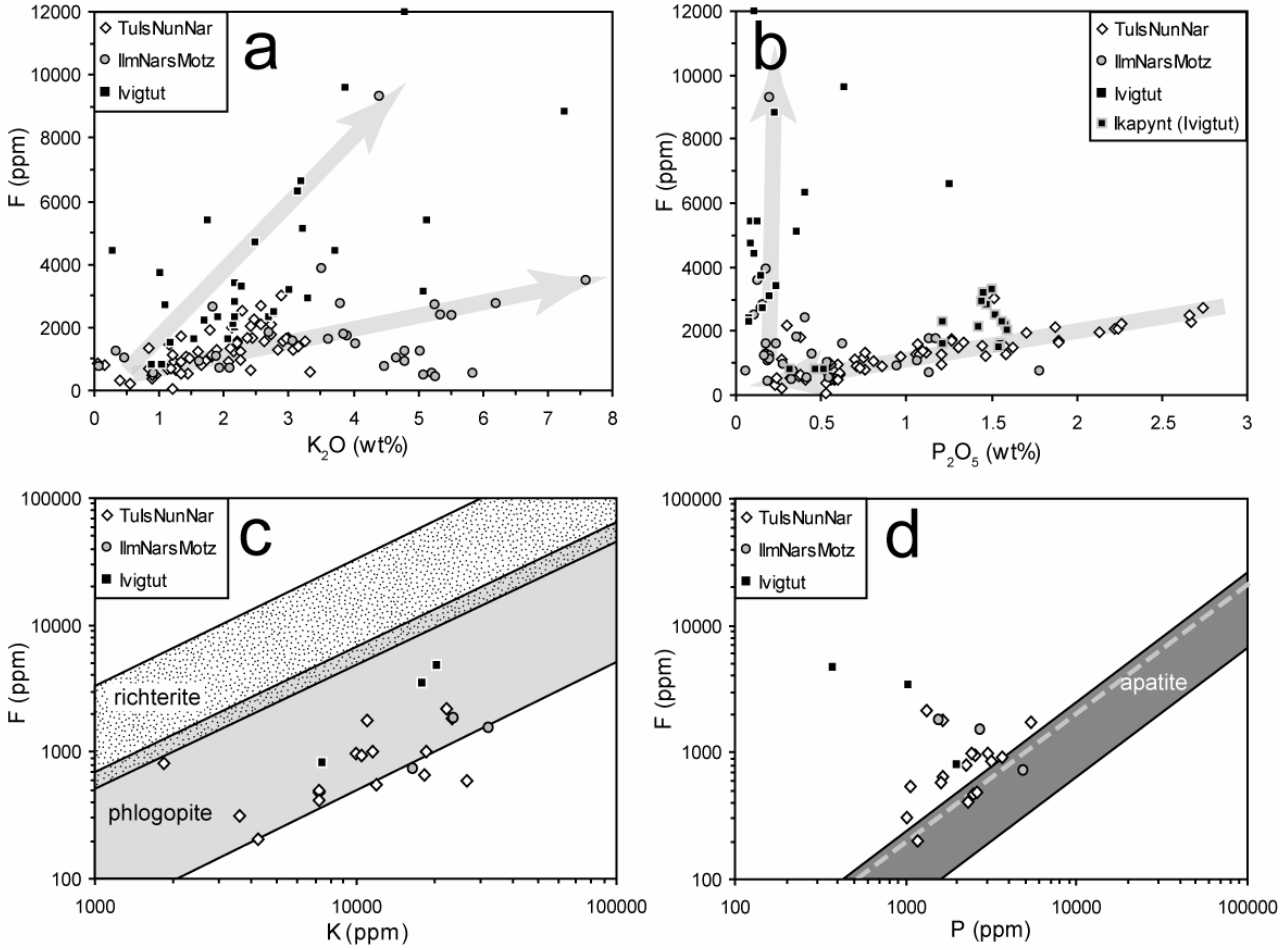

Fig. 9: Diagrams constraining potential mineral reservoirs for F in mantle source. The good correlations between K_2O-F and P_2O_5-F (a, b) suggest F being derived from F-phlogopite and F-apatite, respectively. This is further evidenced by Figs. 7 c and d that show the typical F-K and F-P range for richterite, phlogopite and apatite, respectively (Hogarth, 1988; Boudreau et al., 1993; Campbell & Henderson, 1997; Deer et al., 1997 and references therein; O'Reilly & Griffin, 2000; Bühn et al., 2001; Chakhmouradian et al., 2002; Fleet, 2003 and references therein). Dashed line in d) refers to hypothetical fluorapatite with a P/F ratio of 4.89 (Smith et al., 1981; Sigvaldason & Óskarsson, 1986) [TuIsNunNar = Tugtutôq-Isortoq-Nunarssuit-Narsarsuaq; IlmNarsMotz = Ilímaussaq-Narsaq-Motzfeldt].

To further constrain which mantle phases may have served as an F-reservoir, the range of K/F ratios in richterite (Deer et al., 1997 and references therein) and phlogopite (Fleet, 2003 and references therein) worldwide were compared to the K/F ratios in the most primitive dykes (Mg# > 50; Fig. 9 c). The large overlap of primitive dykes with the K/F-range of phlogopite is striking. Hence, it can be assumed that phlogopite played a crucial role for F-storage in the mantle and that richterite can be neglected. Fig. 9 c also illustrates that only few dykes fall off the phlogopite range suggesting an additional F-rich phase.

8. Mantle metasomatism

The largest part of the Gardar Province is situated within the 1855-1795 Ma old Ketilidian orogen (Fig. 1). This post-collisional belt is the result of the convergence between the Archaean craton and an oceanic plate subducting northward (Chadwick & Garde, 1996).
It is believed that subduction-related processes during the Ketilidian orogeny led to metasomatism of the mantle beneath Gardar resulting in an enrichment of LILE, LREE and other incompatible elements (Upton & Emeleus, 1987; Goodenough,1997; Goodenough et al., 2002; Upton et al., 2003). The relation of Gardar magmas to subduction processes and the Ketilidian orogeny is also evidenced by Nd-model ages which basically range from 1850-1720 Ma (Schönenberger & Markl, in prep.; Marks et al., 2004; Goodenough et al., 2002) and largely correspond to the age of the Ketilidian orogen.

Processes causing mantle metasomatism

Generally, fluid influx can modify the mantle wedge during subduction processes (McCulloch & Gamble, 1991; Arculus, 1994) to produce a hybridised mantle from which calcalkaline rocks form (Green & Ringwood, 1972; Nicholls & Ringwood, 1973). McCulloch & Gamble (1991) and Kessler et al. (2005) demonstrated that HFSE and HREE largely remain immobile during slab-fluxing processes. In contrast, LILE (Rb, Cs, Ba, Sr, U, Pb) and LREE become enriched due to their rock-melt incompability and high mobility (Tatsumi et al., 1986; Tatsumi & Nakamura, 1986).

Two potential processes can lead to mantle metasomatism: a) metasomatism through fluids expelled from the subducting slab or b) metasomatism by felsic-siliceous, slab-derived melts (e.g. Arculus, 1994; Yogodzinski et al., 1994). Both mechanisms are closely related and

can hardly be distinguished. However, Wyllie (1984), Peacock (1990) and Peacock et al. (1994) showed that slab melting is restricted to a) young, hot subducting slab, b) slow subduction into a warm mantle wedge and/or c) highly oblique convergence. Moreover, slab melts which are in equilibrium with an eclogitic (grt + cpx) residue typically have La/Nb and Ba/Nb ratios of 7 and 186, respecitvely (Prouteau et al., 2001).

A special process in subduction zones was described by Klemme (2004). He observed fluoride-glass blebs in lherzolitic xenoliths and inferred fluoride-silicate unmixing in the upper mantle. This unmixing also implies element fractionation where the silicate melt becomes enriched in HREE, HFSE, Ti and Cs. In contrast, the fluorite melt preferably retains LREE, Sr and Ba thus exhibiting subduction-related trace element characteristics. Hence, if unequivocal petrographic evidence lacks, it will be impossible to distinguish if the signature was inherited from slab melts/fluids or if it reflects an unmixed fluoride melt fraction.

Little is known regarding subduction processes beneath the Gardar Province. Garde et al. (2002) note lacking evidence of a continent-continent collision and Chadwick & Garde (1996) describe the oblique convergence between the Archaean craton and an oceanic plate leading to the assumption that slab melting occurred during the Ketilidian orogeny. Rollinson & Tarney (2005) suggested that a magma source with near-constant K/Rb ratios must have been enriched by a fluid rather than melt. The great majority of Gardar dykes has almost constant K/Rb ratios between 350 and 450 suggesting that the mantle wedge was metasomatised by slab fluid-related processes which is also strengthened by both the very low La/Nb (1-3) and Ba/Nb (mean at 39) ratios.

Moreover, samples of this study do not show any evidence for a mantle fluoride-silicate melt immiscibility in the sense of Klemme (2004). The studied thin sections neither comprise any fluoride glass blebs along grain boundaries nor any melt pockets. However, if discussing such immiscibility, the Ivigtut cryolite deposit in the NW of the Gardar Province must be mentioned. The deposit hosts the most F-rich rocks worldwide and actually evolved from fluoride-silicate melt immiscibility. However, this unmixing did not take place in the mantle, but rather at shallow crustal levels and hydrothermal conditions (Pauly & Bailey, 1999; Köhler et al., in press). Furthermore, recalculations assuming 25 ppm F in the primitive mantle (McDonough & Sun, 1994) and the fluorine content of the Ivigtut deposit (Pauly & Bailey, 1999) revealed that only ~ 14 km^3 primitive mantle material would be required to release enough fluorine to form the cryolite deposit at Ivigtut. However, considering the size of the whole Gardar Province (several hundreds of km^2 of outcroping intrusions/dykes), it can be assumed that the total volume of a fluoridic melt in the sense of Klemme (2004) would be

much higher. Moreover, if such an unmixing process had occurred in the Gardar Province, the silicate melt would have been enriched in HREE and HFSE, but the opposite is the case for the dykes (Fig. 5).

9. Summary and Conclusions

The detailed XRF analyses of dykes from all over the failed-rift Gardar Province revealed their moderately to highly evolved nature. Even though they generally display normal fractionation trends, the dykes can be distinguished chronologically and spatially. Older dykes are higher fractionated than younger ones. Trace element distribution shows an enrichment in LILE and LREE while HREE, HFSE, Nb and Ti are depleted. These features together with the high contents of Sr and K_2O suggest subduction-related mantle metasomatism beneath the Gardar Provine and reveal the dykes' strong affinity with shoshonites. The dykes show evidence for plagioclase, Fe-Ti oxide and pyroxene fractionation. In the Ilímaussaq-Narsaq-Motzfeldt area, the dykes describe a peculiar trend where the content of the transition metals Ni, Co, Fe, Zn and Cr suddenly increases at Mg# below 30. This may be attributed to the very reduced nature of the magma source in which Ni is present as Ni^{2+} and Ni^0 with the latter being retained in the melt and not incorporated into minerals.

Generally, all dykes are rich in F and comparable to equally high F contents in Andean rocks. Hence, it can be assumed that an F enrichment may be typical of subduction-related mantle metasomatism, irrespective if it is an active subduction (Andes) or a post-collisional setting (Gardar). In the Gardar Province, this feature can even be observed in dykes (and other rocks) having intruded the crust ca. 700 Ma after the subduction event. Within the Gardar Province, the dykes in the Ivigtut area have the highest content of F suggesting that the extreme F enrichment at the Ivigtut cryolite deposit was not (only) an effect of hydrothermal metasomatic processes, but can also be attributed to a heterogeneously F-enriched mantle. Within the magma source, F may have largely been incorporated into F-phlogopite and F-apatite.

Acknowledgments

Financial support by the Graduiertenförderung des Landes Baden-Württemberg is gratefully acknowledged. Michael Marks kindly provided dyke samples from the Ilímaussaq-Narsaq area. Heiner Taubald, Gisela Bartholomä and Bernd Steinhilber are thanked for performing XRF analyses. Lotte Melchior Larsen from GEUS helped with sample maps and Bjørn Thomassen with GEUS archive material. Gerlind Dreibus gave valuable advice during the set-up of pyrohydrolysis. Thomas Wenzel improved an earlier version of the manuscript significantly. His help is greatly acknowledged.

References

ANDERSEN, T., 1997. Age and petrogenesis of the Qassiarsuk carbonatite-alkaline silicate volcanic complex in the Gardar rift, South Greenland. Mineralogical Magazine 61, 499-514.

ARCULUS, R.J., 1994. Aspects of magma genesis in arcs. Lithos 33, 189-208.

BAGCI, U., PARLAK, O., HÖCK, V., 2005. Whole-rock and mineral chemistry of cumulates from the Kizildağ (Hatay) ophiolite (Turkey): clues for multiple magma generation during crustal accretion in the southern Neotethyan ocean. Mineralogical Magazine, 69, 53-76.

BAILEY, J.C., 1977. Fluorine in granitic rocks and melts: a review. Chemical Geology 19, 1-42.

BAILEY, J.C., Gwozdz, R., Rose-Hansen, J., Sørensen, H., 2001. Geochemical overview of the Ilímaussaq alkaline complex, South Greenland. In: Sørensen, H. (Ed.), The Ilímaussaq Alkaline Complex, South Greenland, Status of Mineralogical Research with New Results. Geology of Greenland Survey Bulletin 190, 35-54.

BLAXLAND, A.B., VAN BREEMEN, O., EMELEUS, C.H., ANDERSON, J.G., 1978. Age and origin of the major syenite centres in the Gardar Province of South Greenland: Rb-Sr studies. Geological Society American Bulletin 89, 231-244.

BOTTOMLEY, D.J., CLARK, I.D., BATTYE, N., KOTZER, T., 2005. Geochemical and isotopic evidence for a genetic link between Canadian Shield brines, dolomitization in the Western Canada Sedimentary Basin, and Devonian calcium-chloridic seawater. Canadian Journal of Earth Sciences 42, 2059-2071.

BOUDREAU, A.E., LOVE, C., HOATSON, D.M., 1993. Variation in the composition of apatite in the Munni Munni Complex and associated intrusions of the Wet Pilbara Block, Western Australia. Geochimica et Cosmochimica Acta 57, 4467-4477.

BRENAN, J.M., 1993. Partitioning of fluorine and chlorine between apatite and aqueous fluids at high pressure and temperature: implications for the F and Cl content of high P-T fluids. Earth and Planetary Science Letters 117, 251-263.

BROMILEY, D.V., KOHN, S.C., 2007. Comparisons between fluoride and hydroxide incorporation in nominally anhydrous and fluorine-free mantle minerals. Geochimica et Cosmochimica Acta 71, Goldschmidt Conference Abstracts, A124.

BUREAU, H., METRICH, N., 2003. An experimental study of bromine behaviour in water-saturated silicic melts. Geochimica et Cosmochimica Acta 67, 1689-1697.

BUREAU, H., KEPPLER, H., METRICH, N., 2000. Volcanic degassing of bromine and iodine: experimental fluid/melt partitioning data and applications to stratospheric chemistr. Earth and Planetary Science Letters 183, 51-60.

BÜHN, B., WALL, F., LE BAS M.J., 2001. Rare-earth element systematics of carbonatitic fluorapatites, and their significance for carbonatite magma evolution. Contributions to Mineralogy and Petrology 141, 572-591.

CAMPBELL, L.S., HENDERSON, P., 1997. Apatite paragenesis in the Bayan Obo REE-Nb-Fe ore deposit, Inner Mongolia, China. Lithos 42, 89-103.

CANDELA, P.A., 1986. Toward a thermodynamic model for the halogens in magmatic systems; an application to melt-vapor-apatite equilibria. Chemical Geology 57, 289-301.

CARMICHAEL, I.S.E., TURNER, F.J., VERHOOGEN, J., 1974. Igneous petrology. McGraw-Hill Books Co., New York. 739 p.

CARROLL, M.R., WEBSTER, J.D., 1994. Solubilities of sulfur, noble gases, nitrogen, chlorine, and fluorine in magmas. In: Carroll, M.R., Holloway, J.R. (Eds.), Volatiles in Magmas, Reviews in Mineralogy 30, Mineralogical Society of America.

CHADWICK, B., GARDE, A.A., 1996. Palaeoproterozoic oblique plate convergence in South Greenland: a re-appraisal of the Ketilidian orogen. From: Brewer, T.S., Atkin, B.P. (Eds.), Precambrian crustal evolution in the North Atlantic Region. Geological Society of London, Special Publication 112, 179-196.

CHAKHMOURADIAN, A.R., REGUIR, EKATARINA, MITCHELL, R.H., 2002. Strontium-apatite: new occurrences, and the extent of Sr-FOR-Ca Substitution in apatite-group minerals. The Canadian Mineralogist 40, 121-136.

COATS, R.R., 1953. Geology of Buldir Island, Aleutian Islands, Alaska. U.S. Geological Survey Bulletin 989-A, 1-26.

COATS, R.R., NELSON, W.H., LEWIS, R.Q., POWERS, H.A., 1959. Geological reconnaissance of Kiska Island, Aleutian Islands, Alaska. U.S. Geological Service Bulletin 1028-R, 563-581.

DEER, W.A., HOWIE, R.A., ZUSSMAN, J., 1997. Rock-forming minerals. Volume 2B: Double-chain silicates. The Geological Society, London, 616-634.

DEFANT, M.J., DRUMMOND, M.S., 1990. Derivation of some modern arc magmas by melting of young subducted lithosphere. Nature 347, 662-665.

DOLEJS, D., BAKER, R., 2007 a. Liquidus Equilibria in the System K_2O-Na_2O-Al_2O_3-SiO_2-F_2O_{-1}-H_2O to 100 Mpa: I. Silicate-Fluoride Liquid Immiscibility in Anhydrous Systems. Journal of Petrology 48, 785-806.

DOLEJS, D., BAKER, R., 2007 b. Liquidus Equilibria in the System K_2O-Na_2O-Al_2O_3-SiO_2-F_2O_{-1}-H_2O to 100 Mpa: II. Differentiation Paths of Fluorosilicic Magmas in Hydrous Systems. Journal of Petrology 48, 807-828.

DREIBUS, G., SPETTEL, B., WANKE, H., 1979. Halogens in meteorites and their primordial abundances. In: Ahrens, L.H. (Ed.), Origin and Distribution of the Elements. Wiley, 33-38.

DREWES, H., FRASER, D.G., SNYDER, G.L., BARNETT, H.F., 1961. Geology of Unalaska Ilsand and adjacent insular shelf, Aleutian Islands, Alaska. U.S. Geological Survey Bulletin 1028-S, 583-676.

DRUMMOND, M.S., DEFANT, M.J., KEPEZHINSKAS, P.K., 1996. Petrogenesis of slab-derived trondhjemite-tonalite-dacite/adakite magmas. Transactions of the Royal Society of Edinburgh: Earth Sciences 87, 205-215.

EDGAR, A.D., ARIMA, M., 1985. Fluorine and chlorine contents of phlogopite crystallized from ultrapotassic rock compositions in high pressure experiments: Implications for halogen reservoirs in source rocks. American Mineralogist 70, 529-536.

EDGAR, A.D., PIZZOLATO, L.A., SHEEN, J., 1996. Fluorine in igneous rocks and minerals with emphasis on ultrapotassic mafic and ultramafic magmas and their mantle source regions. Mineralogical Magazine 60, 243-257.

ESCHER, A., WATT, W.S., 1976. Geology of Greenland. Geological Survey of Greenland, Copenhagen, 603 p.

FLEET, M.E., 2003. Micas. In: Deer, W.A., Howie, R.A., Zussman, J. (Eds.), Rock-forming minerals, Volume 2B. The Geological Society, London, 354-369.

GARDE, A.A., HAMILTON, M.A., CHADWICK, B., GROCOTT, J., MCCAFFREY, K.J.W., 2002. The Ketilidian orogen of South Greenland: geochronology, tectonics, magmatism, and fore-arc accretion during Palaeoproterozoic oblique convergence. Canadian Journal of Earth Sciences 39, 765-793.

GOVINDARAJU, K. 1994. Compilation of working values and sample description for 383 geostandards. Geostandards Newsletter 18, 158 p.

GRASER, G., POTTER, J., KÖHLER, J., MARKL, G., submitted to Lithos. Isotopic, major, minor and trace element geochemistry of late-stage fluids in the peralkaline Ilímaussq intrusion, South Greenland.

GREEN, T.H., RINGWOOD, A.E., 1972. Crystallization of garnet-bearing rhyodacite under high pressure hydrous conditions. Journal of the Geological Society of Australia 19, 203-212.

GOODENOUGH, K.M., 1997. Geochemistry of Gardar Intrusions in the Ivigtut area, South Greenland. PhD thesis, Edinburgh.

GOODENOUGH, K.M., UPTON, B.G.J., ELLAM, R.M., 2002. Long-term memory of subduction processes in the lithospheric mantle: evidence from the geochemistry of basic dykes in the Gardar Province of South Greenland. Journal of the Geological Society, London 159, 705-714.

HALAMA, R., WAIGHT, T., MARKL, G., 2002. Geochemical and isotopic zoning patterns of plagioclase megacrysts in gabbroic dykes from the Gardar Province, South Greenland; implications for crystallisation processes in anorthositic magmas. Contributions to Mineralogy and Petrology 144, 109-127.

HALAMA, R., MARKS, M., BRÜGMANN, G., SIEBEL, W., WENZEL, T., MARKL, G., 2004. Crustal contamination of mafic magmas; evidence from a petrological and Sr-Nd-Os-O isotopic study of the Proterozoic Isortoq dike swarm, South Greenland. Lithos 74, 3-4, 199-232.

HALTER, W.E., BAIN, N., BECKER, K., HEINRICH, C.A., LANDTWING, M., VONQUADT, A., CLARK, A.H., SASSO, A.M., BISSIG, T., TOSDAL, R. M., 2004. From andesitic volcansim to the formation of a porphyry Cu-Au mineralizing magma chamber : the Farallón Negro Volcanic Complex, northwestern Argentina. Journal of Volcanology and Geothermal Research 136, 1-30.

HARLOW, G.E., DAVIES, R., 2004. Status report on stability of K-rich phases at mantle conditions. Lithos 77, 647-653.

HOGARTH, D.D., 1988. Chemical composition of fluorapatite and associated minerals from skarn near Gatineau, Quebec. Mineralogical Magazine 52, 347-358.

KELEMEN, P.B., 1995. Genesis of high Mg# andesites and the continental crust. Contributions to Mineralogy and Petrolog 120, 1-19.

KESSLER, R., SCHMIDT, M.W., ULMER, P., PETTKE, T., 2005. Trace element signature of subduction-zone fluids, melts and supercritical liquids at 120-180 km depth. Nature 437, 724-727.

KLEMME, S., 2004. Evidence for fluoride melts in Earth's mantle formed by liquid immiscibility. Geology 32, 441-444.

KOGARKO, L.N., 1974. Role of Volatiles. In: Sørensen, H. (Ed.), The Alkaline Rocks. London: John Wiley & Sons., 474-487.

KOGARKO, L.N., RYABCHIKOV, I.D., 1978. Volatile components in magmatic processes. Geochemistry International 15, 9-32.

KÖHLER, J., KONNERUP-MADSEN, J., MARKL, G., in press. Fluid geochemistry in the Ivigtut cryolite deposit, South Greenland. Lithos. doi: 10.1016/j.lithos.2007.10.005

KONNERUP-MADSEN, J., 1984. Compositions of fluid inclusions in granites and quartz syenites from the gardar continental rift province (South Greenland). Bulletin de Minéralogie 107, 327-340.

KONNERUP-MADSEN, J., DUBESSY, J., ROSE-HANSEN, J., 1985. Combined Raman microprobe spectrometry and microthermometry of fluid inclusions in minerals from igneous rocks of the Gardar province (south Greenland). Lithos 18, 271-280.

KONZETT, J., 1997. Phase relations and chemistry of Ti-rich K-richterite-bearing mantle assemblages: an experimental study at 8.0 GPa in a Ti-KNCMASH system. Contributions to Mineralogy and Petrology 128, 385-404.

KONZETT, J., SWEENEY, R.J., THOMPSON, A.B., ULMER, P., 1997. Potassium Amphibole Stability in the Upper Mantle: an Experimental Study in a Peralkaline KNCMASH System to 8.5 GPa. Journal of Petrology 38, 537-568.

KRUMREI, T.V., VILLA, I.M., MARKS, M., MARKL, G., 2006. A 40Ar/39Ar and U/Pb isotopic study of the Ilímaussaq Complex, South Greeland; implications for the 40K decay constant and for the duration of magmatic activity in a peralkaline complex. Chemical Geology 227, 258-273.

KULLERUD, K., 1996. Chlorine-rich amphiboles: interplay between amphibole composition and an evolving fluid. European Journal of Mineralogy 8, 355-370.

KUSHIRO, I., SYONO, Y., AKIMOTO, S., 1967. Stability of phlogopite at high pressures and possible presence of phlogopite in the Earth's upper mantle. Earth and Planetary Science Letters 3, 197-203.

LE MAITRE, R.W., BATEMAN, P., DUDEK, A., KELLER, J., LAMEYRE LE BAS, M.J., SABINE, P.A., SCHMID, R., SØRENSEN, H., STRECKEISEN, A., WOOLLEY, A.R., ZANETTIN, B., 1989. A classification of igneous rocks and glossary of terms. Blackwell, Oxford, 193 p.

LE ROEX, A., SPÄTH, A., ZARTMAN, R.E., 2001. Lithospheric thickness beneath the southern Kenya Rift : implications from basalt geochemistry. Contribution to Mineralogy and Petrology 142, 89-106.

LOWENSTERN, J.B., 1994. Chlorine, fluid immiscibility, and degassing in peralkaline magmas from Pantelleria, Italy. American Mineralogist 79, 353-369.

MARKL, G., SCHUMACHER, J.C., 1996. Spatial variations in temperature and composition of greisen-forming fluids; an example from the Variscan Triberg granite complex, Germany. Economic Geology and the Bulletin of the Society of Economic Geologists 91, 576-589.

MARKS, M., MARKL, G., 2001. Fractionation and Assimilation Processes in the Alkaline Augite Syenite Unit of the Ilímaussaq Intrusion, South Greenland, as Deduced from Phase Equilibria. Journal of Petrology 42, 1947-1969.

MARKS, M., VENNEMANN, T., SIEBEL, W., MARKL, G., 2004. Nd-, O-, and H-isotopic evidence for complex, closed-system fluid evolution of the peralkaline Ilímaussaq Intrusion, South Greenland. Geochimica Cosmochimica Acta 68, 3379-3395.

MARTIN, A.R., 1985. The Evolution of the Tugtutôq-Ilímaussaq Dyke Swarm, Southwest Greenland. PhD thesis, Edinburgh.

MARTIN, H., 1999. Adakitic magmas; modern analogues of Archean granitoids. Lithos 46, 411-429.

MARTIN, H., SMITHIES, R.H., RAPP, R., MOYEN, J.-F., CHAMPION, D., 2005. An overview of adakite, tonalite-trondhjemite-granodiorite (TTG), and sanukitoid: relationships and some implications for crustal evolution. Lithos 79, 1-24.

MATTSSON, H.B., OSKARSSON, N., 2005. Petrogenesis of alkaline basalts at the tip of a propragating rift: Evidence from the Heimaey volcanic centre, south Iceland. Journal of Volcanology and Geothermal Research 147, 245-267.

MCCULLOCH, M.T., GAMBLE, J.A., 1991. Geochemical and geodynamic constraints on subduction zone magmatism. Earth and Planetary Science Letters 102, 358-374.

MCDONOUGH, W.F.M., SUN, S.S., 1995. The composition of the Earth. Chemical Geology 120, 223-253.

MCINNES, B.I.A., CAMERON, E.M., 1994. Carbonated, alkaline hybridizing melts from a sub-arc environment: mantle wedge samples from the Tabar-Lihir-Feni arc, Papua New Guinea. Earth and Planetary Science Letters 122, 125-141.

METRICH, N., RUTHERFORD, M.J., 1992. Experimental study of chlorine behavior in hydrous silicic melts. Geochimica Cosmochimica Acta 56, 607-616.

MICHEL, A., VILLEMANT, B., 2003. Determination of Halogens (F,Cl,Br,I), Sulfur and Water in Seventeen Geological Reference Materials. Geostandards Newsletters 27, 163-171.

MIDDLEMOST, E.A.K., 1989. Iron oxidation ratios, norms and the classification of volcanic rocks. Chemical Geology 77, 19-26.

MORGAN, GEORGE, B. VI., LONDON, D., LUEDKE, R.G., 1998. Petrochemistry of Late Miocene Peraluminous Silicic Volcanic Rocks from the Morococala Field, Bolivia. Journal of Petrology 39, 601-632.

MORSE, S.A., RHODES, J.M., NOLAN, K.M., 1991. Redox effect on the partitioning of nickel in olivine. Geochimica et Cosmochimica Acta 55, 2373-2378.

NICHOLLS, I.A., RINGWOOD, A.E., 1973. Effect of water on olivine stability in tholeiites and production of silica-saturated magmas in the island arc environment. Journal of Geology 81, 285-300.

NIJLAND, T.G., JANSEN, J.B.H., MAIJER, C., 1993. Halogen geochemistry of fluid during amphibolite-granulite metamorphism as indicated by apatite and hydrous silicates in basic rocks from the Bamble sector, South Norway. Lithos 30, 167-189.

NYE, C.J., TURNER, D.L., 1990. Petrology, geochemistry and age of the Spurr Volcanic Complex, Eastern Aleutian Arc. Bulletin of Volcanology 52, 205-226.

O'REILLY, S.Y., GRIFFIN, W.L., 2000. Apatite in the mantle: implications for metasomatic processes and high heat production in Phanerozoic mantle, Lithos 53, 217-232.

PAN, Y., FLEET, M.E., 1996. Rare element mobility during prograde granulite facies metamorphism: significance of fluorine. Contributions to Mineralogy and Petrology 123, 251-262.

PAULY, H., BAILEY, J.C., 1999. Genesis and evolution of the Ivigtut cryolite deposit, SW Greenland. Meddelelser om Grønland, Geoscience 37, 60 p.

PEACOCK, S.M., 1990. Fluid processes in subduction zones. Science 248, 329-337.

PEACOCK, S.M., RUSHMER, T., THOMPSON, A.B., 1994. Partial melting of subducting oceanic crust. Earth and Planetary Science Letters 121, 227-244.

PEARCE, N.J.G., LENG, M.J., 1996. The origin of carbonatites and related rocks from the Igaliko Dyke Swarm, Gardar Province, South Greenland: field, geochemical and C-O-Sr-Nd isotope evidence. Lithos 39, 21-40.

PROUTEAU, G., SCAILLET, B., PICHAVANT, M., MAURY, R., 2001. Evidence for mantle metasomatism by hydrous silicic melts derived from subducted oceanic crust. Nature 410, 197-200.

ROLLINSON, H.R., TARNEY, J., 2005 Adakites – the key to understanding LILE depletion in granulites. Lithos 79, 61-81.

SALVI, S., FONTAN, F., MONCHOUX, P., WILLIAMS-JONES, A.E., MOINE, B., 2000. Hydrothermal Mobilization of High Field Strength Elements in Alkaline Igneous Systems: Evidence from the Tamazeght Complex (Morocco). Economomic Geology 95, 559-576.

SCHMIDBERGER, S., SIMONETTI, A., HEAMAN, L.M., CREASER, R.A., WHITEFORD, S., 2007. Lu–Hf, in-situ Sr and Pb isotope and trace element systematics for mantle eclogites from the Diavik diamond mine: Evidence for Paleoproterozoic subduction beneath the Slave craton, Canada. Earth and Planetary Science Letters 254, 55–68.

SCHÖNENBERGER, J., KÖHLER, J., MARKL, G., 2007. REE systematics of fluorides, calcite and siderite in peralkaline plutonic rocks from the Gardar Province, South Greenland. Chemical Geology, doi : 10.1016/j.chemgeo.2007.10.002.

SHEARER, C.K., PAPIKE, J.J., 2005. Early crustal building processes on the Moon; models for the petrogenesis of the magnesian suite. Geochimica et Cosmochimica Acta 69, 3445-3461.

SIGVALDASON, G.E., ÓSKARSSON, N., 1986. Fluorine in basalts from Iceland. Contributions to Mineralogy and Petrology 94, 263-271.

SMITH, J.V., DELANEY, J.S., HERVIG, R.L., DAWSON, J.B., 1981. Storage of F and Cl in the upper mantle; geochemical implications. Lithos 2, 133-147.

SØRENSEN, H., BOHSE, H., BAILEY, J.C., 2006. The origin and mode of emplacement of lujavrites in the Ilimaussaq alkaline complex, South Greenland. Lithos 91, 286-300.

TAGIROV, B., SCHOTT, J., HARRICHOURRY, J.C., SALVI, S., 2002. Experimental study of aluminum speciation in fluoride-rich supercritical fluids. Geochimica et Cosmochimica Acta 66, 2013-2024.

TATSUMI, Y., HAMILTON, D.L., NESBITT, R.W., 1986. Chemical characteristics of fluid phase from a subducted lithosphere and origin of arc magmas: evidence from high-pressure experiments and natural rocks, Journal of Volcanology and Geothermal Reasearch 29, 293-309.

TATSUMI, Y., NAKAMURA, N., 1986. Composition of aqueous fluid from serpentinite in the subducted slab. Geochemical Journal 30, 191-196.

TAYLOR, P.N., UPTON, B.G.J., 1993. Contrasting Pb isotopic compositions in two intrusive complexes of the Gardar Magmatic Province of South Greenland. Chemical Geology 104, 261-268.

TAYLOR, S.R. & MCLENNAN, S.M., 1985. The Continental Crust: its Composition and Evolution. Oxford: Blackwell Scientific, 312 p.

TSUCHIYA, N., SUZUKI, S., KIMURA, J.-I., KAGAMI, H., 2005. Evidence for slab melt/mantle reaction: petrogenesis of Early Cretaceous and Eocene high-Mg andesites from the Kitakami Mountains, Japan. Lithos 79, 179-206.

UPTON, B.G.J., 1962. Geology of Tugtutôq and neighbouring islands, South Greenland. Part I. Meddelelser om Grønland, Grønlands Geologiske Undersøgelse 169, p.60.

UPTON, B.G.J., THOMAS, J.E., 1980. The Tugtutôq Younger Giant Dyke Complex, South Greenland; fractional crystallization of transitional olivine basalt magma. Journal of Petrology 21, 167-198.

UPTON, B.G.J., STEPHENSON, D., MARTIN, A.R., 1985. The Tugtutôq older giant dyke complex: mineralogy and geochemistry of an alkali gabbro-augite-syenite-foyaite association in the Gardar Province of South Greenland. Mineralogical Magazine 49, 623-642.

UPTON, B.G.J., EMELEUS, C.H., 1987. Mid-Proterozoic alkaline magmatism in southern Greenland: the Gardar province. From: Fitton, J.G. & Upton, B.G.J. (Eds.), Alkaline Igneous Rocks. Geological Society Special Publication No. 30, 449-471.

UPTON, B.G.J., 1991. Gardar mantle xenoliths; Igdlutalik, South Greenland. Rapport – Grønlands Geologiske Undersøgelse, Report – Geological Survey of Greenland 150, 37-43.

UPTON, B.G.J., EMELEUS, C.H., HEAMAN, L.M., GOODENOUGH, K.M, FINCH, A.A., 2003. Magmatism of the mid-Proterozoic Gardar Province, South Greenland: chronology, petrogenesis and geological setting. Lithos 68, 43-65.

VEKSLER, I., 2004. Liquid immiscibility and its role at the magmatic-hydrothermal transition: a summary of experimental studies. Chemical Geology 210, 7-31.

WATSON, E.B., 1980. Apatite and phosphorus in mantle source regions: an experimental study of apatite/melt equilibria at pressures to 25 kbar. Earth and Planetary Science Letters 51, 322-335.

WEBSTER, J.D., 1990. Partitioning of F between H_2O and CO_2 fluids and topaz rhyolite melt. Implications for mineralizing magmatic-hydrothermal fluids in F-rich granitic systems. Contributions to Mineralogy and Petrology 104, 424-438.

WILLIAMS-JONES, A.E., SAMSON, I.M., OLIVIO, G.R., 2000. The genesis of hydrothermal fluorite-REE deposits in the Gallinas Mountains, New Mexico. Economic Geology and the Bulletin of the Society of Economic Geologists 95, 327-341.

WOOD, S.A., 2003. The geochemistry of rare earth elements and ytttrium in geothermal waters. In: Simmons, S.F., Graham, I. (Eds.), Volcanic, geothermal, and ore-forming fluids; rules and witnesses of processes within the Earth. Special Publication (Society of Economic Geologists (U.S.) 10, 133-158.

WYLLIE, P.J., 1984. Sources of granitoid magmas at convergent plate boundaries. Physics of The Earth and Planetary Interiors 35, 12-18.

YOGODZINSKI, G.M., VOLYNETS, O.N., KOLOSKOV, A.V., SELIVERSTOV, N.I., MATVENKOV, V.V., 1994. Magnesian andesites and the subduction component in a strong calc-alkaline series at Piip volcano, Far Western Aleutians. Journal of Petrology 35, 163-204.

Fluid geochemistry in the Ivigtut cryolite deposit, South Greenland

Jasmin Köhler[1], Jens Konnerup-Madsen[2] and Gregor Markl[1*]

[1]Eberhard-Karls Universität Tübingen
Institut für Geowissenschaften
AB Mineralogie und Geodynamik
Wilhelmstraße 56
72074 Tübingen
GERMANY

[2]Københavns Universitet
Geologisk Institut
Øster Voldgade 10
1350 København K
DENMARK

in press bei Lithos: doi: 10.1016/j.lithos.2007.10.005

*Corresponding author

Telephone: +49 7071 2972930
Fax: +49 7071 293060
e-mail: markl@uni-tuebingen.de

Abstract

The 1.27 Ga old Ivigtut (Ivittuut) intrusion in South Greenland is world-famous for its hydrothermal cryolite deposit [Na_3AlF_6] situated within a strongly metasomatised A-type granite stock. This detailed fluid inclusion study characterises the fluid present during the formation of the cryolite deposit and thermodynamic modelling allows to constrain its formation conditions.

Microthermometry revealed three different types of inclusions: (1) pure CO_2, (2) aqueous carbonic and (3) saline aqueous inclusions. Melting temperatures range between -23 to -15 °C for type 2 and from -15 to -10 °C for type 3 inclusions. Most inclusions homogenise between 110 and 150 °C into the liquid.

Stable isotope compositions of CO_2 and H_2O were measured from crushed inclusions in quartz, cryolite, fluorite and siderite. The $\delta^{13}C$ values of about -5 ‰ PDB are typical of mantle-derived magmas. The differences between $\delta^{18}O$ of CO_2 (+21 to +42 ‰ VSMOW) and $\delta^{18}O$ of H_2O (-1 to -21.7 ‰ VSMOW) suggest low-temperature isotope exchange. δD (H_2O) ranges from -19 to -144 ‰ VSMOW. The isotopic composition of inclusion water closely follows the meteoric water line and is comparable to Canadian Shield brines. Ion chromatography revealed the fluid's predominance in Na, Cl and F. Cl/Br ratios range between 56 and 110 and may imply intensive fluid-rock interaction with the host granite.

Isochores deduced from microthermometry in conjunction with estimates for the solidification of the Ivigtut granite suggest a formation pressure of approximately 1-1.5 kbar for the fluid inclusions. Formation temperatures of different types of fluid inclusions vary between 100 and 400 °C. Thermodynamic modelling of phase assemblages and the extraordinary high concentration in F (and Na) may indicate that the cryolite body and its associated fluid inclusions could have formed during the continuous transition from a volatile-rich melt to a solute-rich fluid.

Keywords: peralkaline, fluid inclusions, cryolite, Ivigtut, fluorine

1. Introduction

Fluids associated with (per)alkaline rocks play an important role in the mobilisation, transport and enrichment of elements like Zr, Ta, Nb or the REE which are normally immobile: This "fenitisation" is a common metasomatism feature in and around alkaline silicate rocks or carbonatites. During this process, these elements are highly mobile (Sindern & Kramm, 2000; Ranløv & Dymek, 1991; Kresten, 1988; Sturt & Ramsay, 1965; Rock, 1976) and can be redeposited even to economic levels (Kogarko, 1980; Salvi & Williams-Jones, 1990; 2006). Their transport capability is often explained by the high contents of F in the fluid and by complexation phenomena (Wood, 1990; 2003; Irber, 1999). Moreover, the possibility of a continuous liquid-fluid transition has been discussed (Veksler, 2004; Badanina et al., 2004; Sowerby & Keppler, 2002; Thomas et al., 2000) which would render the fluid composition much more concentrated in elements that commonly partition into the silicate melt during normal fluid exsolution process.

Previous fluid inclusion studies in (per)alkaline igneous systems like the Strange Lake Pluton//Labrador, Mt. St. Hilaire Complex/Quebec or Lovozero & Khibina/Kola Peninsula showed remarkable similiarities: the fluid is generally methane- and/or CO_2-dominated with the aqueous component being enriched in sodium (Currie et al., 1986; Salvi & Williams-Jones, 1990; Potter et al., 2004; Nivin et al., 2001; 2002; 2005; Beeskow et al., 2006).

Extensive research on peralkaline fluids has been conducted in the Gardar Province, South Greenland where silica-undersaturated and silica-oversaturated igneous complexes occur (Upton et al., 2003). The studies have focused on the Ilímaussaq intrusion which is the type locality of agpaitic rocks (Sørensen, 2001; Larsen & Sørensen, 1987; Marks & Markl, 2001; Markl et al., 2001). The origin and development of the magmatic, hydrocarbon-dominated Ilímaussaq fluid was studied in detail by Konnerup-Madsen & Rose-Hansen (1984), Konnerup-Madsen et al. (1988) and Graser et al. (in review). Konnerup-Madsen & Rose-Hansen (1982), Konnerup-Madsen (1984; 2001) and Konnerup-Madsen et al. (1985) further compared fluid inclusions from Ilímaussaq with other alkaline complexes in the Gardar Province. Their results showed that Gardar fluid inclusions vary in composition from CO_2-CH_4 and CO_2-CH_4-H_2O mixtures to aqueous saline fluids with the latter being the most abundant type. The either methane-dominated or rather oxidised nature of fluid inclusions from Gardar complexes is interpreted to result from highly varying redox conditions in the melt which in turn govern the redox state in the fluid (Marks et al., 2003; Marks et al., 2004; Markl et al., 2001)

The Ivigtut complex (also known as *Ivittuut*) is world-famous for its unique cryolite deposit. The occurrence of cryolite is restricted to a few places world-wide (e.g. Mt. Rosa area/Colorado (Gross & Heinrich, 1966), Jos Plateau/Nigeria (Williams et al., 1956), Miask/Russia (Palache et al., 1951)). It is commonly a late phase in alkalic granites/pegmatites (Gross & Heinrich, 1966) which is also the case for Ivigtut (Pauly & Bailey, 1999; Goodenough et al., 2000). In order to understand the origin and formation conditions of this unique deposit, it is essential to constrain the fluid's characteristics, since the fluid played the major part in the formation of the deposit.

2. Geological Setting of the Ivigtut cryolite deposit

The Ivigtut intrusion belongs to the Gardar Province (1.35-1.14 Ga) in South Greenland which represents a failed rift structure between the Archaean craton in the north and the 1.85-1.72 Ga old Ketilidan orogen in the south. Its granitoid basement was intruded by numerous dyke swarms and 12 major alkaline to peralkaline complexes (Upton et al., 2003) .

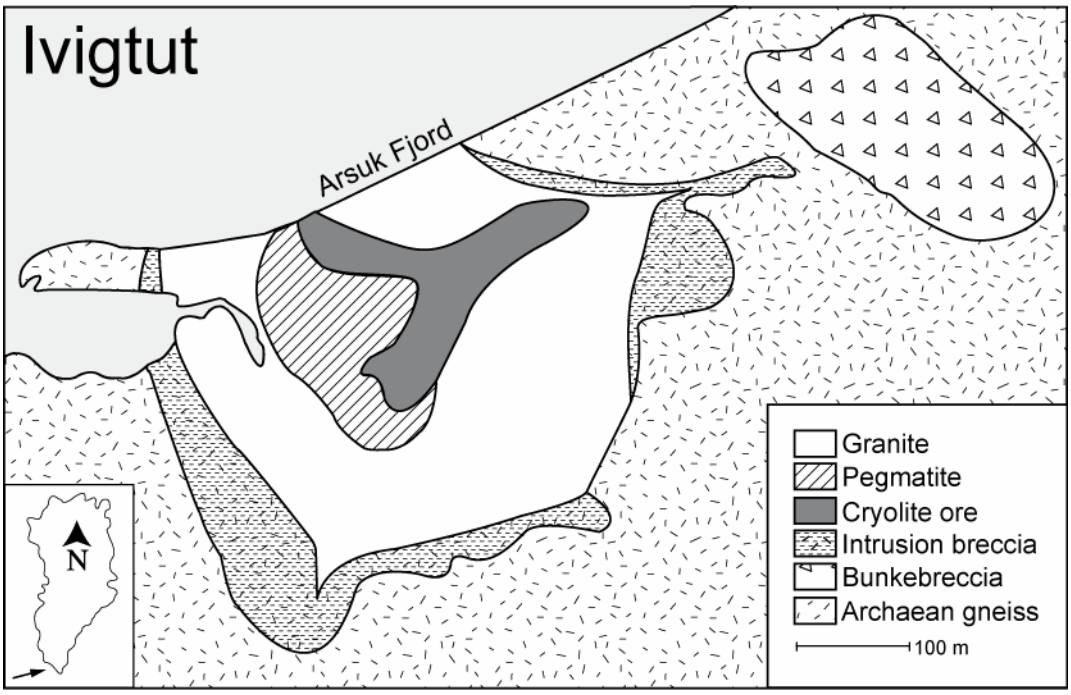

Fig. 1: Geological map of the Ivigtut intrusion and the cryolite deposit situated in Archaean gneiss. Modified after Pauly & Bailey (1999).

The 1.27 Ga old (Upton, unpublished data) Ivigtut intrusion (Fig. 1) is world-famous for its cryolite [Na_3AlF_6] deposit of 12.3 million tons. The complex intruded Archaean gneisses and consists of a A-type granite stock which is surrounded by an intrusion breccia. The 150 m wide cryolite body is situated between an upper hypersolvus and a lower subsolvus granite (Goodenough et al., 2000). Pauly & Bailey (1999) proposed the following evolution model for the deposit: The subsolvus granite developed during intensive metasomatism caused by F-rich, post-magmatic fluids from depth leading to recrystallisation of the feldspar. During metasomatism, a hydrous aluminofluoride melt formed which subsequently separated into fluoride and siliceous melt fractions. Cryolite and associated minerals crystallised from the fluoride melt during three distinct evolutionary stages: Stage 1 began with the brecciation of the granite wall rocks, the formation of xenoliths within the upper part of the deposit and the crystallisation of the main units of siderite-quartz and siderite-cryolite. The latter consolidated between 500-600 °C and displays a layered structure. During stage 2, gas-driven explosions led to a partial collapse of the cryolite roof and the formation of cryptocrystalline topaz in cavities. The fluorite-topaz units and the fluorite-cryolite breccia formed and unusual hydrous minerals like weberite or jarlite precipitated from highly fractionated fluids. Cryolite pockets formed within the breccias due to the plastic, glacier-like movement of cryolite. In the course of stage 3, the explosive release of water pressure formed vertical fissures in which prosopite and cryolite crystallised. Secondary aluminofluorides like pachnolite, ralstonite and thomsenolite formed in cavernous masses (Pauly & Bailey, 1999).

3. Sample petrography

The samples were either collected from the mining dump or were provided by the Geological Museum of Copenhagen. Their approximate original position was reconstructed based on typical mineral assemblages (Bailey, pers. comm., 2007). The cross section of the intrusion (Fig. 2) shows the relative position of the samples within one unit. The black circles are samples from J. Köhler whereas the white ones are from J. Konnerup-Madsen. Fig. 3 a-f shows hand specimens and double-polished wafers of some of the analysed samples. The sample description follows the geological sequence and begins with rocks surrounding the deposit: the two breccia samples (samples “Brekzie 1 & 2”; Fig. 3 f) consist of fragments of brown cryolite, purple fluorite, reddish-brown siderite and white quartz. The fragments are of variable size and the matrix is mainly made up of a phengitic mica called “ivigtite” (Pauly &

Bailey, 1999). The host granite is represented by samples 1454, 47 and 65. The two latter samples are derived from drill cores at a depth of 229 and 502 m, respectively. In all three samples, quartz only occurs interstitially and is associated with alkali feldspar, opaque minerals and rarely with amphibole (sample 1454). Sample 1475 (Fig. 3 b) comprises quartz, brown cryolite and siderite which form a vein of few cm width that cuts "ivigtite"-rich, greisenised granite. It seems to be derived from the transition zone between the breccia and the granite (Bailey, pers. comm., 2007).

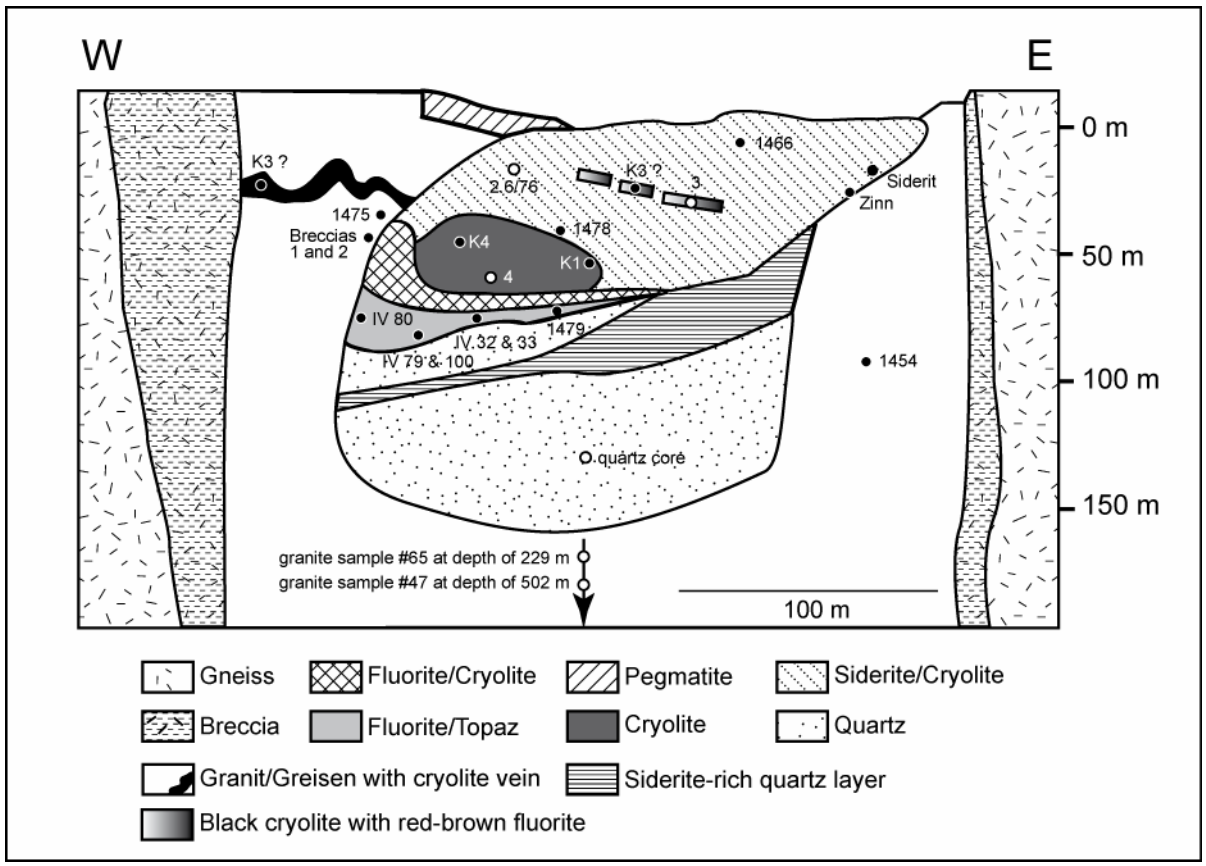

Fig. 2: Cross section of the cryolite deposit at Ivigtut modified after Pauly & Bailey (1999). The relative position of the analysed samples within the different units is indicated. The black circles represent samples investigated by J. Köhler whereas the white ones are from J. Konnerup-Madsen.

From their mineralogy and textures, the following samples appear to be derived from stage 1 of the deposit. Bailey (pers. comm., 2007) suggested samples "Siderit" and "Zinn" to be derived from the eastern extension. They probably represent the early stage of the deposit's development. The two siderite samples are reddish-brown and form cm-large crystals. Sample "Zinn" is fine-grained and composed of light brown cryolite, quartz and black cassiterite. White to light brown cryolite from samples K4 and K1, respectively, come from the pure

cryolite mass. In contrast, dark-brown cryolite (sample K3) may either be derived from a cryolite-rich vein within the greisen or from the black cryolite/red-brown fluorite sheet. Samples 1466 and 2.6/76 come from the siderite-cryolite unit and contain white clouds of quartz and light-brown cryolite that are associated with rust-coloured siderite. The sample "quartz core" is derived from the deposit's lowest part, i.e. the (siderite-)quartz mass.

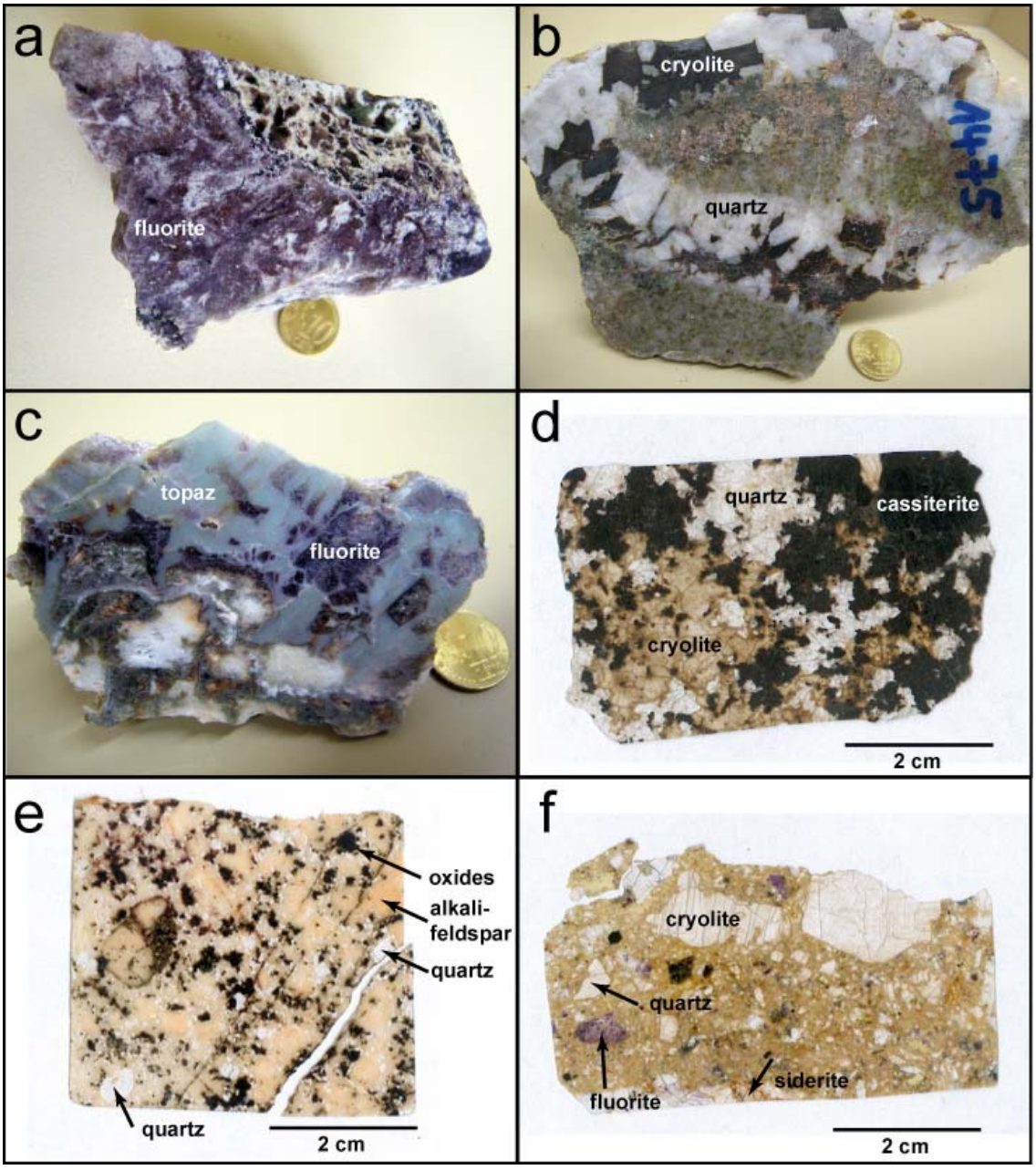

Fig. 3: Three hand specimens and three double-polished thick wafers of the analysed samples. a) According to Pauly & Bailey (1999), sample IV 80 represents a breccia with fluorite and topaz cementing fragments of cryolite. b) Sample 1475 with a cryolite-quartz vein cutting through fine-grained, phengite-bearing greisen. c) Sample 1479 with purple fluorite intergrown with bluish topaz. d) Thick section of "Zinn" with brownish cryolite, quartz and black cassiterite. e) Thick section of granite sample 1454 mainly consisting of quartz and pink alkali-feldspar. f) Thick section of "Brekzie 1" having a greenish, phengite-bearing greisen-matrix with fragments of cryolite, quartz, siderite and fluorite. Scale coin has a diameter of 2 cm.

All analysed fluorites formed during stage 2 and are derived from the fluorite-topaz unit, because they are always associated with cryptocrystalline, bluish-green to light blue topaz. Fluorite is commonly purple (Fig. 3 a, c) and in some samples, it displays colour zonation in thick sections.

4. Methodology

Fluid petrography and microthermometric studies were carried out at the Geologisk Institut, University of Copenhagen, Denmark and at the Institut für Geowissenschaften, University of Tübingen, Germany with any additional investigations conducted in the latter. $\delta^{13}C$ values of inclusion methane were determined by J. Potter at the University of Western Ontario/London, Canada.

Double-polished, 150-200 µm thick wafers were used for fluid inclusion studies in quartz, cryolite, fluorite and siderite. Microthermometric measurements were carried out on a Linkam THMS 600 heating-cooling stage mounted on a Leica DMLP microscope. It was calibrated using the triple point temperature (-56.6 °C) of a CO_2 standard and the melting and critical homogenisation temperatures of a pure H_2O standard (0.0 and 374.1 °C). The accuracy of the final melting temperatures is ±0.2 °C and for the homogenisation temperatures ±1.0 °C. For aqueous inclusions, salinities were calculated from the final melting temperature of ice according to Bodnar et al. (1993) and are expressed in weight percent (wt%) NaCl equivalents. The salinity of the H_2O-CO_2 inclusions was calculated from the clathrate melting temperature using the program ICE of Bakker (1997).

Qualitative Raman spectroscopy was carried out on a Dilor Jobin Yvor Raman spectroscope. Fluid inclusions and the mineral matrix were analysed using a blue argon laser (488 nm) for a wave number range between 600 to 4500 cm^{-1}. Counting times were 10 s.

Crush leach analyses were performed on a Dionex ICS 1000 system with the cation chromatography column CS12-A and the anion column AS9-HC. Before analysis, all samples except for siderite were treated with concentrated (65 %) HNO_3 at 60-70 °C in a sand bath for 2 hours. Subsequently, they were washed with triple deionised water for a week. Since cryolite is water-soluble, aliquots were washed for 4 h, 12 h and 72 h, respectively. However, the results were approximately the same for the three aliquots. Anions (F^-, Cl^-, Br^-, NO_3^- and SO_4^{2-}) and cations (Li^+, Na^+, K^+, Mg^{2+} Ca^{2+}, Sr^{2+}, Ba^{2+}) in inclusions in quartz, siderite and fluorite were analysed separately from 1 g of crushed sample. For cryolite, anions and cations were analysed simultaneously from 10 ml leachate of 2 g of sample. All samples were ground

for 1-2 minutes in an agate mortar. The powder was then leached with 5 ml triple deionised water. For cation analysis, 10 µl of 33 % HNO_3 were additionally added to ensure the right pH value for the chromatography column. Injection volume was 100 µl and running time was 30 min.

Carbon, hydrogen and oxygen isotope measurements of fluid inclusions were performed on a vacuum extraction line according to the techniques described by Friedman (1953), Craig (1961 b) and Vennemann & O'Neil (1993) with samples being mechanically crushed. δD, $\delta^{18}O$ and $\delta^{13}C$ values of CO_2 and H_2O, respectively, were measured on a Finnigan MAT-252 mass spectrometer at the University of Tübingen, Germany. $\delta^{13}C$ values of methane in fluid inclusions were determined through gas chromatography at the University of Western Ontario, Canada. The hydrogen values were calibrated against an internal kaolinite standard with δD = -125 ± 5 ‰. The analytical precision is better than 0.3 ‰ for oxygen and carbon and better than 6 ‰ for hydrogen. δD and $\delta^{18}O$ results are reported relative to VSMOW, $\delta^{13}C$ values relative to VPDB.

5. Analytical Results

5.1 Fluid petrography and microthermometry

Fluid inclusions were analysed in quartz, cryolite, fluorite and siderite. Even though fluid inclusions were analysed in samples from various units of the deposit, no systematic changes were observed. They all comprise the same kind of fluid regardless of their stratigraphic position. Basically, three different types of fluid inclusions can be distinguished (Fig. 4 and 5, Tab. 1): (1) pure CO_2, (2) a CO_2-H_2O mixture and (3) a saline aqueous solution. The results are in general agreement with fluid inclusion data from cryolite and siderite from Prokof'ev et al. (1991).

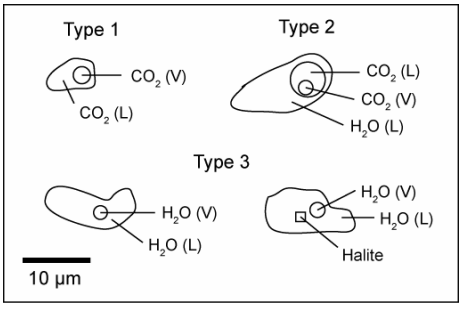

Fig. 4: Schematic sketch of typical appearances of fluid inclusions (type 1-3). See text for further details.

Tab. 1: Microthermometric data for fluid inclusions from Ivigtut analysed by J. Köhler.

Origin	Sample	Mineral	#	Type	T(f)	T(me)	Tm (CO2)	T(m) H2O***	T(m) cla	T(h) CO2	T(h) H2O***	Salinity
												(wt% NaCl eq.)
Rocks surrounding the deposit	1454	quartz	6	pure CO_2	-95 to -88	-90 to -80	-56.1 to -55.9	x	x	12.1 to 16.8	x	x
			13	CO_2-H_2O	double or triple freezing	-45 to -30	-56.3 to -56.1	-17.5 to -12.5	-5.6 to 2.3	8.1 to 28.9	183 to 239	16.43 to 20.6
			25	pure H_2O	-70 to -35	-50 to -30	x	-14.2 to -9.2	x	x	103 to 130	13.07 to 17.96
	Breccia	cryolite	36	pure CO_2	-95 to -82	-93 to -85	-56.8 to -56.4	x	x	-11.8 to 26.7	x	x
	1 & 2		2	CO_2-H_2O	double or triple freezing	-43 to -30	no CO_2 phase	-17.4 to -16.9	-2.7 to 0.6	no CO_2 phase	no data	20.5 to 20.1
		quartz	4	pure CO_2	-94 to -93	-89	-56.9 to -56.3	x	x	-7.6 to 14.1	x	x
			13	CO_2-H_2O	double or triple freezing	-45 to -30	-57.0 to -56.4	-25.3 to -12.6	-12.5 to 2.7	x	154 to 185	16.56 to 25.68
			5	pure H_2O	-73 to -41	-48 to -38	x	-16.4 to -11.3	x	x	95 to 105	15.29 to 19.74
		fluorite	27	CO_2-H_2O	double or triple freezing	-40 to -35	-58.3 to -55.7	-23.0 to -13.1	1.1 to 1.5	15.8 to 28.7	171 to 193	17.02 to 24.31
			5	pure H_2O	-56 to -45	-40 to -35	x	-10.8 to -14.8	x	x	212 to 258	14.78 to 18.73
	1475_Qtz	quartz	31	CO_2-H_2O	double or triple freezing	-45 to -30	-55.6 to -57	-23.8 to -19.4	-3.8 to 1.0	15.9 to 27.5	116 to 257	21.97 to 24.85
			22	pure H_2O	-65 to -38	-40 to -30	x	-16.8 to -13.3	x	x	116 to 152	17.2 to 20.07
	1475_Kry	cryolite	38	CO_2-H_2O	double or triple freezing	-40 to -25	-55.8 to -55.3	-22.8 to -9.0	-13.8 to 3.2	22.6 to 27.9	130 to 266	12.86 to 24.22
			15	pure H_2O	-55 to -37	-35 to '-25	x	-16.8 to -10.2	x	x	123 to 158	14.13 to 20.05
	1475_Sid	siderite	50	pure H_2O	-64 to -24	-50 to -20	x	-13,0 to -10.5	x	x	90 to 250	14.5 to 16.89
Stage 1	1466	quartz	37	pure CO_2	-95 to -89	-90 to -80	-57.1 to -56.0	x	x	0.3 to 25.1	x	x
			3	CO_2-H_2O	double or triple freezing	-65 to -46	-56.3	-21.14 to -18.3	-4.4 to -2.4	28.6	no data	23.2 to 24.49
			9	pure H_2O	-56 to -31	-50 to -25	x	-10.4 to -1.2	x	x	103 to 142	2.07 to 14.37
		cryolite	23	pure CO_2	-97 to -71	-92 to -86	-57.5 to -56.5	x	x	-8.2 to 16.8	x	x
			7	CO_2-H_2O	double or triple freezing	-45	-56.6 to -56.3	-27.1 to -16.8	-14.9 to 5.7	15.9 to 19.2	142	20.1 to 26.8
			21	pure H_2O	-46 to -35	-35	x	-14.4 to -10.3	x	x	103 to 131	14.26 to 18.17
	K1	cryolite	5	pure H_2O	-56 to -44	-35	x	-5.7 to -4.9	x	x	no data	7.71 to 8.8
	K3	cryolite	3	pure CO_2	-97 to -96	x	-57.4 to -57.2	x	x	-9.1 to -8.7	x	x
			3	CO_2-H_2O	double or triple freezing	-45 to -30	no CO_2 phase	-13.5 to -10.5	-2.6 to 1.1	no CO_2 phase	no data	14.45 to 17.36
			4	pure H_2O	-45 to -35	-35 to -30	x	-12.4 to -10.4	x	x	no data	14.35 to 16.35
	K4	cryolite	5	CO_2-H_2O	double or triple freezing	-35 to -30	no CO_2 phase	-9.6 to -6.3	2.6 to 4.6	no CO_2 phase	no data	9.54 to 13.49
	1478	cryolite	45	CO_2-H_2O	double or triple freezing	-50 to -30	no CO_2 phase	-15.9 to -9.1	-11.5 to 1.8	no CO_2 phase	104 to 140	12.95 to 19.36
			9	pure H_2O	-60 to -37	-50 to -35	x	-13.4 to -8.8	x	x	173 to 245	12.63 to 17.29
	Zinn	cryolite	20	pure CO_2	-96 to -71	-92 to -86	-56.4 to -56.2	x	x	-12.2 to -1.9	x	x
			37	pure H_2O**	-70 to -30	-45 to -25	x	-15.5 to -10.2	x	x	103 to 240	14.16 to 19.08
		quartz	17	pure CO_2	-95 to -82	x	-56.9 to -56.1	x	x	-3.9 to 21.3	x	x
			32	pure H_2O	-67 to -41	-50 to -30	x	-18.3 to -13.3	x	x	103 to 118	17.19 to 21.18
	Siderit	siderite	4	pure H_2O	-48 to -46	-35 to -30	x	-11.5 to -11.1	x	x	171 to 199	15.07 to 15.47
Stage 2	1479	fluorite	8	pure CO_2	-88 to -78	x	-56.4 to -55.5	x	x	-25.5 to -2.3	x	x
			1	CO_2-H_2O	double or triple freezing	-30	no CO_2 phase	-11.5	3.7	no CO_2 phase	89	15.9
			40	pure H_2O	-60 to -38	-45 to -27	x	-13.8 to -9.4	x	x	136 to 177	13.3 to 17.58
	IV 100	fluorite	6	pure CO_2	-97 to -85	x	-56.9 to -56.8	x	x	21.6 to 27.9	x	x
			4	CO_2-H_2O	double or triple freezing	-25	no CO_2 phase	-12.8 to -11.6	no data	no CO_2 phase	no data	15.73 to 16.49
			4	pure H_2O	-55 to -51	-30 to -40	x	-6.7 to -5.9	x	x	no data	9.12 to 10.15
	IV 32+33	fluorite	5	pure H_2O	-45 to -42	-25	x	-2.3 to -1.8	x	x	234 to 242	3.02 to 3.82
	IV 80	fluorite	5	pure H_2O	-48 to -42	-35 to -30	x	-3.9 to -3.1	x	x	158 to 240	5.04 to 6.37
	IV 79	fluorite	2	CO_2-H_2O	double or triple freezing	-30	no CO_2 phase	-10.6	3.9	no CO_2 phase	no data	14.62
			2	pure H_2O	-56 to -53	-40 to -30	x	-12.1 to -11.0	x	x	no data	14.62 to 15.02

T(f) double or triple freezing due to freezing of water, clathrate (and CO_2)
T(me) eutectic melting of water
T(m) final melting
T(h) homogenisation temperature

* salinity of CO_2-H_2O inclusions calculated from clathrate melting temperature
** seldom with hydrohalite
*** temperature range for majority of fluid inclusions
cla CO_2 clathrate

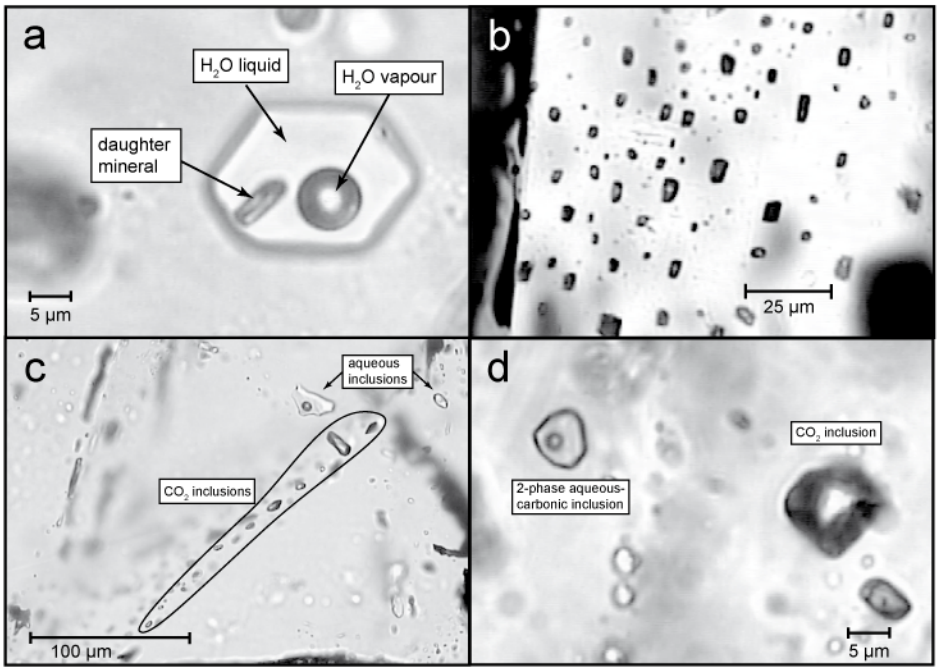

Fig. 5: Photos of typical fluid inclusions at Ivigtut. a) Hexagonal saline aqueous inclusion (type 3) in quartz with unknown daughter mineral (sample 1475). b) Rectangular, secondary saline aqueous inclusions in siderite (sample 1475). c) Saline aqueous inclusions right next to a trail of pure CO_2 inclusions in fluorite (sample 1479). d) A two-phase aqueous carbonic inclusion (type 2) next to a pure CO_2 inclusion (type 1) in quartz (sample 1466).

5.1.1 Type 1: pure CO_2 inclusions

Type 1 inclusions are dark, monophase at room temperature and predominately occur in cryolite and quartz. They have a rounded shape and a diameter of 6 to 11 µm. Secondary type 1 inclusions clearly dominate over primary ones. They melt between -57.5 to -55.9 °C, but generally cluster around the triple point temperature of pure CO_2 at -56.6 °C. The shift towards lower temperatures indicates the presence of CH_4 with a possible maximum CH_4 content of ~ 3 mole % (Fig. 6). Homogenisation occurs between -40 and +30 °C into the liquid phase with a correspondingly large variation in molar volumes from 40 to more than 60 cm^3.

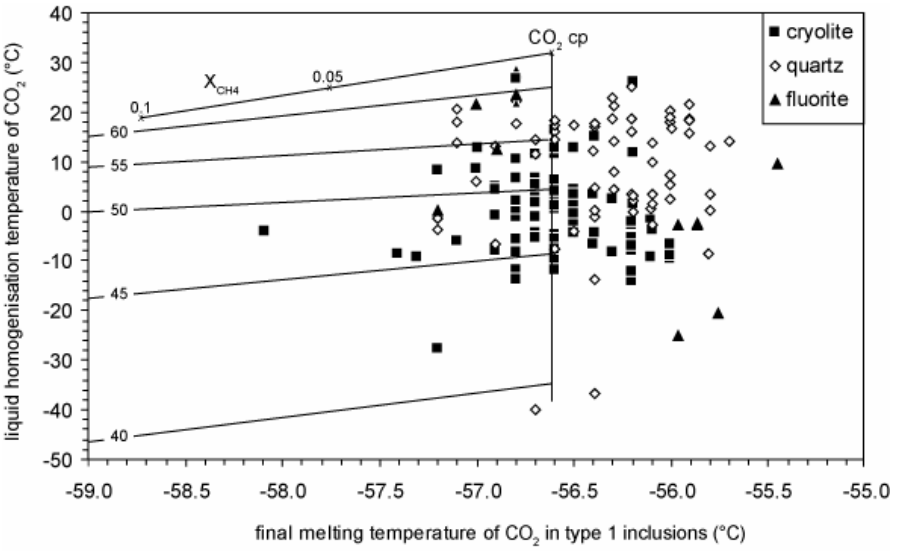

Fig. 6: Liquid homogenisation temperature versus final melting temperature of solid CO_2 in type 1 inclusions in different host minerals. Also shown is part of the critical curve for CO_2-CH_4 mixtures with mole fractions of CH_4 as indicated. CO_2cp is the critical point for pure CO_2. The curves show the corresponding molar volumes in cm³.

5.1.2 Type 2: aqueous carbonic inclusions

Fluid inclusions of type 2 are angular to rounded, up to 12 µm across and mostly secondary. The liquid volume fraction varies between 0.65 and 0.95. Only some of them contain three phases at room temperature, i.e. two liquids and a vapour phase. However, they always comprise clathrate during cooling runs and occasionally hydrohalite or halite (e.g. sample "Zinn"). The CO_2 phase in type 2 inclusions melts at ~ -56.6 °C and homogenises between -5 and +28 °C. The aqueous liquid melts between -18 and -22 °C and only rarely between -13 and -15 °C. CO_2 clathrate melts from -9 to +4 °C with a mean at -2.1 °C which corresponds to an average salinity of approximately 17 wt% NaCl eq. Total homogenisation of type 2 inclusions occurs between 210 and 240 °C into the liquid, in some samples also above 300 °C (Fig. 7; 8). However, most inclusions decrepitate before complete homogenisation. Qualitative Raman spectroscopy showed many inclusions also comprise CH_4.

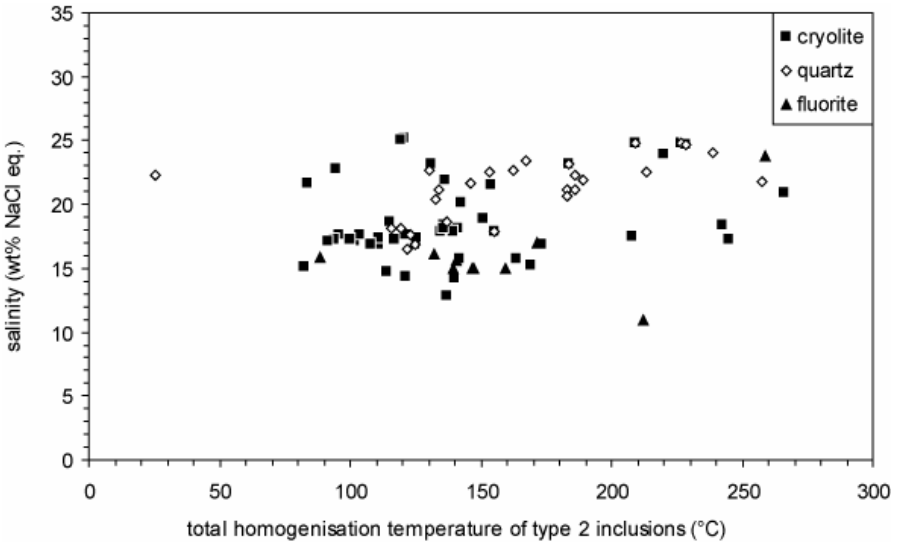

Fig. 7: Salinity of the aqueous liquid versus total homogenisation temperature of aqueous-carbonic inclusions (type 2). The vast majority of inclusions is restricted to salinities of 15-25 wt% NaCl eq., but show a wide range of homogenisation temperatures.

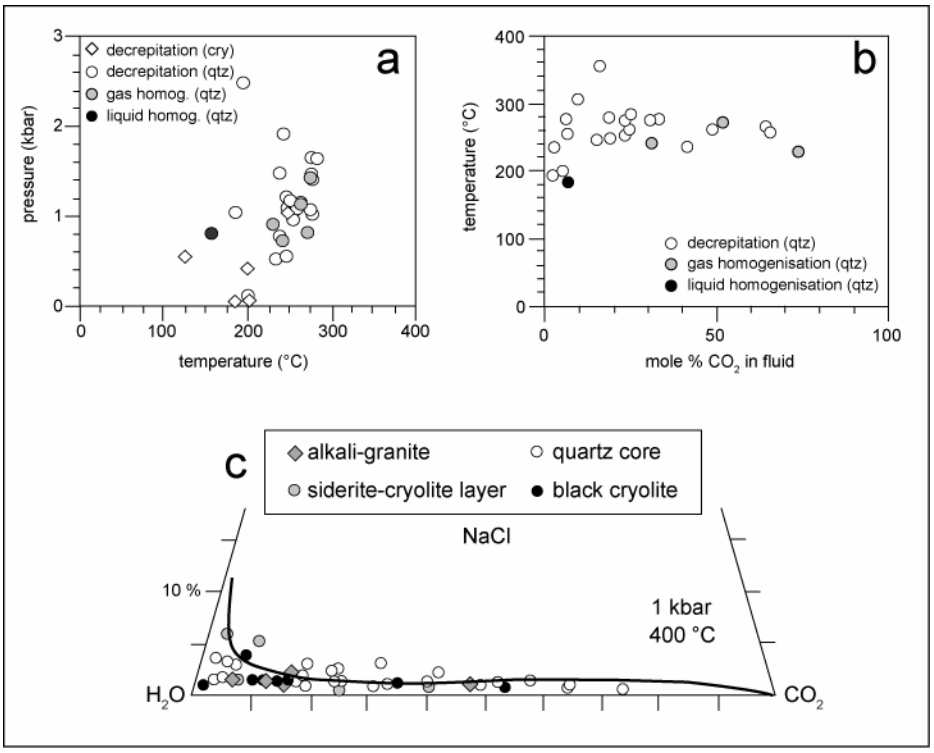

Fig. 8: Selected data on the type 2 aqueous-carbonic inclusions. a) Calculated pressures at the temperature of total homogenisation or decrepitation for fluid inclusions in quartz and cryolite. b) Total homogenisation or decrepitation temperature versus bulk H_2O-CO_2 composition of the inclusions in quartz. c) The bulk molar H_2O-CO_2-NaCl compositions of individual inclusions in different host minerals. The limiting solvus curve at 1 kbar and 400 °C is included for comparison.

5.1.3 Type 3: saline aqueous inclusions

Type 3 inclusions are predominately secondary and occur in all analysed minerals. They are commonly 7-30 μm in diameter and their shape varies from hexagonal in cryolite, rectangular in siderite to rounded or irregular within the other minerals. The degree of fill is typically 0.95 with a few inclusions having one between 0.80 and 0.90. The aqueous inclusions melt between -10 and -15 °C which corresponds to a salinity of approximately 14 – 19 wt% NaCl eq. The majority of type 3 inclusions homogenises into the liquid between 100 and 130 °C (Fig. 9). Densities obtained from the final melting and homogenisation temperatures vary between 0.85 for the low salinity fluids to about 1.1 g/cm³ for higher saline fluids. Qualitative Raman analysis revealed the presence of small amounts of C_3H_8. Only very few type 3 inclusions in quartz from the host granite comprise halite.

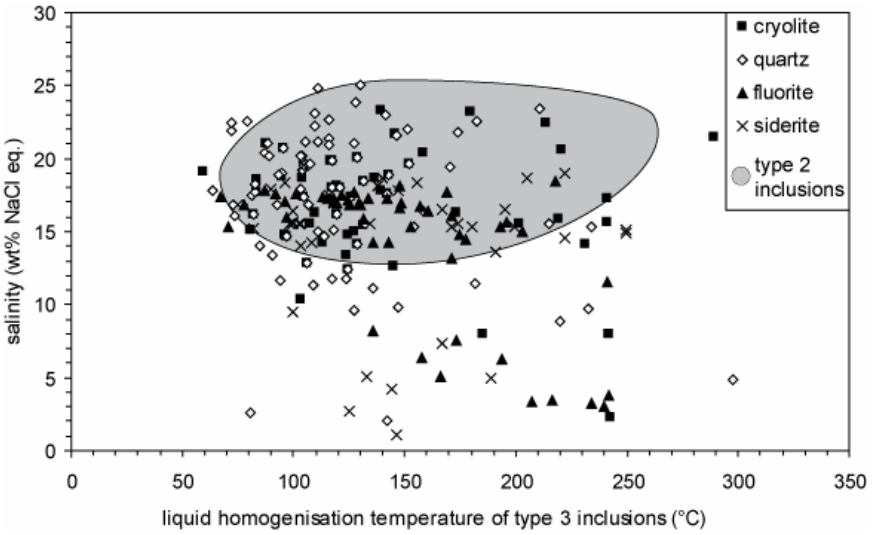

Fig. 9: Salinity versus liquid homogenisation temperature for aqueous type 3 inclusions. The grey field shows salinity-homogenisation data for type 2 aqueous-carbonic inclusions.

In inclusions of type 2 and rarely of type 3, a darkish, elongate daughter mineral occurs. This mineral melts between 40 and 80 °C and recrystallises quickly upon cooling. Raman spectroscopy showed no signal. Hence it is assumed that the mineral is either Raman inactive or too small for analysis. Fluid inclusions of type 2 and 3 generally show low eutectic melting temperatures between -50 and -30 °C (Tab. 1). During cooling runs, the inclusions often become brown which might argue for other cations like Ca^{2+}, Fe^{2+}, Mg^{2+} and possibly Li^{+} (Dubois et al., 1994; Borovikov et al., 2001; Davis et al., 1989; Shepherd et al., 1985).

5.2 Stable Isotopes

Isotopic studies on fluid inclusions were carried out for two quartz (1466, 1475), four cryolite (1478, K1, K3, K4), two fluorite (IV 32, IV 33) and two siderite samples (1475, Siderit; Tab. 2). Like the microthermometric results, the isotope data show no systematic change among the different units of the deposit. Even though the samples comprise fluid inclusions of types 1-3, a bulk analysis is reasonable, because the few primary inclusions show the same microthermometric properties as the dominating secondary ones and are hence of the same major composition. Furthermore, we suggest that the different types of inclusions (water-rich and carbonic inclusions) were trapped contemporaneously, probably from two immiscible fluids, i.e. a brine and a carbonic-rich fluid (see 6.1).

δD of H_2O in the inclusions varies from -19 to -144 ‰ with the majority lying between -45 and -107 ‰. The corresponding $\delta^{18}O$ values of H_2O range widely from -1.5 to -21.7 ‰. The analysed inclusion CO_2 has a $\delta^{13}C$ of -4.4 to -9.3 ‰ with the vast majority at -

5.0 ‰ which is typical of most mantle-derived magmas (Pineau & Javoy, 1983). The corresponding $\delta^{18}O$ of CO_2 ranges from +20.7 to +42.0 ‰.

In most inclusions in quartz, cryolite and fluorite, additional methane (and higher hydrocarbons) were present. The $\delta^{13}C$ value for methane is much more depleted than for CO_2 and ranges between -28.0 and -40.8 ‰. δD in methane could not be analysed because the extracted amount of hydrogen was below the detection limit.

Three quartz samples were additionally analysed for their oxygen isotope composition. Quartz from the host granite (sample 1454) yielded a $\delta^{18}O$ value of 8.4 ‰ which falls in the range of the whole rock $\delta^{18}O$ value for the metasomatised granite of 8.4 to 9.7 ‰ given by Pauly & Bailey (1999). Quartz from the deposit itself and the breccia gave a $\delta^{18}O$ of 10.5 and 9.6 ‰, respectively. This is in accordance with a $\delta^{18}O$ of 10.5 ‰ for the bulk cryolite body (Pauly & Bailey, 1999).

5.3 Ion chromatography

Crush leach analyses were performed on four quartz (1454, 1466, 1475, Brekzie 1) two siderite (1475, Siderite), five fluorite (IV 32, IV 33, IV 79, IV 80, IV 100) and six cryolite samples (1475, 1478, K1, K3, K4, Brekzie 1).

The method does not allow the analysis of the main elements of the host mineral. The bulk crush leach method applied in this study slightly differs from the one described by Bottrell et al. (1988), Banks & Yardley (1992) and Yardley et al. (1993) due to the disuse of $LaCl_3$ the effect of which is discussed below.

5.3.1 Analysis of divalent cations without $LaCl_3$

When crushing fluid inclusions, cations are adsorbed onto the powder surface. Univalent cations are washed off with triple deionised water whereas divalent cations should be exchanged from the powder surface and brought into solution by a trivalent cation which is commonly La^{3+} (Bottrell et al., 1988). However, the amount of $LaCl_3$ required (~ 200 ppm La) for the exchange process led to an overload of the chromatography column. To test the effect of crushing without $LaCl_3$, we simulated the crushing procedure with a standard of divalent cations dissolved in deionised water. The solution had different known divalent cation concentrations (Sr^{2+}, Ca^{2+}, Mg^{2+}, Ba^{2+}) and was dripped onto cleaned quartz powder. One solution was vaporised overnight and washed with triple deionised water; the other

Tab. 2: Stable isotope analyses of fluid inclusions from Ivigtut.

Origin	Sample	Mineral	δD_{H2O} VSMOW	$\delta^{18}O_{H2O}$ VSMOW	$\delta^{13}C_{CO2}$ VPDB	$\delta^{18}O_{CO2}$ VSMOW	$\delta^{13}C_{CH4}$ VPDB	T(eq.) between $\delta^{18}O_{H2O}$ and $\delta^{18}O_{CO2}$ *	T(eq.) between $\delta^{13}C_{CO2}$ and $\delta^{13}C_{CH4}$ **	Fractionation range water-CO_2 ($\delta^{18}O$)	$\delta^{18}O$ in quartz mineral
Rocks surrounding the deposit	1454	quartz									8.4
	Bre_1 Qz	quartz									9.6
	1475_Qz	quartz	-43	-13.72	-4.47	29.8		52.95	172.7	43.52	
					-4.34	28.8			171.7		
					-5.73		-40.78		182.6		10.5
	1475_Sid	siderite	-67.7	-10.76	-9.3	34.77		44.6		45.53	
Stage 1	K3	cryolite	-123.4	-21.7	-4.89	28.62	-27.97	23.3	320.5	50.32	
	K1	cryolite	-106.6	-16.47	-5.74	32.6		29.05		49.07	
	K4	cryolite	-45	-7.02	-4.9	39.18		42.5	296	46.2	
	1478	cryolite	-144.1	-19.14	-5.25	23.99		53.65	187.1	43.13	
					-5.82		-39.79		191.9		
					-6.63		-29.61		321.4		
	1466	quartz	-85.3	-20.14	-4.14	20.69		64.5		40.83	11.2
	Siderit	siderite			-6.12	32.65					
Stage 2	IV 32	fluorite	-58.7	-6.6	-6.16	42.01			280		
					-4.44	41.55		34.55	258.7	48.15	
					-5.68		-31.99		273.9		
	IV 33	fluorite	-18.7	-1.49	-4.52	35.65			174.6		
					-4.5	36.5		83.35	174.4	37.99	
					-5.26		-40.59		180.4		
			-80.3	-13.82	-8.64	32.96					
					-5.33	36.7		24.05		50.52	

* calculated after Friedman & O'Neil (1977)
** calculated after Ohmoto & Goldhaber (1997)
all values in ‰

sample solution was directly analysed after having stirred the powder in the standard solution. Both times and even for different standard concentrations, we were able to reproduce the added divalent cation concentration with a relative error of max. 20 %.

5.3.2 Calculating the absolute ion concentration

The absolute concentration of dissolved ions was calculated using the inclusion's average salinity. Depending on inclusion type, the salinity was calculated in two ways: a) from the final ice-melting temperature for aqueous inclusions and b) from the clathrate-melting temperature for CO_2-H_2O inclusions. Since both inclusion types occur in various proportions within the samples, it is impossible to indicate the exact salinity. However, the absolute ion concentrations vary 12 % at most if the salinity is calculated from the ice-melting or from clathrate-melting. For the calculations, a constant Na- or Cl-factor was used for cations and anions having the denotation:

Cl *or* Na = (atom weight Cl *or* Na / atom weight NaCl) * 10000 * salinity (wt% NaCl eq.) (1)

Fluid inclusions in cryolite were analysed from one single aliquot with the absolute concentration for all ions being calculated via the Cl-factor.

5.3.3 Washing and crushing experiments with cryolite

Since cryolite is soluble in water, it was necessary to test if the host mineral itself influences the anion content in the inclusions' leachate. A piece of cryolite (sample K4) was successively crushed from coarse grains to a fine powder. The different fractions were leached in triple deionised water for one minute which approximately corresponds to the time the sample powder is washed until the leachate is put into the syringe. From the uncrushed cryolite, only minor amounts of Cl^-, NO_3^- and SO_4^{2-}, but no bromine were leached. The finer cryolite fraction showed more Cl^-, SO_4^{2-} and Br^- in solution, probably because more inclusions were cracked. The Cl/Br ratio decreased successively until the fine powder had about the same ratio as the aliquot which was powdered at once. Chlorine leached from the uncrushed cryolite makes up less than 10% of the final Cl^- concentration. Therefore, the error caused by cryolite solubility is negligible and the measured Cl/Br ratios reflect true fluid inclusion values.

5.3.4 Anion-Cation-Balance

To check the accuracy of the crush leach analyses, the molar ratio of all negative charges versus the sum of all positive charges should equal 1. However, as stated by Banks et al. (2000), this is rarely the case for natural waters, for example due to solid impurities within the host mineral or the presence of daughter minerals (i.e. halite) as observed for some fluid inclusions (e.g. cryolite in sample 1475).

The ratio >>1 for one siderite and two quartz samples can be ascribed to the extremely high fluorine which – in two samples – even exceeds the chlorine content (Tab. 3). These samples were measured twice to rule out possible contamination and/or analytical errors, but the fluorine content remained unusually high. The lack of cations to balance the anions could be ascribed to elevated contents of aluminium. This element was not analysed during ion chromatography, because due to its trivalent oxidation state it would have been impossible to leach (see 5.3.1). Tagirov & Schott (2001) showed that besides hydroxide complexes, F and Na (+ Si) are the main complexing ligands responsible for Al-transport. They further demonstrated that Al forms stable complexes with F and might be present as a $NaAl(OH)_3F$ complex at 400-450 °C (Tagirov et al., 2002 a & b) or an $Al(OH)_2F_2^-$ complex between 300 and 600 °C (Zaraisky, 1994).

The charge-balance test has limited applicability for the cryolite and fluorite samples, because elements also present in the host mineral could not be measured. Therefore, the ratio of Σanions/Σcations for inclusions in cryolite and fluorite varies between 0.7 and 0.9 (Tab. 3).

5.3.5 Results of analysed cations

Sodium reaches up to 7 wt% and dominates over the others by one or two orders of magnitude (Tab. 3). Potassium is the second most abundant cation with an average concentration of 9 300 ppm. In some samples (cf. cryolite), lithium is even more concentrated than calcium. This is not surprising given the occurrence of cryolithionite at Ivigtut (Pauly & Bailey, 1999). Magnesium is a subordinate component in fluid inclusions from cryolite (usually < 100 ppm), but can reach higher concentrations (> 500 ppm) in fluorite and quartz.
The predominance of sodium is in agreement with microthermometry. The eutectic temperatures between -30 and -50 °C can be attributed to the additional presence of $MgCl_2$ and $LiCl_2$ (Davis et al., 1989; Dubois et al., 2007) with $CaCl_2$ playing an insignificant role.

Tab. 3: Absolute ion concentrations (ppm) in fluid inclusions from crush leach analyses.

Origin	Sample	Mineral	Salinity	F^-	Cl^-	Br^-	NO_3^-	SO_4^{2-}	Cl/Br	Na^+	K^+	Li^+	Mg^{2+}	Sr^{2+}	Ba^{2+}	Ca^{2+}	Σanion/Σcation (molar)
rocks surrounding the deposit	1454	quartz	**17.4**	5 052	105 000	427	6 123	108	**246**	69 000	39 453	775	500	201	344	15 620	0.7
	Bre_1 Qz	quartz	**18.76**	522 663	113 207	1 308	1 184	1 202	**87**	74 393	2 435	90	16 550	24	9	149	6.6
	Bre_1 Kry	cryolite	**20.32**	n.a.	122 621	1 284	3 600	3 332	**95**	*80 562*	28 280	1 967	933	x	x	432	0.8
	1475_Qz	quartz	**19.32**	2 934	116 586	1 863	698	122	**63**	76 614	8 791	1 306	447	438	34	854	0.9
	1475_Kry	cryolite	**19.04**	n.a.	114 897	438	1 713	2 453	**262**	*75 487*	3 612	1 271	790	x	x	588	0.9
	1475_Sid	siderite	**13.88**	13 511	83 759	1 305	1 046	111	**64**	55 041	4 515	203	494	x	x	n.a.	1.2
Stage 1	K3	cryolite	**17**	n.a.	102 586	1 047	2 901	2 107	**98**	*67 399*	4 452	3 148	95	15	x	336	0.9
	K1 24 h	cryolite	**9.136**	n.a.	55 131	651	2 332	429	**85**	*36 221*	5 385	1 692	34	x	x	152	0.8
	K4	cryolite	**11.17**	n.a.	67 405	706	2 408	770	**96**	*44 285*	6 977	1 120	55	x	x	163	0.9
	1478	cryolite	**16.44**	n.a.	99 207	1 762	2 000	551	**56**	*65 179*	5 945	1 521	38	x	x	125	0.9
	1466	quartz	**15.18**	92 450	91 603	1 134	12 559	229	**81**	60 197	3 262	289	288	520	408	580	2.7
	Siderit	siderite	**15.27**	69 981	92 147	981	3 711	x	**94**	60 553	2 868	196	1584	x	x	n.a.	2.2
Stage 2	IV 32	fluorite	**3.374**	n.a.	20 360	199	406	x	**102**	13 380	31 150	248	477	322	602	n.a.	0.4
	IV 33	fluorite	**15**	n.a.	90 517	1 697	742	x	**53**	59 483	32 612	238	2 685	3 640	4 985	n.a.	0.7
	IV 79	fluorite	**15.08**	n.a.	91 015	1 301	1 331	126	**70**	59 810	7 301	115	196	513	364	n.a.	0.9
	IV 80	fluorite	**8.598**	n.a.	51 884	470	651	30	**110**	34 096	3 704	864	620	3 145	2 717	n.a.	0.8
	IV 100	fluorite	**12.36**	n.a.	74 586	858	605	<14	**87**	49 014	10 737	202	905	22 295	10 384	n.a.	0.7

Note: The Na-content of fluid inclusions in cryolite is re-calculated from the measured Cl-conentration and the constant Na/Cl ratio of 0.657.

x = below detection limit

n.a. = not analysed due to host mineral

Cryolite: additional trace amounts of nitrite and bromate

Siderite, fluorite, quartz: additional trace amounts of nitrite and chlorite

5.3.6 Results of analysed anions

Chlorine reaches up to 10 wt% and is closely followed by fluorine with highly variable contents that range between 0.3 and 9 wt% (Tab. 3). Even the high amounts of F appear reasonable, because for example the F-content of 69 981 ppm in sample "Siderit" is in very close agreement with analyses from Prokof'ev et al. (1991) who obtained an F-content of 74 500 and 71 700 ppm in two siderite samples from Ivigtut. Bromine generally ranges from 700 to 1 300 ppm. The Cl/Br ratio lies between 53 and 110. Only fluid inclusions in quartz from the granite and one cryolite sample have a higher Cl/Br ratio of 246 and 262, respectively, and seem to approach the ratio of seawater (i.e. 288; Millero, 2004). Nitrate is highest in fluid inclusions in cryolite (~ 2 400 ppm) whereas it seldomly exceeds 1 300 ppm in the other minerals. Regardless of the host minerals, all inclusions additionally contain minor amounts of nitrite. Sulfate is subordinate with an average ~ 480 ppm, but is slightly more concentrated in cryolite. Negligible amounts of chlorite and bromate are also present. The oxidised equivalents of Cl^- and Br^- may have been generated during crushing.

6. Discussion

6.1 Evidence for fluid immiscibility

Even though most aqueous-carbonic inclusions homogenise to the liquid phase, it is obvious that fluid immiscibility must have occurred. This is evidenced by the spatially close relationship of the different inclusion types (Fig. 5 c), by varying degrees of fill and the wide compositional range between the (saline) H_2O and CO_2 end members. Post-entrapment processes that subsequently changed the phase proportions (e.g. necking down) might have happened for some irregularly shaped inclusions (e.g. Loucks, 2000) which were not analysed. However, the vast majority of fluid inclusions in Ivigtut have a rounded or hexagonal shape which make recrystallisation unlikely.

It is known from experimental studies (e.g. Frantz et al., 1992, Sterner et al., 1984) that synthetic inclusions with different proportions of H_2O, NaCl and CO_2 exhibit fluid immiscibility at different temperatures and pressures. Pauly & Bailey (1999) derived a formation pressure of 1-1.5 kbar from phase relations between the unaltered Ivigtut granite and earlier granophyre dykes (cf. Goodenough et al., 2000). At this pressure, isochores deduced from microthermometry suggest a formation temperature for primary CO_2-H_2O inclusions of 180-400 °C (see below). Frantz et al. (1992) showed that for 300-400 °C and 1

kbar, the immiscibility field in the system NaCl-H_2O-CO_2 is rather large. Furthermore, Duan et al. (1995) demonstrated that the NaCl-H_2O-CO_2 immiscibility field is minimal between 400-500 °C and expands above and below this temperature range at a constant pressure.

In general, there are two kinds of simultaneous entrapment of immiscible fluids: The fluid inclusions are either the result of exsolution from a homogeneous parent fluid or they were derived from the heterogeneous trapping of a mechanical mixture (Anderson et al., 1992). Ramboz et al. (1982) described criteria for the presence of two immiscible phases and heterogeneous trapping: a) occurrence of different inclusion types within the same regions of one sample, b) evidence that the distinct inclusions were contemporaneously trapped in the same region, c) strongly varying volume phase fractions, d) a wide range of composition and e) no signs of leakage or necking down. As discussed above, all these criteria are fulfilled for the Ivigtut inclusions except for occasional leakage phenomena. It is therefore suggested that the fluid inclusions at Ivigtut resulted from heterogeneous trapping of a brine and a carbonic-rich fluid.

6.2 $\delta^{13}C$ and $\delta^{18}O$ in CO_2 from fluid inclusions

The $\delta^{13}C$ value of CO_2 extracted from fluid inclusions varies between -4.1 and -9.3 ‰ which corresponds to typical mantle values (Taylor et al., 1967; Tab. 2). Therefore, we assume that the CO_2 analysed in fluid inclusions in minerals from Ivigtut are derived from a carbonatitic magma, because carbonatitic rocks occur as minor components in the whole Gardar Province (Upton et al., 2003). From the abundance of siderite at Ivigtut (Pauly & Bailey, 1999), the nearby carbonatitic complex of Grønnedal-Ika (Halama et al., 2005) and a geochemical and isotope study of the Ivigtut granite, Goodenough et al. (2000) suggested that the Ivigtut granite might have been derived from F-rich carbonatites. C- and O-isotopes in siderite from Ivigtut (Goodenough et al., 2000) and calcite from carbonatites at Grønnedal-Ika (Halama et al., 2005) fall into the primary carbonatite field (Taylor et al., 1967; Fig. 10).

However, Fig. 10 also clearly shows that the enriched $\delta^{18}O$ values of inclusion CO_2 (+20.7 to +42.0 ‰) differ significantly from the other Gardar carbonatitic rocks, but are identical to the isotopic composition of CO_2 vesicles from MOR basalts (Pineau & Javoy, 1983). Whereas the carbon appears to be mantle-derived, the enriched $\delta^{18}O$ value of inclusion CO_2 can be explained by isotope exchange with oxygen from inclusion water whose $\delta^{18}O$ varies between -1.5 and –21.7 ‰ (see 6.4). Richet et al. (1977) stated that at room temperature, the fractionation between CO_2 and liquid water is between 41.2 to 44.1 ‰.

Additional variation can be caused by the presence of different dissolved salts (Pineau & Javoy, 1983). This fractionation range agrees with $\delta^{18}O$ values of CO_2 and H_2O extracted from fluid inclusions from Ivigtut (Tab. 2). The fractionation varies between 38 and 50.5 ‰ with a mean at 45.5 ‰ comparable to Richet et al. (1977). The calculation of equilibrium temperatures between $\delta^{18}O_{CO2}$ and $\delta^{18}O_{H2O}$ after Friedman & O'Neil (1977) yielded similarily low temperatures between 23.3 and 83.4 °C with an average value of 45.2 °C (Tab. 2). This again indicates that CO_2 and H_2O must have isotopically exchanged within the inclusions even down to low temperatures.

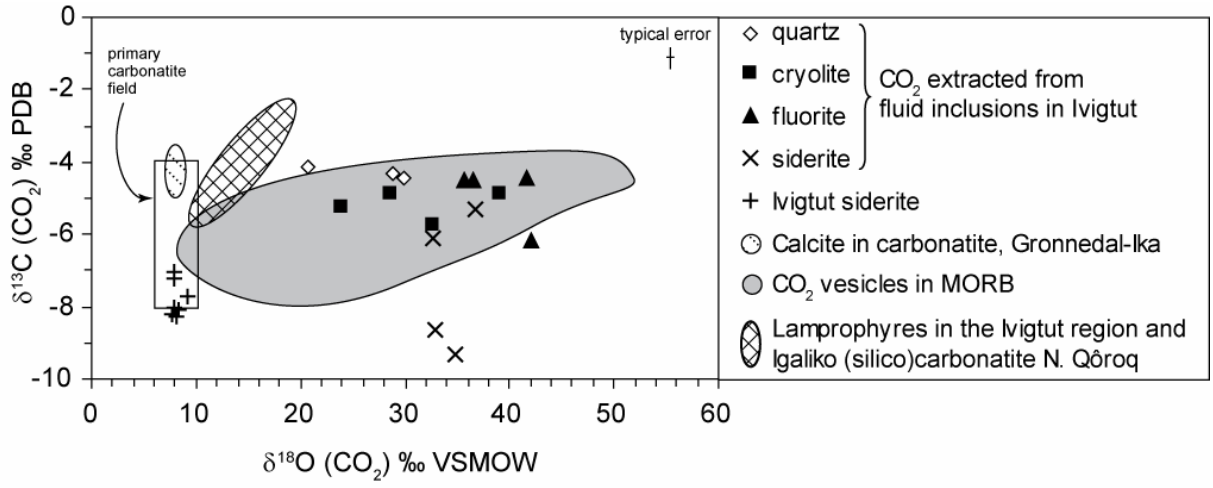

Fig. 10: $\delta^{13}C_{CO2}$ vs. $\delta^{18}O_{CO2}$ from fluid inclusions. Even though the $\delta^{13}C$ value of the analysed samples falls into the range of primary carbonatites, the isotopic composition of the fluid inclusion CO_2 is more similar to isotopic data from CO_2 vesicles in MOR basalts analysed by Pineau & Javoy (1983). The $\delta^{13}C$ value is typical of primitive mantle. The $\delta^{18}O$, however, is the result of low-temperature isotope exchange with oxygen from the water-rich inclusion part. See text for further discussion. Comparative data are from: a) CO_2 vesicles in MORB (Pineau & Javoy, 1983), b) calcite in carbonatites from Grønnedal-Ika (Halama et al., 2005), c) Ivigtut siderite (Goodenough et al., 2000), d) lamprophyres from Ivigtut, Igaliko and (silico)carbonatites from North Qôroq (Coulson et al., 2003), e) primary carbonatite field (Taylor et al., 1967).

Calculation of equilibrium temperatures using the fractionation factors of Richet et al. (1977; Fig. 11) and Ohmoto & Goldhaber (1997; Tab. 2) yielded temperatures between 175 and 321 °C. The samples in equilibrium at higher temperatures are comparable to fluorites derived from the non-agpaitic parts of the Motzfeldt complex (Schönenberger & Markl, in prep.) whereas the ones at lower temperatures correspond to late-magmatic quartz of the Ilímaussaq intrusion (Graser et al., in review).

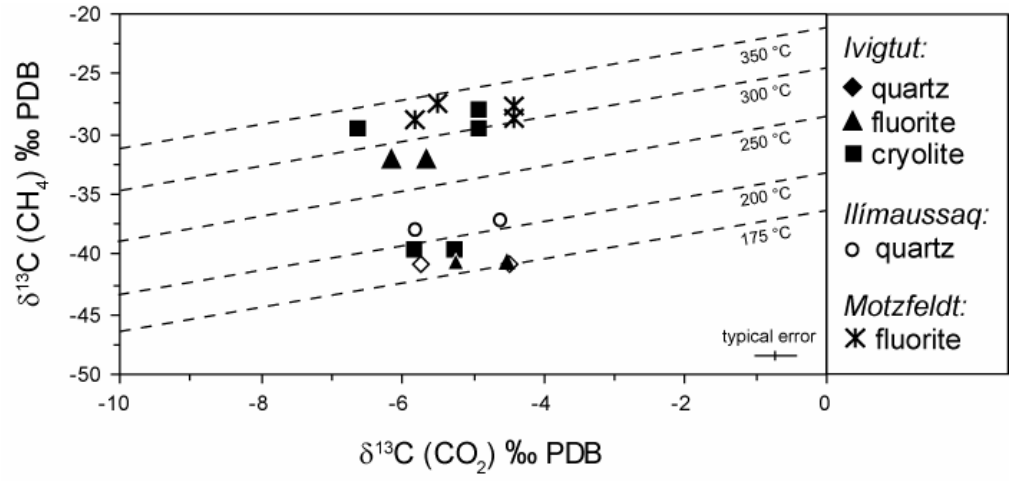

Fig. 11: $\delta^{13}C_{CO2}$ vs. $\delta^{13}C_{CH4}$ from fluid inclusions. Given the fractionation by Richet et al. (1977), carbon dioxide and methane are in isotopic equilibrium at temperatures between 175 and 320 °C. The higher temperatures are comparable to fluid inclusions in fluorite from Motzfeldt (Schönenberger & Markl, in prep.) whereas the the lower equilibrium temperatures are similar to inclusions in quartz veins from Ilímaussaq (Graser et al., in review).

Even though methane makes up only a minor part of the fluid inclusions at Ivigtut, its origin is enigmatic. There are generally two major sources of methane: organic or inorganic. In the analysed fluid inclusions, the very depleted $\delta^{13}C_{CH4}$ value (-28.0 to -40.8 ‰; samples 1475_Qz, 1478, K1, K3, K4, IV 32, IV33) is usually explained by a thermogenic origin, i.e. it results from the thermal decomposition of organic matter at temperatures above 100 °C (Des Marais, 1981; Schoell, 1988). However, a biogenic origin does not apply to Ivigtut, since there are no organic sediments in its close vicinity, but only the basement rocks of the Archaean craton and the Ivigtut granite itself (Fig. 1). Thus, it is reasonable to assume an inorganic source of the methane.

In contrast to CO_2, the $\delta^{13}C$ value of methane is strongly depleted (-28.0 to -40.8 ‰;). Based on thermodynamic calculations, Ryabchikov & Kogarko (2006) showed that at oxygen fugacities close to the QFM buffer, progressively more methane forms in a C-H-O gas during cooling with significant amounts of CH_4 present only below 400 °C. According to their calculations and assuming formation conditions of about 500 °C, 1 kbar and f_{O2} ~ QFM for the Ivigtut cryolite deposit, the gas would have approximately the following mole fraction composition: H_2O 0.75, CO_2 0.24, CH_4 0.008, ± CO, H_2. During cooling to 400 °C, this fluid would change to H_2O 0.7, CO_2, 0.1, CH_4 0.08, ± CO, H_2. Thus, we suggest that the formation of methane in our C-H-O fluid inclusions is the result of respeciation of an original CO_2-H_2O fluid as proposed by Konnerup-Madsen et al. (1985).

6.4 δD and $\delta^{18}O$ in H_2O from fluid inclusions

Quartz in sample 1466 from the deposit and quartz from the host granite (sample 1454) have a $\delta^{18}O$ of 11.2 and 8.4, respectively. Pauly & Bailey (1999) yielded similar $\delta^{18}O$ values for quartz and suggested that these are consistent with crystallisation from granitic oxygen during decreasing temperatures. The $\delta^{18}O$ of water which would be in equilibrium with such quartz for a temperature range from 400 to 800 °C would vary between 3.9 to 10.0 ‰ (Zheng, 1993) which is in strong contrast to the analysed $\delta^{18}O$ of inclusion water (-1.5 to -21.7 ‰). The δD and $\delta^{18}O$ of inclusion water largely fall above the meteoric water line (Craig, 1961 a) and mostly overlap with brines from the Canadian Shield (Tab.2; Fig. 12; Frape & Fritz, 1982; Frape et al., 1984; Bottomley et al., 1994). The shift of the $\delta^{18}O_{H2O}$ value to the left of themeteoric water line can be attributed to low-temperature equilibration with CO_2 with a fractionation factor of approximately 41-44 ‰ (Richet et al., 1977).

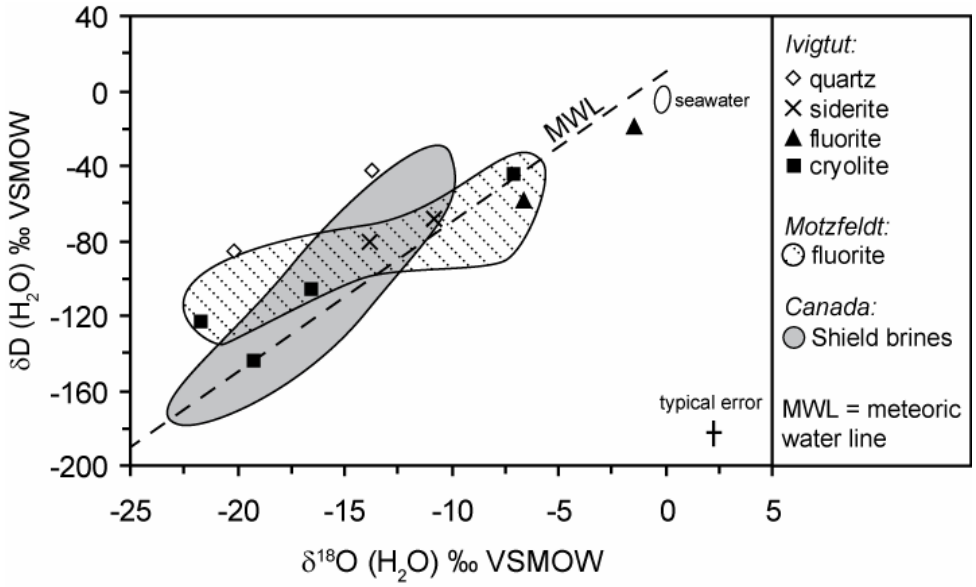

Fig. 12: The isotopic composition of inclusion water from Ivigtut in comparison to Canadian Shield brines (Frape & Fritz, 1982; Frape et al., 1984; Bottomley et al., 1994) and fluid inclusions from Motzfeldt (Schönenberger & Markl, in prep). Fluid inclusions at Ivigtut strongly overlap with Canadian Shield brines and follow the meteoric water line (MWL).

However, mass balance calculations showed that the $\delta^{18}O$ value of H_2O prior to low-temperature CO_2-H_2O equilibration would only change the water's $\delta^{18}O$ value by 2 or 3 ‰ at most, because the H_2O/CO_2 ratio is so high and H_2O normally makes up 92 to 96 mol% in the inclusions. Therefore, equilibration alone cannot account for the depletion in $\delta^{18}O$ of water.

According to Frape & Fritz (1982) and Kelly et al. (1986), the $\delta^{18}O$ depletion of Canadian Shield brines can result from low temperature isotopic equilibration with silicate host rocks under a low water/rock ratio. An intensive water-rock interaction at Ivigtut may also have contributed to the decrease in the $\delta^{18}O$ of the inclusions' water.

6.5 Chemistry of fluid inclusions

Crush leach analyses and microthermometry of fluid inclusions in different minerals from Ivigtut showed that the fluid can be referred to as a brine (Fig. 13). Its total dissolved solids (TDS) amount to more than 10^5 mg/l (Bottomley et al., 1994) which corresponds to > 10 wt% NaCl eq. assuming a density of 1 g/cm^3. This is in agreement with microthermometric results in which most inclusions have a salinity between 11 and 20 wt% NaCl eq. Only three samples contain inclusions with a lower salinity and thus lie in the field of saline groundwaters defined by 10^4-10^5 mg/l TDS (Bottomley et al., 1994).

Different types of groundwater from the Canadian Shield are compared to fluids at Ivigtut, Ilímaussaq and Motzfeldt (Fig. 13). In contrast to the saline character of the Motzfeldt fluid (Schönenberger & Markl, in prep.), the fluids at Ivigtut and Ilímaussaq (Graser et al., in review) clearly fall into the narrow range for brines with only two fluorite samples (IV 32 & 80) being of the saline type. The Cl/Br ratio of the Ivigtut fluid generally ranges between 56 and 110 with a mean of 84 and is less than that of seawater (288; Tab. 3). Stober & Bucher (1999) conducted leaching experiments with granites and gneisses from the Schwarzwald area, Germany. The leachate had Cl/Br ratios between 80 and 100 which is comparable to the Ivigtut fluid. Stober & Bucher (1999) argued if the fluid was of marine origin, it would have Cl/Br ratios similar to that of seawater (i.e. 288). They ascribed lower Cl/Br ratios to the interaction with Br-bearing hydrate minerals in the host rocks. Thus, we can also assume that the low halogen ratio typical of the Ivigtut fluid is the result of intensive water-rock interaction.

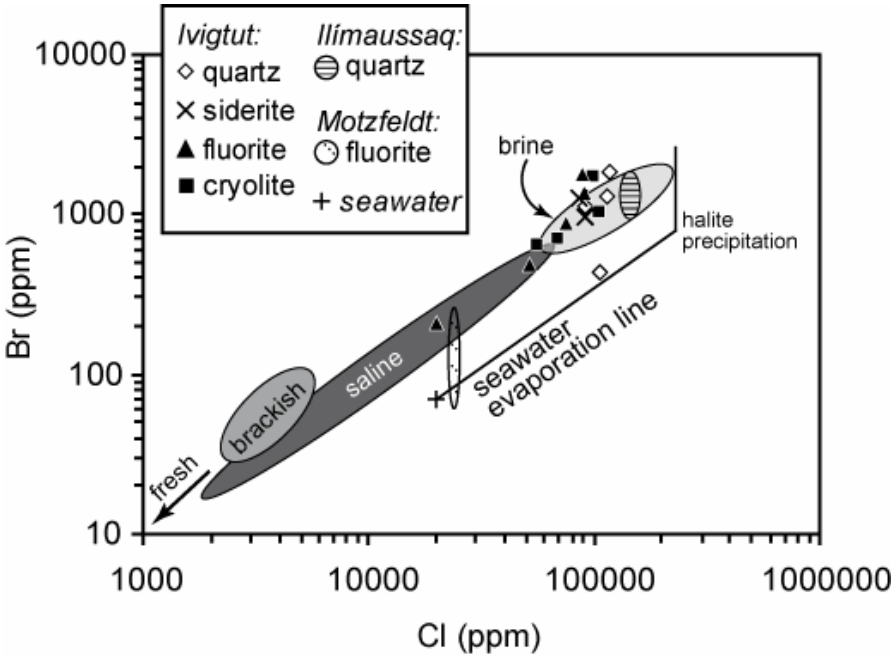

Fig. 13: Chlorine and bromine content from fluid inclusions at Ivigtut analysed by ion chromatography in comparison to Canadian Shield waters (Frape et al., 1984; Bottomley et al., 1994), fluid inclusions in fluorite from Motzfeldt (Schoenenberger et al., in prep.) and inclusions in quartz veins from Ilímaussaq (Graser et al., in prep.). The fluid at Ivigtut can be referred to as a brine with Cl/Br ratios ranging between 53 and 110 that clearly contrast that of seawater (288). Typical error 20 %.

Source of the fluid

Our isotope studies above showed that the inclusions comprise two components of different origin: while the carbon seems to be mantle-derived, the saline-aqueous part of the inclusions clearly displays a meteoric signature.

The halogens Cl and Br may trace the origin of dissolved ions in the fluid, because they behave conservatively in seawater and during water-rock interactions (Bottomley et al., 2005). Lithium, however, is not conservative and its ratios of Li/Cl and Li/Br are strongly dependent on different minerals and rocks (Bottomley et al., 1999). Marine Li shows a good correlation with Cl and Br if the halogens are derived from seawater. Fig. 14 clearly shows that the Ivigtut fluid does neither follow the seawater ratio of Li/Br nor that of Li/Cl. The values rather cluster above the line implying that the salinity is not of marine origin assuming that today's seawater composition is similar to the Proterozoic one.

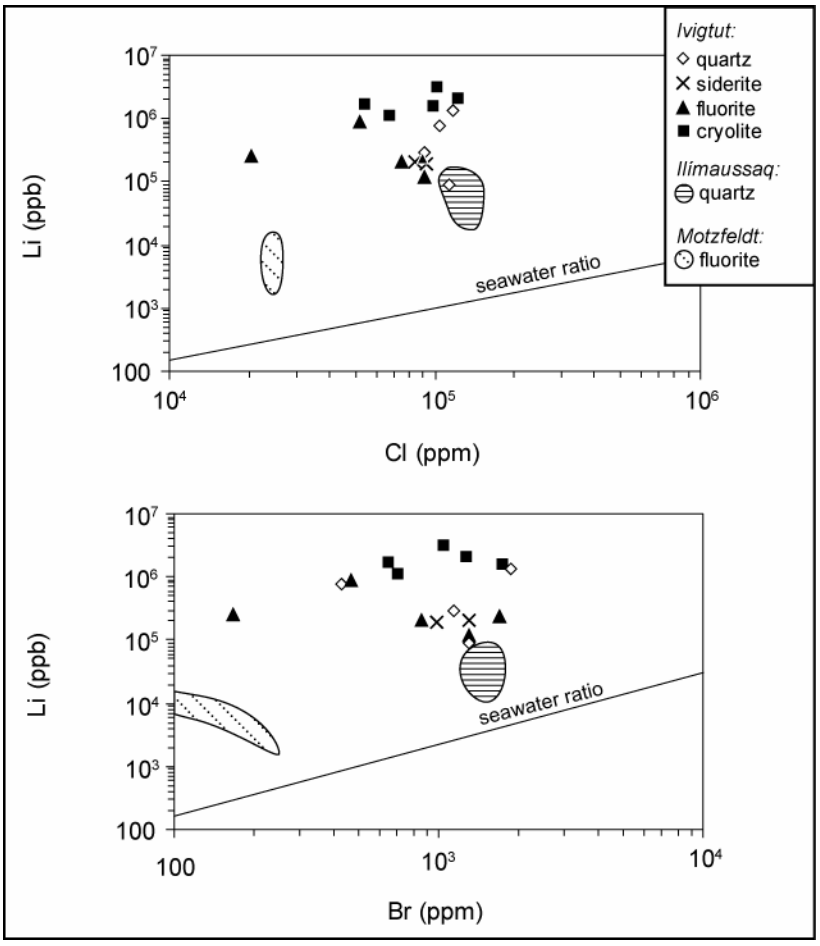

Fig. 14: Chlorine and bromine vs. lithium in fluid inclusions at Ivigtut compared to inclusions from Motzfeldt (Schönenberger & Markl, in prep.) and Ilímaussaq (Graser et al., in review). The lithium-enriched fluid at Ivigtut clearly falls off the Cl-Li and Cl-Br trend of seawater (Bottomley et al., 1999) which thus strengthens its non-marine origin. Typical error 20 %.

The Na-abundance of the Ivigtut fluid might be the result of the distribution of Na and K during crystallisation processes. Goodenough et al. (2000) described the top granite of Ivigtut as hypersolvus whereas the lower part consists of a strongly metasomatised, subsolvus granite that comprises albite and microcline. If a fluid is in equilibrium with two alkali feldspar end members, then the fluid's activities of Na^+ and K^+ are buffered by the following reaction (Orville, 1963):

$$\text{albite} + K^+ \leftrightarrow \text{microcline} + Na^+ \qquad (2)$$

Orville (1963) discussed fractionation processes between the two feldspars and a coexisting fluid. With falling temperature, the fluid becomes progressively enriched in Na as the

feldspars incorporate more K than Na. As a consequence, late-stage crystallisation products are strongly enriched in sodium (e.g. Müller-Lorch et al., 2007). This could explain late albitisation processes and other Na-enriched assemblages in the Ivigtut granite (Goodenough et al., 2000).

7. Formation conditions of fluid inclusions and phase assemblages at Ivigtut

Prokof'ev et al. (1987, 1991) conducted thermodynamic modelling of the Ivigtut mineral assemblages with regard to variable fluorine, sodium and calcium activities. Their calculations showed that cryolite is more stable under acidic conditions (Prokof'ev et al., 1991). The same applies to chiolite and the association of cryolite with topaz. In contrast, less acidic conditions favour the occurrence of cryolite with albite (Prokof'ev et al., 1987). They further demonstrated that at hydrothermal conditions (100-300 °C), the sodium activity must exceed the calcium one by 2-4 orders of magnitude to trigger crystallisation of cryolite.

7.1 Isochores deduced from microthermometry

Isochores deduced from microthermometry provide constraints on the formation conditions of fluid inclusions. At a formation pressure of 1-1.5 kbar (Pauly & Bailey, 1999; Goodenough et al., 2000), calculated isochores for CO_2, primary CO_2-H_2O and aqueous inclusions (Bakker, 2003) indicate that the different inclusion types were formed at 100-400 °C. This could be evidence for the influence of external fluids which is also supported by the isotopic composition of inclusion water. The primary CO_2-H_2O fluid inclusions indicate the highest formation temperatures up to 400 °C (Fig. 15) suggesting that the other inclusion types originated from an already immiscible fluid during cooling.

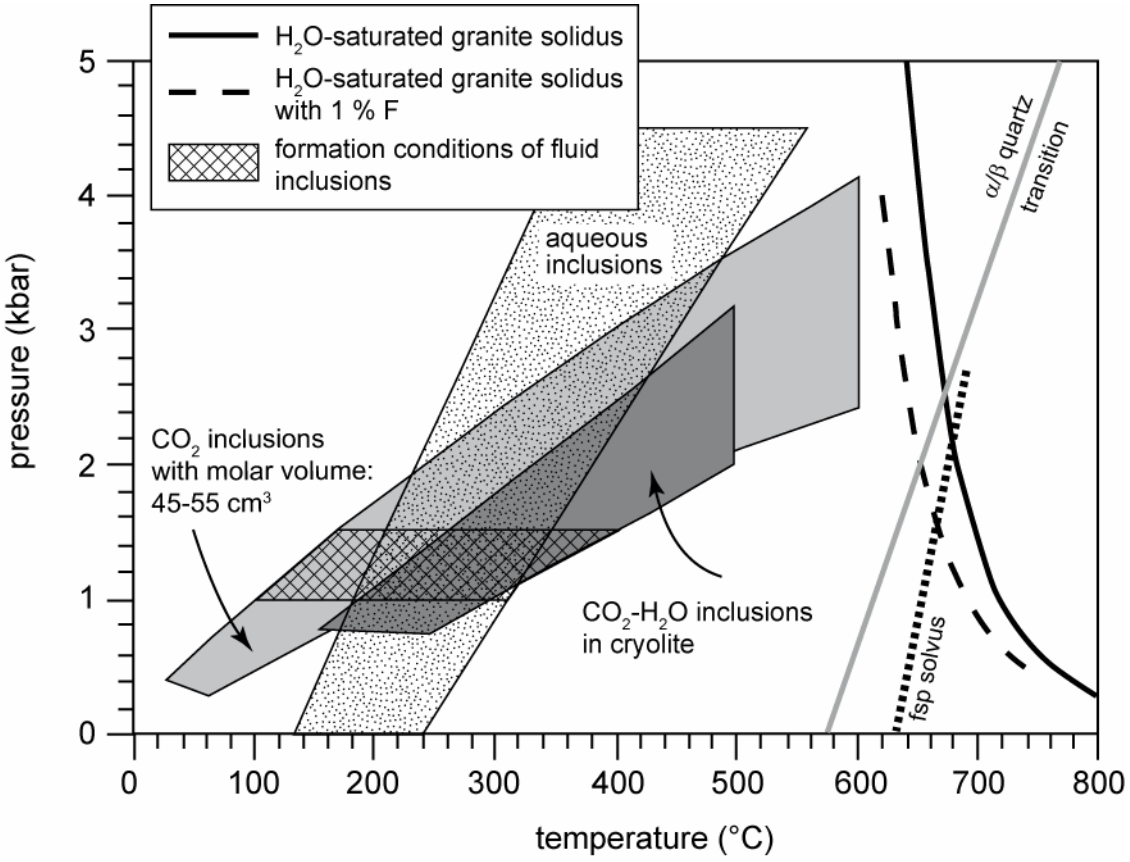

Fig. 15: p-T formation conditions for the analysed fluid inclusions. The pressure of 1-1.5 kbar was suggested by Pauly & Bailey (1999) and Goodenough et al. (2000), but is also derived from the intersection of the feldspar solvus (Boettcher, 1980) with the solidus of H_2O-saturated granite containing 1 % fluorine. For the given pressure, calculated isochores suggest the following formation temperatures for the different inclusion types: a) CO_2 100-300 °C, b) CO_2-H_2O 180-400 °C and c) saline aqueous 180-400 °C. See text for further details.

7.2 Thermodynamic modelling

To further constrain the formation conditions of the cryolite deposit, thermodynamic modelling was carried out using the program TWQ by Berman et al. (1988). The database of Berman (1988) was extended by the thermodynamic properties of cryolite, F-topaz, chiolite and villiaumite from Robie & Hemingway (1995). For rare fluorides like ralstonite, gearksutite or prosopite (Tab. 4), the thermodynamic properties of their fluorine-end members had to be approximated using the models by Van Hinsberg et al. (2005) and Mostafa et al. (1995). Calculations were carried out for pure, fluorine-rich end members unless indicated differently (Fig. 16 a-d).

It must be noted, however, that the modelling only serves as an approximation of the intensive formation parameters using a single set of parameters. The grey-shaded areas (Fig. 16 a-d) represent the stability fields of possible mineral assemblages which are limited by phases that do not occur in the deposit (e.g. villiaumite, pectolite, the alumosilicates). However, since the minerals are closely related within the deposit, it is believed that the stability fields in fact do closely (though not precisely) reflect their formation conditions even if not all assemblages are present in the deposit. All potential assemblages are stable at ≤ 450 °C at high water- and silica-activities evidenced by the occurrence of quartz, hydrous minerals from stage 3 and saline aqueous inclusions in minerals of stage 1 and 2.

Recent experimental studies by Dolejš & Baker (2007 a,b) largely agree with our modelling. For example, the reaction *5 cry + 2 toz + 8 HF = 3 cio + 2 qtz + 4 H_2O* (Fig. 16 b) has approximately the same slope in the T-log a(HF) space as in the diagram by Dolejš & Baker (2007 a). In both studies, the reaction *2 HF + and = toz + H_2O* shows that the "high-fluorination" phases like chiolite become stable at higher log a(HF) (Fig. 16 b; Dolejš & Baker, 2007 a).

Even though Ivigtut is characterised by the predominance of sodium, Ca-bearing minerals like fluorite, gearksutite or prosopite also occur (Pauly & Bailey, 1999). The assemblages of Na- and Ca-bearing minerals are illustrated in Fig 16 c. Even though crush leach analyses revealed the fluid's poverty in Ca, fluorite does occur in the deposit. This is attributed to the low solubility product of fluorite which is easily exceeded in an F-rich (peralkaline) environment (Scaillet & Macdonald, 2004). However, it is the extremely high sodium activity that favours cryolite over fluorite (Prokof'ev et al., 1987) which also explains why the occurrence of fluorite in the deposit is rather restricted. Despite the abundance of sodium and fluorine, villiaumite does not occur in Ivigtut, because of the low temperatures. This is in agreement with Prokof'ev et al. (1987) who stated that villiaumite hardly ever occurs in hydrothermal deposits. In our calculations, villiaumite became stable at temperatures above 450 °C (Fig. 16 a-c).

Mineral	Abbreviation	Formula
Cryolite	cry	Na_3AlF_6
Chiolite	chio	$Na_5Al_3F_{14}$
Gearksutite	gear	$CaAlF_5*H_2O$
Pectolite	pct	$NaCa_2Si_3O_8(OH)$
Prosopite	pro	$CaAl_2F_8$
Ralstonite	ral	$Al_2F_6*H_2O$
Topaz	toz	$Al_2SiO_4F_2$
Villiaumite	vill	NaF

Tab. 4: Fluorides used for thermodynamic phase modelling.

Fig. 16 d clearly shows that the formation of cryolite and chiolite is not only dependent on the Na^+ and F^- activities, but is also sensitive to changes in Al^{3+} activity (and pH) in the fluid. With data from crush leach analysis, we modelled the fluid's activity of Na^+ and F^- and it is evident that cryolite can indeed precipitate from fluids with the analysed composition.

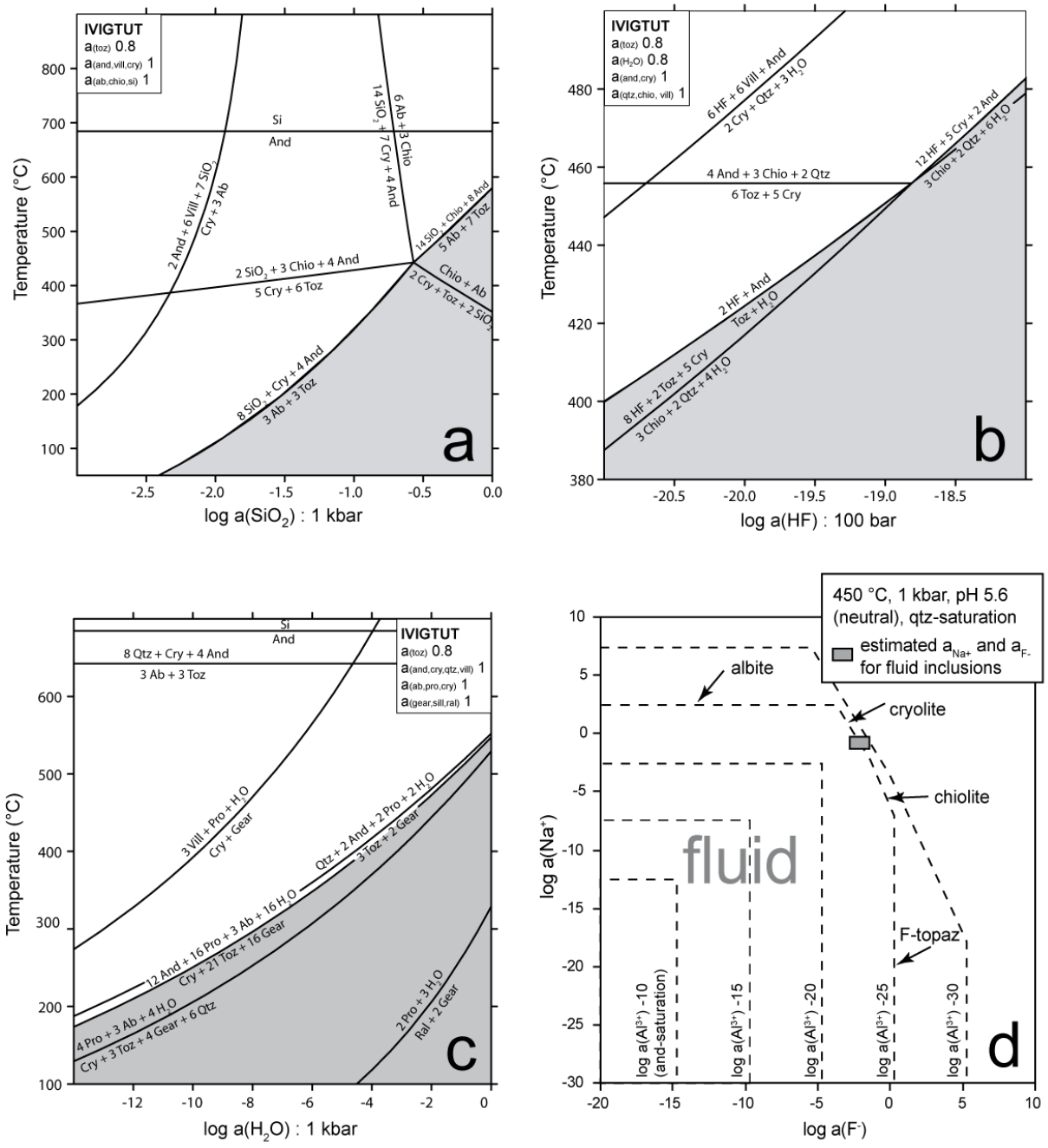

Fig. 16: Approximation of intensive formation parameters of potential stable (grey-shaded) phase assemblages of typical Ivigtut fluorides in dependence of temperature, silica-, water-, HF-, Na^+- and F^--activities. Calculations were carried out for the fluorine-rich end members unless indicated differently. Mineral activities are taken as 1 unless indicated differently. Note that diagram b) was calculated for 100 bar. Abbreviations: ab = albite, and = andalusite, chio = chiolite, cry = cryolite, gear = gearksutite, pct = pectolite, pro = prosopite, qtz = quartz, ral = ralstonite, sill = sillimanite, toz = F-topaz, vill = villiaumite.

8. Discussion of the deposit's evolution

8.1 A true hydrothermal origin?

The term "hydrothermal" has been used to describe formation temperatures of about 400-450 °C for Ivigtut phase assemblages and fluid inclusion isochores (cf. Oen & Pauly, 1967). However, in the case of Ivigtut, this term may not be simply applied because of the extraordinarily F-rich composition. Like water, fluorine depresses the melting temperature and decreases the silicate melt density/viscosity (e.g. Dingwell et al., 1993; Webster et al., 1987; Baker & Vaillancourt, 1995). Veksler (2004) and Thomas et al. (2000) demonstrated that silicate, alkali-rich melts with a high content of volatiles (H, F, Cl or B) can persist down to low temperatures where they coexist with a hydrothermal fluid over a broad p-T range. For example, recent studies by Dolejš & Baker (2007 b) showed that addition of F causes a depression in granite crystallisation temperatures down to 540 °C at 1 kbar. The high abundance of F in Ivigtut may have led to this circumstance where the melt still existed at 400-450 °C and was in the process of evolving to a supercritical fluid.

8.2 Comparison with the model of Pauly & Bailey (1999)

8.2.1 General aspects

Pauly & Bailey (1999) suggested that the deposit formed after the solidification of the host granite. F-H_2O-rich fluids from depth led to greisenisation, later became enriched in Na and Al due to the breakup of feldspars and formed a hydrous aluminofluoride melt. According to their model, this hydrous melt subsequently unmixed into a fluoridic and a siliceous melt at temperatures of about 500-600 °C, the latter leading to the formation of the (siderite-)quartz unit in the lower part of the deposit whereas the cryolite body itself originated from the fluoride-rich melt. We assume that the formation of the deposit had two stages: first, the fluoride-silicate liquid-liquid immiscibility which may have taken place at 500-600 °C and second, the continuous evolution of the fluoridic melt to a solute-rich fluid at temperatures around and below 450 °C.

Our observations do not allow to decide on the first of these steps, as we did not find any unequivocal indication for the separation of the siliceous and fluoridic melts. However, our fluid inclusion data can be used to shed light on the second step. The fact that there are no compositional differences between primary and secondary fluid inclusions indicates that these

fluids share a common history and coexisted with large volumes of the cryolite deposit and surrounding rocks. These fluids could have gradually evolved from the stage 1 melts around or below 450 °C.

8.2.2 Fluid evolution

Pauly & Bailey's (1999) three-stage evolution model implies a change in the fluid's composition: while the early stages are assumed to have consisted of a viscous fluoridic mass poor in H_2O, stage 2 may have been characterised by a Ca-F-Al-rich, still H_2O-poor fluid. Pauly (1992) suggested stage 3 to have been dominated by a fluid rich in H_2O, Ca, Mg and poor in CO_2.

These assumptions are not consistent with our interpretation of the data gathered here. Inclusions from stages 1 and 2 of the deposit (e.g. samples "Zinn" or K4) neither show isotopic nor chemical changes in composition, but they all comprise NaCl-H_2O-CO_2 mixtures of highly varying proportions. However, NaCl-H_2O and CO_2 are of different origin: the brine appears to be ancient meteoric water converted to a crustal brine due to intensive water-rock interaction. The carbonic-rich fluid, however, seems to be derived from the mantle and largely overlaps with $\delta^{13}C$ values from Gardar carbonatites (Coulson et al., 2003). The mode in which these two contrasting fluids mixed is enigmatic. They may have circulated independently through the surrounding crustal rocks, may then have mixed and were heterogeneously trapped during the formation of the cryolite deposit.

8.3 Comparison with experimental results by Dolejš & Baker (2007)

We note that the liquid-liquid immiscibility at 500-600 °C (Pauly & Bailey, 1999) and our proposed continuous fluoridic melt-fluid transition are not supported by the experiments of Dolejš & Baker (2007 a,b) who assumed an immiscibility gap above 1100 °C and 1 kbar in a simplified silica-cryolite system. Moreover, Dolejš & Baker (2007 b) believe that a continuous transition from a volatile-rich melt to a solute-rich fluid only occurs at high alkali and/or high fluorine concentrations which, however, they consider unlikely in natural systems where crystallisation of fluorides inhibits an F-enrichment in residual melts.

However, the experiments by Dolejš & Baker (2007 a,b) were carried out under closed-system conditions in which an F-rich melt fractionated. In contrast, Ivigtut has to be regarded as an open system, as indicated by the granite's strong alteration (Pauly & Bailey, 1999; Goodenough et al., 2000) and by the cryolite- and fluorite-bearing breccia pipes which

document release of fluids/melts during crystallisation of the ore body. The assumption of an open system is also in agreement with the isotopic composition of inclusion water which suggests a meteoric origin. Therefore, the internal F-buffering during fractionation of an F-rich system described by Dolejš & Baker (2007 b) cannot be simply transferred to the Ivigtut complex and hence, experimental proof or disproof of a miscibility gap in this system, which would correspond to Pauly & Bailey's (1999) model, is still lacking.

9. Conclusions

The results of this study contribute to the knowledge of the evolution of the Ivigtut cryolite deposit and provides further insight into the evolution model proposed by Pauly & Bailey (1999):

- Primary and secondary inclusions seem to be derived from the same immiscible $NaCl/H_2O$-CO_2 fluid and do not support Pauly & Bailey's (1999) assumption of a fluid which gradually changed its composition during the deposit's evolution.
- The isotopic composition of CO_2 from fluid inclusions argues for a mantle-derived origin of the carbon. Oxygen of CO_2, however, appears to have equilibrated with oxygen from inclusion water at low temperatures.
- The depletion in $\delta^{18}O$ of water must be ascribed to low-temperature isotope exchange with CO_2 and to intensive water-rock interaction. Both δD and $\delta^{18}O$ values of inclusion water closely follow the meteoric water line, are comparable with Canadian Shield brines (Fritz & Frape, 1982; Frape et al., 1984; Bottomley et al., 1994) and appear to be neither of marine nor magmatic origin. This is in contrast to Pauly & Bailey (1999) who assume that a post-magmatic and not meteoric fluid accounted for leaching processes within the granite.
- Isochores for different inclusion types suggest formation temperatures between 100 and 400 °C. Thermodynamic modelling served as an approximation of intensive formation parameters of typical Ivigtut fluorides and support the deposit's hydrothermal origin.

Acknowledgments

Financial support by the Graduiertenförderung des Landes Baden-Württemberg is gratefully acknowledged. Joanne Potter and Frederick J. Longstaffe are thanked for carbon isotope analyses of inclusion methane at the University of Western Ontario/London, Canada. Ole Petersen kindly provided rock samples from the Geological Musuem of Copenhagen. Collaboration with Johannes Schönenberger and Gabi Stoschek was invaluable to optimise the ion chromatography technique. Thomas Wagner ist thanked for activity modelling. Bernd Steinhilber helped with isotope analyses and Verena Krasz with hand-picking of crush leach samples. Ralf-Thomas Schmitt from the Museum für Naturkunde at the Humboldt University of Berlin provided specimens of late-stage fluorides from Ivigtut even though they were not used in this study. John Bailey and an anonymous reviewer are thanked for their valuable comments and suggestions.

References

ANDERSON, M.R., RANKIN, A.H., SPIRO, B., 1992. Fluid mixing in the generation of mesothermal gold mineralisation in the Transvaal Sequence, Transvaal, South Africa. European Journal of Mineralogy 4, 933-948.

BADANINA, E.V., VEKSLER, I.V., THOMAS, R., SYRITSO, L.F., TRUMBULL, R.B., 2004. Magmatic evolution of Li-F, rare-metal granites: a case study of melt inclusions in the Khangilay complex, Eastern Transbaikalia (Russia). Chemical Geology 210, 113-133.

BAKER, D.R. & VAILLANCOURT, J., 1995. The low viscosities of F-H_2O-bearing granitic melts and implications for melt extraction and transport. Earth and Planetary Science Letters 132, 199-211.

BAKKER, R.J., 1997. Clathrates: computer programs to calculate fluid inclusion V-X properties using clathrate melting temperatures. Computers & Geosciences 23, 1-18.

BAKKER, R.J., 2003. Package FLUIDS 1. Computer programs for analysis of fluid inclusion data and for modelling bulk fluid properties. Chemical Geology 194, 3-23.

BANKS, D.A., YARDLEY, B.W.D., 1992. Crush-leach analysis of fluid inclusions in small natural and synthetic samples. Geochimica et Cosmochimica Acta 56, 245-248.

BANKS, D.A., GIULIANI, G., YARDLEY, B.W.D., CHEILLETZ, A., 2000. Emerald mineralisation in Colombia: fluid chemistry and the role of brine mixing. Mineralium Deposita 35, 699-713.

BEESKOW, B., TRELOAR, P.J., RANKIN, A.H., VENNEMANN, T.W., SPANGENBERG, J., 2006. A reassessment of models for hydrocarbons generation in the Khibiny nepheline syenite complex, Kola Peninsual, Russia. Lithos 91, 1-18.

BERMAN, R.G., 1988. Internally-consistent thermodynamic data for minerals of the system Na_2O-CaO-MgO-FeO-Fe_2O_3-Al_2O_3-SiO_2-TiO_2-H_2O-CO_2. J. Pet. 29, 2, 445-552.

BERMAN, R.G., BROWN, T.H., PERKINS, E.H., 1988. GEO-CALC update; software for calculation of pressure-temperature-X_{CO2} activity phase diagrams. In: Geological Association of Canada, Mineralogical Association of Canada, Canadian Society of Petroleum Geologists, 1988 joint annual meeting. Program with Abstracts – Geological Association of Canada; Mineralogical Association of Canada; Canadian Geophysical Union, Joint Annual Meeting. 13, p. A9.

BODNAR, R.J., 1993. Revised equation and table for determining the freezing point depression of the H2O-NaCl solutions. Geochimica et Cosmochimica Acta 57, 3, 683-684.

BOETTCHER, A.L., 1980. The systems albite-orthoclase-water and albite-orthoclase-quartz-water: Chemographic phase relationships. Journal of Geophysical Research 85, 6955-6962.

BOROVIKOV, A.A., GUSHCHINA, L.N., BORISEKNO, A.S., 2001. Specific features of $FeCl_2$ and $FeCl_3$ solution behaviour at low temperatures (cryometry of fluid incluions). XVI ECROFI European Current Research On Fluid Incluions, Faculdade de Ciências do Porto, Departamento de Geologia, Memória 7, 61-63.

BOTTOMLEY, D.J., GREGOIRE, D.C., RAVEN, K.G., 1994. Saline groundwaters and brines in the Canadian Shield: Geochemical and isotopic evidence for a residual evaporite brine component. Geochimica et Cosmochimica Acta 58, 1483-1498.

BOTTOMLEY, D.J., KATZ, A., CHAN, L.H., STARINSKY, A., DOUGLAS, M., CLARK, I.D., RAVEN, K.G., 1999. The origin and evolution of Canadian Shield brines: evaporation of freezing of seawater? New lithium isotope and geochemical evidence from the Slave craton. Chemical Geology 155, 295-320.

BOTTOMLEY, D.J., CLARK, I.D., BATTYE, N., KOTZER, T., 2005. Geochemical and isotopic evidence for a genetic link between Canadian Shield brines, dolomitization in the Western Canada Sedimentary Basin, and Devonian calcium-chloridic seawater. Canadian Journal of Earth Sciences 42, 2059-2071.

BOTTRELL, S.H., YARDLEY, B.W.D., BUCKLEY, F., 1988. A modified crush-leach method for the analysis of fluid inclusion electrolytes. Bulletin de Minéralogie 111, 279-290.

COULSON, I.M., GOODENOUGH, K.M., PEARCE, N.J.G., LENG, M.J., 2003. Carbonatites and lamprophyres of the Gardar Province – a "window" to the sub-Gardar mantle? Mineralogical Maganzine 67, 855-872.

CRAIG, H., 1961 a. Isotopic variations in meteoric waters. Science 133, 1702.

CRAIG, H., 1961 b. Standards for reporting concentrations of deuterium and oxygen 18 in natural waters. Science 133, 1833-1834.

CURRIE, K.L., EBY, N.G., GITTINS, J., 1986. The petrology of the Mont Saint Hilaire complex, southern Quebec: An alkaline gabbro-peralkaline syenite association. Lithos 19, 65-81.

DAVIS, W.D., LOWENSTEIN, T.K., SPENCER, R.J., 1989. Melting behaviour of fluid inclusions in laboratory-grown halite crystals in the systems NaCl-H_2O, NaCl-KCl-H_2O, NaCl-$MgCl_2$-H_2O and NaCl-$CaCl_2$-H_2O. Geochimica et Cosmochimica Acta 54, 591-601.

DES MARAIS, D.J., DONCHIN, J.H., NEHRING, M.L., TRUESDELL, A.H., 1981. Molecular carbon isotopic evidence for the origin of geothermal hydrocarbons. Nature 292, 826.

DINGWELL, D.B., KNOCHE, R., WEBB, S.L., 1993. The effect of F on the density of haplogranite melt. American Mineralogist 78, 325-330.

DOLEJŠ, D., BAKER, R., 2007 a. Liquidus Equilibria in the System K_2O-Na_2O-Al_2O_3-SiO_2-F_2O-1-H_2O to 100 Mpa: I. Silicate-Fluoride Liquid Immiscibility in Anhydrous Systems. Journal of Petrology 48, 785-806.

DOLEJŠ, D., BAKER, R., 2007 b. Liquidus Equilibria in the System K_2O-Na_2O-Al_2O_3-SiO_2-F_2O-1-H_2O to 100 Mpa: II. Differentiation Paths of Fluorosilicic Magmas in Hydrous Systems. Journal of Petrology 48, 807-828.

DUAN, Z., MØLLER, N., WEARE, J.H., 1995. Equation of state for the NaCl-H_2O-CO_2 system: Prediction of phase equilibria and volumetric properties. Geochimica et Cosmochimica Acta 59, 2869-2882.

DUBOIS, M., WEISBROD, A., SHTUKA, A., 1994. Experimental determination of the the two-phase (liquid and vapor) region in water-alkali chloride binary systems at 500 ° and 600 °C using synthetic fluid inclusions. Chemical Geology 115, 227-238.

DUBOIS, M., COQUINOT, Y., CASTELAIN, T., MONNIN, C., GOUY, S., GOFFÉ, B., 2007. Phase relationships in the H_2O-NaCl-$LiCl_2$ system: A synthesis. European Current Research of Fluid Inclusions (ECROFI-XIX) Abstract Volume, 28.

FRANTZ, J.D., POPP, R.K., HOERING, T.C., 1992. The compositional imits of fluid immiscibility in the system H_2O-NaCl-CO_2 as determined wit the use of synthetic fluid inclusions in conjuction with mass spectrometry. Chemical Geology 98, 237-255.

FRAPE, S.K., FRITZ, P., 1982. The chemistry and isotopic composition of saline groundwaters from the Sudbury Basin, Ontario. Canadian Journal of Earth Sciences 19, 645-661.

FRAPE, S.K., FRITZ, P., MCNUTT, R.H., 1984. Water-rock interaction and chemistry of groundwaters from the Canadian Shield. Geochimica et Cosmochimica Acta 48, 1617-1627.

FRIEDMAN, I., 1953. Deuterium content of natural waters and other substances. Geochimica et Cosmochimica Acta 4, 89-103.

FRIEDMAN, I., O'Neil, J.R., 1977. Compilation of stable isotope fractionation factors of geochemical interest. In: Fleischer, M. (Ed.), Data of geochemistry. U.S. Geological Survey Professional Paper 440-KK, 12.

GRASER, G., POTTER, J., KOEHLER, J., MARKL, G., in review. Isotopic, major, minor and trace element geochemistry of late-stage fluids in the peralkaline Ilímaussq intrusion, South Greenland.

GROSS, E.B., HEINRICH, E.W., 1966. Petrology and Mineralogy of the Mount Rosa area, El Paso and Teller County, Colorado. II. Pegmatites. American Mineralogist 51, 229-323.

GOODENOUGH, K.M., UPTON, B.G.J., ELLAM, R.M., 2000. Geochemical evolution of the Ivigtut granite, South Greenland: a fluorine-rich "A-type" intrusion. Lithos 51, 205-221.

HALAMA, R., VENNEMANN, T., SIEBEL, W., MARKL, G., 2005. The Grønnedal-Ika Carbonatite-Syenite Complex, South Greenland: Carbonatite Formation by Liquid Immiscibility. Journal of Petrology 46, 191-217.

IRBER, W., 1999. The lanthanide tetrad effect and its correlation with K/Rb, Eu/Eu*, Sr/Eu, Y/Ho, and Zr/Hf of evolving peraluminous granite suites. Geochimica et Cosmochimica Acta 63, 489-508.

KELLY, W.C., RYE, R.O., LIVNAT, A., 1986. Saline minewaters of the Keweenaw Peninsula, Northern Michigan: Their natural origin and relation to similar deep waters in the Precambrian crystalline rocks of the Canadian Shield. American Journal of Science 286, 281-308.

KOGARKO, L.N., 1980. Ore-forming potential of alkaline magma. Lithos 26, 167-175.

KONNERUP-MADSEN, J., 1984. Compositions of fluid inclusions in granites and quartz syenites from the gardar continental rift province (South Greenland). Bulletin de Minéralogie 107, 327-340.

KONNERUP-MADSEN, J., 2001. A review of the composition and evolution of hydrocarbon gases during solidification of the Ilímaussaq alkaline complex, South Greenland. Geology of Greenland Survey Bulletin 301, 159-166.

KONNERUP-MADSEN, J., ROSE-HANSEN, J., 1982. Volatiles associated with alkaline igneous rift activity; fluid inclusions in the Ilímaussaq Intrusion and the Gardar granitic complexes (South Greenland). Chemical Geology 37, 79-93.

KONNERUP-MADSEN, J., ROSE-HANSEN, J., 1984. Composition and significance of fluid inclusions in the Ilímaussaq peralkaline granite, South Greenland. Bulletin de Minéralogie 107, 317-326.

KONNERUP-MADSEN, J., DUBESSY, J., ROSE-HANSEN, J., 1985. Combined Raman microprobe spectrometry and microthermometry of fluid inclusions in minerals from igneous rocks of the Gardar province (south Greenland). Lithos 18, 271-280.

KONNERUP-MADSEN, J., KREULEN, R., ROSE-HANSEN, J., 1988. Stable isotope characteristics of hydrocarbon gases in the alkaline Ilímaussaq Complex, South Greenland. Bulletin de Minéralogie 111, 567-576.

KRESTEN, P., 1988. The chemistry of fenitization: examples from Fen, Norway. Chemical Geology 68, 329-349.

LARSEN, L., SØRENSEN, H., 1987. The Ilímaussaq intrusion – progressive crystallization and formation of layering in an agpaitic magma. In: Fitton, J.G., Upton, B.G.J. (Eds.), Alkaline Igneous Rocks. Geological Society Special Publication 30, 473-488.

LOUCKS, R.R., 2000. Precise geothermometry on fluid inclusion populations that trapped mixtures of immiscible fluids. American Journal of Science 300, 23-59.

MARKL, G., MARKS, M., SCHWINN, G., SOMMER, H., 2001. Phase Equilibrium Constraints on Intensive Crystallization Parameters of the Ilímaussaq Complex, South Greenland. Journal of Petrology 42, 2231-2258.

MARKS, M., MARKL, G., 2001. Fractionation and Assimilation Processes in the Alkaline Augite Syenite Unit of the Ilímaussaq Intrusion, South Greenland, as Deduced from Phase Equilibria. Journal of Petrology 42, 1947-1969.

MARKS, M., VENNEMANN, T., SIEBEL, W., MARKL, G., 2003. Quantification of Magmatic and Hydrothermal Processes in a Peralkaline Syenite-Alkali Granite Complex Based on Textures, Phase Equilibria, and Stable and Radiogenic Isotopes. Journal of Petrology 44, 1247-1280.

MARKS, M., VENNEMANN, T., SIEBEL, W., MARKL, G., 2004. Nd-, O-, and H-isotopic evidence for complex, closed-system fluid evolution of the peralkaline Ilímaussaq Intrusion, South Greenland. Geochimica Cosmochimica Acta 68, 3379-3395.

MILLERO, F.J., 2004. Physicochemical Controls on Seawater. In: Elderfield, H., Holland, H.D., Turekian, K.K. (Eds.), Treatise on Geochemistry, Volume 6, The Oceans and Marine Geochemistry. Elsevier Pergamon, Amsterdam.

MOSTAFA, A.T.M., EAKMAN, J.M., YARBRO, S.L., 1995. Prediction of Standard Heat and Gibbs Free Energies of Formation of Solid Inorganic Salts from Group Contributions. Industrial & Engineering Chemistry Research 34, 4577-4582.

MÜLLER-LORCH, D., MARKS, M.A.W., MARKL, G., 2007. Na and K distribution in agpaitic pegmatites. Lithos 95, 315-330.

NIVIN, V.A., BELOV, N.I., TRELOAR, P.J., TIMOFEYEV, V.V., 2001. Relationships between gas geochemistry and release rates and the geochemical state of igneous rock massifs. Tectonophysics 336, 233-244.

NIVIN, V.A., IKORSKII, S.V., TRELOAR, P.J., 2002. Bulk gas content variations in fluid inclusions of minerals from the Khibina and Lovozero nepheline-syenite plutons (NE Baltic Shield, Russia); implication for origin of hydrocarbon gases. Abstracts of the 18th General Meeting of the International Mineralogical Association 18, 248.

NIVIN, V.A., TRELOAR, P.J., KONOPLEVA, N.G., IKORSKY, S.V., 2005. A review of the occurrence, form and origin of C-bearing species in the Khibiny alkaline igeneous complex, Kola Peninsula, NW Russia. Lithos 85, 93-112.

ORVILLE, P.M., 1963. Alkali ion exchange between vapor and feldspar phases. American Journal of Science 261, 201-237.

OEN, I.S., PAULY, H., 1967. A sulphide paragenesis with pyrrhotite and marcasite in the siderite-cryolite ore of Ivigtut, South Greeland. Meddelelser om Grønland 175, 55p.

OHMOTO, H., GOLDHABER, M.B., 1997. Sulfur and carbon isotopes. In: Barnes, H.L. (Ed.), Geochemistry of hydrothermal ore deposits. 3rd ed., Wiley, New York, 517-611.

PALACHE, C., BERMAN, H., FRONDEL, C., 1951. The System of Mineralogy, 7th Ed., Vol. II. John Wiley & Sons, Inc.

PAULY, H., 1992. Topaz, prospoite and closing stage of formation of the Ivigtut cryolite deposit, South Greenland. Meddelelster om Grønland, Geoscience 28, 22 p.

PAULY, H., BAILEY, J.C., 1999. Genesis and evolution of the Ivigtut cryolite deposit, SW Greenland. Meddelelser om Grønland, Geoscience 37, 60 p.

PINEAU, F., JAVOY, M., 1983. Carbon isotopes and concentrations in mid-oceanic ridge basalts. Earth and Planetary Science Letters 62, 239-257.

POTTER, J., RANKIN, A.H., TRELOAR, P.J., 2004. Abiogenic Fischer-Tropsch synthesis of hydrocarbons in alkaline igneous rocks; fluid inclusion, textural and isotopic evidence from the Lovozero Complex, N.W. Russia. Lithos 75, 311-330.

PROKOF'EV, V.Y., SEMENOV, Y.V., RYABENKO, S.V., KORYTOV, F.Y., 1987. Hydrothermal conditions of formation of mineral assemblages containing cryolite. Geokhimiya 6, 824-832.

PROKOF'EV, V.B., NAUMOV, V.B., IVANOVA, G.F., SAVEL'EVA, N.I., 1991. Fluid inclusion studies in cryolite and siderite of the Ivigtut deposit (Greenland). Neues Jahrbuch für Mineralogie, Monatshefte 1, 32-38.

RAMBOZ, C., PICHAVANT, M., WEISBROD, A., 1982. Fluid immiscibility in natural processes: Usa and misuse of fluid inclusion data. II. Interpretation of fluid inclusion data in terms of immiscibility. Chemical Geology 37, 29-48.

RANLØV, J., DYMEK, R.F., 1991. Compositional zoning in hydrothermal aegirine from fenites in the Proterozoic Gardar Province, south Greenland. European Journal of Mineralogy 3, 837-853.

RICHET, P., BOTTINGA, Y., JAVOY, A., 1977. A review of hydrogen, carbon, nitrogen, oxygen, sulphur and chlorine stable isotope fractionation among gaseous molecules. Annual Reviews Earth Planetary Science 5, 65-110.

ROBIE, R.A., HEMINGWAY, B.S., 1995. Thermodynamic properties of minerals and related substances at 298,15 K and 1 bar pressure and at higher temperatures. U.S. Geological Survey Bulletin 2131.

ROCK, N.M.S., 1976. Fenitisation around the Monchique alkaline complex, Portugal. Lithos 9, 263-279.

RYABCHIKOV, I.D., KOGARKO, L.N., 2006. Magnetite compositions and oxygen fugacities of the Khibina magmatic system. Lithos 91, 35-45.

SALVI, S., WILLIAMS-JONES, A.E., 1990. The role of hydrothermal processes in the granite hosted Zr, Y, REE deposit at Strange Lake, Quebec/Labrador: evidence from fluid inclusions. Geochimica Cosmochimica Acta 54, 2403–2418.

SALVI, S., WILLIAMS-JONES, A.E., 2006. Alteration, HFSE mineralisation and hydrocarbon fromation in peralkaline igneous systems: Insights from the Strang Lake Pluton, Canada. Lithos 91, 19-34.

SCAILLET, B., MACDONALD, R., 2004. Fluorite stability in silicic magmas. Contributions to Mineralogy and Petrology 147, 319-329.

SCHOELL, M., 1988. Multiple origins of methane in the Earth. Chemical Geology 71, 1-10.

SHEPHERD, T.J., RANKIN, A.H., ALDERTON, D.H.M., 1985. A practical guide to fluid inclusion studies. Glasgow, Blackie, 239.

SINDERN, S., KRAMM, U., 2000. Volume characteristics and element transfer of fenite aureoles: a case study from the Iivaara alkaline complex, Finland. Lithos 51, 75-93.

SØRENSEN, H., 2001. Brief introduction to the geology of the Ilímaussaq alkaline complex, South Greenland, and its exploration history. Geology of Greenland Survey Bulletin 190, 7-23.

SOWERBY, J.R., KEPPLER, H., 2002. The effect of fluorine, boron and excess sodium on the critical curve in the albite-H_2O system. Contributions to Mineralogy and Petrology 143. 32-37.

STERNER, S.M., KERRICK, D.M., BODNAR, R.J., 1984. Experimental determination of unmixing in CO_2-H_2O-NaCl fluids at 500 °C and 1 kbar using synthetic fluid inclusions: Metamorphic implications. Geological Society of America, Abstract with Programs 16, 668.

STOBER, I., BUCHER, K., 1999. Origin of salinity of deep groundwater in crystalline rocks. Terra Nova 11, 181-185.

STURT, B.A., RAMSAY, D.M., 1965. The alkalic complex of the Breivikbotn area, Sørøy, Norway. Norsk Geologisk Undersogelse 231, 1-142.

TAGIROV, B., SCHOTT, J., 2001. Aluminium speciation in crustal fluids revisited. Geochimica et Cosmochimia Acta 65, 3965-3992.

TAGIROV, B., SCHOTT, J., HARRICHOURY, J.-C., 2002 a. Experimental study of aluminium-fluoride complexation in near-neutral and alkaline solutions to 300 °C. Chemical Geology 184, 301-310.

TAGIROV, B., SCHOTT, J., HARRICHOURRY, J.-C., SALVI, S., 2002 b. Experimental study of aluminium speciation in chloride- and fluoride-rich supercritical fluids. Geochimica et Cosmochimica Acta 66, 2013-2024.

TAYLOR, H.P.JR., FRECHEN, J., DEGENS, E.T., 1967. Oxygen and carbon isotope studies of carbonatites from the Laacher See District, West Germany and the Alno District, Sweden. Geochimica et Cosmochimia Acta 31, 407-430.

THOMAS, R., WEBSTER, J.D., HEINRICH, W., 2000. Melt inclusions in pegmatite quartz: complete miscibility between silicate melts and hydrous fluids at low pressure. Contributions to Mineralogy and Petrology 139, 394-401.

UPTON, B.G.J., EMELEUS, C.H., HEAMAN, L.M., GOODENOUGH, K.M, FINCH, A.A., 2003. Magmatism of the mid-Proterozoic Gardar Province, South Greenland: chronology, petrogenesis and geological setting. Lithos 68, 43-65.

VAN HINSBERG, V.J., VRIEND, S.P., SCHUMACHER, J.C., 2005. A new method to calculate end-member thermodynamic properties of minerals from their constituent polyhedra; II, Heat capacity, compressibility and thermal expansion. Journal of Metamorphic Geology 23, 681-693.

VEKSLER, I., 2004. Liquid immiscibility and its role at the magmatic-hydrothermal transition: a summary of experimental studies. Chemical Geology 210, 7-31.

VENNEMANN, T., O'NEIL, J.R., 1993. A simple and inexpensive method of hydrogen isotope and water analyses of minerals and rocks based on zinc reagent. Chemical Geology 103, 227-234.

WEBSTER, J.D., HOLLOWAY, J. R. & HERVIG, R.L., 1987. Phase equilibria of a Be, U and F-enriched vitrophyre from Spor Mountain, Utah. Geochimica et Cosmochimica Acta 51, 389-402.

WILLIAMS, F.A., MEEHAN, J.A., PAULO, K.L., JOHN, T.V., RUSHTON, H.G., 1956. Economic geology of the decomposed columbite-bearing granites, Jos Plateau, Nigeria. Economic Geology 51, 303-322.

WOOD, S.A., 1990. The aqueous geochemistry of the rare-earth elements and yttrium. 2. Theoretical predictions of speciation in hydrothermal solutions to 350 °C at saturation water vapor pressure. Chemical Geology 88, 99-125.

WOOD, S.A., 2003. The geochemistry of rare earth elements and yttrium in geothermal waters. In: Simmons, S.F., Graham, I. (Eds.), Volcanic, geothermal, and ore-forming fluids; rulers and witnesses of processes within the Earth. Special Publication (Society of Economic Geologists (U.S.)) 10, 133-158.

YARDLEY, B.W.D., BANKS, D.A., BOTTRELL, S.H., 1993. Post-metamorphic gold-quartz veins from NW Italy: the composition and origin of the ore fluid. Mineralogical Magazine 57, 407-422.

ZARAISKY, G.P., 1994. The influence of acidic fluoride and chloride solutions on the geochemical behaviour of Al, Si and W. In: Shmulovich, K.I., Yardley, B.W.D., Gonchar, G.G. (Eds.), Fluids in the Crust: Equilibrium and Transport Properties. Chapman and Hall, 139-161.

ZHENG, Y.G., 1993. Calculation of oxygen isotope fractionation in anhydrous silicate minerals. Geochimica et Cosmochimica Acta 57, 1079-1091.

REE-systematics of fluorides, calcite and siderite in peralkaline plutonic rocks from the Gardar Province, South Greenland[1]

Johannes Schönenberger, Jasmin Köhler, and Gregor Markl*

Institut für Geowissenschaften
AB Mineralogie und Geodynamik
Eberhard-Karls-Universität
Wilhelmstrasse 56
D-72074 Tübingen
Germany

in press bei Chemical Geology: doi: 10.1016/j.chemgeo.2007.10.002.

*Corresponding author.

Telephone: +49 7071 2972930
Fax: +49 7071 293060
e-mail: markl@uni-tuebingen.de

[1]Contribution to the Mineralogy of Ilímaussaq # 140

Abstract

The Gardar failed-rift Province is world-famous for its (per-)alkaline plutonic rocks. Elevated contents of F in the mantle source and F-enrichment in the parental melts have been suggested to account for the peculiarities of the Gardar rocks (e.g. their rare mineralogy extreme enrichment of HFSE elements, Be or REE in the Ilímaussaq agpaites, and the formation of the unique Ivigtut cryolite deposit). To constrain the formation and chemical evolution of F-bearing melts and fluids, fluorides (fluorite, cryolite, viliaumite, cryolithionite), calcite and siderite from the Ilímaussaq, Motzfeldt and Ivigtut complexes were analysed for their trace element content focusing on the rare earth elements and yttrium (REE).

The various generations of fluorite occurring in the granitic Ivigtut, agpaitic Ilímaussaq and miaskitic to agpaitic Motzfeldt intrusions all share a negative Eu anomaly which is attributed to (earlier) feldspar fractionation in the parental alkali basaltic melts. This interpretation is supported by the abundance of anorthositic xenoliths in many Gardar plutonic rocks.

The primary magmatic fluorites from Ilímaussaq and Motzfeldt display very similar REE patterns suggesting a formation from closely related parental melts under similar conditions. Hydrothermal fluorites from these intrusions were used to constrain the multiple effects responsible for the incorporation of trace elements into fluorides: temperature dependence, fluid migration/interaction and complexation resulting in REE fractionation. Generally, the REE patterns of Gardar fluorides reflect the evolution and migration of a F/CO_2-rich fluid leading to the formation of fluorite and fluorite/calcite veins. In certain units, this fluid inherited the REE patterns of altered host rocks. In addition, there is evidence of an even younger fluid of high REE abundance which resulted in highly variable REE concentrations (up to three orders of magnitude) within one sample of hydrothermal fluorite.

The REE patterns of the granitic Ivigtut intrusion show flat to slightly heavy-REE-enriched patterns characterised by a strong tetrad effect. This effect is interpreted to record extensive fluid- rock interaction in highly fractionated, Si-rich systems.

Interestingly, the fluorides appear to record different source REE patterns, as the spatially close Motzfeldt and Ilímaussaq intrusions show strong similarities and contrast with the Ivigtut intrusion located 100 km NE. These variations may be attributed to differences in the tectonic position of the intrusions or mantle heterogeneities.

Keywords: Gardar, fluorite, REE, fractionation, alkaline

1. Introduction

Fluorine plays a crucial role in the crystallisation of magmas, as it drastically reduces the melting temperature and the melt's viscosity/density (Webster, 1990; Manning, 1981; Dingwell, 1988). In magmatic processes, fluorine-rich fluids are capable of transporting and enriching elements like HFSE, the rare earth elements and yttrium (REE) to economic amounts (Stähle et al., 1987; Rubin et al., 1993; Pan and Fleet, 1996; Rudnick et al., 2000; Salvi et al., 2000; Williams-Jones et al., 2000; Tagirov et al., 2002). Nowadays, fluorite is widely used as a geochemical exploration tool (e.g. Hill et al., 2000; Eppinger & Closs, 1990) as it is often associated with economically important elements like Pb, Zn, Ag and Au in hydrothermal deposits.

The study of REE incorporation into fluorite and associated minerals (e.g. calcite, siderite, cryolite and villiaumite) of different intrusions and evolutionary stages (e.g. primary magmatic, pegmatitic or hydrothermal; e.g. Möller et al., 1976; Kempe et al., 1999; Trinkler et al., 2005) can provide insight into fluid evolution, fluid-rock interaction and element behaviour in highly fractionated rocks during ortho- to late-magmatic processes (e.g. Gagnon et al., 2003). These mechanisms include chemical complexation, redox characteristics, mineral/rock leaching, chemical composition of the precipitating melt/fluid (e.g. Ekambaram et al., 1986; Bau, 1991; Bau & Möller, 1992; Liu et al., 2005).

Furthermore, melts and fluids can become considerably enriched in fluorine during fractionation processes leading to the crystallisation of fluorite and minerals like topaz and cryolite (Scaillet & MacDonald, 2004, Dolejš & Baker, 2007 a, b). Scaillet & Macdonald (2001; 2004) summarised the stability of magmatic fluorite in peralkaline rhyolitic melts. They stated that even in very low Ca, highly peralkaline melts, fluorite can be stabilised by high F activities.

The Gardar failed-rift Province in South Greenland comprises numerous alkaline igneous complexes (Upton et al., 2003) of which the Motzfeldt, Ilímaussaq and Ivigtut intrusions are the focus of this study. Their common rift-related origin, but their very different evolutionary paths (Ivigtut: A-type granites, Motzfeldt: miaskitic nepheline syenites, Ilímaussaq: agpaitic nepheline syenites) and the extensive literature on their petrology and geochemistry make these intrusions ideal study objects for the systematics of trace elements. The province's overall high abundance in fluorine led to the crystallisation of considerable amounts of fluorite and other fluorides (e.g. Upton & Emeleus, 1987; Pauly & Bailey, 1999; Petersen, 2001). They do not occur in all, but are associated only with certain magmatic

complexes and/or are typical of distinct crystallisation sequences. The comparison of various generations of fluorides of the Gardar Province provides insight into the different processes governing the incorporation mechanisms of trace elements into these minerals. The combination of highly resolving analytical methods (e.g. CL & LA ICP-MS) help to reveal those mechanisms.

2. Regional Geology

The 1.35 – 1.14 Ga old Gardar Province in South Greenland is considered as a failed rift system (Upton et al., 2003; Fig. 1) and is characterised by 12 major (per-) alkaline intrusive complexes along with numerous (giant) dyke swarms and a succession of volcanic-sedimentary rocks.

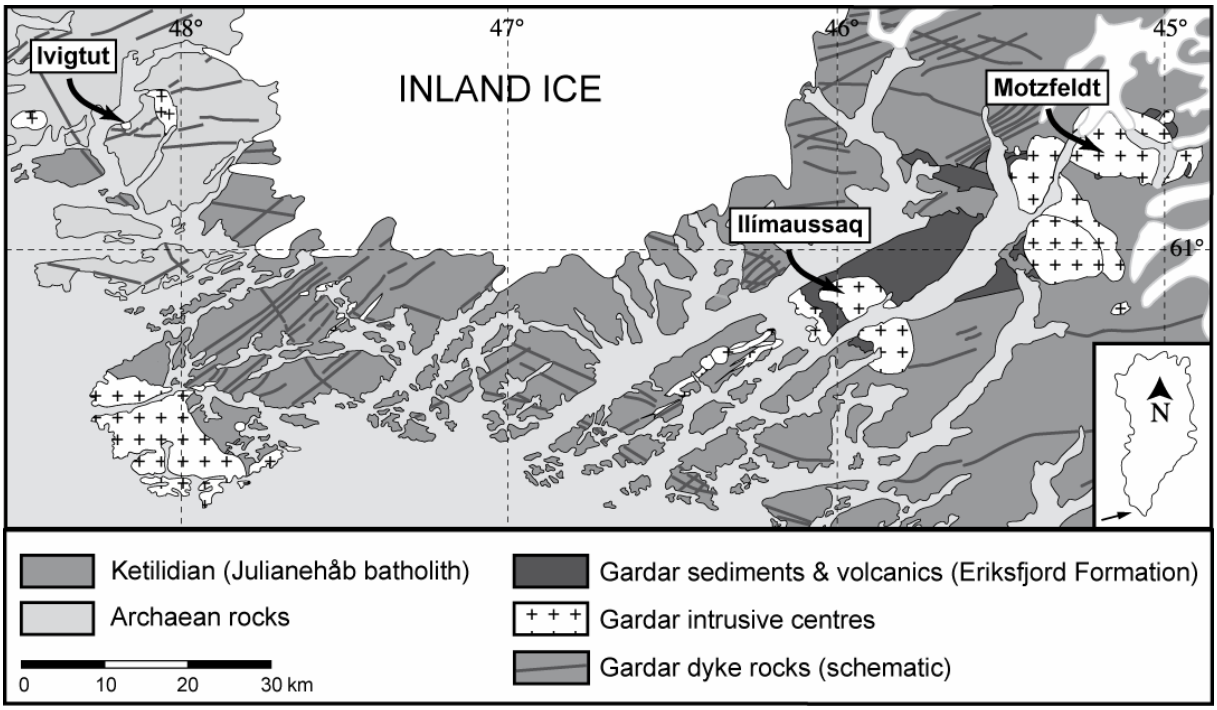

Fig. 1: Overview of the Gardar Province with the investigated intrusions Motzfeldt, Ilímaussaq and Ivigtut. Modified after Escher & Watt (1976).

The composition of the Gardar intrusions ranges from silica-over- to silica-undersaturated rocks. The province is world-famous for the type locality of agpaitic rocks in the Ilímaussaq intrusion and for the unique cryolite [Na_3AlF_6] deposit at Ivigtut. Agpaitic rocks are defined as peralkaline nepheline syenites which crystallised complex Na-Zr-Ti minerals like eudialyte instead of "normal" miaskitic rocks which comprise Fe-Ti oxides and

zircon (Sørensen, 1997). These two intrusions, together with a third intrusion, the Motzfeldt complex, represent most of the compositional range of highly evolved silicate rocks occurring in the Gardar Province. The Ilímaussaq and Motzfeldt complexes intruded the 1.8 Ga old Julianehåb batholith of the Ketilidian orogen (Garde et al., 2002) whereas the Ivigtut intrusion was emplaced in the Archaean craton (Fig. 1). Detailed descriptions of the crystallisation of the three intrusions can be found in e.g. Sørensen et al. (2006), Markl et al. (2001), Goodenough et al. (2000), Pauly & Bailey (1999), Larsen & Sørensen (1987), Jones (1984), Jones (1980), Köhler et al. (in press) and are very briefly summarised below.

Motzfeldt

The Motzfeldt intrusion can be divided into six different intrusive phases (SM1 to SM6, Emeleus & Harry, 1970; Jones, 1980; 1984). SM1 to SM5 are (per-)alkaline, miaskitic rocks, whereas SM6 is of agpaitic composition (occurrence of eudialyte; Sørensen, 1997). Since four phases (SM1, SM4-6) comprise the whole crystallisation sequence (Jones, 1984), we focused on samples from these units. The rocks mainly consist of feldspar, nepheline, Ca-Na amphiboles, augitic to aegirine-augitic pyroxene and Fe-Ti oxides (Jones, 1984). SM6 only crystallised aegirine and neither amphibole nor Fe-Ti oxides, while zircon is replaced by eudialyte. Fluorite occurs as a primary phase in SM1 and SM6, whereas late- to post-magmatic fluorite ± calcite veins are very common in SM1, SM4 and SM5.

Ilímaussaq

The Ilímaussaq intrusion developed from four magmatic batches consisting of miaskitic augite syenite and alkali granite followed by a succession of agpaitic rocks including roof cumulates (naujaites), floor cumulates (kakortokites) and a "sandwich" horizon (lujavrites; Sørensen et al., 2006). The agpaitic rocks consist of arfvedsonite, aegirine, sodalite, eudialyte, feldspar and nepheline in variable modal compositions. Fluorite and villiaumite occur as magmatic phases in the naujaites (Markl et al., 2001), but also crystallised in pegmatites and occur as late-stage and hydrothermal alteration products.

Ivigtut

The Ivigtut (Ivittuut) complex is situated in the northwest of the Gardar Province (Fig. 1). It is about 350 m across and world-famous for its unique cryolite [Na_3AlF_6] deposit that is now mined out. The deposit itself is situated within an A-type granite stock which was intensely metasomatised by F- and CO_2-rich fluids (Goodenough et al., 2000). According to

Pauly & Bailey (1999), these fluids became enriched in Na, Al and Si during the breakup of feldspars and subsequently formed an aluminofluoride-rich melt which later exsolved into a silicate- and a fluoride-rich melt at 500-600 °C. With decreasing temperature, i.e. at hydrothermal conditions, the siliceous melt led to the formation of the large (siderite-)quartz layer in the lower part of the deposit while the cryolite body itself originated from the fluoride-rich melt. It is suggested that this volatile-, F-rich melt gradually evolved to a solute-rich fluid at around and below 450 °C (Pauly & Bailey, 1999; Köhler et al., in press). Within the deposit, cryolite is mainly associated with siderite, quartz, fluorite, topaz and fluorides such as cryolithionite [$Na_3Li_3Al_2F_{12}$], chiolite, ralstonite, pachnolite, prosopite and others (Pauly & Bailey, 1999).

3. Sample preparation and analytical procedures

Polished sections of fluorite, cryolite, calcite, cryolithionite, siderite and villiaumite samples were studied by conventional microscopy, cathodoluminescence (CL) and laser ablation ICP-MS. CL imagery was performed on a CITL CCL 8200 stage at the University of Tübingen, Germany, with the CL chamber being mounted on a Zeiss microscope. Beam current was 300 µA and acceleration voltage 14.5 kV. Exposure times were usually 3 to 6 seconds.

The laser ablation ICP-MS measurements were performed at the University of Würzburg, Germany. A Merchantek 266 LUV, 266 nm laser at 10 Hz and 0.71-0.84 mJ pulse energy for a spot size of 50 µm and an Agilent 7500i quadrupole mass spectrometer were used. ^{44}Ca for fluorite and calcite,^{27}Al for cryolite and crylithionite, ^{57}Fe for siderite and ^{23}Na for villiaumite served as internal standards. The NIST SRM 614 was used as an external standard (Pearce et al., 1997) and was measured frequently during the course of the analyses. Deduced from multiple measurements of the NIST SRM 614 standard, the precision (1 σ level) is usually better than 10 rel.%. However, errors may be larger for analyses with very low REE contents. Minimum detection limits generally lie below 50 ppb.

4. Petrography and Results

We chose 48 samples (Table 1) for detailed study according to distinct generations within one intrusion, their association with other minerals, their different CL colours and

zonations. The analysed REE contents were normalised to chondrite (McDonough & Sun, 1995). The pseudo-lanthanide yttrium was added between Dy and Ho because of its trivalent oxidation state and its geochemical similarity to the REE (Bau & Dulski, 1995). Representative REE analyses can be found in Table 2. The whole data set can be found online (see Appendix A).

Tab. 1: Samples analysed in this study. P and s represent fluorites which are interpreted as primary magmatic (p) or secondary/late stage, hydrothermal (s); columns "Eu" and "Y" refer to the respective anomalies. All samples from Ivigtut are of hydrothermal origin.

Intrusion	unit	mineral	p/s	samples	characteristics	Eu	Y	tetrad
Ilímaussaq	Naujaite	fluorite	p	Ilm133, Ilm225, Ilm259, Ilm260	LREE enriched	neg.	pos.	none
60°56' N	Kakortokite	fluorite	p	XL30	LREE enriched	neg.	pos.	none
45°56' W	Naujaite	fluorite	s	Ilm77, Ilm99, Ilm325	low REE concentration	neg.	pos.	none
	Naujaite	villiaumite	p	villiaumite	REE below det. limit	neg.	pos.	none
Motzfeldt	SM1	fluorite	p	JS193, JS195, JS197	LREE enriched	neg.	pos.	none
61°08' N 45°06' W	SM1	fluorite	s	JS2, JS4, JS6, JS10, JS16	variably LREE enriched	neg.	pos.	none
	SM1	fluorite	s	JS9, JS10	low REE concentration	neg.	pos.	none
	SM4	fluorite	s	JS34, JS38, JS67, JS86, JS90, JS91, JS152, JS168, JS225, JS226	MREE enriched	neg.	pos.	none
	SM4	calcite	s	JS67, JS152, JS226	flat to MREE enriched	neg.	pos.	none
	SM5	fluorite	s	JS109, JS110, JS175, JS183	LREE enriched, anomalies less pronounced	neg.	pos.	none
	SM6	fluorite	p	JS88, JS122	LREE enriched	neg.	pos.	none
Ivigtut		siderite	s	IV-CPH, IV1475, IV-Sid	HREE enriched	neg.	neg.	not quant.
61°12' N 48°10' W		cryolithionite	s	IV30	flat REE pattern, low concentration	neg.	neg.	not quant.
		cryolite	s	IV20, IV30, IV33, IV35, IV-K1, IV-K4	flat REE pattern, low concentration	neg.	neg.	strong
		fluorite	s	IV31, IV 32	low REE concentration	neg.	neg.	strong
		fluorite	s	IV80, IV79a, IV1479, IV33	slightly HREE enriched	neg.	neg.	strong
		fluorite	s	IV30, IV20	flat REE pattern	neg.	neg.	strong

Tab. 2: Representative REE analyses of fluorides, siderite and calcite (in ppm except Y/Ho and Y/Y*) and three standard analyses (one from the lab at Würzburg and two from the literature (Horn et al., 1997; Lahaye et al., 1997) for comparison).

Ivigtut	# 9001	# 9002	# 9009	# 9012A	# 9032	# 9033	# 5026	# 5020
Sample	IV30	IV30	IV30	IV30	IV80	IV80	1479	1479
Mineral	Fluorite	Fluorite	Cryolite	Cryolithion.	Fluorite	Fluorite	Fluorite	Fluorite
La	1541	335	5.75	0.018	2.52	1.76	0.798	0.327
Ce	3772	1076	15.2	0.038	13.4	9.25	8.42	1.24
Pr	559	141	2.54	<0.01	2.98	1.99	3.06	0.236
Nd	2019	463	7.93	<0.03	18.5	9.42	18.6	1.07
Sm	1119	228	4.12	<0.02	47.7	13.9	22.4	0.676
Eu	94.8	33.3	0.604	<0.01	1.42	0.47	0.798	0.021
Gd	1129	126	4.06	0.044	57.7	17.6	22.7	0.734
Tb	280	32.7	0.817	0.011	22.6	6.79	8.32	0.287
Dy	1826	208	5.58	<0.02	177	61.3	67.8	2.62
Y	4620	291	7.53	0.054	225	102	106	9.68
Ho	286	25.1	0.784	<0.01	30.2	12.6	11.8	0.641
Er	804	76.7	2.37	<0.02	88.8	37.7	33.9	1.94
Tm	127	16.9	0.466	0.007	13.9	5.98	5.26	0.315
Yb	901	133	3.17	0.045	82.4	33.7	33.2	2.12
Lu	91.8	13.6	0.318	<0.01	7.19	3.16	2.43	0.228
Sr	5798	3544	230	0.281	502	842	576	8342
Y/Ho	16.2	11.6	9.6	-	7.5	8.1	9	15.1
Y/Y*	0.5	0.3	0.3	-	0.2	0.3	0.3	0.6

unit			SM1					
Ivigtut	BA0014	**Motzfeldt**	# 2002	# 1012	# 3010	# 3016	# 8017	# 8013
Sample	Sid		JS195	JS193	JS10	JS9	JS6	JS6
Mineral	Siderite		Fluorite	Fluorite	Fluorite	Fluorite	Fluorite	Fluorite
La	<0.02		255	209	3.63	1.24	378	50.5
Ce	0.014		454	353	1.74	3.4	771	81.3
Pr	<0.01		58.6	47.1	0.797	0.728	122	9.79
Nd	<0.08		269	212	3.37	3.34	590	39.5
Sm	<0.06		62.5	51.0	1.66	2.06	116	8.42
Eu	<0.03		6.79	4.14	0.201	0.388	8.44	0.976
Gd	0.094		66.5	56.7	3.79	2.42	98.3	11.2
Tb	0.026		9.86	9.18	0.653	0.653	10.3	1.33
Dy	0.145		66.5	59.3	3.88	4.04	51.4	6.84
Y	0.261		820	774	93.3	34.5	681	152
Ho	0.056		13.8	11.9	0.579	0.698	8.71	1.29
Er	0.158		34.1	32.4	1.16	1.77	15.8	2.61
Tm	0.036		4.2	3.67	0.106	0.227	1.32	0.282
Yb	0.528		22.6	20.6	0.469	2.08	7.57	1.47
Lu	0.058		2.52	2.26	0.05	0.186	0.669	0.152
Sr	0.019		751	430	142	300	1432	955
Y/Ho	4.7		59.4	65	161	49	78.2	117.8
Y/Y*	0.21		2	2.2	4.6	1.5	2.4	3.8

Tab. 2 continued

unit	SM4	SM4		SM5		SM6		Naujaite
Motzfeldt	# 8003	# 7019	# 7016	# 1027	# 1028	# 1015	**Ilímaussaq**	# 6002
Sample	JS168	JS152	JS152	JS175	JS109	JS122		ILM225
Mineral	Fluorite	Calcite	Fluorite	Fluorite	Fluorite	Fluorite		Fluorite
La	30.7	322	18.4	46.8	13.4	182		163
Ce	87.2	833	57.5	108	33.3	377		327
Pr	17.1	128	13	16.5	4.97	58.2		52.5
Nd	95.5	610	84	85.5	20.4	305		275
Sm	26.3	186	30.4	17	4.94	66.4		55.7
Eu	2.28	15.7	3.09	1.89	1.83	4.88		4.9
Gd	34.3	224	43.5	14.6	3.81	63.4		56.5
Tb	4.97	41.4	6.65	1.67	0.481	7.3		6.43
Dy	32.8	293	42.6	8.71	2.68	42.5		34.8
Y	372	2371	795	108	10.7	470		430
Ho	6.19	58.8	8.48	1.36	0.283	7.24		6.17
Er	15	177	20.7	2.48	0.753	15.8		13
Tm	1.77	26	2.22	0.245	0.055	1.49		1.28
Yb	8.77	162	12.4	1	0.259	6.49		5.88
Lu	0.965	20.4	1.24	0.126	0.017	0.613		0.618
Sr	495	1127	905	498	95	1066		124
Y/Ho	60.1	40	94	79	37.8	64.9		69.7
Y/Y*	1.9	1.3	3.1	2.3	0.9	2		2.2

	Naujaite			Kakortokite		**Standards**		
Ilímaussaq	# 6661	# 5007	# 5003	# 3003		NIST-614	NIST-614	NIST-614
Sample	ILM259	ILM99	ILM77	XL30		Würzburg	Horn et al. (1997)	Lahaye et al. (1997)
Mineral	Fluorite	Fluorite	Fluorite	Fluorite				
La	120	3.88	0.005	217		0.70	0.74	0.72
Ce	243	5.56	0.01	426		0.76	0.79	0.82
Pr	36.9	1.02	<0.01	75.2		0.70	0.78	0.75
Nd	200	3.81	0.027	385		0.78	0.75	0.74
Sm	47.2	0.894	0.039	78.7		0.74	0.77	0.74
Eu	4.63	0.081	<0.01	7.21		0.74	0.77	0.77
Gd	52.6	0.919	0.071	80.1		0.68	0.73	0.75
Tb	7.42	0.111	0.009	8.27		0.70	0.77	0.69
Dy	39.5	0.806	0.086	46.6		0.69	0.76	0.69
Y	423	14.9	16.7	582		0.74	0.79	0.75
Ho	7.47	0.144	0.018	7.75		0.74	0.78	0.71
Er	18.1	0.385	0.058	17.7		0.65	0.78	0.70
Tm	1.85	0.04	<0.01	1.66		0.71	0.77	0.67
Yb	9.03	0.248	<0.03	8.85		0.76	0.76	0.70
Lu	0.958	0.022	<0.01	0.792		0.73	0.78	0.69
Sr	70.5	19.9	54.1	636		43.80	45.50	48.58
Y/Ho	56.6	103	928	75.1				
Y/Y*	1.8	3.2	31.3	2.3				

Motzfeldt

The primary magmatic fluorites occur in SM1 and SM6 (Figs. 2 & 3). In SM1 samples (JS193, JS195, JS197; Table 1), fluorite forms interstitial grains with a diameter up to 1 mm within the feldspar matrix. They have a rounded to subhedral shape (Fig. 2 a) and are interpreted to be of primary origin. Their colour varies from light blue to white. Purple fluorite occurs as small (up to 1 mm) interstitial grains in JS88 and JS122 of unit SM6 and are similar to primary magmatic fluorite grains from SM1. They are intergrown with feldspar and aegirine and reach sizes of up to 0.5 cm. The REE patterns of all primary magmatic fluorites are characterised by an enrichment in LREE, a negative Eu and a positive Y anomaly. Fluorite from SM1 has slightly lower HREE (Fig. 3) than fluorite from SM6.

Hydrothermal fluorites either occur as patchy fluorite or in veins which show rhythmic zonation of darker and lighter parts. Patchy fluorite does not exhibit any zonation, but has randomly oriented lighter CL parts. The observed REE patterns can be divided into groups according to the different intrusive units.

Hydrothermal fluorites from SM1 developed in different textures (Fig. 2c, d). They occur as small, up to 2 cm thick veins cutting through SM1 (JS10, JS16) or as large fluorite crystals up to 10 cm (JS9). Furthermore, some fluorites up to 2 cm are irregularly associated with feldspar and/or amphibole (JS2, JS4, JS6). Their colour in hand specimen is mostly bluish/purple with some colourless parts (e.g. JS6). The hydrothermal fluorites are characterised by an enrichment of the LREE, a negative Eu anomaly and a positive Y anomaly which varies in size within the same sample (e.g. Fig. 3). Two samples (JS9 and JS10) are enriched in MREE and one (JS10) additionally has a pronounced negative Ce anomaly. Lighter CL parts tend to be more enriched in REE compared to the darker ones.

In unit SM4, fluorite mostly occurs as small veins (Fig. 2f) some of which comprise aegirine and fluorite (JS90, JS91). In these veins, fluorite occurs as 1 to 2 cm large crystals in an aegirine matrix. Other veins consist of fluorite and calcite intergrowths (JS67, JS152, JS226; Fig. 2e). Furthermore, there are large (< 5 cm) pegmatitic crystals which are not associated with veins (JS168, JS225). In fine-grained parts of SM4, fluorite is disseminated (JS38) or forms very thin veinlets (< 0.5 cm; JS34, JS86). The colour of the fluorites ranges from purple/blue to colourless. Fluorites from SM4 incorporate less REE than fluorite from SM1 (Figure 4). The patterns are either flat (e.g. JS152) or exhibit enrichments in MREE (e.g. JS168, 225). Calcite solely occurs in three samples from SM4 and is intergrown with fluorite. Its REE patterns are very similar to the patterns of the associated fluorite.

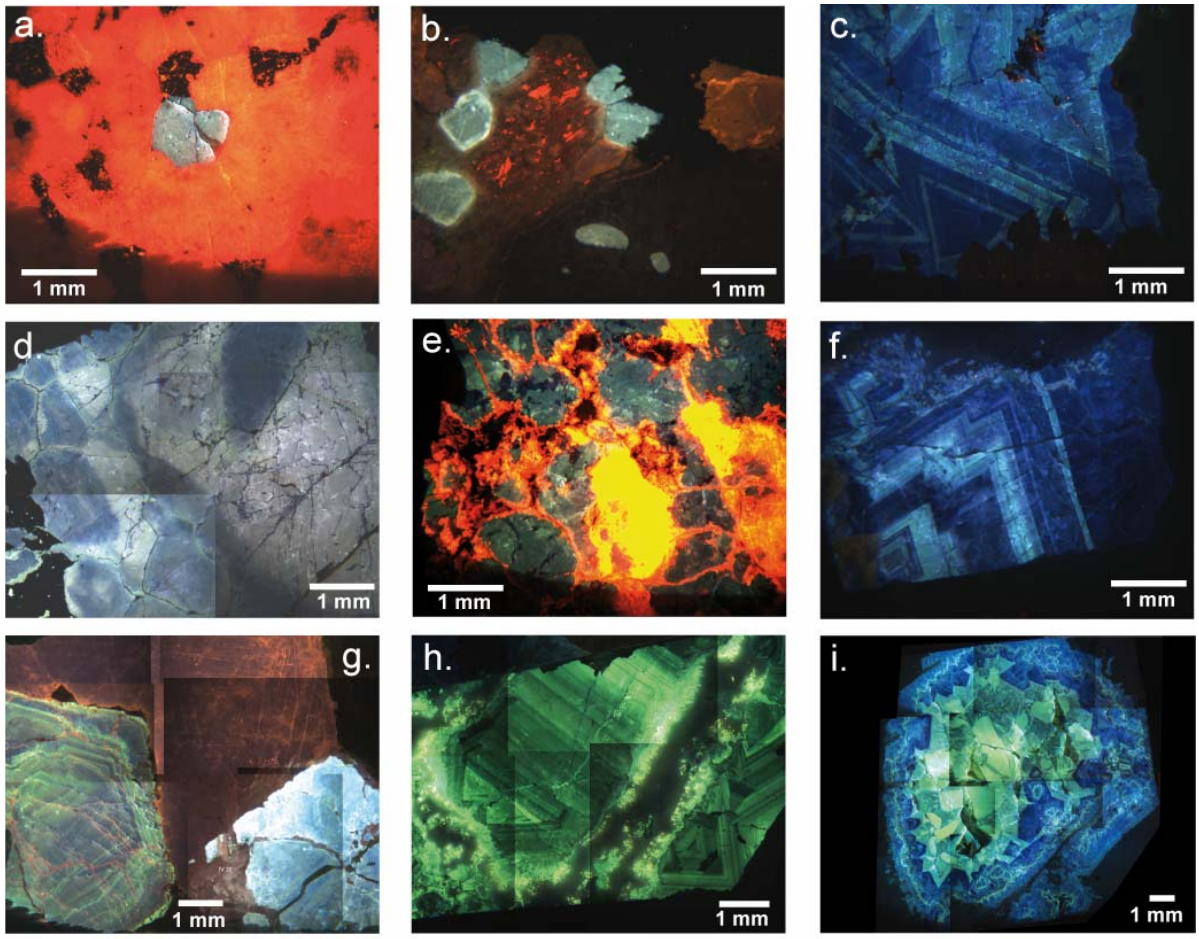

Fig. 2: Cathodoluminescence images of some of the studied samples. a) and b) primary amphiboles from Motzfeldt and Ilímaussaq, respectively, which are associated with feldspar; c) zoned fluorite from the Motzfeldt intrusion (SM1; JS10); d) patchy-grown fluorite from SM1 (JS6); e) fluorite intergrown with calcite from SM4 (JS152); f) strongly zoned fluorite from SM5 (JS175); g) zoned, euhedral fluorite (lower left), cryolite (top) and cryolithionite (lower right) from the Ivigtut deposit (IV 30); h) strongly zoned fluorite from Ivigtut (IV 80) rimmed by cryptocrystalline topaz; i) zoned fluorite from Ivigtut (IV 1479) with a green core and blue rim (CL colours).

Bluish fluorites from SM5 occur in up to several cm thick veins commonnly intergrown with white alkali feldspar (JS109, JS110, JS175). In some samples, fluorite only forms a thin layer. JS183 originates from a feldspar- and biotite-rich sample which occured in close association with supracrustal basaltic rocks within unit SM5. In this sample, the fluorite is interstitial and surrounded by (albitic) feldspar. The fluorite patterns of SM5 are characterised by an enrichment of LREE or flat to slightly MREE enriched. The Eu and Y anomalies are not as pronounced as in samples from other units, and few analyses even show a positive Eu anomaly (Fig. 4).

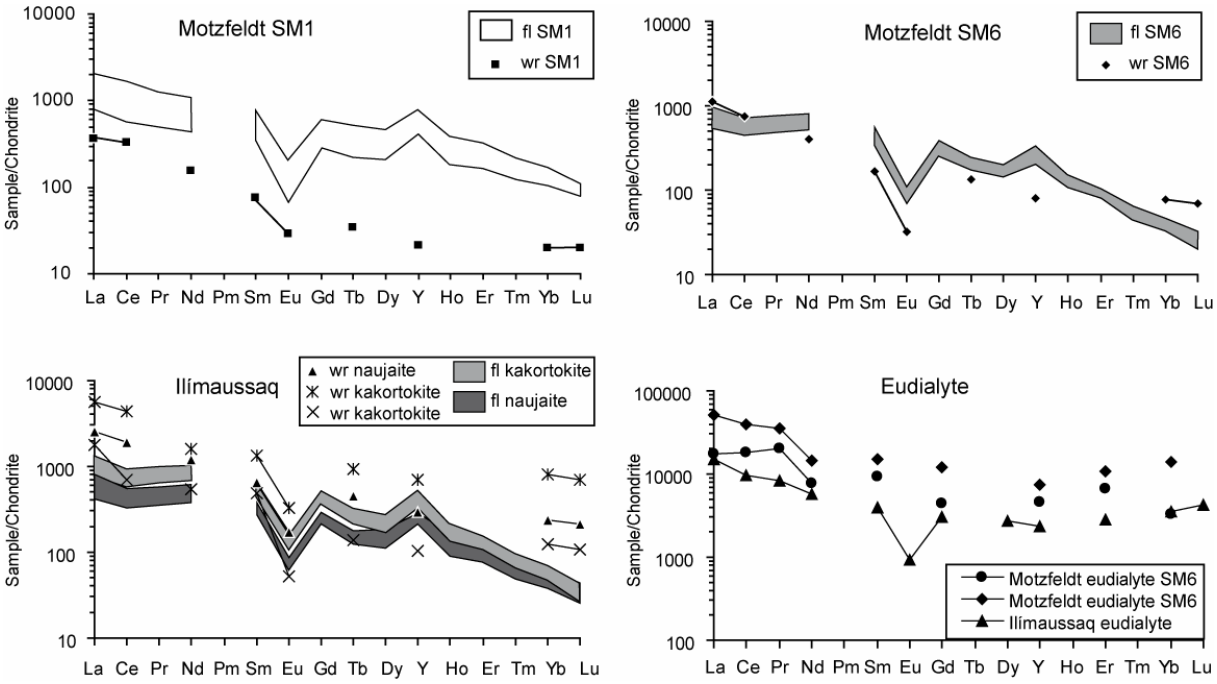

Fig. 3: Representative REE patterns of primary fluorites from Motzfeldt (a. & b.) and Ilímaussaq (c.) compared with whole rock data from Jones (1980), Bradshaw (1988) & Bailey et al. (2001) along with REE mineral data from eudialyte from Motzfeldt (SM6) and Ilímaussaq (Jones, 1980; Fryer & Edgar, 1977). wr = whole rock, fl = fluorite.

Whole rock data from Jones (1980) and Bradshaw (1988) are similar to the REE patterns of primary magmatic fluorite (Fig. 3) regarding the overall enrichment in LREE and the negative Eu anomaly. While primary magmatic SM1 fluorite has more REE than the whole rocks, primary SM6 fluorite is equally enriched. This is attributed to the occurrence of REE-enriched minerals (i.e. eudialyte of SM6) which lead to overall high REE concentrations in the bulk rock. Mineral REE patterns of eudialyte (Fig. 3) or rinkite (Jones, 1980) also show an enrichment of LREE similar to the fluorites.

Whole rock data of unit SM5 partially show a positive Eu anomaly which is in agreement with REE patterns of fluorite from this unit. These fluorites (samples JS109 & JS175) are the only ones which do not exhibit a pronounced negative Eu anomaly, but partially a slightly positive one. All in all, the fluorites show REE patterns very similar to their immediate host rocks and to other REE-enriched minerals such as eudialyte.

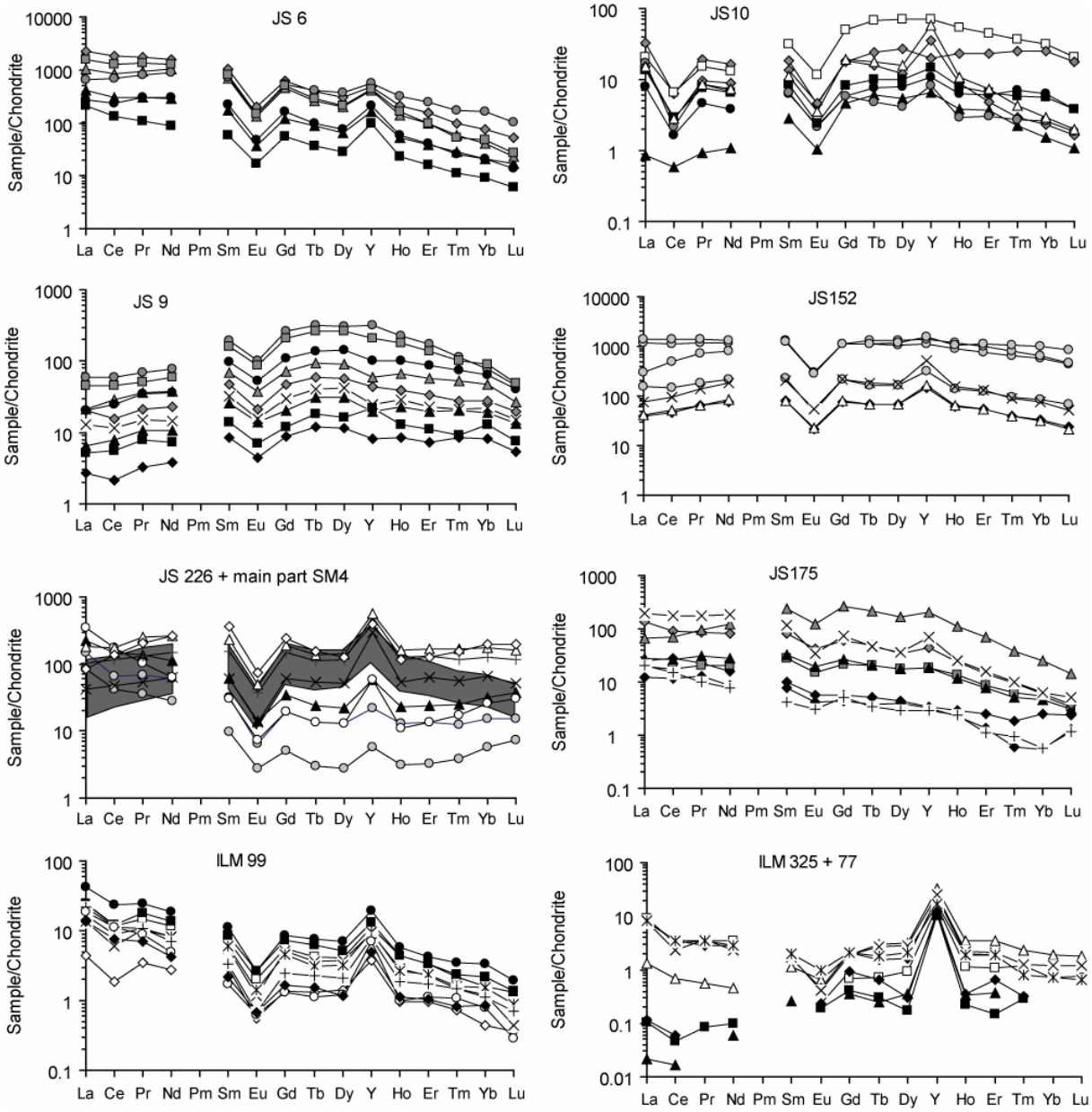

Fig. 4: REE patterns of hydrothermal fluorites from Motzfeldt (SM1: JS6, JS9 & JS10; SM4: JS152; JS226; grey shaded field: JS34, JS38, JS90, JS91, JS168, JS225; SM5: JS 175) and Ilímaussaq (Ilm 77, Ilm99, Ilm325).

Ilímaussaq

The Ilímaussaq fluorites Ilm133, Ilm225, Ilm259 and Ilm260 are subhedral to euhedral and form up to 1 mm large grains in the feldspar matrix of the naujaitic rocks (roof cumulate; Fig. 2b). Fluorites from similar samples were interpreted to be early crystallising phases (Markl et al., 2001). XL30 is the only sample from the kakortokites (floor cumulates) which occurs in a pegmatite. This pegmatite consists of fluorite, arfvedsonite, feldspar and aegirine as main crystallisation phases. Sample XL30 was described in detail by Müller-Lorch et al.

(2007) who suggested that fluorite was the first crystallising mineral. These primary magmatic fluorites are enriched in LREE, have a negative Eu and a positive Y anomaly and are very similar to fluorite patterns in units SM1 and SM6 from Motzfeldt (Fig. 3).

The samples Ilm77, Ilm99 and Ilm325 are derived from the naujaitic part (roof cumulates) of the intrusion and occur in heavily altered samples or as secondary crusts. In sample Ilm99, white albite and purple to black fluorite are finely intergrown. The few single crystals are approximately 2-3 mm. Ilm77 is a heavily altered, vuggy sample in which small (< 5 mm), deep purple fluorite grains are associated with alkali feldspar. The fluorite of Ilm325 forms a crust on altered, fine-grained, feldspar-rich rock. These secondary fluorites show no or only a slight zonation in CL. Generally, secondary fluorites have a considerably lower REE concentration than the primary magmatic ones. The chondrite-normalised REE patterns exhibit a slightly negative Ce anomaly and pronounced negative Eu and positive Y anomalies (Fig. 4). Ilm99 is characterised by an enrichment of LREE whereas Ilm325 shows flatter patterns and Ilm77 is enriched in MREE to HREE. The overall concentration of REE decreases in the order Ilm99 > Ilm325 > Ilm77. Villiaumite occurs as 3 to 4 mm large red crystals and is derived from the lujavritic part (sandwich horizon) of the intrusion. This late-stage, hydrothermal villiaumite (NaF) has REE contents mostly below the detection limits.

Whole rock Ilímaussaq REE patterns from the naujaites (Bailey et al., 2001) and eudialyte data from Fryer & Edgar (1977) are similar to fluorite. All analyses exhibit an enrichment in LREE and a negative Eu anomaly (Fig. 3). The whole rock analyses are generally more enriched in REE than the fluorites which reflects the high modal abundance of REE-bearing minerals (eudialyte) in the bulk samples which control their absolute amount of REE.

Ivigtut

The association of cryolite *or* topaz decides whether the fluorite samples are derived from the fluorite-cryolite zone or from the fluorite-topaz unit underneath. Fluorites in samples IV32, IV79a, IV80 and IV1479 (Table 1) are all finely intergrown with cryptocrystalline, bluish or green topaz. Their colours range from lightgreen (IV79a) and whitish/purple (IV32) to dark green (IV80). In sample IV1479, fluorite is ~ 1 cm across and has a brown core with a purple rim. Fluorites in association with cryolite are generally deep purple except for U-Th-rich (this study; Pauly & Bailey, 1999), red-brown fluorite in sample IV30.

The fluorites display rather smooth REE patterns with some showing a slight enrichment of HREE (Fig. 5). CL images of fluorites generally show strong zonations (Fig. 2

g,h,i) even if fluorite is finely intergrown with cryolite. Zones with bright CL-colours are more enriched in REE than the darker parts. Generally, the fluorites are 2 to 4 orders of magnitude enriched relative to chondrite (Fig. 5). The most REE-enriched sample is a U-Th-rich fluorite (IV30; cf. Pauly & Bailey, 1999; Fig. 5). Light brownish and green fluorites incorporate approximately the same amount of REE whereas purple fluorite is slightly more depleted (Fig. 5). Sample IV31 is a thin fluorite crust possibly formed from a gel-like liquid and has very low concentrations of YREE.

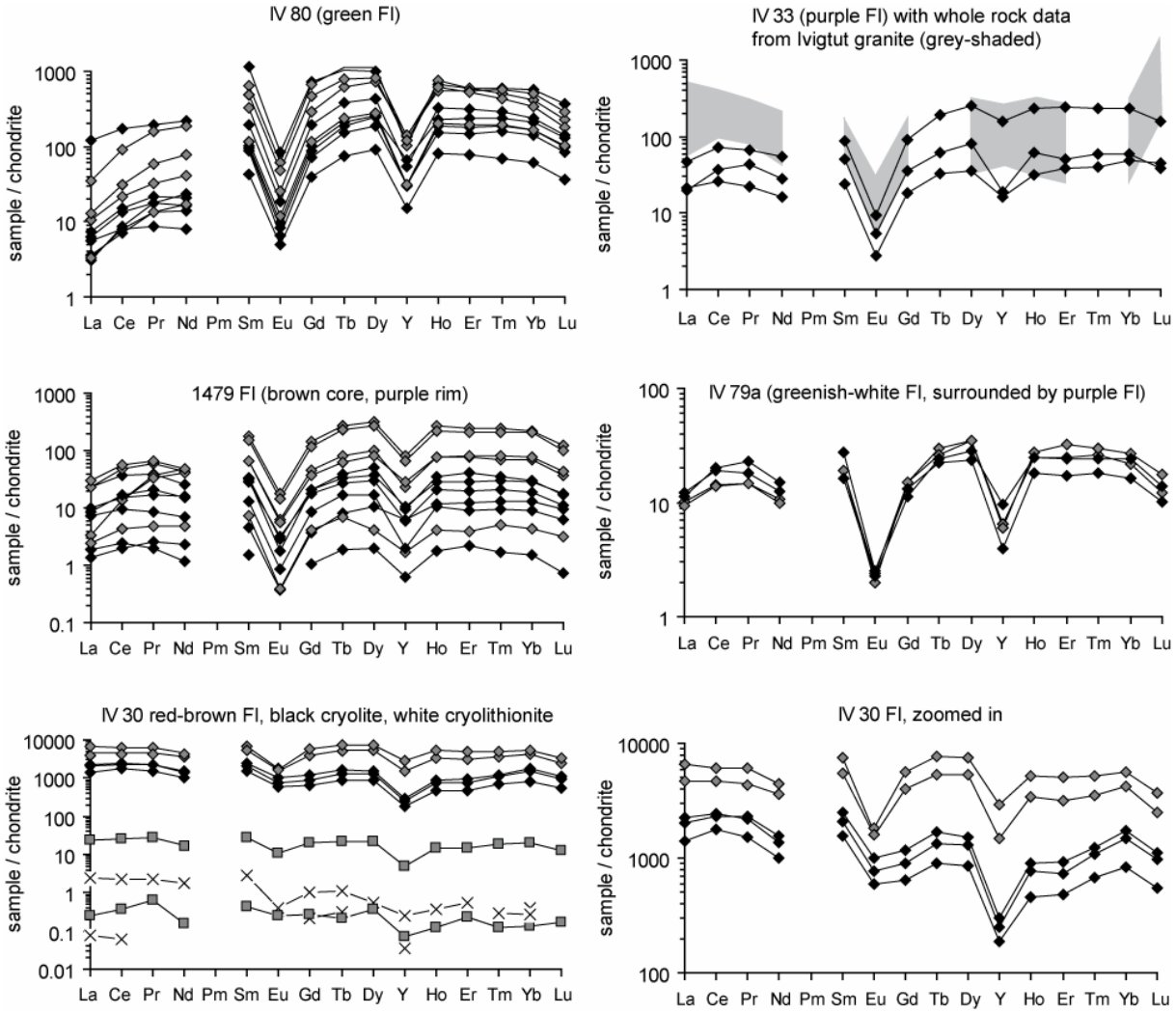

Fig. 5: REE patterns of fluorides from the Ivigtut intrusion; grey-shaded field: comparative whole rock data from the Ivigtut granite from Goodenough et al. (2000). Symbols: rhomb = fluorite; square = cryolite; cross = cryolithionite.

The typical colour of cryolite varies from white to brown. In sample IV30, however, cryolite is black due to radioactive damage of neighbouring U-Th-rich fluorite (Pauly & Bailey, 1999). Both minerals are associated with white cryolithionite. White to light brown cryolite from samples K4 and K1, respectively, forms various cm-sized masses and comes from the deposit's pure cryolite mass. IV35 is a transparent single cryolite crystal of pseudocubic shape of about 0.5-0.7 cm. Light brown cryolite has lower REE concentrations than white or black cryolite and is mostly 1 or 2 orders of magnitude depleted relative to chondrite. In contrast, white or black cryolite is 10 to 100 times enriched relative to chondrite. Similar to fluorite, the REE patterns in cryolite are very flat and exhibit negative Eu and Y anomalies.

In all samples, siderite is reddish-brown and forms cm-large crystals. In sample IV1475, it is associated with quartz and dark-brown cryolite. The three minerals form a vein which is a few cm wide. Bailey (pers. comm., 2007) suggested sample IV Sid to be derived from the eastern extension of the cryolite deposit. The same may apply to IV CPH, but it could also be derived from the siderite-cryolite unit. Siderite very depleted in REE and exhibits a negative Y anomaly. Concentrations in siderite are sub-chondritic and in many samples below the detection limit.

The analysed cryolithionite occurs in close association with reddish-brown fluorite and black cryolite (IV30). The REE are even more depleted than in cryolite, but similar regarding the slight Eu and Y anomalies and comparable to siderite.

In summary, the chondrite-normalised patterns from the Ivigtut deposit are all very much alike and only differ in their absolute REE concentrations. Fluorite is always more enriched in REE than cryolite whereas siderite and cryolithionite hardly incorporate any REE. All minerals show strong negative Eu and negative Y anomalies which is in contrast to the positive Y anomaly in minerals from Motzfeldt and Ilímaussaq.

Whole rock analyses of the Ivigtut granite (Goodenough et al., 2000) and whole rock data of peralkaline granites from China (Jahn et al., 2001; Zhao et al., 2002; Fig. 5) are as enriched in REE as the Ivigtut fluorites and exhibit a similarly pronounced Eu anomaly. In contrast to the distinctive negative Y anomaly in fluorite and cryolite from Ivigtut, only few whole rock samples of the Ivigtut granite have a slightly negative one. The Chinese and Ivigtut granites display rather smooth patterns with the latter showing a strong enrichment in Yb and Lu. Even though the analysed fluorites and cryolites are generally enriched in HREE, their concentration gradually decreases from Yb to Lu.

6. Discussion

The REE patterns do not only differ among the three intrusive complexes, but also vary systematically within one intrusion. Generally, the patterns of different intrusive units and different evolutionary stages can be roughly grouped (Table 1). There are various processes and mechanisms which account for the large diversity of the REE patterns. These include crystallographic control, sorption on mineral surfaces, source-related effects, formation of anomalies, fractionation during crystallisation and complexation.

6.1 Common features

The characteristics discussed in this section apply to both magmatic as well as hydrothermal fluorites or fluorides. Specific aspects typical of magmatic fluorites or hydrothermal fluorides will be discussed in chapters 6.3 and 6.4.

6.1.1 Crystallographic control

In fluorite (and calcite), REE replace Ca according to the following schematic substitutions in which □ is a vacancy (e.g. Möller et al., 1998):

$2\ REE^{3+} + \square \Leftrightarrow 3\ Ca^{2+}$; $REE^{3+} + Na^{+} \Leftrightarrow 2\ Ca^{2+}$; $REE^{3+} + F^{-} \Leftrightarrow Ca^{2+}$

The substitution involving Na^{+} may be crucial as the molar Na^{+} content generally balances the REE^{3+} content even considering the fact that error of the Na^{+} measurements is very high (2 σ up to 50 %).

The enrichment of HREE in siderite from the Ivigtut intrusion can be explained by differences in the ionic size of Ca^{2+} and Fe^{2+} as pointed out by Bau & Möller (1992) and by Morgan & Wandless (1980). Due to the smaller size and higher charge/volume ratio, the HREE are incorporated into the siderite crystal lattice more easily than the LREE according to the following substitution: $2\ REE^{3+} + \square \Leftrightarrow 3\ Fe^{2+}$.

The analyses of REE in villiaumite (NaF) from the Ilímaussaq intrusion are mostly below the detection limit. Although Na^{+} (1.02 Å) has a similar ionic radius compared to the REE^{3+} (1.16 – 0.98 Å), the REE do not fit into the crystal lattice of villiaumite. This is most probably due to charge balance effects as the trivalent REE would require simultaneous formation of two vacancies for each REE cation.

Cryolite [Na_3AlF_6] and cryolithionite [$Na_3Li_3Al_2F_{12}$] incorporate more REE than villiaumite but less REE than fluorite (Fig. 5). This may be due to the different charges of Na (univalent) and Ca (divalent) compared to the REE even though they have similar ionic radii

(1.02 and 1.00 Å, respectively). However, due to the presence of trivalent Al in cryolite and cryolithionite, the charge balance can be achieved more easily than in villiaumite where only univalent Na is present. The lower amount of REE in cryolithionite compared to cryolite (Fig. 5) might be explained by the substitution of Na by small Li (radius 0.76 Å) which renders the incorporation of the larger REE more difficult.

6.1.2 Fluorite reflecting source (fluid/melt) composition

Fleischer & Altschuler (1969) stated that the geological environment (i.e. chemistry of the rocks) control the distribution of REE. This is in agreement with our fluorides which closely match the REE abundance of their host rocks. Fluorites in alkaline nepheline syenites from Motzfeldt and Ilímaussaq generally display an enrichment in LREE in early crystallisation products. Minerals in the granitic Ivigtut intrusion, however, have a (slight) enrichment in HREE representative of the quartz-saturated, pegmatitic character of the deposit.

The amount of trace elements incorporated into fluorides largely depends on their availability in the melt/fluid. Therefore, REE patterns and trace element contents reflect the source (i.e. fluid or melt) from which they crystallised or precipitated (e.g. Sallet et al., 2005) and REE in fluorites are often used to trace the REE content of an associated hydrothermal fluid (e.g. Gagnon et al., 2003; Schwinn & Markl, 2005; Hill et al., 2000 and references therein). The REE distribution in some analysed samples is potentially governed by the trace element content of the surrounding rocks, the precipitation or breakdown of minerals or the abundance of REE in the fluid (Bau, 1991). The fluorites from SM5 (Motzfeldt) are unique as they have no pronounced negative Eu anomalies (JS109 & 175) comparable to the whole rock data (Jones, 1980). An intensive interaction of the fluid with the surrounding rocks from unit SM5 can be assumed for the origin of the REE pattern in these fluorites. Therefore, it is suggested that the fluid, from which these fluorites precipitated, had leached parts of the feldspar-rich unit SM5. Subsequently, it was fixed in the fluorite/feldspar veins at low hydrothermal temperatures and/or high oxygen fugacities (Hill et al., 2000).

6.1.3 Formation of anomalies

The negative Eu anomaly is typical of all analysed samples irrespective of mineral type, intrusion, unit or evolution stage and also occurs in whole rock analyses from the investigated intrusions (Figs. 3 to 5). The Eu anomaly can be attributed to early magmatic

plagioclase fractionation, i.e. the large occurrence of anorthositic rocks underlying the Gardar Province (e.g. Halama et al., 2002).

The negative Ce anomaly in JS10 and JS9 from Motzfeldt and in ILM77, ILM99 and ILM325 from Ilímaussaq may indicate more oxidised conditions and low temperatures (Hollings & Wyman, 2005; Bau & Möller, 1992; Constantopoulos, 1988) or changes in pH (e.g. Bau & Möller, 1992) during the evolution of the fluid from which these fluorites precipitated. The more oxidised conditions during the late stages are well documented for the Ilímaussaq intrusion (Markl et al., 2001) where hematite and aegirine are common (Marks et al., 2003). The same applies to the Motzfeldt intrusion where large parts of SM1 are heavily altered and contain large amounts of hematite along with aegirine and secondary fluorite.
The pronounced Y anomaly will be discussed in further detail below.

6.2 Primary magmatic fluorites

Deducing from the textures, the early fluorites were derived from a magma, because they are closely related to other magmatic phases and do not show any sign of (hydrothermal) alteration. Sallet et al. (2000) observed that primary magmatic fluorites associated with a granite have similar REE patterns as the host rock. The same applies to fluorites from this study which are not only similar to each other but also to the associated whole rock patterns. Therefore, they are interpreted to be of early magmatic origin. The distribution of REE in the primary magmatic fluorites seems to be closely controlled by the overall availability of REE within the whole rock (e.g. Fig. 3) and hence in the magma. This suggests that the distribution coefficient is similar for all REE and thus show similar patterns. The primary magmatic fluorites from the Motzfeldt (units SM1 and SM6) and Ilímaussaq intrusions (naujaites and kakortokites; roof & floor cumulates) define a very narrow range in the Tb/Ca-Tb/La diagram (Möller et al., 1976; Fig. 7) within the pegmatitic field which reflects similar REE contents of the fluorites (cf. Figs. 3-5) suggesting similar formation processes.

All primary magmatic fluorites have Y/Ho ratios between 60 and 70 (average Y/Ho SM1 = 63, SM6 = 68, Ilm = 64) which is in contrast to the chondritic Y/Ho ratios of 28. The constant values argue for similar crystallisation conditions (Bau & Dulski, 1995). Furthermore, Bau & Dulski (1995) observed that the Y/Ho ratio does not change during magmatic fractionation processes which is evidenced by the constant Y/Ho ratios of the studied samples. Veksler et al. (2005) and Marshall et al. (1998) showed that the distribution

coefficient (K_d Fluorite-melt) for Y is higher than that for Ho which would result in a positive Y anomaly in the normalised REE pattern. This could explain the high Y content of the fluorites. On the other hand, Bau & Dulski (1995) suggested that the Y/Ho ratio may reflect source values. According to that, the magma source of the Ilímaussaq and Motzfeldt complexes must have been already either Y-enriched and/or Ho-depleted due to the high Y/Ho ratio.

The primary magmatic fluorites, the whole rock data from Motzfeldt and Ilímaussaq and REE data from dykes all over the Gardar Province (Goodenough et al., 2002; Halama et al., 2007; Köhler et al., in prep.) show an enrichment of LREE implying the source of the Gardar magmas must already have been enriched in LREE. Upton & Emeleus (1987) suggested that the mantle beneath the Gardar Province was metasomatised and enriched in fluorine, LREE and LILE. It is believed that this happened during subduction processes leading to the Ketilidian orogen (Garde et al., 2002; Goodenough et al., 2002; Upton & Emeleus, 1987). A metasomatic exchange associated with the mobilisation of LREE and other trace elements is common in arc related magmas (e.g. You et al., 1996; Drummond et al., 1996) and was also demonstrated experimentally (You et al., 1996; Kessel et al., 2005).

Despite the similar REE patterns which argue for the same processes during crystallisation from a magma, there are differences in the fluorite composition. This is evidenced e.g. in the variable Sr-content of the different magmatic fluorites from Motzfeldt and Ilímaussaq. Even though they have identical amounts of REE, the Sr content is higher in Motzfeldt than in Ilímaussaq (Fig. 6). This indicates different availability of Sr in the magma.

6.3 Hydrothermal (secondary) fluorites and associated minerals

Hydrothermal fluorites are the predominant samples in this study and either occur in veins or as secondary alteration products. Apart from the effects outlined in chapters 6.1-6.3, some additional processes can govern the REE distribution:

According to Bau (1991), sorption of REE on mineral surfaces is an important process in the incorporation of REE into minerals during fluid-rock interactions. He stated that sorption and complexation are opponent mechanisms: whereas the latter increases the content of REE in the fluid, sorption leads to the incorporation of REE into minerals. The effect of sorption generally leads to a preferred incorporation of HREE into the crystal lattice (Bau, 1991). However, the chemical environment in which the studied samples formed suggests that ligands like F^-, CO_3^{2-} and OH^- were highly concentrated. Therefore, sorption processes are

assumed to be of minor importance compared to chemical complexation (of the REE; Bau & Möller, 1992). Additionally, as the fluorides of this study are rather large crystals, it can be assumed that they would only offer a small reactive specific surface area for sorption.

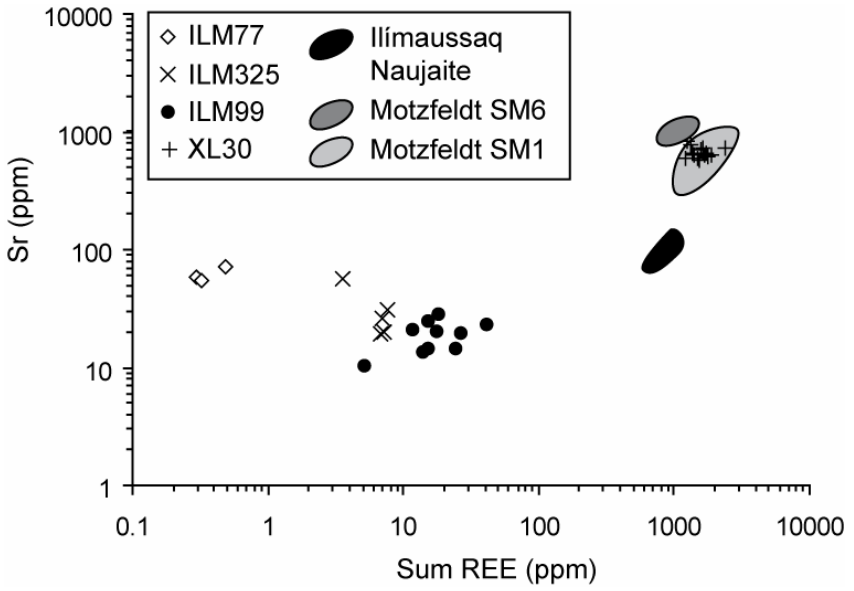

Fig. 6: Sr (ppm) vs. total REE content (ppm) of primary and hydrothermal Ilímaussaq and primary Motzfeldt fluorites.

6.3.1 Evidence for a changing fluid composition

The distribution of REE into minerals changes systematically in the course of crystallisation. It is suggested that early crystallising phases preferentially incorporate LREE whereas later formed ones are more MREE and particularly HREE enriched (Lüders et al., 1993; Schwinn & Markl, 2005; Kempe et al., 1999; Trinkler et al., 2005; Wagner & Erzinger, 2001; Möller et al., 1976). Early primary magmatic fluorites (JS193, JS195, JS197) are enriched in LREE whereas the patterns of hydrothermal vein fluorites are generally flatter (e.g. JS175) or become enriched in MREE (e.g. samples from SM4, JS10). Very late fluorites which form thin crusts or are alteration products even show a (slight) enrichment in HREE (Ilm325, Ilm77, IV31). Additionally, later fluorites commonly show decreasing REE contents indicating that the fluid or melt became depleted in REE in the course of the crystallisation or fluid migration, respectively (c.f. fluorites from Ilímaussaq, Fig. 6).

Möller et al. (1976) proposed the Tb/Ca-Tb/La diagram (Fig. 7) in order to distinguish fluorites of pegmatitic from hydrothermal or sedimentary origin. For this diagram, fluorite was assumed to be stoichiometrically composed of calcium and fluorine. The small amount of

trace elements incorporated into fluorite does not change the overall position of data points in the diagram as discussed by Gagnon et al. (2003).

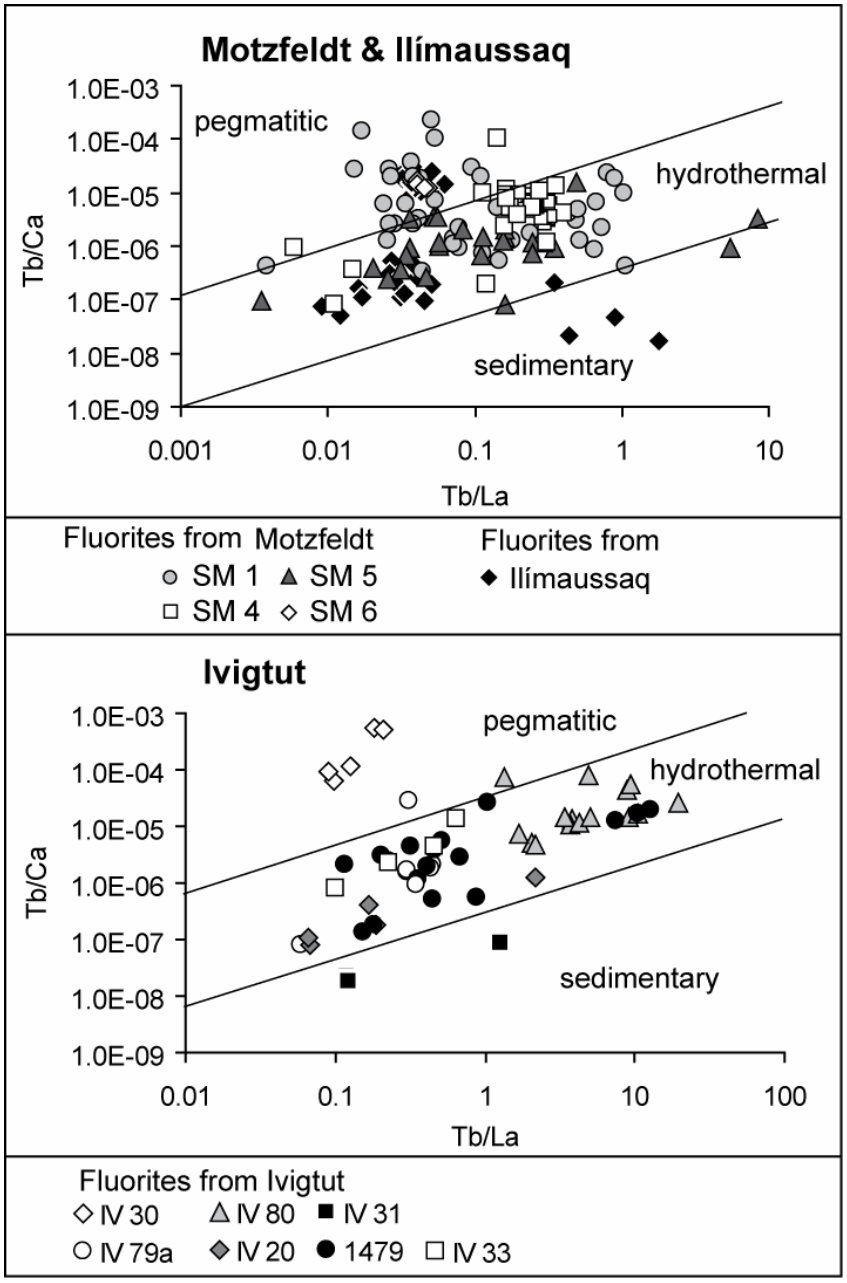

Fig. 7: Tb/Ca-Tb/La diagram (after Möller et al., 1976) of fluorites from Motzfeldt, Ilímaussaq and Ivigtut. The fields which distinguish pegmatitic, hydrothermal and sedimentary formation conditions are more gradual than sharp and "sedimentary" may be better referred to as "low temperature".

The hydrothermal fluorites of the Motzfeldt intrusion are heterogeneously distributed in Fig. 7. Two samples from SM1 (JS9 and JS10) fall into the hydrothermal field whereas almost all other hydrothermal fluorites from SM1 scatter around the field of the primary magmatic ones (Fig. 7, see above). This clearly shows that the Tb/Ca-Tb/La diagram must be used with care as analyses plotting in a particular field do not necessarily reflect those formation conditions. It is important that the textural relationships as well as any precursor material/rocks are also taken into account (for a further discussion see Gagnon et al., 2003). Fluorites from SM4 and SM5 define fields in the Tb/Ca-Tb/La diagram and do not show any clear correlations within one sample. SM4 fluorites plot between the pegmatitic and hydrothermal fields whereas fluorites from SM5 appear to have formed hydrothermally. The secondary Ilímaussaq fluorite samples Ilm99 and Ilm325 fall into the hydrothermal field. Ilm77 is the only sample which lies within the sedimentary field indicating a very late, low-temperature formation which is in agreement with the occurrence of that fluorite in a heavily altered, vuggy sample.

Fluorites from Ivigtut (Fig. 7) are mostly of hydrothermal origin with sample IV30 being the only one that suggests a pegmatitic derivation. The thin fluorite crust of sample IV31 falls into the sedimentary field. All fluorites from Ivigtut describe a positive trend in the Tb/Ca-Tb/La diagram suggesting REE-fractionation during mineralisation. However, the lower points do not necessarily represent the fluorite cores. They are rather characteristic of the dark CL colours while the higher points generally reflect the bright areas in the CL images. This agrees well with the highly variable REE concentrations in the different colour zones.

6.3.2 Grainscale variations (zonations)

If a fluid progressively changed its composition, this fractionation should be observed in continuously evolving REE profiles (e.g. Schwinn & Markl, 2005). In this study, however, differences in REE patterns are rather typical of distinct units and/or intrusions and do not occur within one sample. The zonation of lighter and darker CL zones seen in some fluorite samples from Motzfeldt and Ivigtut most likely formed by abrupt changes of the REE content in the fluid.

Fluorite grains of SM1 from Motzfeldt partly show strong variations in their REE content within one sample. Their concentration varies by two orders of magnitude even over a short distance (< 1 mm). The CL images show that these samples consist of bright, REE-enriched parts whereas the dark ones are depleted in REE (Fig. 2d). Multiple fluorite generations are believed to account for this texture and the variable patterns. This can be

clearly seen in Figure 2d where the white (earlier) parts are replaced by later-formed, darker parts. Accordingly, there must have been an overprint of these fluorites by a fluid which transported less REE. However, there are other samples which show an opposite evolution, suggesting the presence of variably REE-enriched, late-stage fluids in these peralkaline intrusions.

6.3.3 Complexation

The complexation of REE with various ligands is a crucial mechanism that strongly controls the distribution of the REE (Möller et al., 1976; Bau, 1991; Bau & Möller, 1992). Apart from complexes involving Cl^-, the stability of REE complexes with F^-, OH^- and CO_3^{2-} increases from La to Lu and with increasing temperature (e.g. Möller et al., 1976; Ekambaran et al., 1986; Luo & Byrne, 2004; Wood, 1990 a,b; Haas et al., 1995). The continuous change in the relative complex stabilities eventually leads to REE fractionation in aqueous solutions and results in LREE-enriched patterns in the precipitating mineral and a progressive enrichment of HREE in the fluid. The importance of complexes involving F^-, CO_3^{2-}, hydroxide and Cl^- can be inferred from distinct REE characteristics and fluid inclusion data.

Complexation with fluoride may be an important mechanism in the transport of REE (e.g. Pan & Fleet, 1996; Salvi et al., 2000; Tagirov et al., 2002). Bau (1996) suggested Y-F complexes to be more stable than Ho-F ones. Therefore, the Y/Ho ratio increases during migration of F-rich hydrothermal fluids (Bau & Dulski, 1995). This is in agreement with Veksler et al. (2005) who demonstrated that in the presence of F-rich liquids, Y is more enriched than Ho and the Y/Ho ratio is greater than the chondritic one of 28 (Anders & Grevesse, 1989; McDonough & Sun, 1995; Irber, 1999). These findings are in accordance with Y/Ho ratios in fluorites from Motzfeldt and Ilímaussaq which reach up to 1375 (Ilm77; see below). However, they do not hold for fluorite and cryolite from Ivigtut whose Y/Ho ratios vary between 3 and 15 with a mean at 8-9. However, this does not necessarily preclude the effect of F-complexation at Ivigtut, because Irber (1996) showed that A-type granites (as in the case of the Ivigtut granite) normally have Y/Ho ratios below 28. Furthermore, crush leach analyses of fluid inclusions revealed the predominance of F.

In addition to fluoride complexes, carbonate ones may also play an important role in Motzfeldt and Ivigtut. The latter is dominated by abundant siderite and CO_2-rich fluid inclusions (Pauly & Bailey, 1999; Köhler et al., in press) while in the Motzfeldt intrusion, not only calcite in veins, but also calcite daughter minerals in fluid inclusions are common (Schönenberger & Markl, in prep.). In contrast, carbonates or CO_2-bearing fluid inclusions are

rare or absent in Ilímaussaq (Graser et al., in review) and therefore, REE complexation by (bi)carbonate seems highly unlikely.

Apart from the aforementioned processes in 6.3, the negative Ce anomaly (JS9, JS10, Ilm77, ILM325) may also be due to complexation with hydroxides. The stability of $Ce(OH)_3^0$ complexes are higher than those with other REE (Haas et al., 1995). This would lead to an increase in the solubility in the fluid and a negative Ce anomaly in the precipitating mineral. In Ivigtut, hydroxide complexation may have also influenced the distribution of REE, because fluid inclusions predominantly consist of an F-rich, CO_2-H_2O solution (Köhler et al., in press). Additionally, various (late-stage) OH-bearing minerals like gearksutite, jarlite, pachnolite, ralstonite occur in the cryolite deposit (Pauly & Bailey, 1999).

Chloride complexes do not play an important role in the formation of complexes with "hard" ions (Pearson, 1963) at 25 °C (Wood, 1990a; Haas et al., 1995). However, they are important in more acidic fluid compositions. This may be the case at Ivigtut since thermodynamic modelling has shown that cryolite is stabilised under more acidic conditions (Köhler et al., in press; Prokof'ev et al., 1991).

It must be noted, however, that the current data on complex stability constants of the REE with various ligands are from theoretical pressure-temperature extrapolations by Haas et al. (1995) and Wood (1990). New data on the stability of Nd and Er complexes with Cl^-, F^- and SO_4^{2-} were recently published by Migdisov & Williams-Jones (2002), Migdisov et al. (2006) and Migdisov & Williams-Jones (2007). Their results suggest that particularly at higher temperatures, Cl^- complexation may be more important than assumed by Haas et al. (1995) and Wood (1990).

To conclude, it is assumed that the REE patterns of the Motzfeldt and Ivigtut intrusions are most likely controlled by F^-, CO_3^{2-} and OH^- complexation in the fluid phase whereas for the Ilímaussaq intrusion only F^- and OH^- are suggested to have played a significant role.

6.3.4 Tetrad effect

The tetrad effect typically occurs in highly evolved silicate magmas (i.e. granites) and is attributed to strong fluid-rock interaction. It becomes visible in chondrite-normalised REE patterns. Masuda et al. (1987) classified the four tetrads as: T1 = La-Nd, T2 = (Pm)Sm-Gd, T3 = Gd-Ho and T4 = Er-Lu which can be either M- or W-shaped. The quantification of the tetrad effect in our samples was carried out after the method proposed by Monecke et al. (2002) excluding the second tetrad (Pm does not occur in nature) and considering the Ce-anomaly.

The tetrad effect does not play any role in the Motzfeldt and Ilímaussaq intrusions since its values are usually well below 0.2 which is below statistical significance (Monecke et al., 2002). In Ivigtut, however, fluorite and cryolite constantly display pronounced tetrad effects with values as high as 1 (Fig. 8). In all analysed samples, the tetrad effect describes a convex, M-shaped pattern. However, Veksler et al. (2005) concluded from tetrad patterns involving the distribution coefficient that only silicate melts produce M-shaped patterns. The conjugate fluoride liquid, however, should have a W-shape which is not in accordance with the studied samples.

The pronounced tetrad effect in the Ivigtut deposit implies that it formed from highly evolved (granitic) melts which strongly interacted with a (F-rich) fluid (Zhao et al., 2002; Liu et al., 2005; Irber, 1999). The tetrad effect cannot be explained by fractionation of REE-rich accessory minerals (monazite, xenotime, garnet, eudialyte etc.; c.f. Liu et al., 2005; Irber, 1999) as no significant tetrad effect was observed in the unaltered Ivigtut granite surrounding the Ivigtut deposit. The fluid-rock interaction which is evidenced by the strong metasomatism of the host granite (Pauly & Bailey, 1999) is the most likely explanation for the REE distribution found in the fluorides from the Ivigtut cryolite deposit.

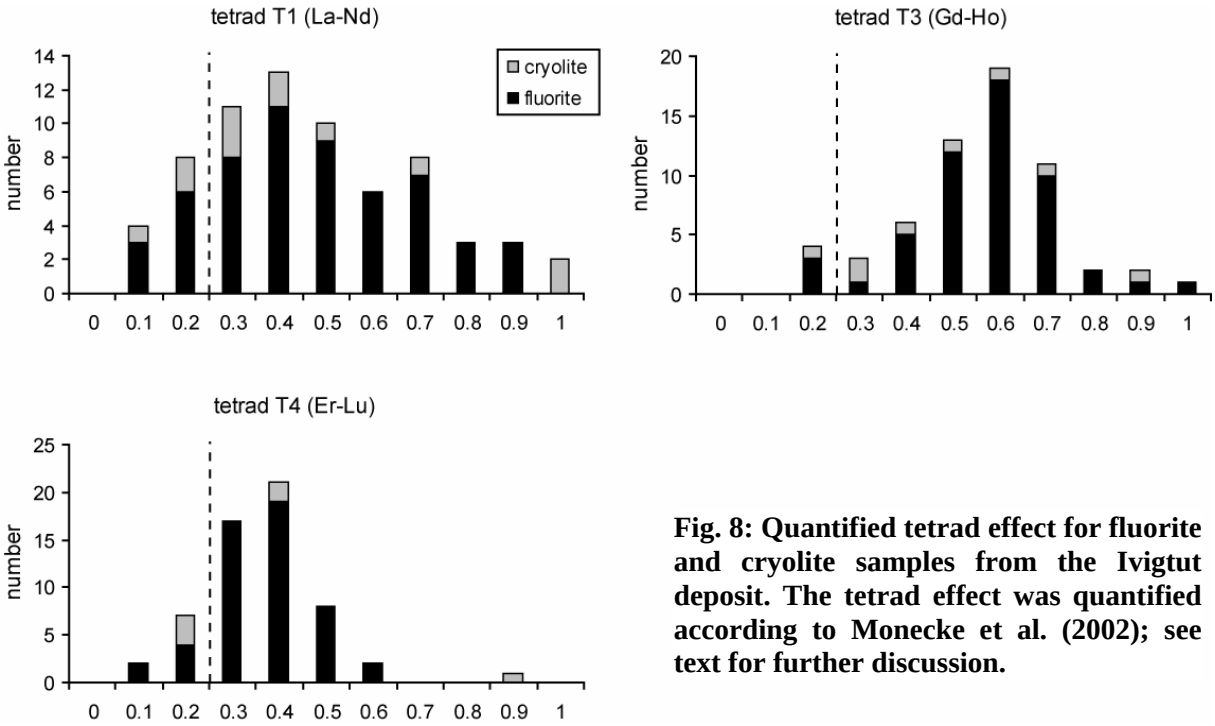

Fig. 8: Quantified tetrad effect for fluorite and cryolite samples from the Ivigtut deposit. The tetrad effect was quantified according to Monecke et al. (2002); see text for further discussion.

6.3.5 Y/Ho fractionation

Hydrothermal fluorites from Motzfeldt and Ilímaussaq

In Ilímaussaq and Motzfeldt, the hydrothermal fluorites are variable in their Y/Ho ratios that can reach up to 1370 (Ilm77). This argues for a decoupling of Y from Ho during the hydrothermal stage during which these fluorites formed. Bau & Dulski (1995) suggested that in fluorine-rich environments, the Y/Ho ratio and the positive Y anomaly increase during the migration and interaction of a fluorine-rich aqueous fluid. This is the most likely explanation for the increasing Y/Ho ratios of hydrothermal fluorites from the Ilímaussaq intrusion with ratios > 1300 (Fig. 9 & 10). Fluorites which are interpreted to have formed at a later stage (i.e. at lower temperatures) show a decreasing content of REE coupled with an increasing Y anomaly (e.g. very late formed Ilm77).

The fluorites from Motzfeldt and Ilímaussaq define steep trends in the Y against Ho diagram with slopes between 50 and 80 (R^2 = 0.7 to 0.9; Fig. 10). The Y/Ho ratios of fluorites from SM1 are widely scattered suggesting the influence of coupled effects of fluid interaction, remobilisation and/or various generations of fluorite. Additionally, the highly varying Y/Ho and La/Ho ratios may further indicate that these fluorites are not cogenetic (Bau & Dulski, 1995). It is obvious that the Y/Ho ratio decreases with increasing REE content in certain samples from SM1 (Fig. 2, JS6; JS16, JS4). This could be related to different origins of the different fluorite parts. Another hypothesis suggests that Y was complexed with F and therefore was retained in the fluid whereas the REE were incorporated in the fluorites. A migrating fluid would then show an increasing Y anomaly with decreasing REE content (Bau & Dulski, 1995).

The Y/Ho and La/Ho ratios of most fluorites from unit SM4 (Motzfeldt) have similar values implying precipitation from a similar hydrothermal fluid (Bau & Dulski, 1995). SM5 shows slightly lower Y/Ho and higher La/Ho ratios. The slightly decreasing Y/Ho ratio from SM4 to SM5 (Motzfeldt) could account for interaction with a (bi)carbonate-rich solution (Bau & Dulski, 1995). This is further supported by vein fluorites associated with carbonates and calcite daughter minerals in fluid inclusions of the Motzfeldt intrusion (Schönenberger & Markl, in prep.).

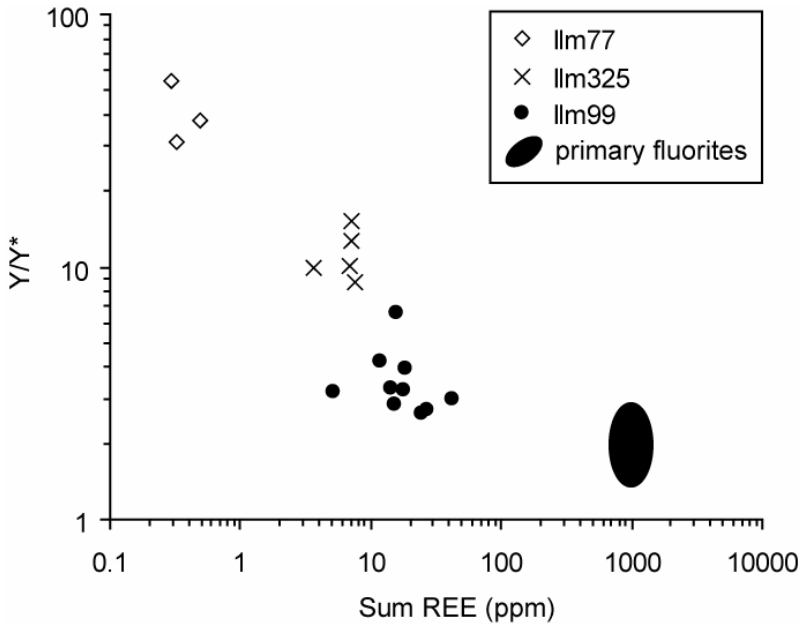

Fig. 9: Y anomaly (Y/Y* with $Y^* = (Dy_n * Ho_n)^{0.5}$) vs. total REE content (ppm) of the Ilímaussaq fluorites. Primary fluorites show the highest REE content whereas the Y anomaly increases in the order primary fluorites < Ilm 99 < Ilm 325 < Ilm 77.

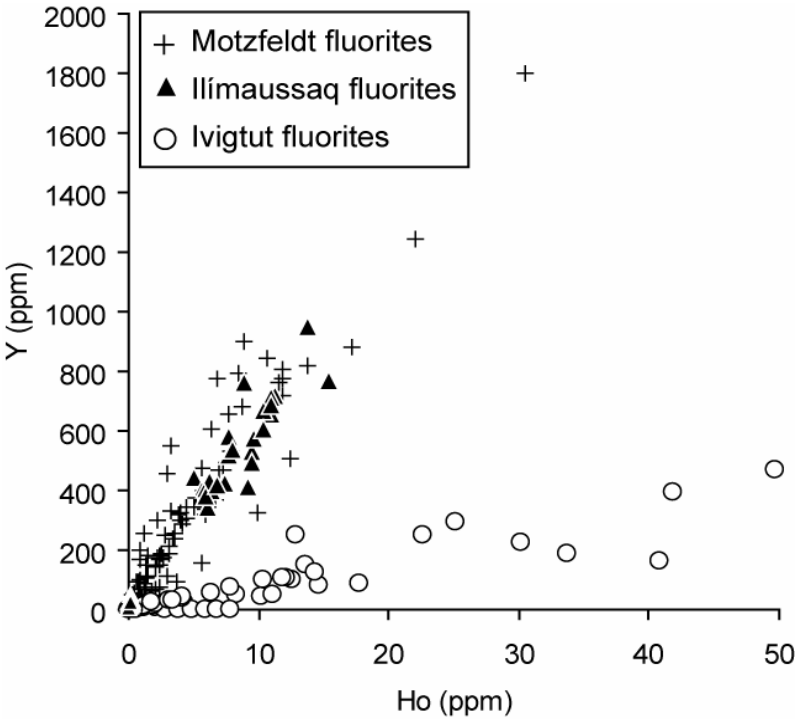

Fig. 10: Y (ppm) vs. Ho (ppm) of Motzfeldt, Ilímaussaq and Ivigtut fluorites. The Motzfeldt and Ilímaussaq fluorites describe a much steeper trend than the Ivigtut fluorites.

Hydrothermal fluorites from the Ivigtut deposit

The low Y/Ho ratio in samples from Ivigtut is in strong contrast to the rather high ratios in fluorites from Motzfeldt and Ilímaussaq. In Ivigtut, the Y/Ho ratios of cryolite and fluorite are below the chondritic value of 28 and vary between 3 and 15 with a mean at 8-9. In the Y-Ho diagram, the data points define a flat slope of about 8 ($R^2 = 0.91$; Fig. 10). Veksler et al. (2005) observed a decoupling of Y from Ho and a strong Y/Ho anomaly in cryolite which they ascribed not only to the influence of F itself, but rather to REE-aluminofluoride complexes. However, they also pointed out that fluoride liquids are more enriched in Y than in Ho. This is not in agreement with samples from Ivigtut, because if the analysed cryolite samples precipitated from such a fluoride liquid, much higher Y/Ho ratios would be expected. The low Y/Ho ratios could be explained by an abnormally low Y content in the fluid. Strikingly, however, bulk rock analyses from the Ivigtut granite exhibit near-chondritic Y/Ho ratios from 16 to 40 with a mean at 28 (Goodenough et al., 2000). The fact that the unaltered Ivigtut granite does have chondritic Y/Ho ratios, but fluorite and cryolite from the deposit do not, may be explained with experimental results by Veksler et al. (2005). They showed that the cryolite/fluoride or silicate melt D_Y is lower than that of Ho. This may explain the low Y/Ho ratio in cryolite, but not the low ratio in fluorite which is commonly below 10. It may be possible that some change in the Y-Ho content took place before/during the deposit's formation. Pauly & Bailey (1999) suggested that the granite had already been solidified when greisenisation and metasomatism led to its alteration. These altering fluids formed an aluminofluoride melt which later unmixed into a silica- and a fluorine-rich melt. It may be possible that during greisenisation, Y and Ho were decoupled. Y was most likely retained in the granite whereas Ho was preferably leached leading to the low Y/Ho ratios of the deposit.

7. Conclusions

In the present study, REE patterns of fluorides from three plutonic complexes in a magmatic province record distinct conditions of formation. The fluorites from the Motzfeldt and Ilímaussaq intrusions appear to have formed in a similar environment and from a similar source. Primary magmatic fluorites have (almost) identical characteristics regarding their Y/Ho ratios, REE content and patterns irrespective of their association with an agpaitic or miaskitic mineral assemblage. The most likely process having led to these comparable LREE enriched patterns is the similar K_D and/or the whole-rock control. The latter also accounted for the LREE enriched peralkaline magmatic rocks from Motzfeldt and Ilímaussaq.

The CL imagery and REE patterns of hydrothermal fluorites from Motzfeldt suggest multiple fluorite generations within one unit (SM1). Furthermore, different physico-chemical formation conditions are reflected by low REE contents and a negative Ce anomaly indicating more oxidised conditions. Fluorites from SM5 show evidence of fluid interaction with the surrounding rocks from which they appear to have partly inherited the positive Eu anomaly.

The HREE-enriched or smooth patterns in minerals from the Ivigtut deposit are very different from Motzfeldt and Ilímaussaq and appear to reflect hydrothermal formation conditions. The incorporation of REE into fluorides from Ivigtut seems to be mostly driven by F-complexation resulting in the tetrad effect. This effect typically reflects strong interaction of a fluid with highly evolved granitic rocks. In contrast, the tetrad effect is not seen in highly evolved, Si-undersaturated rocks like those from Motzfeldt and Ilímaussaq.

These observations lead to the conclusion that the abundance and distribution of REE is strongly source-dependent. The heterogeneous mantle source assumed beneath the Gardar Province may be an important factor controlling the distribution of trace elements. Additionally, silica-rich, granitic systems like Ivigtut favour HREE whereas the low-Si, alkaline nepheline-syenites from Motzfeldt and Ilímaussaq appear to preferentially incorporate LREE. Apart from source features, it is the size and charge of the cation and the availability of complexing agents in the fluid that govern the incorporation of REE into minerals.

Acknowledgments

Financial support by the German Science Foundation (DFG) and the Graduiertenförderung des Landes Baden-Württemberg is gratefully acknowledged. Helene Brätz is thanked for performing the LA-ICP MS measurements in Würzburg. Ole V. Petersen kindly provided rock samples from Ivigtut from the Geological Musuem of Copenhagen, Denmark. Gesa Graser and Thomas Krumrei are thanked for providing samples from the Ilímaussaq intrusion. Adrian Finch is thanked for fruitful discussions. Thomas Wagner kindly helped to improve an earlier version of the manuscript. The useful comments and suggestions of two anonymous reviewer are greatly acknowledged.

Appendix A. Supplementary data

Supplementary data associated with this article can be found in the online version.

References

ANDERS, E., GREVESSE, N., 1989. Abundances of the elements: meteoritic and solar. Geochimica et Cosmochimica Acta 53, 197-214.

BAILEY, J.C., GWOZDZ, R., ROSE-HANSEN, J. & SØRENSEN, H., 2001: Geochemical overview of the Ilímaussaq alkaline complex, South Greenland. In: Sørensen, H. (Ed.), The Ilímaussaq complex, South Greenland: status of mineralogical research with new results. Geology of Greenland Survey Bulletin 190, 35-53.

BAU, M., 1991. Rare earth element mobility during hydrothermal and metamorphic fluid-rock interaction and the significance of the oxidation state of europium. Chemical Geology 93, 219-230.

BAU, M., 1996. Controls on the fractionation of isovalent trace elements in magmatic and aqueous systems: evidence from Y/Ho, Zr/Hf, and the lanthanide tetrad effect. Contributions to Mineralogy and Petrology 123, 323-333.

BAU, M., 1997. The lanthanide tetrad effect in highly evolved felsic igneous rocks—a reply to the comment by Y. Pan. Contrib. Mineral. Petrol. 128, 409– 412.

BAU, M., DULSKI, P., 1995. Comparative study of yttrium and rare-earth element behaviours in fluorine-rich hydrothermal fluids. Contributions to Mineralogy and Petrology 119, 213-223.

BAU, M., MÖLLER, P., 1992. Rare Earth Element Fractionation in Metamorphogenic Hydrothermal Calcite, Magnesite and Siderite. Mineralogy and Petrology 45, 231-246.

BRADSHAW, C., 1988. A Petrographic, Structural and Geochemical study of the Alkaline Igneous rocks of the Motzfeldt centre, South Greenland. PhD thesis, Univ. of Durham, UK.

CONSTANTOPOULOS, J., 1988. Fluid Inclusions and Rare Earth Element Geochemistry of Fluorite from South-Central Idaho. Economic Geology 83, 626-636.

DINGWELL, D.B., 1988. The structures and properties of fluorine-rich magmas: a review of experimental studies. CIM Special Volume 39, 1-12.

DOLEJS, D., BAKER, D.R., 2007a. Liquidus Equilibria in the System K_2O-Na_2O-Al_2O_3-SiO_2-F_2O_{-1}-H_2O to100MPa: I. Silicate-Fluoride Liquid Immiscibility in Anhydrous Systems. Journal of Petrology 48, 785-806.

DOLEJS, D., BAKER, D.R., 2007b. Liquidus Equilibria in the System K_2O-Na_2O-Al_2O_3-SiO_2-F_2O_{-1}-H_2O to100 MPa: II. Differentiation Paths of Fluorosilicic Magmas in Hydrous Systems. Journal of Petrology 48, 807-828.

DRUMMOND, M.S., DEFANT, M.J., KEPEZHINSKAS, P.K., 1996. Petrogenesis of slab-derived trondhjemite-tonalite-dacite/adakite magmas. Transactions of the Royal Society of Edinburgh: Earth Sciences 87, 205-215.

EKAMBARAM, V., BROOKINS, D.G., ROSENBERG, P.E., EMANUEL, K.M., 1986. Rare-Earth Element Geochemistry of fluorite-carbonate deposits in western Montana, USA. Chemical Geology 54, 319-331.

EMELEUS, C.H., HARRY, W.T., 1970. The Igaliko nepheline syenite complex; general description. Meddelelser om Grønland, 186, 115.

EPPINGER, R.C., CLOSS, L.G., 1990. Variation of trace elements and rare earth elements in fluorite: A possible tool for exploration. Economic Geology 85, 1896-1907.

ESCHER, A., WATT, W.S., 1976. Geology of Greenland. Geological Survey of Greenland, Copenhagen, 603 p.

FLEISCHER, M., ALTSCHULER, Z.S., 1969. The relationship of the rare-earth composition of minerals to geological environment. Geochimica et Cosmochimia Acta 33, 725-732.

FRYER, B.J., EDGAR, A.D., 1977. Significance of rare earth distributions in coexisting minerals of peralkaline undersaturated rocks. Contributions to Mineralogy and Petrology 61, 35-48.

GAGNON, J.E., SAMSON, I.M., FRYER, B.J., WILLIAMS-JONES, A.E., 2003. Compositional heterogeneity in fluorite and the genesis of fluorite deposits: insights from LA-ICP-MS analysis. Canadian Mineralogist 41, 365-382.

GARDE, A.A., HAMILTON, M.A., CHADWICK, B., GROCOTT, J., MCGAFFREY, K.J.W., 2002. The Ketilidian orogen of South Greenland: geochronology, tectonics, magmatism, and fore-arc accretion during Palaeoproterozoic oblique convergence. Canadian Journal of Earth Sciences 39, 765-793.

GOODENOUGH, K.M., UPTON, B.G.J., ELLAM, R.M., 2000. Geochemical evolution of the Ivigtut granite, South Greenland: a fluorine-rich "A-type" intrusion. Lithos 51, 205-221.

GOODENOUGH, K.M., UPTON, B.G.J., ELLAM, R.M., 2002. Long-term memory of subduction processes in the lithospheric mantle: evidence from the geochemistry of basic dykes in the Gardar Province of South Greenland. Journal of the Geological Society, London 159, 705-714.

GRASER, G., POTTER, J., KÖHLER, J., MARKL, G., in review. Isotopic, major, minor and trace element geochemistry of late-stage fluids in the peralkaline Ilímaussq intrusion, South Greenland. Lithos.

HAAS J.R., SHOCK E.L., AND SASSANI D.C., 1995. Rare earth elements in hydrothermal systems: estimates of standard partial molal thermodynamic properties of aqueous complexes of the rare earth elements at high pressures and temperatures. Geochim. Cosmochim. Acta 59, 4329–4350.

HALAMA, R., WAIGHT, T., MARKL, G., 2002. Geochemical and isotopic zoning patterns of plagioclase megacrysts in gabbroic dykes from the Gardar Province, South Greenland: implications for crystallisation processes in anorthositic magmas. Contributions to Mineralogy and Petrology 144, 109-127.

HALAMA, R., JORON, J.L., VILLEMANT, B., MARKL, G., TREUIL, M., 2007. Trace element constraints on mantle sources druing mid-Proterozoic magmatism: evidence for a link between the Gardar (South Greenland) and Abitibi (Canadian Shield) mafic rocks. Canadian Journal of Earth Sciences 44, 1-20.

HILL, G.T., CAMPBELL, A.R., KYLE, P.R., 2000. Geochemistry of southwestern New Mexico fluorite occurrences implications for precious metals exploration in fluorite-bearing systems. Journal of Geochemical Exploration 68, 1-20.

HOLLINGS, P., WYMAN, D., 2005. The geochemistry of trace elements in igneous systems: principles and examples from basaltic systems. In: Linnen, R.L., Samson, I.M. (Eds.), Rare-Element Geochemistry and Mineral Deposits: Geological Association of Canada, GAC Short Course Notes 17, 1-16.

HORN, I., HINTON, R.W., JACKSON, S.E., LONGERICH, H.P., 1997. Ultra-trace element analysis of NIST SRM 616 and 614 using laser ablation microprobe-inductively coupled plasma-mass spectrometry (LAM-ICP-MS); a comparison with secondary ion mass spectrometry (SIMS). Geostandards Newsletter 21, 191-203.

IRBER, W., 1996. Laugungsexperimente an peralumischen Graniten als Sonde für Alterationsprozesse im finalen Stadium der Granitkristallisation mit Anwendung auf das Rb-Sr-Isotopensystem. Ph.D. dissertation (German with English abstract), FU Berlin.

IRBER, W., 1999. The lanthanide tetrad effect and its correlation with K/Rb, Eu/Eu*, Sr/Eu, Y/Ho, and Zr/Hf of evolving peraluminous granite suites. Geochimica et Cosmochimica Acta 63, 489-508.

JAHN, B., WU, F., CAPDEVILA, R., MARTINEAU, F., ZHAO, Z., WANG, Y., 2001. Highly evolved juvenile granites with tetrad REE patterns: the Woduhe and Baerzhe granites from the Great Xing'an Mountains in NE China. Lithos 59, 171-198.

JONES, A.P., 1980. Petrology and structure of the Motzfeldt centre, Igaliko complex, South Greenland. PhD thesis, Univ. of Durham, UK.

JONES, A.P., 1984. Mafic silicates from the nepheline syenites of the Motzfeldt centre, south Greenland. Mineralogical Magazine, 48, 1-12.

KEMPE, U., MONECKE, T., OBERTHÜR, T., KREMENETSKY, A.A., 1999. Trace elements in scheelite and quartz from the Muruntau/Myutenbai gold deposit, Uzbekistan: constraints on the nature of ore-forming fluids. In: Stanley, C.J., et al. (eds). Mineral Deposits: Processes to Processing. Balkema, Rotterdam, The Netherlands, 373-376.

KESSEL, R., SCHMIDT, M.W., ULMER, P., PETTKE, T., 2005. Trace element signature of subduction-zone fluids, melts and supercritical liquids at 120-180 km depth. Nature 437, 724-727.

KÖHLER, J., KONNERUP-MADSEN, J., MARKL, G., in press. Fluid geochemistry in the Ivigtut cryolite deposit, South Greenland. Lithos. doi: 10.1016/j.lithos.2007.10.005.

LAHAYE, Y., LAMBER, D., WALTERS, S., 1997. Ultraviolet laser sampling and high-resolution inductively coupled plasma mass spectrometry of NIST and BCR-2G glass reference materials. Geostandards Newsletter 21, 205-214.

LARSEN, L.M., SØRENSEN, H., 1987: The Ilímaussaq intrusion . progressive crystallization and formation of layering in an agpaitic magma. In Fitton, J. G., Upton, B. G. J. (eds.), Alkaline Igneous Rocks, Geol. Soc. Spec. Pub. 30, 473-488.

LIU, C.Q., ZHAN, H., 2005. The lanthanide tetrad effect in apatite from the Altay No. 3 pegmatite, Xingjiang, China: an intrinsic feature of the the pegmatitic magma. Chemical Geology 214, 61-77.

LÜDERS, V., MÖLLER, P., DULSKI, P., 1993. REE Fractionation in Carbonates and Fluorite. Monograph Series on Mineral Deposits 30, 133-150.

LUO, Y.-R., BYRNE, R.H., 2004. Carbonate Complexation of Yttrium and the Rare Earth Elements in Natural Waters. Geochimica et Cosmochimica Acta 68, 691-699.

MANNING, D.A.C., 1981. The effect of fluorine on liquidus phase relationships in the system Qz-Ab-Or with excess water at 1 kb. Contributions to Mineralogy and Petrology 104, 424-438.

MARKL, G., MARKS, M., SCHWINN, G., SOMMER, H., 2001. Phase Equilibrium Constraints on Intensive Crystallization Parameters of the Ilímaussaq Complex, South Greenland. Journal of Petrology 42, 2231-2258.

MARKS, M., VENNEMANN, T., SIEBEL, W., MARKL, G., 2003. Quantification of Magmatic and Hydrothermal Processes in a Peralkaline Syenite-Alkali Granite Complex Based on Textures, Phase Equilibria, And Stable and Radiogenic Isotopes. Journal of Petrology 44, 1247-1280.

MARSHALL, A.S., HINTON, R.W., MACDONALD, R., 1998. Phenocrystic fluorite in peralkaline rhyolites, Olkaria, Kenya Rift Valley. Mineralogical Magazine 62, 477-486.

MASUDA, A., KAWAKAMI, O., DOHMOTO, Y., TAKENAKA, T., 1987. Lanthanide tetrad effect in nature: two mutually opposite types, W and M. Geochemical Journal 21, 119-124.

MCDONOUGH, W.F.M., SUN, S.S., 1995. The composition of the Earth. Chemical Geology 120, 223-253.

MIGDISOV A.A., WILLIAMS-JONES A.E., 2002. A spectrophotometric study of neodymium(III) complexation in chloride solutions. Geochimica et Cosmochimica Acta 66, 4311–4323.

MIGDISOV A.A., REUKOV V.V., WILLIAMS-JONES A.E., 2006. A spectrophotometric study of neodymium(III) complexation in sulfate solutions at elevated temperatures. Geochimica et Cosmochimica Acta 70, 983–992.

MIGDISOV, A.A., WILLIAMS-JONES, A.E., 2007. An experimental study of the solubility and speciation of neodymium (III) fluoride in F-bearing aqueous solutions. Geochimica et Cosmochimica Acta 71, 3056-3069.

MÖLLER, P., PAREKH, P., SCHNEIDER, H.-J., 1976. The application of Tb/Ca-Tb/La abundance ratios to problems of fluorspar genesis. Mineralium Deposita 11, 111-116.

MÖLLER, P., BAU, M., DULSKI, P., LÜDERS, V., 1998. REE and Y fractionation in fluorite and their bearing on fluorite formation. Proceedings of the Ninth Quadrennial IAGOD Symposium. Schweizerbart, Stuttgart, 575-592.

MONECKE, T., KEMPE, U., MONECKE, J., SALA, M., WOLF, D., 2002. Tetrad effect in rare earth element distribution patterns: A method of quantification with application to rock an mineral samples from granite-related rare metal deposits. Geochimica et Cosmochimica Acta 66, 1185-1196.

MORGAN, J.W., WANDLESS, G.A., 1980. Rare earth element distribution in some hydrothermal minerals: evidence for crystallographic control. Geochmicia et Cosmochimica Acta 44, 973-980.

MÜLLER-LORCH, D., MARKS, M.A.W., MARKL, G., 2007. Na and K distribution in agpaitic pegmatites. Lithos 95, 315-330.

PAN, Y., FLEET, M.E., 1996. Rare element mobility during prograde granulite facies metamorphism: significance of fluorine. Contributions to Mineralogy and Petrology 123, 251-262.

PAULY, H., BAILEY, J.C., 1999. Genesis and evolution of the Ivigtut cryolite deposit, SW Greenland. Meddelelser om Grønland, Geoscience 37, 60.

PEARCE N.J.G., PERKINS W.T., WESTGATE J.A., GORTON M.P., JACKSON S.E, NEAL C.R, CHENERY S.P., 1997. A compilation of new and published major and trace element data for NIST SRM 610 and NIST SRM 612 glass reference materials. Geostandards Newsletter 21, 115-144.

PEARSON, R.G., 1963. Hard and soft acids and bases. Journal of the American Chemical Society 85, 3533-3539.

PETERSEN, O.V., 2001: List of minerals identified in the Ilimaussaq alkaline complex, South Greenland. Geology of Greenland Survey Bulletin 190, 25-33.

PROKOF'EV, V.B., NAUMOV, V.B., IVANOVA, G.F., SAVEL'EVA, N.I., 1991. Fluid inclusion studies in cryolite and siderite of the Ivigtut deposit (Greenland). Neues Jahrbuch für Mineralogie, Monatshefte 1, 32-38.

RUBIN, J.N., HENRY, C.D., PRICE, J.G., 1993. The mobility of zirconium and other "immobile" elements during hydrothermal alteration. Chemical Geology 110, 29-47.

RUDNICK, R.L., BARTH, M., HORN, I., MCDONOUGH, W.F., 2000. Rutile-bearing refractory eclogites: missing link between continents and depleted mantle. Science 287, 278-281.

SALLET, R., MORITZ, R., FONTIGNIE, D., 2000. Fluorite $^{87}Sr/^{86}Sr$ and REE constraints on fluid-melt relations, crystallization time span and bulk D^{Sr} of evolved high-silica granites, Tabuleiro granites, Santa Catarina, Brazil. Chemical Geology 164, 81-92.

SALLET, R., MORITZ, R., FONTIGNIE, D., 2005. The use of vein fluorite as probe for paleofluid REE and Sr–Nd isotope geochemistry: The Santa Catarina Fluorite District, Southern Brazil. Chemical Geology 223, 227-248.

SALVI, S., FONTAN, F., MONCHOUX, P., WILLIAMS-JONES, A.E., MOINE, B., 2000. Hydrothermal Mobilization of High Field Strength Elements in Alkaline Igneous Systems: Evidence from the Tamazeght Complex (Morocco). Economomic Geology 95, 559-576.

SCAILLET, B., MACDONALD, R., 2004. Fluorite stability in silicic magmas. Contributions to Mineralogy and Petrology 147, 319-329.

SCAILLET, B., MACDONALD, R., 2001. Phase Relations of Peralkaline Silicic Magmas and Petrogenetic Implications. Journal of Petrology 42, 825-845.

SCHWINN, G., MARKL, G., 2005. REE systematics in hydrothermal fluorite Chemical Geology, 216, 225-248.

SØRENSEN, H., 1997. The agpaitic rocks – a review. Mineralogical Magazine 61, 485-498.

SØRENSEN, H., BOHSE, H., BAILEY, J.C., 2006. The origin and mode of emplacement of lujavrites in the Ilímaussaq alkaline complex, South Greenland. Lithos 91, 286-300.

STÄHLE, H.J., RAITH, M., HOERNES, S., DELFS, A., 1987. Element mobility during incipient granulite formation at Kabbadurga, Southern India. Journal of Petrolgy 28, 803-834.

TAGIROV, B., SCHOTT, J., HARRICHOURRY, J.C., SALVI, S., 2002. Experimental study of aluminum speciation in fluoride-rich supercritical fluids. Geochimica et Cosmochimica Acta 66, 2013-2024.

TRINKLER, M., MONECKE, T., THOMAS, R., 2005. Constraints on the genesis of yellow fluorite in hydrothermal barite-fluorite veins of the Erzgebirge, Eastern Germany: Evidence from optical absorption spectroscopy, rare-earth-element data and fluid-inclusion investigations. The Canadian Mineralogist 43, 883-898.

UPTON, B.G.J., EMELEUS, C.H., HEAMAN, L.M., GOODENOUGH, K.M, FINCH, A.A., 2003. Magmatism of the mid-Proterozoic Gardar Province, South Greenland: chronology, petrogenesis and geological setting. Lithos 68, 43-65.

UPTON, B.G.J., EMELEUS, C.H., 1987. Mid-Proterozoic alkaline magmatism in southern Greenland: the Gardar Province. In: Fitton, J.G. & Upton, B.G.J. (Eds.), Alkaline Igneous Rocks, Geological Society Special Publication 30, 449-471.

VEKLSER, I.V., DORFMAN, A.M., KAMENETSKY, M., DULSKI, P., DINGWELL, D., 2005. Partitioning of lanthanides and Y between immischible silicate and fluoride melts, fluorite and cryolite and the origin of the lanthanide tetrad effect in igneous systems. Geochimica et Cosmochimica Acta 69, 2847-2860.

WAGNER, T., ERZINGER, J., 2001. REE geochemistry of fluid-rock interaction processes related to Alpine-type fissure vein mineralisation, Rheinisches Schiefergebirge, Germany. In: Piestrzynski, A. et al. (Eds.), Mineral deposits at the beginning of the 21st century. Proc. joint 6th biennial SGA-SEG meeting, Krakow, 929-932. Society for Geology Applied to Mineral Deposits (SGA).

WEBSTER, J.D., 1990. Partition of F between H_2O and CO_2 fluids and topaz rhyolite melt. Contrib. Mineral. Petrol. 104, 424–438.

WILLIAMS-JONES, A.E., SAMSON, I.M., OLIVIO, G.R., 2000. The genesis of hydrothermal fluorite-REE deposits in the Gallinas Mountains, New Mexico. Economic Geology and the Bulletin of the Society of Economic Geologists 95, 327-341.

WOOD, S.A., 1990A. The aqueous geochemistry of the rare-earth elements and yttrium. 1. Review of available low-temperature data for inorganic complexes and the inorganic REE speciation of natural waters. Chemical Geology 88, 159-186.

WOOD, S.A., 1990B. The aqueous geochemistry of the rare-earth elements and yttrium. 2. Theoretical predictions of speciation in hydrothermal solutions to 350 °C at saturation water vapor pressure. Chemical Geology 88, 99-125.

YOU, C.F., CASTILLO, P.R., GIESKES, J.M., CHAN, L.H., SPIVACK, A.J., 1996. Trace element behavior in hydrothermal experiments: Implications for fluid processes at shallow depths in subduction zones. Earth and Planetary Science Letters 140, 41-52.

ZHAO, Z., XIONG, X., HAN, X., WANG, Y., WANG, Q., BAO, Z., JAHN, B., 2002. Controls on the REE tetrad effect in granites: Evidence from the Qianlishan and Baerzhe Granites, China. Geochemical Journal 36, 527-543.

Eidesstattliche Erklärung

Hiermit erkläre ich, dass ich die Arbeit selbstständig und nur mit den angegebenen Hilfsmitteln angefertigt habe, und dass alle Stellen, die dem Wortlaut oder dem Sinne nach anderen Werken entnommen sind, durch Angabe der Quellen als Entlehnung kenntlich gemacht worden sind.

Ferner erkläre ich, dass ich nicht anderweitig mit oder ohne Erfolg versucht habe, eine Dissertation einzureichen.

Tübingen, im Dezember 2007

Jasmin Köhler